Elena Surra

Licenciada em Geologia

Pós-Graduada em Energia e BioEnergia

BioCH$_4$ from the Anaerobic co-Digestion of the Organic Fraction of Municipal Solid Waste and Maize Cob Wastes

Dissertação para obtenção do Grau de Doutora em
Energia e Bioenergia

Orientador: Nuno Carlos Lapa dos Santos Nunes, Assistant Professor, Faculdade de Ciências e Tecnologia da Universidade Nova de Lisboa

Co-orientadora: Isabel Alexandra de Almeida Caneto Esteves Esperança, Assistant Researcher, Faculdade de Ciências e Tecnologia da Universidade Nova de Lisboa

Júri:

Presidente: Professor Doutor Manuel Luís Magalhães Nunes da Ponte (FCT/UNL)

Arguentes: Professora Doutora Elizabeth da Costa Neves Fernandes de Almeida Duarte (ISA/UL)
Professora Doutora Margarida Maria João de Quina (FCT/UC)

Vogais: Professora Doutora Isabel Maria de Figueiredo Ligeiro da Fonseca (FCT/UNL)
Professor Doutor Nuno Carlos Lapa dos Santos Nunes (FCT/UNL)

FACULDADE DE CIÊNCIAS E TECNOLOGIA
UNIVERSIDADE NOVA DE LISBOA

October 2019

BioCH$_4$ from the Anaerobic co-Digestion of the Organic Fraction of Municipal Solid Waste and Maize Cob Wastes

To my husband Marco and to our sons, Tommaso and Federico

Agradecimentos

Antes de tudo, os meus mais profundos e sinceros agradecimentos vão ao meu Orientador, o Professor **Nuno Lapa**, sem o seu profissionalismo, suporte técnico e psicológico, seriedade, perseverança e paciência, tudo isso teria sido impossível.

Agradeço à minha coorientadora, a Doutora Isabel Esteves pela oportunidade que me deu e pelo apoio financeiro nestes anos de tão intenso trabalho, para as condições laboratoriais que disponibilizou, pelo trabalho importantíssimo de correção da tese e, o mais importante, por todos os desafios que me tornaram mais confiante e forte.

Gostaria de agradecer a iniciativa ERANet LAC e a Fundação para a Ciência e a Tecnologia (FCT / MCIES) através do projeto ELAC2014/BEE0367 e IF/01016/2014, por financiar a minha tese de doutoramento de fevereiro de 2015 até maio 2019. Agradeço também pelo parcial apoio econômico dado pelo LAQV-REQUIMTE, por sua vez financiado pelos fundos nacionais FCT/MCTES (UID/QUI/50006/2013) e co-financiado pelo ERDF ao abrigo do protocolo de cooperação PT2020 (POCI01-0145-FEDER-007265).

Ao longo deste percurso cruzei-me com muitas pessoas, todas elas contribuíram para enriquecer com a sua própria experiência, genialidade e disponibilidade este trabalho, mas, mais do que tudo, os meus dias. Todos eles foram marcantes, sem dúvida. Começando pela FCT gostava de agradecer a Professora Isabel Fonseca, a Doutora Maria Bernardo e o Mestre Miguel Costa Nogueira, por ter sido um suporte fundamental na produção, caraterização e uso dos carvões ativados, tal como na escrita do artigo relativo a essa parte. Agradeço ao Professor José Paulo Mota, ao Professor Mário Eusébio, ao Doutor Rui Ribeiro e ao aluno de Doutoramento Tiago Santos pelo importantíssimo suporte técnico, pelo carinho, pela disponibilidade e simpatia nestes longos meses de trabalho numa área por mim completamente nova e desafiante. Agradeço também aos Professores que acompanharam a parte curricular do meu programa Doutoral, nomeadamente ao Professor João Lourenço, por ter me ensinado e apoiado na aprendizagem e uso do Latex, ao Professor João Joanaz de Melo, ao Professor Tomás Ramos, ao Professor Paolo Limão, à Professora Ana Luísa Fernando, à Professora Margarida Gonçalves, e à Professora Benilde Mendes por me ter aceite no programa doutoral. Agradeço os alunos de mestrado que ao longo destes anos contribuíram para este projeto ser mais completo e rico, nomeadamente a Mestre Susana Lancinha e os Mestres Hélio Pereira e Alexandre Deodato, e os futuros

Mestres Ricardo Carvalho e Inês Martins. Agradeço também ao aluno de Doutoramento Diogo Dias, pela ajuda em algumas análises químicas de bancada, mas sobretudo pelos muitos risos e pela partilha de muitos momentos divertidos.

Agradeço à ETVO da Valorsul Lda, for ter fornecido as amostras de pré-hidrolisado e digerido e, em particular à Eng.ª Anália Torres, à Dr.ª Constância Correia e ao Eng.º Sérgio Lopes por terem facilitado as nossas idas à ETVO, para além de terem demonstrado interesse nesse trabalho. Agradeço à ANPROMIS, na pessoa do Eng.º Tiago Silva Pinto pelo suporte e por nos ter posto em contacto com a Quinta da Cholda, que forneceu o carolo de milho, e com o Eng.º João Coimbra, um exemplo de empreendedorismo perspicaz e sustentável. Agradeço a Cabot-Norit por nos ter fornecido as amostras de carvões ativados comerciais, que foram um importante termo de comparação com os carvões ativados produzidos neste trabalho.

E agora gostava de agradecer a umas pessoas especiais, que participaram de diferentes formas esta viagem tão marcante. São pessoas que me inspiraram nos momentos difíceis porque eles próprios, aos meus olhos, são um exemplo de excelência, inteligência e entregue completa. Começamos por Alexandre Testagrossa e Vasco Alves, dois amigos queridos e insubstituíveis, que me ensinaram a ver o mundo e a vida de uma perspetiva muito mais abrangente e completa. Agradeço à minha grande amiga Rita Gomes de Sousa, companheira de muitas aventuras desportivas e suporte nos momentos difíceis, ao seu marido Rui Camacho Palma, um dos homens mais inteligentes que eu já conheci, à minha amiga Dora Russo Angelino e ao seu marido Tiago Mora, que tiveram um papel fundamental na nossa integração em Portugal, à minha amiga Núria Baylina e ao Jõao Falcato pela inspiração que e deram através do contributo que eles diariamente dão à conservação dos Oceanos e do nosso Planeta, à minha amiga Rita Macedo e aos pais dela, que sempre estiveram presentes e, sem eles saberem, deram-me coragem. Agradeço ao meu amigo, quase irmão, Alessandro Frozzi, por estar sempre ao meu lado, mesmo estando longe, por me fazer rir do nada, sempre, hoje tal como quando eramos miúdos.

Agradeço ao meu tio Bruno, à minha mãe Anna, aos meus sogros Marcello e Giovanna que me suportaram sempre, como sempre. E agradeço ao meu **pai Renzo**, que mesmo não estando ainda por aqui, sempre olhou por mim, disso tenho a certeza absoluta. Agradeço aos meus adorados filhos Tommaso e Federico pela paciência que tiveram comigo quando estava mais cansada e por me lembrarem, com a alegria deles, o que é verdadeiramente importante na vida.

Finalmente e o mais importante, o meu mais profundo Obrigada vai para o meu Marido **Marco**, sem os seus conselhos, perspicácia, exemplo diário de força e instinto de competitividade, apoio, paciência, e amor incondicional, tudo isto teria sido impossível, mais uma vez.

Caparica, 9 de Setembro de 2019

Elena Surra

Abstract

Maize Cob Waste (MCW) is available in high amounts, as maize is the most produced cereal in the world. MCW is generally left in the fields despite its negligible impact in soil fertility. It can be used as substrate in Anaerobic co-Digestion (AcoD) and as precursor to produce Activated Carbons (ACs). In this context, a biorefinery concept was developed based on two purposes: 1) the pre-treated MCW can be valorised as co-substrate in the AcoD with Organic Fraction of Municipal Solid Wastes (OFMSW), and 2) MCW can be used as a precursor of ACs for biomethane (bioCH_4) conditioning.

The AcoD of OFMSW with chemically pre-treated MCW in presence of H_2O_2 at 23 ºC increased the biogas and CH_4 yields by 65% and 48%, respectively, when compared to AD of standalone OFMSW., providing higher biogas quality and a more stable AcoD process than with non-pre-treated MCW.

Among the ACs produced, the physically MCW(PA)3h AC performed better in H_2S removal than commercial and impregnated by liquid digestate ACs. Textural properties seemed to be more important than the mineral content for H_2S removal and the presence of O_2 on MCW(PA)3h surface may have favoured H_2S catalytic oxidation.

The MCW(PA)3h AC was also the most suitable candidate for CO_2 separation due to its more favourable textural properties, sufficient selectivity and higher working capacity than the others ACs produced. The adsorption equilibrium measurements of CO_2 and CH_4 showed that the Sips isotherm model and the Adsorption Potential Theory (APT) can be confidently employed to correlate the experimental data, as well as the axial dispersed plug-flow and Linear Driving Force (LDF) model is able to correlate the fixed bed experimental data.

The environmental Life Cycle Assessment of a biorefinery case study was performed on the hypothesis of implementing, at an existing Portuguese Anaerobic Digestion plant processing OFMSW, (i) an AcoD unit using MCW as co-substrate; (ii) an H_2S unit using MCW(PA)3h as adsorbent, and (iii) a Pressure Swing Adsorption (PSA) upgrading unit. The cogeneration of the biogas produced during AcoD with non-pre-treated MCW is more sustainable than with pre-treated MCW. The environmental impacts associated with biogas upgrading to bioCH_4 at optimized H_2S adsorption capacity of MCW(PA)3h, if fossil natural gas used for the OFMSW transport is substituted by the produced bioCH_4, decreased significantly, giving lower impacts than cogeneration in five categories.

Keywords: Activated Carbon, Anaerobic Digestion, Biorefinery, Biogas Upgrading to Biomethane, Maize Cob Waste, Pre-treatment

Resumo

O carolo de milho (CM) está disponível em grande quantidade, sendo o milho o cereal mais produzido no mundo. O CM geralmente é deixado no solo como ferilizante, apesar do seu impacto ser negligivél. O CM pode ser valorizado tal como co-substrato no processo de codigestão anaeróbica (co-DA), tal como precursor na produção de carvão ativado (CA). Com base nestas premissas, foi desenvolvido um conceito de bio refinaria, onde o CM é usado para a produção de CA e como co-substrato na co-AD com a Fração Orgânica de Resíduos Sólidos Urbanos (FORSU) para produzir bioCH_4.

A co-DA de FORSU com CM quimicamente pré-tratado na presença de H_2O_2 a 23 ºC aumentou o rendimento de biogás e CH_4 em 65% e 48%, respetivamente, em comparação com a DA de FORSU. O biogás obtido foi de melhor qualidade e o processo de co-DA mais estável do que com CM sem pré-tratamento.

Entre os carvões produzidos, o CA ativado fisicamente MCW (PA)3h teve um desempenho melhor na remoção de H_2S do que o CA comercial e do que os impregnados com digerido líquido. As propriedades texturais pareceram ser mais importantes do que o seu conteúdo mineral para a remoção de H_2S e a presença de O_2 na superfície do CA pode ter favorecido a oxidação catalítica do H_2S.

O carvão ativado MCW (PA)3h foi também o melhor candidato para a separação de CO_2 do biogás, devido às suas propriedades texturais favoráveis, seletividade e capacidade de adsorção. O modelo isotérmico de adsorção de Sips e a Teoria do Potencial de Adsorção (TPA), revelaram-se adequados para correlacionar os dados experimentais de equilíbrio de adsorção. O modelo de fluxo axial disperso e LDF podem ser usados para correlacionar os dados experimentais de rutura em leito-fixo.

A Analise de Ciclo de Vida de uma biorefinaria como caso de estudo foi realizada considerando a hipótese da sua implementação, numa unidade Portuguesa já existente de DA que processa FORSU, de (i) uma unidade co-AD usando CM como co-substrato; (ii) de uma unidade de adsorção de H_2S usando MCW(PA)3h como adsorvente; e (iii) de uma unidade de PSA para condicionar o biogás a bioCH_4. A cogeração do biogás produzido durante a co-DA de FORSU com CM não pré-tratado é mais sustentável do que com CM pré-tratado. Se o gás natural fóssil usado para o transporte de FORSU for substituído pelo bioCH_4 produzido, em condições otimizadas de adsorção de H_2S pelo MCW(PA)3h, os impactos associados ao condicionamento a bioCH_4 diminuíram significativamente, mostrando impactos inferiores à cogeração em 5 categorias de impacto.

Palavras-chave: Carvão ativado, Digestão Anaeróbica, Biorrefinaria, Condicionamento de biogás a bioCH_4, Carolo de Milho, Pré-tratamento

List of Symbols

A, B, C, D	parameters of the Wagner equation
b, b_0, b_∞	parameters of Sips isotherm, 1/bar
C_i	concentration of solids or COD, g/L or mg/O_2/L, and concentration of component i in the gas phase, mol/m^3
C_0	concentration of the inlet gas, ppmv or mol/ m^3
C_t	concentration of the outlet gas at time t, ppmv or mol/ m^3
D_iL	axial dispersion coefficient, m^2/s
D_i	diffusivity coefficient, m^2/s
D_0	parameter
E	adsorption activation energy, KJ/mol
F	gas flow rate, cm^3/min or m^3/s
HRT	hydraulic retention time, d
L	bed length, m
m	mass, g or kg
M_w	molecular weight, mg/mol or g/mol
n, n_0	parameters of Sips isotherm
OLR	organic load rate, g VS/L.d
P	Pressure, bar, Pa
P_c	Critical pressure, bar or Pa

Pe	Peclét number
P_i	partial pressure of component i, bar
P_s	saturation pressure, bar or Pa
q_i	concentration of component *i* in the adsorbed phase, mol/ kg
q_s	concentration of the component *i* at saturation in the adsorbed phase– monolayer coverage, mol/kg
q_{s0}	concentration of the component *i* at saturation in the adsorbed phase at the reference temperature T_0, mol/kg
q_{H2S}	concentration of H_2S in the adsorbed phase, mg/g
q_t	total concentration of component *i* in the adsorbed phase, mol/kg
Q_i	heat of adsorption of component i, J/mol
Q_s, ΔH_i	isosteric heat of adsorption of component i, J/mol
R	universal gas constant, J/mol.K
r_p	mean pore radius, m
R_p	particle radius, m
S_{BET}	BET surface area, m^2
sCOD	soluble chemical oxygen demand, mgO_2/L
T	temperature, K or °C
T	time, s or min or h or days
t_{br}	time breakthrough, s or min
T_c	critical temperature, K
tCOD	total chemical oxygen demand mgO_2/L

TS	total solids, g/L
U	interstitial fluid velocity, m/s
V	volume, m^3 or L (STP)
V_M	molar volume, cm^3/mol
v	superficial fluid velocity, m/s or cm/s
V_b	molar volume of the liquid adsorbate at the normal boiling point, m^3/mol
V_m	adsorbed-phase molar volume, m^3/mol
V_{meso}	mesopore volume, cm^3/g
VS	volatile solids, g/L
V_{total}	total pore volume, cm^3/g
Z_{RA}	Rackett compressibility factor
W	volume of the adsorbed phase, cm^3/g
W_s, V_{micro}	micropore volume, cm^3/g
x_i	mole fraction of component i in the adsorbed-phase
y_i	mole fraction of component i

Greek Symbols

$\eta_i\ removal$	removal efficiencies of VS, TS, tCOD, and sCOD, % w/w
η_α	biogas or methane efficiency production, g VS/d
ϕ	adsorption potential, bar m^2/mol

β	affinity coefficient
χ, α	parameter of Sips isotherm
$\alpha\ removal$	lignin, hemicellulose, cellulose removals, % w/w
γ	parameters of D-A equation
ε	total voidage
ε_b	interparticle porosity or (external) void fraction of packing
ε_p	intraparticle porosity
θ	fractional loading (q/q_s)
ρ_b	bulk density, kg/m
ρ_p	particle density, kg/m
ρ_s	carbon matrix density, kg/m
τ	tortuosity factor
Ω	thermal expansion coefficient, 1/K

Subscripts

b	normal boiling point
c	critical conditions
ex	excess adsorption
i	component i
s	saturated conditions

Table of Contents

List of Figures

List of Tables

1

Introduction

The management of bio-wastes has become a critical issue in terms of global warming and contamination of natural resources.

Anaerobic Digestion (AD) offers the opportunity to produce biogas from organic waste (Liu et al., 2015). Biogas can be upgraded to a higher methane content (>97% v/v), so that it can resemble the quality of natural gas (NG). The biomethane (bioCH_4) produced is then suitable for grid injection, or to be used as transportation fuel, thus being economically more profitable than the direct biogas combustion. Also, it can contribute to satisfy the increasing demand of renewable fuels (EBA, 2015).

Two types of wastes are quite suitable to AD: they are the Organic Fraction of Municipal Solid Waste (OFMSW) and Maize Cob Waste (MCW).

OFMSW is produced worldwide in high amounts. Assuming that about 40% of municipal waste is bio-waste, in 2017 were produced in Europe approximately 195 kg/per capita, with an estimated total amount of 140 million tons per year of OFMSW (Eurostat, 2019).

Maize is one of the most important crops worldwide with a total production, in 2018, of around 1060 million tons (IGC - International Grain Council, 2018). For 1 kg of dry corn grains, about 150 g cobs are generated (Zhang et al., 2012), which resulted by the end of 2018, in approximately 159 million tons of corn cobs.

Maize generates residual stover (leaves, stalks and maize cob) that are usually left in the field as natural fertilizers (J Zheng et al., 2014). Unlike to stover,

standalone Maize Cob Waste (MCW), due to its low biodegradability, has a negligible impact on soil carbon content and its removal can increase the maize yield (Jeschke and Heggenstaller, 2012).

MCW is sometimes harvested as feedstock for full-scale production of ethanol and xylitol (Wang et al., 2012a), furfural (Li et al., 2014a) and activated carbon (Hou et al., 2013). However, the potentially available MCW worldwide exceeds the current industry and market capacities to process it (Gu et al., 2014).

The OFMSW is enriched in proteins and lipids and is poor in carbohydrates. Its anaerobic biodegradation is not well balanced, and the lack of carbohydrates can lead to ammonia accumulation that is detrimental for methanogenesis. The use of MCW as co-substrate can balance the C:N ratio towards the optimal range, stabilizing AD process and enhancing biogas yield (Lapa et al., 2017).

Currently, most of the European biogas plants that process maize residues, use as co-substrate maize silage that is composed by all the maize plant (leaves, stalks and corn). The silage is produced as an energy crop that affects negatively the availability of arable lands for food production. When MCW is harvested separately from grains, it can be used as carbon source in an Anaerobic co-Digestion (AcoD) process without any significant impact on feed or food chains.

MCW, as a lignocellulosic biomass, is mainly composed of cellulose, hemicellulose and lignin, that are embedded together in a complex matrix (Menon and Rao, 2012). Cellulose and hemicellulose are polysaccharides fermentable after hydrolysis, while lignin, a complex aromatic and hydrophobic amorphous heteropolymer that acts as cement for the cross-linking between cellulose and hemicellulose, cannot be degraded during anaerobic digestion (Palmqvist and Hahn-Hägerdal, 2000). Lignin hinders the digestion of the polysaccharides, reducing the biogas yield (Liu et al., 2015;Xu et al., 2014a). Thus, to use MCW as substrate for AcoD, lignin must be preferentially removed to expose cellulose fibers and hemicellulose to bacteria attack. The selection of a proper pre-treatment and its optimization are crucial for the viability of a AcoD process (Budzianowski and Budzianowska, 2015).

Biogas is composed by 60-70% v/v of CH_4 and 30-40% v/v of CO_2. Other compounds can be present in biogas some of them regarded as contaminants such as H_2O (5-10%), H_2S (0.005- 2%), halogenated hydrocarbons (VOC) (< 0.6%), NH_3 (<1%), O_2 (0-1%), CO (<0.6%), N_2 (0-2%) and siloxanes (0-0.02%) that can be detrimental in several applications if not removed (Ryckebosch et al., 2011). The biogas upgrading to bioCH_4 aims to increase CH_4 content in the biogas stream

by separating CO_2 and trace contaminants, thus enabling its injection in natural gas (NG) networks or use as biofuels after proper conditioning (Scarlat et al., 2018).

There are several commercial technologies available for removing CO_2 from biogas streams, being the most employed ones scrubbing with water or other physical solvent, chemical scrubbing, membranes permeation and adsorption-based processes, such as Pressure Swing Adsorption (PSA)(Grande, 2011).

Among them, PSA is attracting increasing interest for its low energy requirements and limited initial capital investment in comparison with other separation technologies (Ruthven et al., 1994 and Bauer et al., 2013). Moreover, PSA can process high throughputs and produce high-purity CH_4 (Esteves and Mota, 2007).

In a PSA unit for biogas upgrading, an adsorbent is subjected to pressure changes to selectively adsorb and desorb CO_2. The efficiency of adsorption of CO_2 depends, among other factors, specifically on (i) the textural properties, (ii) on the working capacity, (iii) on the CO_2 selectivity and on (iv) the capability of the adsorbent material to be regenerated. Thus, the choice of the adsorbent plays a crucial role in the PSA process efficiency.

This work is part of the Bio-FESS European research project (ERANET-LAC, Ref. ELAC2014/BEE0367), that is developed by a consortium composed by different European (German and Portuguese) and Latin-America (Colombian and Mexican) partners. It aims to study the feasibility of a biorefinery concept able to valorise low-cost materials, such as MCWs, to produce activated carbons (ACs) that can be used either to pre-condition and to upgrade biogas to bioCH_4 or, at least, to be employed for other applications with higher added value (supercapacitors).

The contribution of this work to Bio-FESS Project is illustrated in Figure 1.1 and includes the following Tasks:

- **Task 1:** Literature review. This Task provides a bibliographical review of all the processes involved in the proposed bio-refinery (Figure 1.1). It comes across (i) the possible pre-treatments for MCW prior to AcoD; (ii) the AcoD process using MCW as co-substrate; (iii) the production of ACs, using MCW and liquid digestate as precursors, for the conditioning and upgrading of biogas to bioCH_4, and (iv) an overview on biogas upgrading technologies.

Task 1 provided the basis for the work plan adopted in the following Tasks 2, 3, 4 and 5. The results of Task 1 are reported in Chapter 2. The outputs of the Task 1 were the peer-reviewed publications:

- Elena Surra, Maria Bernardo, Nuno Lapa, Isabel A.A.C. Esteves, Isabel Fonseca, José P.B. Mota, Biomethane Production through Anaerobic co-Digestion with Maize Cob Waste Based on a Biorefinery Concept: A Review, Journal of Environmental Management, 249 (2019) 109351, 21 pp., DOI: 10.1016/j.jenvman.2019.109351

- N. Lapa, E. Surra, I.A.A.C. Esteves, R.P.P.L Ribeiro, J.P.B. Mota, Production of Biogas and BioH_2 – Biochemical Methods, Chapter 15 in Biofuels Production and Processing Technology, Eds. M.R. Riazi, David Chiaramonti, CRC Press/Taylor & Francis, Boca Raton (USA), October 11th 2017, 690 Pages, ISBN 9781498778930, eBook ISBN: 9781498778947, https://doi.org/10.1201/9781315155067. Book chapter (review) written by invitation

- **Task 2**: Development of a lab-scale AcoD process using the MCWs as co-substrate for OFMSW. Selection of the optimal MCWs pre-treatments for optimization of the AcoD process towards the maximization of biogas production was made. The AcoD operating conditions applied at laboratorial scale were those employed at an industrial biogas plant, located in Lisbon surroundings, Portugal. The results of Task 1 are reported in Chapter 3. The outputs of the Task 2 were the publications:

  - Elena Surra, Maria Bernardo, Nuno Lapa, Isabel Esteves, Isabel Fonseca, José Paulo Mota., 2018. Maize cob waste pre-treatments to enhance biogas production through co-anaerobic digestion with OFMSW. Waste Manag. 72, 193–205 DOI: 10.1016/j.wasman.2017.11.004

  - Elena Surra, Maria Bernardo, Nuno Lapa, Isabel A.A.C. Esteves, Isabel Fonseca, José Paulo Mota, 2018. Enhanced biogas production through anaerobic co-digestion of OFMSW with maize cob waste pre-treated with hydrogen peroxide. Chem. Eng. Trans. 65, 121-126, DOI: 10.3303/CET1865021

- **Task 3:** Production, screening and testing of different activated carbons (ACs) using MCW and Liquid Digestate (LD), the liquid fraction produced during anaerobic digestion, as precursors. The produced ACs were developed both for H_2S removal during pre-conditioning of biogas and for consecutive biogas upgrading to bioCH_4 in a CO_2 adsorption unit.

- **Task 4:** Assessment of H_2S removal capacity from a real biogas stream using the ACs produced during previous Task 3. The results of Tasks 3 and 4 are reported in Chapter 4. The output of Tasks 3 and 4 was the publication:

  - Elena Surra, Miguel Costa Nogueira, Maria Bernardo, Nuno Lapa, Isabel Esteves, Isabel Fonseca, 2019. New adsorbents from maize cob wastes and anaerobic digestate for H2S removal from biogas. Waste Manag. 94, 136–145, DOI: 10.1016/j.wasman.2019.05.048

- **Task 5:** Adsorption equilibrium studies of the main biogas components onto selected ACs produced and tested in the previous Tasks 3 and 4, and study of the kinetics of the adsorption process. This Task provided the basis for future design and modelling works of a PSA cycle built on the use of renewable carbon adsorbents produced from MCW. The results of Task 5 are reported in Chapter 5. A publication with the results obtained in Task 5 is expected as an output and is being prepared.
- **Task 6**: Life Cycle Assessment (LCA) of the proposed biorefinery (Figure 1.1), on the hypothesis of implementing a biogas pre-conditioning and upgrading unit in an existing biogas plant located in Lisbon, Portugal. This plant is currently processing 40000 ton/year of OFMSW. The biogas upgrading unit was hypothesized utilizing as the most suitable configuration among the AD and AcoD tested during Task 2. The biogas pre-conditioning step was developed on the basis of the results of Task 3 and 4, and on the literature data available for the removal of other contaminants different from H_2S. The development of the upgrading unit was also based on the available literature, since the experimental and modelling works developed in herein were still in an early stage to be used as basis for the development of a complete PSA cycle for CO_2 separation. The results of Task 6 are reported in Chapter 6. It is expected that a publication with the results of Task 6 arises as an outcome of this work.

In summary, the work developed has the global aim to provide a comprehensive study of a biorefinery concept based on the valorisation of maize cob that is currently under valorised when looking to its enormous potential. The use of MCW as co-substrate for AcoD can contribute positively to a highly integrated management of maize crops, thus reducing negative environmental impacts currently associated with the maize silage energy crops. Moreover, the use

of MCW to produce ACs for biogas conditioning and upgrading to bioCH_4 allows to integrate and close the cycle of the proposed biorefinery, with the additional development of high added-value sub-products like the activated carbons.

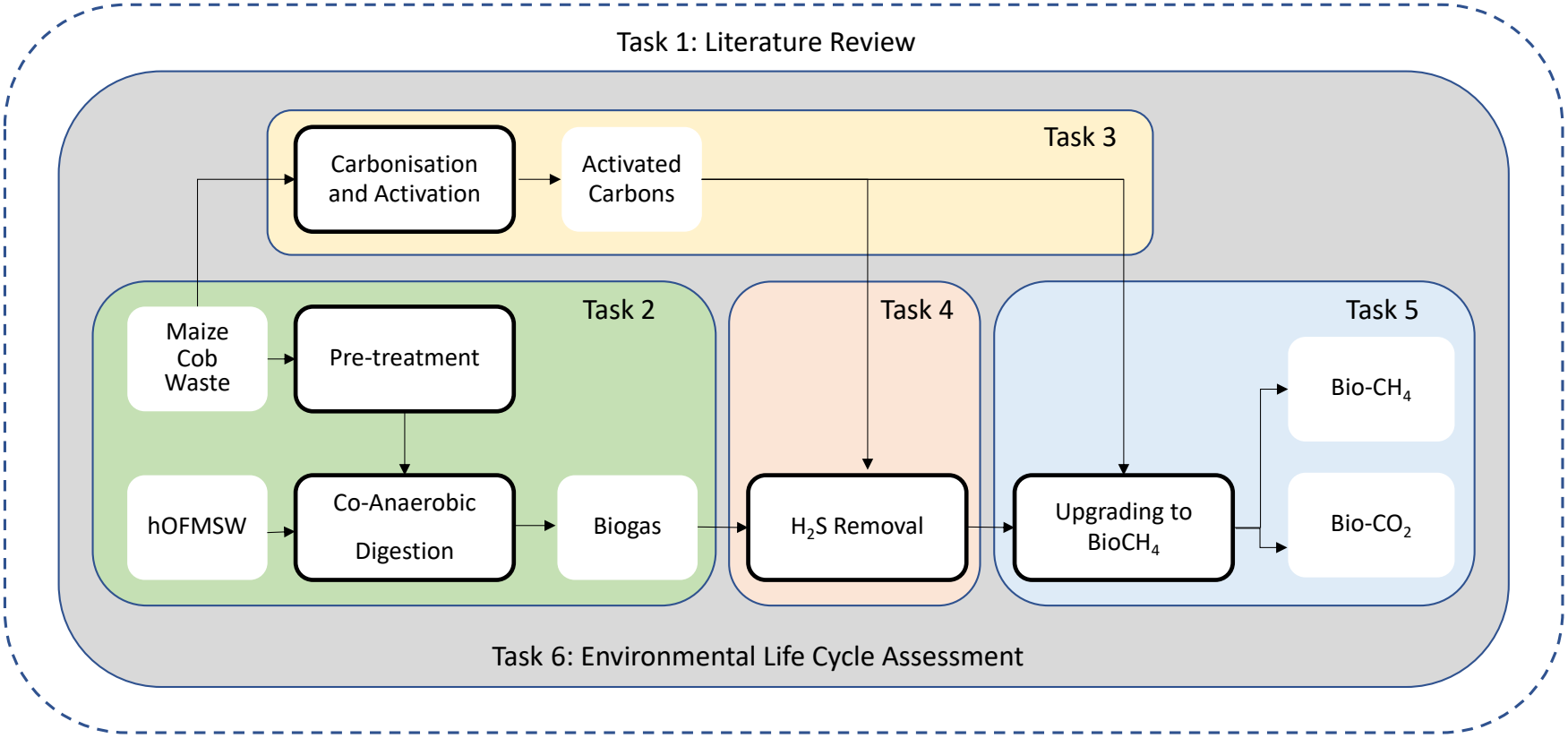

Figure 1.1: Diagram of the bio-refinery proposed in the present work.

2

Literature Review

2.1 Introduction

This Section represents the development of the **Task 1** of this work.

2.2 Pre-Treatments of MCW

MCW is a complex lignocellulosic material composed of cellulose (32-46% wt db), hemicellulose (30-44% wt db), lignin (6-22% wt db), and other trace components (ash, protein, waxes, and sucrose) (Menon and Rao, 2012; Su et al., 2015; Torre et al., 2008). Cellulose, lignin and hemicellulose are linked together by covalent bounds, intermolecular bridges, and van der Waals forces, forming a complex structure. MCW is therefore resistant to biological degradation (Ayeni and Daramola, 2017).

In order to improve the biodegradability of MCW during AcoD, this biomass must be submitted to a proper pre-treatment. The pre-treatment efficiency depends on its ability to deconstruct the lignocellulosic biomass without generating inhibitors to the anaerobic consortia, such as furfurals, hydroxymethilfurfural (HMF), phenolic compounds and carboxylic acids, in concentrations that are toxic for the bacteria involved in anaerobic digestion (Mao et al., 2015). This objective is achievable if lignin is removed and cellulose and hemicellulose structure are weakened enough to offer accessible specific surface area to bacteria degradation (Bernstad et al., 2013; Esposito et al., 2011). Several pre-treatments have been studied at lab-scale for the pre-hydrolysis of MCW: mechanical (S. S. Sun et al., 2015), thermal and thermo-chemical (Diaz et al., 2015; Jun Zheng et al., 2014), chemical (Ayeni and Daramola, 2017; Idrees et al., 2014; Li et al., 2010), biochemical and biological (ensiling, aeration, enzymatic digestion, fungi and

microbial consortium degradation) (Carrere et al., 2016). To date, the biological pre-treatments are the only ones used in industry for biogas production from lignocellulosic biomasses (Carrere et al., 2016).

2.2.1 Mechanical Pre-Treatment: Size Reduction

MCW needs an initial mechanical size reduction in order to increase the surface area exposed to pre-treatment (Kratky and Jirout, 2011).

For biogas production, the mechanical size reduction of MCW is preferentially performed by chipping, grinding, and/or milling techniques, rather than by extrusion techniques, due to its hard structure and high average moisture content (Bhutto et al., 2017; Taherzadeh and Karimi, 2008). Chipping allows obtaining particle sizes of 10-30 mm, while grinding and milling can reduce the particle size up to 0.2 mm (Kumar and Sharma, 2017).

To authors' knowledge, no data are available regarding the optimal particle size of MCW before AD. Herrman and co-workers (Herrmann et al., 2012) worked over corn stover and observed a maximum increase in methane yield of 11-13% with a particle size ranging between 6-33 mm. Although this is a different type of biomass from MCW that may require a different pre-treatment process, it was the closest one that was found in literature.

Regarding other types of biomass materials, biogas production from agricultural and forest residues increases with the decrease of particle size from 0.088 to 30 mm (Sharma et al., 1988). However, Izumi et al. (2010) reported that an excessive biomass comminution may decrease biogas yield, due to the excessive production of Volatile Fatty Acids (VFAs).

Although some studies suggest that it is better to disrupt or shred the lignocellulosic structure rather than to cut it (Taricska et al., 2009), an initial size reduction of about 0.1 to 1 cm (Chongkhong and Tongurai, 2014; Jun Zheng et al., 2014) seems to be an important step before submitting MCW to AD. It must be noted that milling do not produce any inhibitors for AD (Kumar and Sharma, 2017).

2.2.2 Thermal and Thermo-Chemical Pre-treatments

2.2.2.1 Conventional Thermal Route

Thermal pre-treatments are energy demanding processes that can be divided into low temperature (<100 °C) and high temperature (>100 °C) treatments; the latter group is also known as thermal hydrolysis (Nazari et al., 2017). Thermal

pre-treatments performed at low temperatures do not degrade complex molecules, such as carbohydrates, but simply induce the de-flocculation of macromolecules (Prorot et al., 2011). At temperatures higher than 150–180 ºC, hemicellulose starts to solubilize almost at the same time of lignin. In the case of high temperature pre-treatments, the production of compounds with inhibitory effects to the anaerobic consortia is expected (Hendriks and Zeeman, 2009).

Thermal pre-treatments can be carried out in autoclaves, traditional ovens or microwave ovens, and in the presence or absence of a catalyst. At high temperatures and pressures, water can behave as a solvent, catalyst or reactant, originating a set of pre-treatments named as hydrothermal pre-treatments (Patel et al., 2016).

The pre-treatment of MCW at temperatures exceeding 150–180 ºC solubilize lignin and hemicellulose, generating AD inhibitors (Guo et al., 2014), such as heterocyclic compounds like furfural and hydroxyl methyl furfural (HMF) (hemicellulose-derived substances), and phenolic compounds (lignin-derived substances) that may have an inhibitory or toxic effect on the anaerobic consortia (Hendriks and Zeeman, 2009).

Few studies were found on the effect of thermal pre-treatments on maize residues used as feedstock materials for biogas production, and no studies were identified on MCW. Menardo et al. (2012) did not find any enhancement on methane yield after the thermal pre-treatment (90 – 120 ºC for 30 minutes) of maize stalk autoclaved with water for 30 minutes. In contrast, Bondesson et al. (2013), tested the biogas production after a steam pre-treatment (210 ºC for 10 minutes) of corn stover, with and without the addition of diluted H_2SO_4 (0.2% w/w), and found higher methane yields with a biomass pre-treatment with steam and diluted acid, than with a standalone steam pre-treatment. This was probably due to the higher concentrations of furfural, HMF, and formic and acetic acids in the biomass only pre-treated with steam.

2.2.2.2 Steam Explosion

Steam explosion (SE) has been demonstrated to be an efficient biomass pre-treatment method prior to AD (Biswas et al., 2015). During SE, biomass is heated up with high-pressure steam (0.7–5.0 MPa) at a temperature ranging from 180 ºC to 260 ºC for a short period of time (from several seconds to minutes). Suddenly, a quick depressurization is performed, causing biomass defibration and fibres disruption (Chornet and Overend, 1991) and promoting the degradation of hemicellulose and sometimes lignin (Carrere et al., 2016). Acetyl groups produced from the xylan present in hemicellulose turn into acetic acid, catalysing

the chemical reaction known as auto-hydrolysis (Rabemanolontsoa and Saka, 2015). Water at high temperature and pressure can act as well as an acid catalyst.

SE is affected by the following variables: particle size, temperature, residence time, moisture content and combined effect of temperature and time (Maurya et al., 2015; Y. Zheng et al., 2014). Concerning the biomass particle size, its reduction favours the effectiveness of the mechanical and chemical effects provided by SE, due to an effective pressure distribution within the lignocellulosic polymers, although it may consume at least one-third of the power requirement for the entire process (Maurya et al., 2015).

Due to the high temperature used in SE, phenolic compounds (from lignin and furfural) and HMF (from hemicellulose) are produced; thus, SE conditions must be accurately selected. J. Zheng et al. (2014) reported that SE pre-treatments catalysed by diluted acids or alkalis (0.5–5.0% w/w) result in more complete solubilization of hemicellulose, decreasing the production of inhibitory compounds. However, catalysts such as H_2SO_4 or SO_2 also raise issues related to pH adjustments, production of H_2S and sulphate, and increase of process costs (Yang and Wyman, 2008). X. Zhang et al. (2017) observed that acid-catalysed SE can remove hemicellulose from MCW, causing the enrichment of solid residues in lignin that inhibits the hydrolysis.

Only few studies were found on biogas production from SE pre-treated maize wastes. All of them were carried out on maize stover rather than on MCW. For example, J. Li et al. (2015) observed an increase of 64% in methane yield produced from SE pre-treated corn stover (1.2 MPa, 10 minutes, 90% moisture content), during 28 days of mesophilic AD. An increase of 80% in methane yield was observed in the presence of 1.5% KOH.

To authors' knowledge, no full-scale application of SE pre-treatment prior to AD has been reported up to now, mainly due to its complexity and several drawbacks associated to this pre-treatment.

2.2.2.3 Microwave Irradiation

As a non-conventional heating source, microwave irradiation (MWI) heats MCW uniformly, quickly and avoid large temperature gradients, limiting the formation of inhibitors (H. Li et al., 2014; Li et al., 2016). MWI can be carried out either at atmospheric pressure or high pressure. The latter allows lower reaction temperatures and higher hydrolysis ratio (Tong and Yao, 2009) than the former (Li et al., 2016).

Deconstruction of lignocellulosic biomass and sugar release from maize cob are enhanced if the MWI pre-treatment is catalysed by alkalis, acids, or High Boiling Solvents (HBS). Some attempts with promising results were recently performed on corn stover in the absence of catalyst (Aguilar-Reynosa et al., 2017); in this study, it was observed that hemicellulose removal by MWI is higher than by traditional conduction-convection methods.

The available literature agrees that MWI affects the maize cob morphology, producing an increase of its crystallinity index (Diaz et al., 2015; Odhner et al., 2012). Most of the pre-treatments performed on maize cob using MWI are targeted to the bioethanol production (Aguilar-Reynosa et al., 2017), or to the generation of fermentable sugars (Tong and Yao, 2009) rather than for biogas production. All these works agree in the fact that MWI promotes efficiently the hydrolysis of maize cob. Boonsombuti and Luengnaruemitchai (2013) obtained more than 60% of lignin removal and approximately 38% increase of available surface area by using MWI catalysed by 2% w/v NaOH at 100 ºC, for 30 minutes, after enzymatic hydrolysis. Chen et al. (2013) obtained 65% lignin solubilisation by applying MWI to maize stover catalysed by NaOH (NaOH/corn stover ratio = 0.077 w/w), at 95 ºC, for 30 minutes. In contrast, Surra et al. (2018a) observed that MWI of maize cob, for 10 minutes, at 160 ºC and catalysed by NaOH in concentrations between 2-20% NaOH/MCW (w/w), did not produce any delignification, nor cellulose solubilisation. Only moderate hemicellulose removal was obtained. The difference between these studies may be related with the residence time; Surra et al. (2018a) have used a residence time of 10 min, three times lower than the residence time applied by Chen et al. (2013), and Boonsombuti and Luengnaruemitchai (2013) (30 min for both studies), suggesting that MWI time plays a key role in biomass depolymerisation. Similar results were obtained by Zhu et al. (2005) that combined MWI and alkali method to pre-treat a different lignocellulosic biomass (rice straw); the content of cellulose (glucan) increased, while the content of hemicellulose (xylan) and lignin decreased, when MWI time increased from 15 to 70 min, at 300 W.

It must be noticed that MWI catalysed by NaOH in concentrations higher than 6% NaOH/MCW (w/w) is able to produce phenolic compounds in concentrations that are detrimental to methanogens (Surra et al., 2018a), namely in what concerns the threshold-limit for *p*-coumaric acid (50 mg/L)(Akassou et al., 2010). Additionally, Aguilar-Reynosa et al. (2017) suggest that the concentration of catalyst is crucial to limit the production of furfural.

The use of acids as catalysts during MWI was investigated by Chongkhong and Tongurai (2014). The authors tested MWI catalysed by acetic acid on maize

cob to convert the hemicelluloses into soluble sugars in a short reaction time. A significant glucose concentration of 84.2 g/L was obtained at a MCW/acetic acid (0.5 M) ratio of 0.40:1, under 900 W of microwave power, for 10 minutes. Similarly, Tong and Yao (2009) found that coupling MWI with H_2SO_4 (10 g/L) to treat maize stover at 190 ºC, with a reaction time of 3 min and Liquid/Solid (L/S) ratio of 20 L/kg, resulted in a sugar yield of 44.6%.

HBS such as 1,4-butanediol and glycerol are used in MWI of biomass, due to their high-boiling points at atmospheric pressure and their ability to remain in liquid state at high temperatures. MWI catalysed by HBS can break the bonds within the biomass; lignin is dissolved and HBS can be recovered and recycled (Li et al., 2016). Diaz et al. (2015) reported delignification percentages of 29.5% and 22.6% after having immersed maize straw in aqueous glycerol (95% v/v) and alkaline glycerol solution (95% v/v glycerol-NaOH 1.4 M), respectively, for 16 h, before MWI. However, these results are contradictory with those obtained by Surra et al. (2018a) where lignin or cellulose removals were not found with direct MWI catalysed by glycerol, either in the presence or absence of alkaline water. It seems that the residence time of the chemical pre-treatment before MWI, may be more effective for lignin solubilisation than MWI itself.

Another way to use MWI is to couple it with steam explosion that deconstructs the lignocellulosic biomass more efficiently (Beszédes et al., 2009). Pang et al. (2012) registered a sugar yield of 72.1% and obtained a decrease on the crystallinity index of maize stover pre-treated with a combination of SE-MWI.

Based on this review and on a previous work carried out by Surra et al. (2018a), it seems that MWI is not a key technology for maize cob pre-treatment; it is an expensive technology and must be coupled with other catalysts to efficiently degrade the lignocellulosic structure.

2.2.3 Chemical Pre-treatments

2.2.3.1 Alkalis and Acids

Among the chemical methods, alkali pre-treatment is the preferred one and the most studied for AD, as anaerobic bioconversions can support slightly alkaline environments. The most common alkalis are, by decreasing order of efficiency, NaOH > KOH > $Mg(OH)_2$ > $Ca(OH)_2$ (Chandra et al., 2012). Compared with NaOH and $Ca(OH)_2$, KOH has not been widely used (Alqaralleh, 2012).

Few studies were found about alkali pre-treatments on maize wastes prior to biogas production. Zhu et al. (2010) compared different NaOH loadings (1, 2.5,

5.0, and 7.5% w/w) to treat maize stover during 24 h, before submitting it to AD under mesophilic conditions for 40 days. These authors have used an effluent of AD as inoculum and added nitrogen as supplying nutrient. NaOH loading of 1% w/w did not cause significant improvement on biogas yield. The highest biogas yield of 372 L/kg VS was obtained for the corn stover pre-treated with 5% v/v NaOH, which was 37% higher than that of the untreated sample. They also observed that the inhibition of methanogens occurred with 7.5% w/w NaOH. This evidence was confirmed by Calabrò et al. (2015) who found that methanogenesis slows down in the presence of high NaOH dosage used in the pre-treatment of tomato processing wastes.

It must be noticed that according to Zhu et al. (2010), NaOH treatment of maize stover did not improve significantly the biogas production. But, according to Zheng et al. (2009), the total biogas production and methane yield were increased by 72.9% and 73.4%, respectively, when maize stover pre-treated with 2% w/w NaOH, at 20°C, for 3 days and with a moisture content of 88% w/w, was submitted to mesophilic AD.

The use of NaOH pre-treatment may cause Na^+ inhibition of the AD process, especially during methanogenesis, because sodium ion is a well-known AD inhibitor. Additionally, the digestate disposal rich in Na^+ could lead to negative environmental impacts, such as soil and water salinization (Y. Zheng et al., 2014).

Studies on sugar recovery improvement have demonstrated that a sequential acid–alkali pre-treatment on maize stover is able to minimize acetic acid, furfural and HMF production (Lee et al., 2015). The idea of gathering sequentially acidic and alkaline pre-treatments to mitigate the generation of AD inhibitors can open a new window of research to minimise inhibitors formation. Otherwise, the high investment, operation and management costs, as well as operational difficulties and environmental impacts, reduce the potential use of acids and alkalis in the pre-treatment of MCW at an industrial-scale (Modenbach and Nokes, 2013).

2.2.3.2 Oxidative Pre-treatments

Oxidative pre-treatments use peroxides or ozone as catalysts. Peroxides are widely used to enhance the biological conversion of lignocellulosic biomass into bioethanol, whereas only few attempts were done with these catalysts for biogas production (Shahriari et al., 2013; Surra et al., 2018b). The most used peroxide compound is H_2O_2 followed by peracetic acid, dimethyldioxirane, and peroxy monosulphate.

The potential of peroxides lies in their ability to be transformed into hydroxyl radicals, which are more powerful than peroxides themselves to remove lignin and enhance biomass degradability during AD. The treatments with peroxides are non-selective oxidation processes that may cause losses on digestible sugars (Y. Zheng et al., 2014). H_2O_2 requires an alkaline pH (usually 11.5) to produce the oxidizing radicals needed to degrade lignin. However, recent studies demonstrated that pH values as lower as 9.8 can be enough to support an suitable MCW depolymerization for AcoD (Surra et al., 2018b). In this chemical context, this type of pre-treatment is known as Alkaline Hydrogen Peroxide (AHP) pre-treatment.

During an AHP pre-treatment, the reaction time strongly affects lignin removal (Banerjee et al., 2011; Saha and Cotta, 2007). This result was confirmed by Surra et al. (2018a), who tested the pre-treatment of MCW with AHP under a H_2O_2/MCW ratio of 0.5 w/w, pH of 9.8, and MCW mass of 10% w/v. The solubilization percentage of lignin with a reaction time of 3 days was 90% and 50% higher than those obtained with 4 hours and 1 day, respectively.

Literature presents contradictory results on the effect of temperature in an AHP pre-treatment. Selig et al. (2009) and Su et al. (2015) showed that sugar yields from maize stems and maize stover increase with temperature. On the contrary, Karagöz et al. (2012) obtained higher yields with rapeseed straw at 50 ºC than at 70 ºC, due to H_2O_2 decomposition at higher temperatures. Oxidizing pre-treatment catalysed by H_2O_2 at 100 ºC, for 10 minutes, with microwave heating did not promote any significant improvements concerning sugar solubilization, when compared to the pre-treatments carried out at room temperature under the same conditions (Surra et al., 2018a, 2018b). Two important factors that affect AHP pre-treatment efficiency are the concentration of solids and H_2O_2 loading.

Tables 2.1 and 2.2 summarize some of the studies of AHP pre-treatments applied on maize wastes. Studies focusing on MCW are very few.

Gould (1984) demonstrated that H_2O_2 can be used as a delignifying agent for maize stover. Approximately, 50% of the lignin in a 2% w/v solution of maize stover can be removed with 1% solution of H_2O_2 (0.5 g H_2O_2/g biomass) at an initial pH of 11.5.

Banerjee et al. (2011) tested different H_2O_2/biomass ratios (0.125, 0.25 and 0.5 g/g) at a biomass concentration of 10%. These authors found a higher glucose conversion yield (95%) with the biomass pre-treated at 0.5 g H_2O_2/g biomass.

Table 2.1: Summary on AHP studies before enzymatic saccharification

Substrate	H_2O_2 load	Biomass load	t	T	Glucose conversion[1]	Initial pH	Reference
	$w_{H_2O_2}/w_{MCW}$	% (v_{H_2O}) MCW	h	ºC	% w/w		
Crop residues [2]	0.50	2.00	4	Ambient	95.0%	11.5	(Gould, 1984)
	0.50	10.0	24	23	95.0%	11.5	(Banerjee et al., 2011)
Maize Stover	0.25	10.0	24	23	83.0%	11.5	(Banerjee et al., 2011)
	0.125	10.0	24		55.0%	Adjustment every 6 h	
	0.125	15.0	48		75.0%	Adjustment required	(Banerjee et al., 2012)
Substrate	H_2O_2 load	Biomass load	t	T	Glucose solubilisation	Lignin solubilisation	Reference
	$w_{H_2O_2}/w_{mcw}$	% MCW/v_{H_2O}	h	ºC	% w/w	mg/L	
Maize Cob	1.00	5.00	0.50	120	72.0%	39.0	(Ayeni and Daramola, 2017)

[1] After enzymatic hydrolysis; [2] Corn stalks, corn husk, wheat straw and kenaf

Table 2.2: Summary on AHP studies for biogas production

Substrate	H_2O_2 load	Biomass load	t	T	Lignin solubilisation	Glucose [1]	AD conditions	AD yield	Refer-ence
	$w_{H_2O_2}/w_{MCW}$	% (v_{H_2O}) MCW	h	ºC	% w/w			mL CH_4/g VS	
Maize Cob	0.50	2.00	4	23	0.00	148	Thermophilic, 30 d	480	(Surra et al., 2018a)
	0.50	10.0	72		68.6	928		500	
	0.50	10.0	4		5.00	653		550	
Corn Straw	3.00	33.0	168	25	6-32		Mesophilic, 35 d	Up to 217	(Song et al., 2014)

[1] Glucose solubilisation in the liquid phase after pre-treatment

The same authors obtained a glucose conversion yield of 75% when the pre-treatment reaction time was extended up to 48 hours, using 15% of solid concentrations and 0.125 g H_2O_2/g biomass (Banerjee et al., 2012).

Song et al. (2014) tested the effect of seven different chemicals on maize straw for biogas production (Table 2.2). The comparison between H_2O_2, H_2SO_4, HCl, CH_3COOH, NaOH, $Ca(OH)_2$ and NH_3H_2O, show that maize straw pre-treated with 3% H_2O_2 w/w gives the highest methane yield when compared with other catalysts (115.4% higher than that of the untreated straw).

In a recent study performed by Surra et al. (2018b), the pre-treatments on MCW were catalysed by H_2O_2 at room temperature, different H_2O_2/biomass ratios (0.125, 0.250, 0.5 and 1.0), different pH values (9.8 and 11.5) and different reaction times (4 hours; 1, 2 and 3 days). The hydrolysed materials were used in AcoD assays with the Organic Fraction of Municipal Solid Wastes (OFMSW). This study showed that the highest lignin and glucose solubilizations (68.6% w/w and 928 mg/L, respectively) were achieved at room temperature in the pre-treatment with a H_2O_2/MCW ratio of 0.5 w/w, pH 9.8, 10% w/v MCW concentration and a reaction time of 3 days. The AcoD of pre-treated MCW under this condition produced a methane yield of 500 mL/g VS, that was slightly lower than that obtained at the same H_2O_2 load, pH and solid concentration, but with 4 hours of reaction time (550 mL/g VS). This was probably due to the higher concentrations of inhibitors produced in the assays with a longer reaction time (3 days).

It must be noticed that a concentration of H_2O_2 higher than 4% w/w can inhibit the AD process, due to the toxic effect of excessive hydroxyl ions to methanogens (Song et al., 2014).

To date, H_2O_2 can be considered as one the most favourable catalysts for improving the methane yield on lignocellulosic biomass, due to its effectiveness and relatively low cost. The work of Banerjee et al. (2012) highlighted that AHP is a readily scalable technology, due to its simplicity and low capital costs. Moreover, Song et al. (2014) performed a comparison between different pre-treatment methods on corn straw, demonstrating that H_2O_2 pre-treatment was one of the most favourable, due to both good economic performance and higher methane yields that promoted in AD.

2.2.3.3 Ionic Liquids

Ionic liquids (ILs) are molten salts at room temperature, characterized for being strong solvents with high polarity, great thermal stability and negligible volatility (Q. Zhang et al., 2017). They are constituted solely by a large asymmetric organic cation and a polyatomic organic or inorganic counterion (Luo et al., 2013). Due to immeasurable combinations of cations and anions that can form ILs, they are often called designer solvents (da Costa Lopes et al., 2013).

ILs have been proven to be highly effective in the dissolution of cellulose, lignin, and hemicellulose over different types of biomass materials, including maize cob and maize stover (Luo et al., 2013). Carbohydrates and lignin can be simultaneously dissolved, due to the activity of phosphate or chloride anions present in ILs (Li et al., 2010). The non-hydrated chloride ions of ILs can form hydrogen bonds with the hydroxyl protons of sugars of lignocellulosic biomass, disrupting the complex non-covalent bonds that inter-link cellulose, hemicellulose, and lignin, with minimal generation of degradation products (Alvira et al., 2010). ILs are 100% recoverable to their initial purity and leave minimum residues for the downstream AD process (Heinze et al., 2005), although the residual solution can become viscous and difficult to handle after several extraction cycles (Li et al., 2010).

Among the published works dealing with the use of ILs to pre-treat biomass for biogas production, N-methylmorpholine-N-oxide monohydrate (NMMO) has been the most frequently used (Aslanzadeh et al., 2014; Kabir et al., 2015; Mancini et al., 2016; Y. Zheng et al., 2014). However, the efficiency of this compound in the pre-treatment of maize wastes before AD is not clear.

Papa et al. (2015) studied the efficiency of a mild ionic liquid (1-ethyl-3-methylimidazolium acetate [C2C1Im][OAc]) on maize stover before AD. The authors observed that the use of this compound, at 100 ºC, for 3 hours, did not affect methane production from maize stover. These results contrast with those of Gao et al. (2013) which showed that the pre-treatment of water hyacinth with 1-N-butyl-3-methyimidazolium chloride ([Bmim]Cl)/dimethyl sulfoxide (DMSO), at 120 ºC, for 120 min, generated a lignin removal of 49.2% and an increase in the biogas yield of 97.6% as compared with non-pre-treated biomass.

The main drawbacks of IL-based pre-treatments are (i) costs (up to 1,000 US$/kg) (URL1, 2018), (ii) energy demand for recycling the compounds, (iii) lack of toxicological data, (iv) lack of knowledge about the IL action on hemicellulose/lignin disruption, and (v) AD inhibition effects (Y. Zheng et al., 2014). The

high cost and difficulties in the recovery of ILs are the most important future challenges for scaling up this technology.

2.2.4 Biological Pre-treatments

Biological pre-treatments can be divided into (i) ensiling, (ii) micro-aeration, (iii) use of enzymes, (iv) fungi activity, and (v) microbial consortia activity.

In several European countries (Germany, Austria, Sweden, France and Finland), maize is the most widely used crop for biogas production at farm-scale, and ensiling is one of the most used pre-treatments (Murphy et al., 2011). Due to its seasonality, ensiling has the double advantage of pre-treating and preserving the maize crop throughout the year (Herrmann et al., 2015; Kreuger et al., 2011). Fresh crops can be used as AD substrate just after harvesting, but ensiling may increase the methane potential (m^3/kg VS) in most anaerobic digesters (Pakarinen et al., 2008).

Maize is chopped through standard combine harvesters and then stored in big silos (6,000 t capacity), silage clamps (shovel loaders covered with plastic blankets), or bale silos (660 kg capacity), depending on the dimension of the AD plant (Murphy et al., 2011).

Ensiling process can be divided in the following four steps: (i) initial aerobic period, in which residual intraparticle oxygen is consumed, (ii) anaerobic fermentation, (iii) stabilization phase, and (iv) feed-out. During the anaerobic fermentation and after all the interparticle oxygen has been consumed (initial aerobic period), the anaerobic microorganisms, such as lactic acid bacteria, enterobacteria, clostridia and yeasts, begin to proliferate and biomass undergo to anaerobic homolactic, acetic acid, heterolactic, ethanolic and butyric fermentations (Kreuger et al., 2011) These fermentation pathways preserve a significant part of the organic matter and nutrients from the attack of other bacteria (McDonald et al., 1991). During the stabilization phase, the pH remains stable and anaerobic conditions are maintained.

Exposure to air during the different steps of ensilage process and during feed-out can cause aerobic deterioration of organic matter, reducing the methane yield (Wilkinson and Davies, 2012). Anaerobic stability and methane yield can be increased by using chemical additives, but the process becomes more expensive (Herrmann et al., 2015; Plöchl et al., 2009).

Good silage preservation may occur for feedstocks with low moisture content, high accessible carbohydrates and low buffering capacity. High packing

density and reduced particle size contribute to minimize energy losses during ensiling (Teixeira Franco et al., 2016).

The recent German practical experience with maize ensilage reports a mean methane yield of 348 m^3/t VS (KTBL, 2009). Negri et al. (2014) observed with BMP test that the highest biomethane production was obtained by harvesting and ensiling the whole maize plant (more than 10000 m^3/ha), including corn; the biomethane production of the ensiled maize without corn was sharply lower (3300 m^3/ha), although it is more sustainable because reduces the competition with food and feed chains.

Fu et al. (2016) pointed out that supplying a limited amount of oxygen, or air (micro-aeration) to corn straw, prior to AD, can improve the methane yield. The reason for this improvement is the shifting of microbial community under micro-aerobic conditions. However, the amount of oxygen supplied has to be carefully dosed to prevent the organic matter oxidation by aerobic bacteria (S. Xu et al., 2014). S Fu et al. (2015) improved the methane yield with Micro-Aerobic Pre-treatment (MAP) on maize straw. The MAP process consisted in a shaking water bath at 130 rpm, in which maize straw was pre-treated with an optimized pure oxygen load of 5 mL/g VS (Shan-fei Fu et al., 2015), under thermophilic conditions (55 °C), and at atmospheric pressure, until all oxygen consumption. Afterwards, the anaerobic digestion of the treated material at batch mesophilic conditions (37 °C) and using animal slurry as inoculum during an incubation time period of 60 days, registered an increase of 10.2% in biomethane when compared with the untreated samples. MAP process stimulates the microorganisms from the *phylum Firmicutes*, which produce extracellular enzymes, allowing an intensive hydrolytic activity over the lignocellulosic biomass (S Fu et al., 2015).

MCW pre-treatment through enzymes for biogas production was tested at lab scale mainly through the BMP test. Pérez-Rodríguez et al. (2016) observed a reduction of more than 4-fold of the initial lignin content after enzymatic pre-treatment with Ultraflo ® L in an amount equivalent to 0.2 U feruloyl esterase per gram of dry milled maize cob, at 150 rpm, 40 ºC, for 3 h. The methane production increased by 14.6% when compared with non-pre-treated maize; however, high concentrations of *p*-coumaric and ferulic acids of 55 and 174 mg/L, respectively, were registered.

The impact of pre-treating lignocellulosic biomass with different enzymes, at different incubation times (0.6 and 24 h) was studied by Schroyen et al. (2014) on maize stover. The methane production assessed by the BMP test showed an

increase of 25%, after 24 h of incubation with laccase, and 17% after 6 h of incubation with peroxidase. Phenolic compounds ranged from 20 mg/L with laccase (with 6 h of reaction time) to 66 mg/L (with 24 h of reaction time) with a combination of enzymes. At lab scale, the enhancement of methane yield with the use of enzymes is a proved concept, although the production of phenolic compounds is higher than that obtained with other cheaper pre-treatments, such as chemical oxidative methods. At full scale, enzymes were tested by direct addition to a mesophilic digester fed with maize silage. Low or even no impact on methane yield were observed (Schimpf et al., 2013).

Microbial consortia, as well as fungi pre-treatments, require long processing time and volume; also, an initial size reduction is needed. Fungal pre-treatments are less complex and expensive than enzymes. Lignocellulosic degrading fungi can be sorted into white-, brown- and soft-rot fungi (Rouches et al., 2016). They are cheap, environment-friendly and potentially suitable for non-easy degradable biomass materials, such as MCW. The increase in biogas production is possible (Liu et al., 2017) but not systematic, because organic matter losses always occur with this pre-treatment (Rouches et al., 2016).

The high overall costs associated with biological pre-treatments, except for ensiling, are presently the bottle neck for their full-scale application.

2.2.5 Future Challenges

New treatment processes, or optimized combinations of the existing ones with low associated costs, are still needed in order to reduce the cost of the final products. This is highly significant to produce electrical energy from biogas, specifically in the countries in which this type of energy is compensated by low revenue rates.

2.3 Potential inhibitors of the AcoD of MCW with OFMSW

2.3.1 Inhibitors Conditions – Generation, effect and toxic thresholds

The type and concentration of AD inhibitors generated after MCW pre-treatment depend on the pre-treatment conditions applied (Redding et al., 2011). The inhibitors produced are mainly (i) furan derivatives (furfural and 5-Hydroxymethylfurfural – 5-HMF), (ii) phenolic compounds, (iii) VFAs, (iv) extractives (acidic resins, tannins, terpene acids), (iv) some alkaline and alkaline-earth

metals (Na, K, Ca), and (v) heavy metals (for example, Fe, Ni, Zn) (Behera et al., 2014; Mussatto and Roberto, 2004; Vaswani et al., 2016).

Furfural and 5-HMF are formed by decomposition of pentoses and hexoses at high temperatures (Kowalski et al., 2013); 5-HMF may decrease cell growth rate (Park et al., 2015) and substrate degradation kinetic during AD (Ask et al., 2013; Makawi et al., 2009). Concentrations of furfural higher than 20 mM (1.92 g/L) can strongly inhibit *Methanococcus deltae* and *Methanococcus deltae* LH, but concentrations lower than 10 mM do not cause cell growth inhibition. Furthermore, furfural in concentrations lower than 10 mM can be transformed into furfuryl alcohol, promoting the medium detoxification, within 48 h of incubation, in *Methanococcus deltae* cultures (Belay et al., 1997). Similarly, Pekařová et al. (2017) found that concentrations of furfural below 1.0 g/L do not produce any significant inhibition, whereas 5-HMF concentrations higher than 0.2 g/L can cause significant inhibition of methanogens.

Taherzadeh and Karimi (2008) reported that neither furfural nor 5-HMF were detected in hydrolysates obtained from alkaline peroxide pre-treatments of lignocellulosic biomass. This evidence was confirmed by Surra et al. (2018a, 2018b) who found concentrations of furfurals and 5-HMF below the detection limits (3.5 mg/L and 3.9 mg/L, respectively) after MCW pre-treatment, at both room temperature and 100 °C, under MWI, for all H_2O_2 loads tested.

Phenolic compounds are produced by the degradation of lignin. They can cause loss of integrity of biological membranes (physiological inhibition), reducing cell growth and further inhibiting sugar assimilation (Campos et al., 2009). Phenolic compounds with low molecular weight are more inhibitory than those with high molecular weight. Additionally, Parajó et al. (1998) reported that low molecular weight phenolic compounds are more toxic to microorganisms than furfural and 5-HMF.

Regarding the inhibitory effect of phenolic compounds, the literature indicates that during AcoD of olive mill wastewater with wine distillery wastewater, by using cattle manure as inoculum, concentrations of *p*-coumaric acid higher than 50 mg/L strongly inhibited methanogenesis (Akassou et al., 2010). On the other hand, Mousa and Forster (1999) stated that gallic acid concentrations below 20 mg/L do not cause inhibition of AD, whereas concentrations of 50 mg/L can cause 15% decrease of methane content in biogas. Finally, Hernandez and Edyvean (2008) observed that 1.0 g/L of caffeic acid and gallic acid can cause

significant inhibition of AD process. Among the phenolic compounds, syringaldehyde and vanillic acid affect strongly the cell growth (Cortez and Roberto, 2010).

Acetic, formic, butyric, propionic and levulinic acids are the most commonly carboxylic acids found in hydrolysates after biomass pre-treatments; they are also known as VFAs. Their concentrations depends upon the type of feedstock used and pre-treatment method applied (Kim, 2018).

Temperature and residence time of the pre-treatment affect the hydrolyzation of the acetyl groups. VFAs can be also considered as AD inhibitors, due to their ability to cause unbalances between hydrolysis, acidogenesis and methanogenesis phases when present in individual or combined concentrations above the thresholds for a stable AD process (D. Li et al., 2015). Khanal (2008) observed that in a stable anaerobic digester, the concentration of total VFAs is in the range of 50–250 mg/L. According to Drosg (2013), AD instability due to VFAs is achieved when the total concentration exceeds 4000 mg/L.

Among individual VFAs, D. Li et al. (2015) observed that during AcoD of rice straw with cow manure, propionate was the strongest inhibitor for biogas production, because its degradation is slower than that of acetate. Propionate must be degraded to acetate before it can be used by bacteria, whereas acetate can be directly bio-converted into methane and carbon dioxide. The concentration of propionate tolerated by methanogens is just below 1000 mg/L (Hanaki et al., 1994; Wang et al., 2009). It has been reported that AD do not fail up to 10000 mg/L for either acetic or butyric acids (Khanal, 2008). Formic acid, that is also formed due to the breakdown of furan derivatives is more inhibitory than acetic acid (Almeida et al., 2007).

According to McMillan (1994), several extractive raw compounds, such as acidic resins, tannin and terpene acids, derived from acetyl groups that are present in the hemicellulose, generate less inhibition of microbial growth than lignin derivatives or acetic acid.

MCW also contains metals such as Na (1.32% w/w), K (1.53% w/w) and Mg (0.42% w/w) (Anukam et al., 2017), which being bioavailable after the pre-treatment in concentrations higher than 8, 12 and 3 g/L, respectively, can act as inhibitors (McCarty, 1964).

Some heavy metals can be originated from the corrosion of equipment used for MCW pre-treatment (Mussatto and Roberto, 2004; Paul and Dutta, 2018), or be present in MCW due to the specific soil nature and environmental factors, or due to the use of pesticide and fertilizers (Cd, Cr(IV), Cu, Mn, Ni, Pb, and Zn)

(Peng et al., 2006). These elements can also act as inhibitors. If present in trace concentrations, some of them (Mn, Fe, Co, Cu, Mo, Ni, Se, W) are essential for the growth of anaerobic microorganisms; however, when present in high concentrations, can lead to AD inhibition (Guo et al., 2019; Minh et al., 2016). Nasr and Shafy (1992) have defined a toxicity ranking of Cu, Cr(VI), Pb, and Zn for AD as follows: Cu > Cr(VI) > Pb > Zn. These four chemical elements can inactivate enzymes, thus inhibiting the growth of bacteria and jeopardizing the digester (Selling et al., 2008).

There are four different approaches to mitigate the presence of inhibitors in hydrolysates generated during biomass pre-treatment: (i) to opt for a pre-treatment that generates less inhibitors; (ii) to implement a detoxifying process of the hydrolysate before fermentation; (iii) to develop species of microorganisms able to support higher concentration of inhibitors; and (iv) to convert toxic compounds into products that do not interfere with the metabolism (Thaerzadeh et al., 2000).

Detoxification of hydrolysate is very expensive; hence, to adapt and develop microorganisms able to support higher concentrations of inhibitory chemical species seems to be a good approach. The inhibition due to toxic chemical species can be partially solved during AD if a long hydraulic retention time is used. Under these conditions, anaerobic consortia can adapt, or even degrade these toxic chemical species (when the biodegradation is possible); however, the kinetic of overall process will be affected (Kabir et al., 2015).

2.3.2 Future Challenge

The generation of inhibitors during biomass pre-treatment and their potential toxicity in the anaerobic consortia is a crucial aspect when biomass is previously submitted to pre-treatment processes prior to AcoD. Therefore, it is essential to develop further studies on the identification of potential toxic compounds, generated during biomass pre-treatments to anaerobic consortia. Also, the study of pre-treatments performed under mild conditions that limit the production of inhibitors, without compromising the efficiency of biomass deconstruction, is highly important and required.

2.4 AD and AcoD of MCW

2.4.1 AD definition and AcoD using MCW as co-Substrate

AD is a biological process in which complex organic substrates are degraded into CH_4, CO_2, and other trace components (H_2O, H_2S, CO and NH_3) in the absence of dissolved oxygen (Deublein and Steinhauser, 2010). AD takes place in four different stages: (i) hydrolysis, (ii) acidogenesis, (iii) acetogenesis and (iv) methanogenesis (Batstone et al., 2002; Deublein and Steinhauser, 2010; Lapa et al., 2017). Figure 2.1 reports a simplified diagram of the AD process.

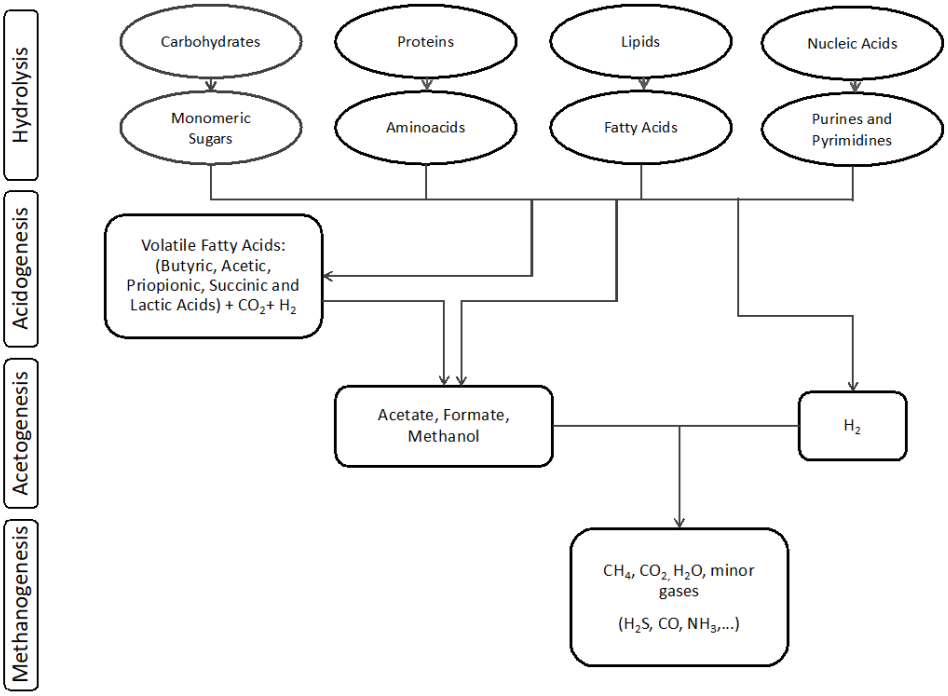

Figure 2.1: Diagram of the anaerobic digestion stages. Adapted from (Batstone et al., 2002; Lapa et al., 2017; Oliveira, 1982)

The rate-limiting stage in the AD of MCW is the hydrolysis, due to the intrinsic recalcitrance characteristic of MCW induced by the presence of cellulose, hemicellulose and lignin.

The AD of standalone MCW shows significant instability caused by the low alkalinity of maize wastes and high C/N ratio. To stabilize the anaerobic process, it is recommended to add a co-substrate with higher N-content than MCW. The AcoD with (i) animal manure and slurry, (ii) sewage sludge, or (iii) OFMSW is highly recommended to achieve adequate biogas and methane yields. The use of co-substrates extremely rich in nitrogen, as fresh meat can lead to the AD process failure, if the relative C/N ratio is not balanced (Hutňan, 2016).

AcoD of MCW can be carried out in liquid phase (LS-AD), when operated at a low concentration of total solids (0.5 to 15% wt) (Owamah and Izinyon, 2015), or in solid phase (SS-AD), if the total solids concentration ranges between 15-40% wt (Y. Li et al., 2015).

Animal manure, sewage sludge and food wastes can be co-processed with MCW via LS-AD, while the OFMSW can be co-processed also through SS-AD (Franchetti, 2013). SS-AD requires smaller bioreactors and has a lower energy demand associated to heating and stirring the bioreactor content (Budzianowski and Budzianowska, 2015), although biogas yield can be lower (Y. Li et al., 2015).

Maize wastes are generally dosed during AcoD in a percentage not exceeing 35% w/w both at laboratory and industrial scales (Ramos-Suárez et al., 2017). Most of the works reported in the literature related to AD of maize wastes, use maize stover, maize husk, maize stalks or maize silage as substrates or co-substrates. Currently, most of the industrial AD plants operating with agricultural residues use maize silage as substrate (Achinas et al., 2017; National Research Institute Poland - Oil and Gas, 2014), which is produced as an energy crop.

MCW rarely is used in laboratory AD assays. No evidence was found in literature about industrial AD plants operating with standalone MCW as substracte or co-substrate. Table 2.3 reports published works selected on AD or AcoD of maize wastes.

The presence of maize wastes only submitted to size reduction (without any other pre-treatment) provides biogas yields comparable to those obtained with pre-treated maize wastes (Table 2.3) (Hutňan, 2016; Surra et al., 2018b). This suggests that using combined pre-treatments before AD is not a guarantee for methane yield enhancement; to find other co-substrates that may stabilise the AcoD process, or even that can also increase the biogas and methane yields is essential.

For example, the use of glycerol as co-substrate was investigated to assess its ability to increase the methane yield during AcoD with maize wastes, and to improve the anaerobic biodegradability of these wastes (Table 2.3). Špalková et al. (2009) compared the results obtained in two laboratory-scale bioreactors operated with an Organic Loading Rate (OLR) of 3.2 kg COD/(m^3.d); one of the bioreactors was fed only with maize silage and the other with a mixture of 4830 g of maize silage and 805 mL of crude glycerol. Authors concluded that the addition of glycerol did not provided any significant improvement on methane yield during AcoD. This was confirmed by (Hutňan (2016) in a pilot-scale

bioreactor which concluded that glycerol is more effective in stabilizing the AcoD process of maize wastes, than in the increase of methane production (Table 2.3).

On the other hand, Amon et al. (2006) observed that adding crude glycerol to a mixture of maize silage (31%), corn (15%) and pig manure (54%) improved the anaerobic biodegradability of the mixture by 17% and 22% when the crude glycerol was added in concentrations of 3% and 6% (v/v), respectively; an increase in the specific biogas and methane yields was also observed (Table 2.3)

Table 2.3: Experimental data available in literature on AD or AcoD assays of maize wastes

Feedstock / Inoculum	Pre-treatment	AD/ AcoD conditions	η_{biogas}	η_{CH_4}	Reference
			mL/g VS		
35% w/w Maize Silage / ASS [1]	Ensiling	OLR: 5.03 kg VS/(m^3.d); T: 35±1 ºC; pH: corrected; HRT[2]: 101 d	569 [3]	310 [4]	(Hutňan, 2016)
Maize Straw (MS)	Ground 2.5-5.0 mm; 0.05-0.15 g CaO/g MS; 1:1 g_{MS}/mL_{H_2O}; or 0.01-0.1 $g_{C_2H_4O_4}/g\ TS_{MS}$; 1:3 g TS_{MS}/mL_{H_2O}; RT [5]: 6 and 12 h	Batch T: 35± 1°C; HRT: 45 d	<400	nr [6]	(Ramos-Suárez et al., 2017)
31% w/w Maize Silage 15% w/w Corn 54% w/w Pig Manure; + 6% glycerine	Not pre-treated	Batch T: 38–40 ºC HRT: 42 d	679	439	(Amon et al., 2006)
75% w/w Food Waste 25% w/w Maize Husk	Dried and ground to powder	OLR: 3.5 g VS/L.d; T: 37±1 °C; pH: 7.4; C/N: 23.4; HRT: 44 d	700	447	(Owamah and Izinyon, 2015)
87% w/w VS OFMSW 13% w/w VS MCW	Ground 2-4 mm; H_2O_2/MCW ratio (w/w): 0.5; 10% MCW w/v; pH: 9.8; T: 23 ºC; RT: 4 h	OLR: 2.48 g VS/(L.d); T: 55±2 °C; pH: 8.0; HRT: 13 d	870	550	(Surra et al., 2018b)
54% w/w Dairy Manure 33% w/w Maize Stover 13% w/w Tomato Wastes	Ground to 40 mm	Batch SS-AD; T: 35±1 ºC; C/N: 22.4; HRT: 45 d	nr	15.0	(Y. Li et al., 2015)
36% w/w Dairy Manure 24% w/w Corn Straw 40% w/w Tomato Wastes	Ground to 40 mm	Batch SS-AD; T: 35±1 ºC; C/N: 14.1; HRT: 35 d	nr	375	(Li et al., 2018)
70% w/w TS Swine Manure 30% w/w TS Maize Stover	Ground to 1 mm	Batch; T: 55±2 ºC; pH: 8; HRT: 35 d	203	64.6	(T. Zhang et al., 2015)

[1] Anaerobic Stabilized Sludge; [2] Hydraulic Retention Time; [3] Assuming ϱ_{biogas}=1.15 kg/m^3, STP, and $VS_{maize\ silage}$ =95.8% TS ; [4] Calculated assuming CH_4 content= 54.5% ; [5] Reaction Time; [6] not referred

2.4.2 Factors affecting AcoD of MCW

The most important factors that affect the AcoD of MCW are the same as for other organic lignocellulosic wastes, namely (i) C/N ratio, (ii) pH, (iii) OLR, and (iv) macro- and micro-nutrients (Deublein and Steinhauser, 2010). All these factors are interlinked and are affected themselves by concentrations of the total and individual VFAs, Total Ammonia Nitrogen (TAN), free Ammonia (NH_3), Ammonium Nitrogen (NH_4^+), and H_2.

2.4.2.1 C/N ratio

Being C and N two macro-nutrients necessary for cell growth, the C/N ratio in the substrate is an important parameter for AD process. A high C/N ratio means the lack of nitrogen, which can be due eventually to the lack of proteins and/or of their solubilization. It reflects low concentrations of TAN and can be related to VFAs accumulation, causing an unavoidable acidification of the medium.

At very high C/N ratios, pH can decrease significantly, and the AD process becomes unstable. In this case, the addition of a co-substrate rich in N is necessary to balance the process. Low C/N ratios may result in N-accumulation in the form of aqueous NH_4^+, which can be toxic for methanogens.

The optimal C/N ratio for AD ranges between 20 and 30, with an optimal value of 25 (Ning et al., 2019; X. Wang et al., 2012). Maize cob is characterized by a typical C/N ratio of approximately 50, thus the use of a N-rich co-substrate is recommended.

2.4.2.2 pH

Methanogenesis is more efficient at a pH range of 6.5-8.2. In one-stage digesters, the optimal pH is around 7.0 to favour methanogenic bacteria (Kondusamy and Kalamdhad, 2014).

The digesters are naturally buffered if the pH of the feedstock is kept between 6.5 and 7.5. pH values lower than 6.5 or higher than 8.2 inhibit AD (Jain et al., 2015). pH values lower than 5.5 cause the accumulation of VFAs. A good strategy to control the pH, in the case of the AcoD of MCW, is to separate the hydrolysis/acidogenesis and acetogenesis/methanogenesis stages in a two-stage anaerobic process (Demirer and Othma, 2008; Kondusamy and Kalamdhad,

2014). Careful dosage of the substrate to control abrupt pH changes and accumulation of VFAs may avoid inhibitory effects (Hutňan, 2016).

Surra et al. (2018a) observed that an increment of 15% in OLR with splintered MCW, during the AcoD with OFMSW, produced an initial slight pH decrease after each bioreactor feeding (from 8.2 to 7.5). Nevertheless, the system recovered again to its natural pH of 8.2 just after 2-3 hours, without any apparent short-term inhibition of the AcoD process. A different behaviour is, however reported in the literature for long-term AD of maize silage used as single substrate. Lebuhn et al. (2008) observed that, even at a low OLR (2 g VS/L.d), a long-term acidification in continuously-stirred AD bioreactor occurs. Similarly, Hutňan (2016) observed that the anaerobic biodegradation of maize silage as a single substrate is an unstable process, due to its low alkalinity that must be compensated by pH adjustment or with other co-substrate.

2.4.2.3 Organic Loading Rate (OLR)

If a high OLR is applied to the bioreactor, VFA accumulation may occur in the early stages of fermentation, leading to acidification and causing methanogenic inhibition (Mao et al., 2015).

The optimal OLR depends on the type and size of bioreactor, its sophistication level of control, but also on the type of substrate used and temperature under which the bioreactor is operated (Velásquez-Piñas et al., 2018). At lab scale, the optimal OLR range for mesophilic bioreactors is within 2.5-5.0 kg VS/(m^3.d) for maize wastes. The maximum OLR allowed in a specific AD system is conditioned by the changes caused in AD critical factors, such as VFAs, pH, Total Alkalinity, and TAN. The type of substrate or even co-substrate used and thermal conditions applied (mesophilic or thermophilic) affect the maximum OLR allowed. Additionally, the relation between the activity of methanogens and activity of carbon dioxide producers, at different OLR values, is important to define the optimal OLR (Owamah and Izinyon, 2015).

Owamah and Izinyon (2015) observed that during AcoD of 75% w/w food waste with 25% w/w maize husk, under mesophilic conditions, the gradual increase of OLR from 1 to 4.5 g VS/(L.d) enhanced the digester stability, due to the increase of TAN that acted as a buffer. These authors found that the OLR of 4.5 g VS/(L.d) allowed higher methane yield than that of 3.5 g VS/(L.d). Similar results were obtained by Li et al. (2014b) that found an optimal OLR for AcoD of chicken manure and maize stover of 4.0 g VS/L.d. OLR higher than 6.0 kg VS/(m^3.d) at lab scale caused a decrease in the specific biogas production

(Hutňan, 2016). At lab scale, Surra et al. (2018b) observed an enhancement in biogas and methane yields with an OLR of 2.48 kg VS/(m^3.d), under thermophilic conditions and in the presence of 13% VS MCW and 87% VS OFMSW (Table 2.3).

2.4.2.4 Macro- and Micro-Nutrients

Macronutrients, such as P, N, S, K, and Mg are fundamental for AD processes, but some of them also play an important role as buffering agents. Micronutrients, such as Fe, Ni, Mo, Co, W, and Se, are crucial co-factors in many enzymatic reactions involved in the AD process (Lo et al., 2012; Schattauer et al., 2011). The optimal C/N/P/S ratio found during AD was of 600:15:5:1 (Mao et al., 2015), and the optimal C/N/P ratio for CH_4 yield enhancement was reported to be 200:5:1 (Ayeni and Daramola, 2017). MCW is characterized by 410 g C/kg MCW, 0.04 g P/kg 620 MCW, 0.2 g S/kg MCW, 7.6 g K/kg MCW, and 3.0 g Mg/kg MCW (Nogueira, 2017), which can be a potential positive contribution of its use as an AD nutrient demand, namely in what concerns to C, K, Mg and S contents.

2.4.2.5 VFA and Alkalinity Ratio

VFAs are short-chained volatile organic acids, such as acetic, propionic, butyric, and valeric acids. They are produced during the AD acidogenic phase as intermediate metabolites. The accumulation of VFAs causes the methanogenesis inhibition (Batstone et al., 2002; Lapa et al., 2017) and can be related to a substrate overload (Ward et al., 2008). The alkalinity ratio contributes for the buffer capacity of the bioreactor content (Batstone et al., 2002; Lapa et al., 2017). A decrease in the buffering capacity caused by the accumulation of VFAs comes earlier than the pH decrease. Therefore,, VFAs/alkalinity ratio is a reliable parameter for monitoring AD process imbalance (Song et al., 2004; T. Zhang et al., 2015; Zhao and Kugel, 1996). The recommended total VFAs and VFA/Alkalinity ratio for a stable AD process are below 1000 mg/L and 0.3, respectively (Lapa et al., 2017).

The stability of an AD process, in terms of VFA accumulation and alkalinity, depends mainly on the type of substrate used and relative percentages of different co-substrates. Owamah and Izinyon (2015) achieved the AD stability in a bioreactor that was kept with a VFA/alkalinity ratio in a range of 0.06-0.22 with 75% food waste and 25% maize husk. Zhang et al., (2015) obtained a VFA/alkalinity ratio lower that 0.4 during the digestion (Hydraulic Retention Time, HRT = 35 days) of 70% swine manure and 30% maize stalk. In this case, when the

percentage of swine manure decreased, the VFA/alkalinity ratio increased, and the system lost the buffer capacity.

2.4.2.6 Ammonium Nitrogen and Free Ammonia

Ammonia (NH_3) is the end-product of anaerobic digestion for proteins, urea and nucleic acids (Yenigün and Demirel, 2013). In the anaerobic digester, NH_3 is present in solution in the form of ammonium nitrogen (NH_4^+) and free ammonia ($NH_{3,aq}$); these two species of nitrogen are in a pH-dependent equilibrium (Wu et al., 2016).

Although ammonia is important for bacterial growth at a low concentration, high concentrations of NH_3 and NH_4^+ can inhibit the AD process (Rajagopal et al., 2013). $NH_{3,aq}$ is considered to be the main cause of metabolic inhibition of bacteria, as it freely crosses the cell membranes. The adaptation of anaerobic bacteria is a key factor to avoid process imbalance by $NH_{3,aq}$ (Drosg, 2013).

Total Ammonia Nitrogen (TAN) (i.e., $NH_{3,aq} + NH_4^+$) is reported to present concentrations of 1700–1800 mg/L (Melbinger et al., 1971), 3000 mg/L (McCarty, 1964), and 3300 mg/L (Hobson and Shaw, 1976). Acclimated inocula may tolerate concentrations of TAN up to 5000 mg/L (Drosg, 2013). Thermophilic AcoD of maize silage and pig manure, with ammonia adapted bio-consortium withstood the critical TAN concentration of 5500 mg/L (Lindorfer et al., 2008). McCarty and McKinney (1961) proposed that $NH_{3,aq}$ in solution is the chemical species responsible for inhibition/toxicity rather than NH_4^+. These authors also found that 150 mg/L $NH_{3,aq}$ was completely inhibitory to AD. $NH_{3,aq}$ inhibition is dependent not only on the NH_4^+ concentration, but also on the medium temperature (Lindorfer et al., 2008) and pH (Drosg, 2013).

According to Drosg (2013), it is preferable to monitor NH_4^+ rather than $NH_{3,aq}$ to assess the ammonia inhibition in an anaerobic digester, because the quantification of the latter is strongly dependent on the accurate determination of pH (pH accuracy <0.02 units). Additionally, even if a high concentration of NH_4^+ can lead to inhibitory concentration of $NH_{3,aq}$, at the same time, it may increase the buffer capacity of the digester. This favours the system tolerance to

high NH_4^+ concentrations, although the AD system becomes more sensible to small changes of pH and OLR.

Hutňan (2016) observed that the long-term operation of a lab-scale anaerobic reactor (4 L) fed with maize silage was affected by significant instability due to the weak ammonia buffer capacity (NH_3/NH_4) and the lack of nitrogen as nutrient. The addition of a co-substrate with higher nitrogen content, such as sewage sludge or animal manure should be used to correct this instability.

2.4.2.7 Hydrogen

Hydrogen is an intermediate metabolite, being produced at various stages of the AD process. H2 concentration must be kept below 100 ppm to maintain the process stability. The change in H2 concentration occurs before the change in VFA or VFA/alkalinity ratio. Therefore, H2 is an earlier indicator of ongoing instability on the process than VFA and alkalinity ratio (Drosg, 2013).

2.4.3 Future challenges

The anaerobic digestion of co-substrates is a topic that still needs future research, since optimal substrates for anaerobic digestion are difficult to find. To assess the local organic substrates available in place, evaluate their compatibility and synergetic effects for anaerobic digestion, and quantify their supply cost to an AcoD plant, are important research topics to follow to obtain a sustainable production of biogas and bioCH_4.

2.5 BioCH_4 Quality Standards

The nature of substrate and operational conditions used during the AD determine the chemical composition of biogas, including CH_4 and CO_2 contents, as well as the type and concentration of contaminants (Angelidaki et al., 2018).

Biogas conditioning and upgrading to bioCH_4 aims to increase the CH_4 content to a certain standard quality (97% v/v), separating CO_2 and removing specific poisoning trace contaminants, such as H_2S. The final objective herein is to enable bioCH_4 injection into the NG grids for consumer usage or its application in the transportation sector as biofuel.

Until 2016, European countries based their national standards of bioCH on national specifications for NG. However, due to the increase of bioCH_4 production and the growing number of vehicles fuelled by NG, new regulations and technical security standards were required to allow easier trade of bioCH_4.

In November 2016, the European Committee for Standardization (CEN) published the specification for bioCH_4 devoted to grid injection (EN 16723-1:2016) and for its use as automotive fuel (EN 16723-2:2016) (Wellinger, 2017). The common parameters, such as methane number (MN), H_2S and carbonyl sulphide (as sulphur) contents, hydrocarbons dew point, CO_2 content, among others, were referred to the quality requirements of NG, standardized in EN 16726:2015 (Gas infrastructure – Quality of gas – Groups H and L). The standards EN16723-1 and EN16723- 2 were accepted by the European member-states in August 2016 and March 2017, respectively.

Table 2.4 and 2.5 show the bioCH_4 quality standards included in EN16723-1 and EN 16723-2. According to the current standard, CO_2 concentration allowed at NG grid entry and interconnection points cannot exceed 4.0% v/v. A lower limit must be defined if the installation sensitiveness is higher (e.g. underground storage systems). Regarding H_2S and carbonyl sulphide, the maximum allowed threshold is 5 mg/m^3 (3.89 ppm), for both grid injection and automotive fuel.

Table 2.4 : Applicable common requirements and test methods for bioCH_4 at the entry point into H and L gas grids

Component	Unit	EN16723-1		Test Method
		Min	Max	
TVS [1]	mg Silicone/m^3		0.3 -1 [2]	EN ISO 16017- 1:2000
Compressor Oil			free	ISO 8573-2:2007
Dust			free	ISO 8573-4:2001
CO	% mol	-	0.10	EN ISO 6974 series
NH_3	mg/ m^3	-	10	EN 2826:1999 or VDI 3496 Blatt 1- 1982-04 NF X 43- 303:2011
Amine	mg/ m^3	-	10	VDI 2467 Blatt 2:1991-08

[1] Total Volatile Silicone; [2] Pure and diluted, respectively

Table 2.5: Requirements, limit values and related test methods for natural gas and bioCH_4 as automotive fuels with normal Methane Number grade

Component	Unit	EN16723-2 Min	EN16723-2 Max	Test Method
TVS [1]	mg Silicone/m^3		0.10-0.50 [2]	SP test Method
H_2	% mol/mol		2.00	EN ISO: 6874-3, 6874-6, 6975
HC dewpoint [3]	°C	-	-2	EN ISO: 23874, ISO/TR: 11150, 12148
O_2	% mol/mol		1.00	EN ISO: 6974 series, 6975
H_2S+COS	mg/m^3		5.00	EN ISO: 6326-1 6326-3, 19739
CO_2	% mol	2.50	4.00 [4]	EN ISO 6974, 6975
Total sulphur	mg S/m^3	nd	nd [5]	EN ISO: 63265, 19739
Methane Number	Index	65.0	-	EN ISO 16726 (Annex A)
Compressor Oil			Free	EN ISO: 85732
Dust			Free	EN ISO: 85734
Amine	mg/m^3		10.0	VDI 2467 Blatt 2:1991-08
H_2O dewpoint	°C	-10.0	-30.0	EN ISO 6327, (20000 kPa)

[1] Total Volatile Silicone; [2] Pure and diluted, respectively; [3] From 0.1 to 7 MPa absolute pressure;

[4] A more restrictive limit may be applied, when the gas does flows to installations sensitive to higher levels of CO_2 ; [5] nd: not defined. Neither an upper limit nor a lower limit for total sulphur were defined. Currently, there is a difference between the automotive industry needs (10 mg S/m^3 including odorisation) and the values that the industry can provide (30 mg S/m^3 including odorisation).

2.6 Activated Carbons from MCW for Biogas Conditioning and Upgrading

Among the different techniques that can be used to remove H_2S and CO_2 from biogas, the adsorption-based technology using ACs is considered a safe, reliable and an environmental friendly technique (Köchermann et al., 2015).

Wang et al. (2010) suggested that MCW can be a potential precursor to produce ACs, since the obtained adsorbent materials may present high surface areas and a well-developed micro and meso porosities. Moreover, the surface of ACs could be functionalized in order to increase their adsorption capacity for the target adsorbates. As mentioned before, MCW is a lignocellulosic biomass characterized by high carbon content (40-45% w/w) and low percentage of ashes (about 1-2% w/w), which makes it an adequate precursor for ACs (Nogueira, 2017).

2.6.1 H_2S Removal

The mechanisms ruling the sorption of H_2S onto ACs may be quite complex and strongly dependent on both the adsorbents, and biogas properties, as well as the operating conditions used during the sorption process (Nowicki et al., 2016).

Physisorption (pore filling) and chemisorption (H_2S dissociation, oxidation and metallic reduction/sulfidation) might be involved individually or combined in H_2S removal (Bamdad et al., 2018; Castrillon et al., 2016; Hervy et al., 2018).

In order to enhance the H_2S adsorption capacity, ACs can be impregnated with alkalis, as sodium (Bagreev and Bandosz, 2002) and potassium (Kaźmierczak-Raźna et al., 2013) hydroxides, potassium iodine (Choi et al., 2008), potassium carbonate (Castrillon et al., 2016), or with several metal oxides (de Falco et al., 2017; Inoue and Matsumoto, 2017). These agents can increase up to 10 times the H_2S loading capacity of ACs, when compared with non-impregnated ACs (Bailón Allegue and Hinge, 2014). This is mainly due to oxidation or sulfidation reactions.

Moreover, nitrogen functionalities in porous carbon materials confer basic character to the carbon surface, enhancing the dissociation of H_2S to HS^- ions, which are subsequently oxidized to elemental sulphur (Seredych and Bandosz, 2008).

Köchermann et al. (2015) reported that the adsorption of H_2S onto ACs without chemical agents proceeds solely by physisorption, while impregnated ACs with different agents, such as NaOH, CuO, KI, and K_2CO_3, can react with H_2S through catalytic oxidation in the presence of oxygen. In the absence of oxygen, catalytic oxidation does not occur, and H_2S is physisorbed.

Bouzaza et al. (2004) found that the oxidation of H_2S on carbon fibres occurs under dry atmosphere and without oxygen, due to the presence of oxygen functional groups at carbon fibre surface. Feng et al. (2005) confirmed this observation with oxidized carbon fibres, demonstrating that oxygen functionalities can act as active sites for H_2S oxidation.

Guo et al. (2007) found that the physisorbed H_2S by ACs produced through physical activation of oil palm could be completely desorbed at room temperature. However, an AC chemically activated with KOH and H_2SO_4 required high temperatures for H_2S desorption, suggesting that chemisorption occurred.

Shen et al. (2018) employed the Density Functional Theory (DFT) to investigate the adsorption mechanisms of H_2S onto ACs. These authors found that these carbon materials favoured the dissociation of H_2S and offered active sites for adsorption. It was suggested that the direct adsorption of H_2S leads to the formations of C-S or C-SH on the surface of the ACs followed by their evolution into stable C-S-C species.

Few attempts were done to producing ACs from MCW for H_2S removal; some studies were based on physical activation (Kaźmierczak-Raźna et al., 2013; Nowicki et al., 2016) and others on chemical activation (Nowicki et al., 2016). Hoewver, more attempts were performed with other biomass wastes, such as coconut shells (Choo et al., 2013), cherry stones, coffee and tobacco wastes (Nowicki et al., 2016), rice husk (Nam et al., 2018), sewage sludge and fish wastes (Ansari et al., 2005; Wallace et al., 2014). Table 2.6 presents a comparison between ACs produced from MCW and from other biomass wastes for H_2S removal.

Nowicki et al. (2016) tested the H_2S adsorption capacity of physical and chemical activated carbons and concluded that, independently of the precursor used (cherry stones, coffee or tobacco wastes) and the activation method, the lowest H_2S adsorption capacities were observed under dry conditions (barely exceeded 20 mg/g (Table 2.6). High surface areas and high mineral content were not enough for an effective H_2S removal without a previous moistening process of the gaseous stream (70% moisture content). These results were also confirmed by Kaźmierczak-Raźna et al. (2013), where it was observed that the presence of water dramatically enhances the H_2S adsorption capacity of ACs.

Table 2.6: Comparison of ACs prepared from MCW and other biomass wastes for H_2S removal.

Precursor	Carbonization conditions	Activation conditions	S_{BET} m^2/g	V_{total} [1] cm^3/g	H_2S adsorption capacity mg/g dry	wet	pre-humidified	References
MCW	700 °C for 1 h (Argon, 0.17 L/min)	800 °C for 0.5 h (CO_2, 0.25 L/min)	495	0.30	27.9	119	88.8	(Nowicki et al., 2016) [3]
Cherry stones			347	0.21	0.60	1.10	1.30	
Coffee wastes (IS [2])			28.0	0.04	11.8	150	119	
Tobacco wastes (IS)			202	0.14	6.70	19.0	21.0	
MCW		700 °C for 0.5 h KOH:char (w/w) = 2:1 (Argon, 0.33 L/min)	941	0.54	8.60	17.4	13.3	
Cherry stones			1181	0.66	7.00	8.60	9.80	
Coffee wastes (IS)			1436	0.95	4.70	7.20	9.20	
Tobacco wastes (IS)			1201	0.73	3.70	76.3	64.7	
MCW		800 °C for 0.5 h (CO_2, 0.25 L/min)	429	0.23	44.7	159	122	
Cherry stones			472	0.28	8.30	17.2	19.5	
Coffee wastes (IS)			23	0.03	6.00	198	216	
Tobacco wastes (IS)			74	0.07	13.0	158	178	
MCW	500 °C for 1 h (Argon, 0.17 L/min)	800 °C for 0.5 h (CO_2, 0.25 L/min)	352	0.21	16.5	18.0	10.8	(Kaźmierczak-Raźna et al., 2013) [4]
		0.5 h KOH:char (w/w) = 2:1	566	0.33	19.5	45.1	5.00	
	800 °C for 1 h (Argon, 0.17 L/min)	800 °C for 0.5 h (CO_2, 0.25 L/min)	1213	0.63	5.00	6.80	29.5	
		0.5 h KOH:char (w/w) = 2:1	747	0.40	4.10	6.30	4.70	
Coconut shell	Commercial activated carbon	-	877	0.46	106	27.0	122	(Seredych and Bandosz, 2006) [5]
Grape seed	Not referred	-	740	0.47	100	31.0	152	

[1] V_{total}: Total pore volume; [2] IS: Industrial source; [3] H_2S adsorption capacity calculated for a breakthrough of 100 ppmv H_2S; [4] Breakthrough at 100 ppmv H_2S; [5] Breakthrough at 350 ppmv H_2S.

These authors found that physically activated MCW produced ACs with a H_2S adsorption capacity of 45.1 mg/g under wet conditions, which was 2.3-fold higher than that obtained at dry conditions (19.5 mg/g) (Table 2.6).

Seredych and Bandosz (2006) observed that the role of water in H_2S adsorption is different whenever the ACs are exposed to moistened gas or pre-humidified one (air with 70% moisture content, during 2 h). These authors concluded that the best adsorption capacities are obtained when the pre-moistening of the carbon adsorbents was done and no water was added to the gas mixture (Seredych and Bandosz, 2006).

2.6.2 CO_2 Removal

ACs are highly promising adsorbents for the separation of CO2 from gaseous streams (Rashidi et al., 2016). Adsorption of CO2 onto ACs can occur by physisorption or by chemisorption. The ACs that act through physisorption can be regenerated (at high temperature and/or low pressure), reducing significantly the operation costs. These ACs should provide (i) high surface area, (ii) considerable microporous volume, (iii) adequate adsorption capacity, (iv) sufficiently large pore network for efficient kinetics (Do, 1998), (v) high selectivity towards CO2 (Grande, 2011), and (vi) a regeneration capacity that allows them operating in multiple cycles in a wide range of temperatures and pressures (Keramati and Ghoreyshi, 2014).

To increase the adsorption capacity of CO2, ACs can be functionalized with nitrogen groups (Keramati and Ghoreyshi, 2014; Pevida et al., 2008; Tiwari et al., 2018), ionic liquids (Yusuf et al., 2017) or Deep Eutectic Solvents (DES) (Zulkurnai et al., 2017). These functionalization's can promote strong or irreversible interactions between the functional groups and CO2, favouring chemisorption. In this case, the ACs lose their regenerative properties, increasing the costs associated to landfilling.

Table 2.7 presents a comparison between ACs produced from agricultural/forest biomasses and MCW for CO_2/CH_4 separation. Agricultural and forest residues are attractive precursors of ACs for CO_2 removal, due to their high availability and low cost (Álvarez-Gutiérrez et al., 2017; Durán et al., 2018). Cherry stone-based ACs demonstrated high potential for biogas upgrading as well as coconut shells (Vilella et al., 2017), pine sawdust (Durán et al., 2018), and

olive stone (Álvarez-Gutiérrez et al., 2014). Considerable CO_2 uptakes were also observed with date seed (Ogungbenro et al., 2018) and MCW (Song et al., 2013).

For industrial application, the adsorbents produced from the mentioned biomasses have to exhibit not only a high CO_2 adsorption capacity and selectivity, but also rapid adsorption/desorption rates. Álvarez-Gutiérrez et al. (2017) observed that the adsorption rate constants, k_A, increased with the increasing of CO_2 concentration, being the mass transfer during the adsorption of CO_2 ruled by a diffusion-based process involving film diffusion and intra-particle diffusion.

CO_2/CH_4 separation at atmospheric pressure onto ACs produced from pine sawdust (Durán et al., 2018) was affected by the presence of both water vapor in the biogas stream and a pre-saturated adsorbent material. Under moistened biogas (wet conditions), the CO_2 uptake decreased in comparison with the dry experiments. However, despite the lower CO_2 uptake under wet conditions and in the presence of a pre-saturated adsorbent, the CO_2 selectivity increased. This result suggests the potential of this adsorbent to be used for CO_2 separation from real biogas not submitted to any preliminary water removal conditioning step (Table 2.7).

2.6.3 Future Challenges

Further studies concerning the development of MCW-derived ACs for H_2S removal from biogas streams are needed. The challenge is in the increase of ACs adsorption capacity of H_2S by limiting the addition of air/oxygen and/or water, since these compounds are problematic for the biogas upgrading technologies.

To authors' knowledge, no studies are available in the literature regarding the use of MCW as precursor to produce adsorbents for cyclic CO_2 adsorption-based separation technologies, such PSA. More work can be done in this field, in order to integrate the use of MCW in biogas purification technologies

Table 2.7: Comparison of ACs prepared from agricultural and forest residues for CO_2 removal.

Precursor	Carbonization and activation conditions	Type of Activation/ Catalyst	S_{BET}	V_{total}[1]	CO_2/CH_4	P	T	Selectivity	CO_2	CH_4	Ref.
			m^2/g	cm^3/g	% v/v	bar	°C		mmol/g		
Cherry stones	Very complex process; please, *see* (Gil et al., 2013)	Physical and Chemical/ H_2O	998	0.53	30/70	1	30	nr[2]	1.04	0.68	(Álvarez-Gutiérrez et al., 2017)
					50/50				1.49	0.37	
					65/35				2.12	0.47	
		Physical and Chemical/ CO_2	1045	0.48	30/70				1.18	0.71	
					50/50				1.63	0.47	
					65/35				1.98	0.39	
Cherry stones	Very complex process; please, *see* (González et al., 2013)	Physical/ CO_2	903	0.34	50/50	3		-	2.89	1.45	(Álvarez-Gutiérrez et al., 2014)
						6		3.29	4.04	2.09	
						10		3.15	4.97	2.66	
						18		2.89	6.04	3.39	
Olive stones	Very complex process; please, *see* (Gil et al., 2013)	Physical and Chemical/ H_2O	925	0.33		3		-	2.79	1.31	
						6		3.28	3.75	1.89	
						10		3.13	4.51	2.36	
						18		2.84	5.34	2.94	
Pine saw-dust	Direct activation 800°C/1h	Physical/ CO_2	788	0.34	30/70	1.2	30	4.51(d) [3]	1.44 (d)	0.65(d)	(Durán et al., 2018)
								2.97(w) [4]	0.96 (w)	0.72(w)	
								6.33(w+h) [5]	0.42(w+h)	0.15(w+h)	
					50/50			5.23(d)	2.00(d)	0.37(d)	
								3.36(w)	1.39(w)	0.43(w)	
								6.2(w+h)	0.65(w+h)	0.11(w+h)	
					65 /35			5.13(d)	2.42(d)	0.26(d)	
								3.09(w)	1.64(w)	0.32(w)	
								5.89(w+h)	0.78(w+h)	0.08(w+h)	

Table 2.7: *Continued.* Comparison of ACs prepared from agricultural and forest residues for CO_2 removal.

Precursor	Carbonization and activation conditions	Type of Activation/ Catalyst	S_{BET}	V_{total}[1]	CO_2/CH_4	P	T	Selectivity	CO_2	CH_4	Ref.
			m^2/g	cm^3/g	% v/v	bar	°C		mmol/g		
Coconut shell	Direct activation 900°C /140 min	Physical/CO_2	1452	0.65	30/70	1	20	0.87	2.20	1.14	(Vilella et al., 2017)
Babassu coconut			809	0.39				2.64	2.43	0.92	
Coconut shell	600°C /3h	Physical/N_2, 30 min Calcination 800°C /2h	1650	0.54	Pure gases	1	25	nr	1.40	0.85	(Yang et al., 2011)
						2			1.80	1.45	
		Chemical H_2PO_4:AC= 1:2 Calcination 600°C /2h	1922	0.68		1			1.70	0.05	
						2			2.55	0.15	
		KOH:AC=1:4 v/w Calcination 800°C /2h	1575	0.53		1			1.20	0.70	
						2			2.20	1.90	
Date Seed	900°C /1h	Physical/CO_2 800°C /1h	798	0.28	100/0	1	20	-	3.21	-	(Ogungbenro et al., 2018)
MCW	400°C /1h	Physical/Steam 800°C /2	980	0.52		1	25	-	1.40	-	(Song et al., 2013)(Song et al., 2013)
	450°C /1h	800°C /2 KOH:AC=3:1	1600	0.62					1.50	-	

[1] Vtotal: Total pore volume. [2] nr: not reported. [3] dry conditions. [4] wet conditions. [5] wet and pre-hydrated conditions

2.7 Biogas Upgrading Technologies

Several technologies can be applied to upgrade biogas to bioCH_4 (Figure 3) (i) absorption, (ii) adsorption, (iii) membrane permeation, and (iv) cryogenic technologies (TUV, 2012).

2.7.1 Absorption based Technologies

2.7.1.1 Amine Scrubbing

One of the most used techniques for biogas upgrading applying chemical absorption is the amine scrubbing. Firstly, CO_2 passes through the amine solution and then is stripped by heating the liquid with steam. The most used amines are methyldietanolamine (MDEA), dietanolamine (DEA), monoethanolamine (MEA) and primary activated dietanolamine (AMDEA). The advantage of amine scrubbing is that high CH_4 purity (>97%) and low CH_4 loss (<1%) are achieved (Q. Sun et al., 2015).

Despite of their efficiency, amines present some disadvantages: (i) high energy intensity, (ii) subsequent compression requirement, (iii) environmental toxicity, and (iv) requirements of heavy equipment (Scholz et al., 2013).

Amine scrubbers can handle biogas without its pre-treatment. Most of the H_2S and ammonia are dissolved in the amine solution and can be removed during regeneration, where there is no strict limitation on air supply (Figure 2.2a). O_2, N_2 and H_2 pass through the absorption column together with bioCH_4 and must be removed downstream, according to the final gas quality requirements (Hoyer et al., 2016).

2.7.1.2 Water Scrubbing

Absorption processes through water scrubbing is an alternative to amine scrubbing. Water scrubbing operates with two columns: in one column, the absorption stage is performed and in the other column the desorption is done in phase, with the presence of a flash column in the middle to recover as much as possible the methane dissolved in the process. Biogas is fed in the first column at a pressure between 6-8 bar. The water is regenerated by decompression and stripping air into the desorption column.

Both gas and air pressurization are energy demanding steps that contribute to increase the overall costs. Water scrubbing can dissolve H_2S, ammonia and some VOCs in water. These contaminants are afterwards released with stripping air (Figure 2.2b). They must be treated accordingly with the national and regional legislations. The outcoming CH_4 is saturated with water, thus it must be dried up to the required dew point. Moreover, water pH control, anti-foam and bactericide agents must be added to the process, increasing the overall costs.

One of the main drawbacks of water scrubbing technology is that the selectivity of water in absorbing CO_2 and CH_4 is limited, resulting in theoretical CH_4 losses of 3–5%, while plant suppliers claim to be only around 2% (Q. Sun et al., 2015) (Table 2.8).

2.7.1.3 Organic Physical Scrubbing

Organic physical scrubbing (Figure 2.2c) is another absorption-based technology in which Genosorb® is commonly used; this substance is a mixture of dymethylethene and polyethyleneglycol. The solubility of CO_2 in Genosorb® is much higher than in water.

The biogas must be pre-compressed to 6-7 bars and cooled down before entering the absorption column. The solvent is regenerated by heating and no corrosion effects take place. Also, this solvent can handle H_2S, VOCs and ammonia, but its performance is much better if the raw biogas is previously pre-treated to remove these contaminants. Furthermore, drying and de-oxygenating steps may have to be included before the final delivery of the stripped-off gas.

2.7.2 Membrane Permeation

Membrane-based separation process for biogas upgrading (Figure 2.2d) is very attractive, because of its high energy efficiency, processing easiness, high reliability and small environmental footprint.

Several membrane materials can separate CO_2 from a biogas stream, namely polymer or polymeric composite materials, due to their low manufacturing cost when compared to other inorganic materials (Scholz et al., 2013).

Membrane fibres are continuously being improved to gain better selectivity and higher permeability with lower methane slip. Membrane technology is preferentially used when the purity level required for bioCH_4 is not very high (<95% v/v) (Table 2.8). Apart from this, other main drawbacks of membrane technology applied to biogas upgrading is the plasticisation that occurs when

high CO_2 partial pressure induces significant sorption of this gas in the polymer matrix. This increases the polymer chain mobility, enhancing the mass transfer of all gas species through the membrane, thus reducing its selectivity (Basu et al., 2010)

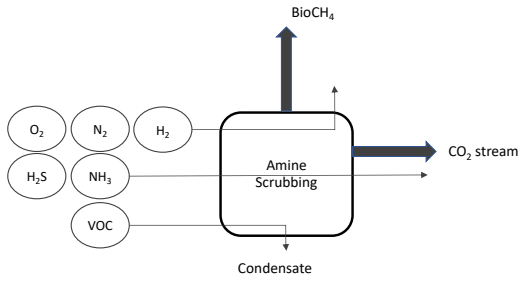

Figure 2.2a) Amine Scrubbing (absorption-based technology)

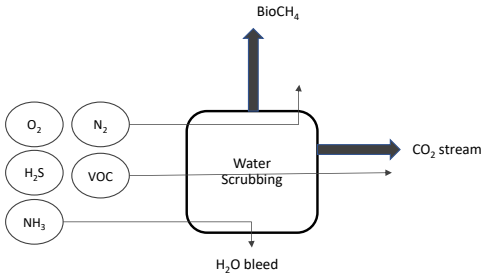

Figure 2.2b) Water Scrubbing (absorption-based technology)

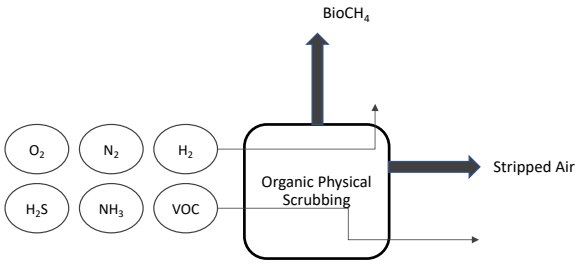

Figure 2.2c) Organic Physical Scrubbing (absorption-based technology)

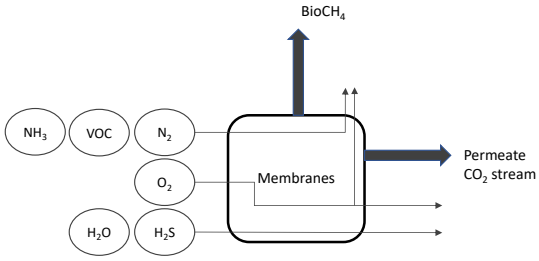

Figure 2.2d) Membrane upgrading (permeation-based technology)

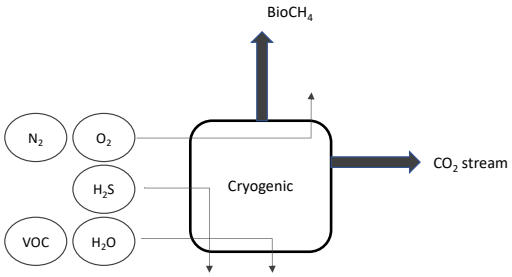

Figure 2.2e) Cryogenic upgrading (cryogenic-based technology)

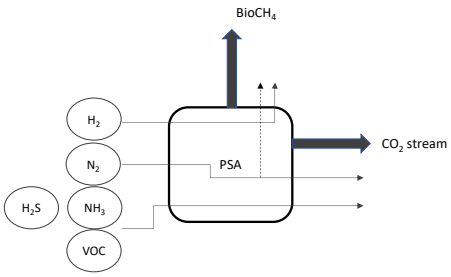

Figure 2.2f) Pressure swing adsorption (PSA) (adsorption-based technology)

Figure 2.2: Biogas trace component pathways in the different upgrading technologies. Adapted from Hoyer et al. (2016)

Membranes are sensitive to liquid water, oil and solid particles. VOCs, H_2S, and ammonia may cause acid formation on the membrane surface, thus requiring their removal prior to biogas upgrading. Biogas shall be maintained below the

dew point during all the process. Downstream de-oxygenation may be required according to the quality demands of final use (Hoyer et al., 2016).

Table 2.8: Comparison between different upgrading technologies. Adapted from CryoPur (2017); Q. Sun et al. (2015); TUV (2012); Kvist and Aryal (2019).

Technology	CH_4 purity	CH_4 slip	Pressure delivery	Energy	Heat
	%		bar	kWh/Nm^3	
Amine scrubbing	97.0–99.0	<1.00	0.00	$0.50_{raw\ gas}$	0.5-1
Water scrubbing	96.0–99.0	2.00	4.00-8-00	$0.45–0.90_{clean\ gas}$	-
Membranes	90.0–95.0	0.50–20.0	4.00-7.00	$0.25–0.43_{clean\ gas}$	-
Cryogenic	99.5	<0.50	0.00	$0.80–1.54_{clean\ gas}$	-
PSA	95.0–99.0	1.00–3.00	4.00-7.00	$0.46_{clean\ gas}$	-

Table 2.9: Capital Costs (CAPX) and operating and maintenance costs (O&M) of different upgrading technologies. Adapted from Q. Sun et al. (2015).

Technology	Capacity	CAPX	O&M	References
	m^3/h	€×$10^3/m^3.h$	€ cent/$m^3.h$	
Ammine	500	3.20	9.00	(Q. Sun et al., 2015)
	1,000	2.50		
	1,500	1.80		
Water scrubbing + reagents	500	3.10	9.10	(Q. Sun et al., 2015)
	1,000	1.80		
	1,500	1.80		
Membranes	500	2.40	6.50-10.1	(Bailón Allegue and Hinge, 2012)
	1,000	2.00	5.00-7.00	
	1,500	2.00		
Cryogenic	600	2.00	6.10	(Tajima et al., 2004)
PSA	500	3.00	6.50-9.20	(Q. Sun et al., 2015)
	1,000	2.00		
	1,500	1.50		

2.7.3 Cryogenic Separation

CO_2 removal from biogas can be performed through cryogenic separation (Figure 2.2e). The gas mixture is chilled down to less than -80 ºC (T < CO_2 sublimation point) in order to freeze and separate CO_2 from the biogas stream. The bioCH_4 stream is than chilled down to -164 ºC (T < CH_4 boiling point) to be obtained as liquid (bioLNG).

The bioCH_4 quality obtained from cryogenic separation is higher than that required for grid injection or automotive fuel. The methane slip is extremely reduced and CO_2 purity obtained allows to use it as a by-product. H_2S is removed

before upgrading in a dedicated de-sulphuring unit, generally through ACs, while VOCs and water vapor are removed during cooling and condensation. O_2 and N_2 are flashed in a bioCH_4 liquefaction step.

Cryogenic separation generally requires larger equipment than other established technologies and it is known to be high energy demanding (0.8-1.54 kWh/Nm^3) (Table 2.8) (Bauer et al., 2013). However, in October 2017, it was commissioned in Northern Ireland the first commercial cryogenic unit based on the patented CryoPur technology, which is able to produce liquid bioCH_4 and liquid CO_2 characterized by high flexibility and low electric energy consumption (0.6-0.7 kWh/Nm^3) (CryoPur, 2017). According to the last technological developments, it seems that cryogenic separation is starting to become commercially competitive.

2.7.4 Pressure Swing Adsorption (PSA)

PSA is an adsorption-based technology used already well stablished for H_2, CO_2, CH_4, N_2, and O_2 separations (Voss, 2005). PSA has been used in the last decade at full-scale for biogas upgrading (Paolini et al., 2018).

PSA can produce highly pure bioCH_4 (CH_4 > 95-99% v/v) with low energy requirements, when compared to other upgrading technologies (Riboldi and Bolland, 2015). It is characterized by excellent reliability and good scalability to medium-small plants (TUV, 2012), allowing adsorbent regeneration that reduces the environmental impacts and some energy penalties (Riboldi and Bolland, 2017).

PSA operates in cycles of adsorption/desorption onto a solid porous material (Kim et al., 2015), during which the adsorbent is subjected to pressure changes to selectively adsorb/desorb the undesired gas components. The selective adsorption occurs due to the different equilibrium capacities (adsorbent equilibrium) or due to different uptaking rates (adsorbent kinetics) provided by the adsorbent used (Augelletti et al., 2017; D. Ruthven et al., 1994).

The basic PSA Skartstrom cycle includes 4 steps (pressurization, adsorption, blowdown, and purge) (D. Ruthven et al., 1994). Biogas is fed into the columns at a pressure that ranges from 6 to 10 bar; CO_2 (heaviest product) is separated from CH_4 (lightest product) during the adsorption step, while CH_4 is withdrawn from the column (Esteves, 2005). The bed regeneration is performed during the blowdown step by reducing the total pressure of the system. Vacuum or temperature can be additionally used for bed regeneration and CO_2 complete desorption; herein, the process is termed Vacuum Swing Adsorption (VSA) or

Temperature Swing Adsorption (TSA), respectively (Shih-Perng, 1999). The purge step ca be performed by the lightest product or by an inert gas at low pressure, in order to prepare the adsorbent bed for the next cycle. During the purging cycle, a less pure heavy by-product is collected.

However, the basic PSA Skarstrom cycle configuration has high CH_4 slip and is characterized by some inefficiencies, due to the presence of some CH_4 and residual pressure in the blowdown gaseous stream. The addition to this basic Skarstrom cycle, one or more pressure equalization steps increases the separation performance and minimizes the energy losses, but also adds complexity to the process (Riboldi and Bolland, 2015).

A trade-off situation is achieved in PSA units with four-columns employing up to two pressure equalization steps before the blowdown step (Grande, 2011; Petersson and Wellinger, 2009). Common adsorbents used in PSA units are ACs, natural and synthetic zeolites, silica-gel, and carbon molecular sieves. Metal-Organic Frameworks (MOFs) are gaining consensus as potential alternatives to ACs (Schell et al., 2013) with promising results (Casas et al., 2013) for PSA application, although further research and production costs reduction are still largely desirable.

Siriwardane et al. (2001) demonstrated that ACs can provide better performances than zeolites when CO_2 partial pressure is higher than 1.7 bar. However, further studies are needed to produce ACs with high selectivity and that do not easily saturate at low CO_2 pressures to allow their easier regeneration (Riboldi and Bolland, 2017). The use of renewable biomasses can be of interest to produce such ACs aiming to reduce the production costs. To authors' knowledge, no PSA system was studied based on the use of ACs produced from MCW.

Regarding the impurity's pathway during PSA process (Figure 2.2f), H_2S irreversibly contaminates the adsorbent; therefore, it must be removed upstream the upgrading process. Likewise, ammonia and VOCs removal are performed in a pre-conditioning column before the upgrading process. H_2 goes with the final product (bioCH_4), while O_2 and N_2 can be removed along with CO_2 during PSA (Hoyer et al., 2016). The presence of these latter contaminants reduces the CO_2 adsorption capacity of the adsorbent.

From the point of view of the investment and operational and maintenance (O&M) costs, there is not the "best technology", because the upgrading cost of all technologies is quite similar, decreasing only with the increase of plant capacity

(Bauer et al., 2013; Petersson and Wellinger, 2009). Bauer et al. (2013) stated that the energy required to upgrade 1 m^3 of biogas is approximately 0.2-0.3 KWh.

The selection of an upgrading technology for biogas depends mainly on (i) local factors, (ii) state of investigation, (iii) economic resources available, and (iv) biogas quality that must be upgraded.

2.7.5 Future Challenges

The biogas upgrading technologies are well stablished and available at industrial scale. Nevertheless, further studies on new materials for scrubbing, permeation and adsorption are needed, in order to improve the efficiency of these technologies, promote their economic sustainability and contribute for the recycling of by-products from agriculture and industrial sectors under the concept of Circular Economy.

2.8 Future challenges for the contribution of MCW to bioCH_4 market

By the end of 2015, there were 430 bioCH_4 plants in the International Energy Agency (IEA) Task 37-member countries, with 188 plants in Germany, 59 in Sweden, 50 in the United Kingdom and 29 in Switzerland. Germany remains the leader in this sector, with 185 bioCH_4 plants and 10,846 biogas plants (Hoyer et al., 2016).

BioCH_4 potential is estimated to increase from 300 x 10^6 Nm^3/y in 2010, up to 18,000 x 10^6 N m^3/y in 2030 (EBA, 2015), suggesting that bioCH_4 is a consolidated marked with a positive trend that will continue in the near future (URL2, 2016). Therefore, opportunities for integrating bioCH_4, particularly in Europe and USA, are rising due to the spread of infrastructures for compressed natural gas (CNG) vehicles and fuel stations. The introduction of the European quality standard for bioCH_4 injection in NG grid networks, as well as for its use as automotive fuel, will contribute to its full integration into the traditional markets.

The maize silage is yet one of the most used lignocellulosic substrates currently used in biogas industry, although it comes, in most of the cases, from dedicated energy crops that inevitably compete with the arable land availability for food production. The substitution of maize silage for MCW as co-substrate for AD can contribute positively to a better integrated management of crops

through residual waste valorisation, thus reducing negative environmental impacts currently associated with energy crops. Additionally, the use of MCW to produce ACs for biogas conditioning and upgrading will allow as well to integrate and close the cycle of the proposed biorefinery, with the development of high added-value sub-products, such as activated carbons of different grade.

3

Pre-Treatment and Anaerobic co-Digestion of MCW with OFMSW

3.1 Introduction

As reviewed in the previous Chapter 2, several pre-treatments may be applied to MCW prior to AD with the aim of enhancing biogas and methane yields during AcoD.

Mechanical pre-treatments are energy demanding, but in most of the cases an initial size reduction seems an important step before any submission of MCW to AD (Chongkhong and Tongurai, 2014 ; Y. Zheng et al., 2014).

Thermal and thermo-chemical pre-treatments can be very effective, although according to the temperature and to the catalyst chosen, the formation of inhibitors, in concentrations that can be detrimental for methanogens, may occur. Microwave Irradiation, as a non-conventional heating source, heats MCW uniformly, quickly and can help to avoid large temperature gradients, limiting the formation of inhibitors (Li et al., 2016).

If a strict chemical pre-treatment is applied, the choice of the catalyst is crucial for the economic viability of the process. Among the catalysts that may be used for MCW pre-treatment, NaOH is the most tested due to its high efficiency and low cost. Recently, the High Boling Solvents, as glycerol, were recognized by some authors to have a high solubilization potential and due to their capacity to remain liquid at high temperatures (Diaz et al., 2015; Moretti De Souza et al., 2014). Finally, H_2O_2 can be considered as one of the most suitable catalysts for improving the methane yield on lignocellulosic biomass, due to its effectiveness

without producing any significant inhibition to the AD process, and to its relatively low cost (Banerjee et al., 2012; Song et al., 2014).

Several studies are available in literature on AcoD of maize waste (Table 2.3). Owamah and Izinyon (2015) demonstrated that maize waste can enhance biogas and methane yields when used as co-substrate along with food waste, while Ramos-Suárez et al (2017) observed that oxidative pre-treatments on maize straw can enhance biogas and methane yields. On the other hand, Hutňan (2016) showed that the presence of standalone maize wastes submitted to size reduction without any other pre-treatment, provides biogas yields comparable to those obtained with pre-treated maize wastes, suggesting that the use of a pre-treatment prior to AcoD is not a guarantee of biogas and methane yields enhancement.

In this Section, the efficiency of selected pre-treatments of MCW are studied towards the enhancement of biogas and methane yields during AcoD with pre-hydrolysed OFMSW (hOFMSW). For this purpose, microwave irradiation (MW) catalysed by NaOH, glycerol and H_2O_2, along with a room temperature chemical pre-treatment catalysed by H_2O_2 were tested.

This Section represents the development of the **Task 2** of this work.

3.2 Material and Methods

3.2.1 Feedstock

For the laboratory assays, a pre-hydrolysed OFMSW (hOFMSW) was used. This hOFMSW was collected from the hydrolysis tank of a Portuguese AD plant, located in Lisbon region. This AD plant collects the OFMSW from canteens, restaurants and malls. The hOFMSW was stored at 4 ºC in glass bottle until use. Samples of the hOFMSW were collected with an adequate frequency to guarantee the freshness of the organic matter along the studies.

MCW was collected from a local farmer located in Coruche area, in Lisbon surroundings. The MCW was air-dried to a final moisture content of 13% w/w and then ground to particles of size within the range of 2-4 mm through a Retsch SM 2000 mill. The grounded MCW was then stored in closed plastic bins at 4 ºC to be used later on.

3.2.2 Feedstock Characterisation

3.2.2.1 hOFMSW

The characterization of hOFMSW included the following parameters: Total Solids (TS), Ashes and Volatile Solids (VS) (method 2540); total Chemical Oxygen Demand (tCOD) and soluble Chemical Oxygen Demand (sCOD)(method 5220 B)(APHA et al., 2005) Total Kjeldal Nitrogen (TKN) (method ISO 5663:1984), Ammonium Nitrogen (NH_4-N) (method ISO 5664:1984), and Organic Nitrogen (o-N); phosphorus (P) (method ISO 6878:2004); Elemental Analysis (EA); Volatile Fatty Acids (VFAs) as Acetic Acid (AA), Formic Acid (FA), Propionic Acid (PA) and Butyric Acid (BA). Each determination was performed in duplicate.

EA was performed on the dried hOFMSW (2h at 105 °C ±1 °C) in a Thermo Finnigan Elemental Analyzer - CE Instruments, model Flash EA 1112 (CHNS). VFAs were analysed with a HPLC system (Dionex ICS3000, USA) equipped with Biorad Aminex 87H column, pre-column and UV detector at 210 nm. The eluent used was H_2SO_4 10 mN, with a flow rate of 0.6 ml/min, at 30 °C. The characterisation of the hOFMSW is reported in Table 3.1.

Table 3.1: Characterisation of the hOFMSW (average ± standard deviation)

Parameters	Units	Values
TS	% w/w	5.63 ± 0.45
VS	% w/w	4.55 ± 0.35
Ashes	% w/w	1.09 ± 0.11
tCOD	gO_2/L	87.7 ± 4.36
sCOD	gO_2/L	32.7 ± 1.88
P	g/L	0.49 ± 0.075
TKN	g/L	2.87 ± 0.66
NH_4-N	g/L	1.50 ± 0.09
o-N	g/L	1.37 ± 0.13
C	% w/w db	52.2 ± 7.66
N	% w/w db	5.41 ± 0.97
H	% w/w db	6.93 ± 0.96
S	% w/w db	1.84 ± 0.23

TS (5.6%) and VS (4.5%) are relatively low, implying that the lab-scale digester had been operated under the liquid state anaerobic digestion condition (L-AD). tCOD and sCOD are significantly higher than typical values found in literature for OFMSW (Cesaro et al., 2012; Cesaro and Belgiorno, 2013).

The C:N ratio of hOFMSW is 9.6 ±0.3, which is considerably lower than the optimal value (25) for AD according to literature. This shows a low carbon contribution useful for cell structure maintenance (X. Wang et al., 2012).

The ratio C:N:P in hOFMSW is 106:11:1. Again, this ratio presents unbalanced values of C relatively to the optimum C:N:P ratio for methane yield, which was reported in literature to be 200:5:1 (Lo et al., 2010).

In the absence of specific references in literature concerning the composition of hOFMSW, CHNS results obtained in dry basis (db) were compared to the average values found for OFMSW for 22 European and non-European countries (Campuzano and González-Martínez, 2016).

C, N and S contents quantified in the present study were 12%, 86% and 613% higher, respectively, than the typical values pointed out for the other countries. This evidence and the high concentrations of tCOD and sCOD are probably due to the fact that, in the local plant, the hOFMSW is mixed with anaerobic sludge pumped back before the hydrolysis take place.

H does not show any significant variation in comparison with literature (6.93 w/w db *vs* 6.6% w/w db in the literature) (Campuzano and González-Martínez, 2016).

3.2.2.2 MCW

The characterization of MCW included the following parameters: moisture content, TS, Ashes, VS, TKN, NH_4-N, o-N, P, EA, lignin, cellulose and hemicellulose. The analytical methodologies were the same as described in the section above. Lignin, cellulose and hemicellulose contents were assessed according to the Forage Fibre Analysis included in the 379th Agriculture handbook (Goering and Van Soest, 1970).

Table 3.2 shows the experimental data obtained from the chemical characterization of MCW.

Hemicellulose and lignin percentages obtained agree with the data reported in the literature. The cellulose percentage found in this work (29.8% w/w db) is slightly lower than the typical values present in literature, which range within 32-46% w/w db (M. Li et al., 2014; Lopez Torres and Ma del C. Espinosa, 2008; Menon and Rao, 2012; Su et al., 2015).

Table 3.2: Chemical characterisation of the MCW (average ± standard deviation).

Parameters	Units	Values
Cellulose	% w/w db	29.8 ± 1.2
Lignin	% w/w db	19.3 ± 1.7
Hemicellulose	% w/w db	45.2 ± 4.0
Moisture	% w/w	13.0 ± 0.1
TS	% w/w	91.0 ± 4.0
VS	% w/w	90.0 ± 4.0
Ashes	% w/w	1.50 ± 0.0
TKN	g/kg	2.30 ± 0.7
P	g/kg	0.40 ± 0.1
C	% w/w db	41.7 ± 0.2
N	% w/w db	<0.10 ± 0.0
H	% w/w db	5.60 ± 0.2
S	% w/w db	<0.01

db: dry basis

The percentages obtained of C and N (41.7% w/w db and <0.1% w/w db, Table 3.2), are in good agreement with the literature data (36.8% w/w db and <1% w/w db) suggesting that MCW is a C-based material that can be used to improve the efficiency and stability of an AD process (Altintig et al., 2016).

The TKN and P percentages obtained are slightly lower (0.23% w/w db and 0.04% w/w db, respectively) than the one reported in literature (0.33% w/w db and 0.11% w/w db, respectively) (National Research Cuncil, 1982).

3.2.3 Pre-Treatments of MCWs

In order to remove lignin and solubilise part of the hemicellulose and cellulose into digestible sugars, MCW was submitted to microwave-assisted chemical pre-treatments and to chemical pre-treatments at room temperature (23 °C) in the presence of different catalysts.

The pre-treatment conditions were chosen based on the best pre-treatment results reported in literature, trying to optimize them with the final aim of saving chemicals (NaOH) and energy (exposure time during microwave irradiation). The pre-treatment conditions applied are reported in the Table 3.3.

For MCW pre-treatments, 0.5 g of grounded MCW was suspended in 40 mL of different catalyst solutions and then transferred to an Ethos 1600 microwave system operating at a frequency of 2450 MHz (Milestone Microwave Laboratory

System, USA). The pre-treatments were performed, at 160 ºC of temperature without stirring during 10 minutes. The chemical pre-treatment was performed at room temperature without stirring in the presence of 1 g of grounded corncob and 40 mL of catalyst solution.

Table 3.3: Experimental conditions of the pre-treatment to which MCW was submitted in the initial screening phase.

Pre-Treatment	Catalyst	Catalyst solution	T	t
			ºC	min
MW[1]	NaOH	2%, 4%, 6%, 10%, 20% wNaOH/wMCW	160	10
	Glycerol + H_2O	95% v/v glycerol + 5% v/vH_2O		
	Glycerol + NaOH	95% v/v glycerol + 5% v/v NaOH (1.0 N) 95% v/v glycerol + 5% v/v NaOH (1.5 N)		
	H_2O_2	H_2O_2/MCW(wH_2O_2/wMCW): 0.125, 0.25, 0.5, 1.0; alkaline water (pH 9.8); 2% MCW w/v		
Chemical[2]	H_2O_2	H_2O_2/MCW (wH_2O_2/wMCW): 0.125, 0.25, 0.5, 1.0; alkaline water (pH 9.8); 2% MCW w/v	23	240

[1]: Microwave assisted pre-treatment, [2]: Chemical pre-treatment at room temperature

All pre-treated samples were filtered through Gooch crucibles under vacuum (Vacuubrand GMBH, Germany). The remaining solid fraction was dried at 105 ºC, during 2 h, and weighed before being submitted to lignin, cellulose and hemicellulose quantifications. The liquid fraction was analysed for glucose, fructose, xylose, arabinose and inhibitors: phenolic compounds, furfural and the most common hydroxymethilfurfural-5-hydroxymethilfurfural (5-HMF). Duplicates have been analysed to check reproducibility.

Glucose, fructose, xylose and arabinose concentrations were determined using a High-Performance Liquid Chromatography (HPLC) (ICS 3000 DIONEX) equipped with DIONEX Carbopac PA10 250x4 mm column, pre-column and Pulsed Amperometric Detection (PAD). A solution of 18 mM NaOH was used as mobile phase, at a column temperature of 30 ºC.

Phenolic compounds were determined in the liquid phase of the pre-treated samples by HPLC (Dionex ICS3000, USA) equipped with Waters NovapaK C18 column and pre-column with PDA photodiode array, able to detect at 280 nm, 320 nm e 365 nm, in presence of a methanol gradient in 2% CH_3COOH, at 30 ºC.

Furfural and 5-HMF were determined in the liquid phase of the pre-treated samples by HPLC (Thermo Surveyor and Dionex ICS3000) equipped with Bio-rad Aminex 87H column, pre-column, and UV 280 nm detector, in the presence of 10 mN H_2SO_4, at a flowrate of 0.6 ml/min, at 40 ºC.

The pre-treatment that presented the best balance between the highest concentration of sugars in the liquid fraction, low inhibitors generation and higher lignin, cellulose and hemicellulose solubilisation (Pre1) was then optimized according to the conditions listed in Table 3.4.

The samples obtained in the pre-treatment optimisation were submitted to the same filtration process and analytical determinations done in the first pre-treatment phase. After this optimisation phase, the pre-treatment that presented the best balance in terms of sugars, lignin, cellulose and hemicellulose solubilisation and inhibitors production was identified as Pre2.

With the aim of assessing the impact of the lignin, cellulose and hemicellulose solubilisation on biogas and methane yields during AcoD, the pre-treatment that provided the best balance in terms of monomeric sugar solubilisation and inhibitors production, but characterised by the lowest lignocellulosic biomass solubilisation, was identified as Pre3.

Table 3.4: Optimisation conditions of the Pre-treatment Pre-1.

Pre-Treatment	Catalyst	Catalyst solution	T	t
			ºC	d
Chemical[1]	H_2O_2	0.5 H_2O_2/MCW (wH_2O_2/wMCW): alkaline water (pH 9.8); 2% MCW (wMCW/v alkaline water)	23	1 and 2
		0.5 H_2O_2/MCW (wH_2O_2/wMCW): alkaline water (pH 11.5); 2% MCW (wMCW/v alkaline water)		0.17, 1 and 2
		0.5 H_2O_2/MCW (wH_2O_2/wMCW): alkaline water (pH 9.8); 10% MCW (wMCW/v alkaline water)		0.17, 1, 2 and 3
		0.5 H_2O_2/MCW (wH_2O_2/wMCW): alkaline water (pH 11.5); 10% MCW (wMCW/v alkaline water)		0.17, 1 and 2

[1] Chemical: Chemical pre-treatment at room temperature

3.2.4 Efficiency Assessment of MCW Pre-treatments

The efficiency assessment of MCW pre-treatments was performed through the quantification of monosaccharides, phenolic compounds, furfural, 5-HMF, lignin, cellulose and hemicellulose.

Lignin, cellulose, and hemicellulose removals were calculated according to Eq. 3.1:

$$\alpha\ removal\ (\%) = \left(1 - \frac{\%\ \alpha\ after\ pre-treatmment}{\%\ \ \alpha\ in\ MCW}\right), \qquad (Eq\ 3.1)$$

where α stands for lignin, cellulose, and hemicellulose percentages, respectively.

The lignin, cellulose and hemicellulose removals were statistically analysed through t-Student test and ANOVA ($p<0.05$) using SPSS IBM software in order to compare different pre-treatment conditions.

3.2.5 Anaerobic Digestion Assays

AD assays were carried out in a 2.1 L lab-scale stirred reactor (New Brunswick Scientific, NY, USA), equipped with controlling systems for temperature, pH (Hanna Instruments HI8711E) and redox potential (Orion, 290A).

The AD assays were carried out under thermophilic conditions (50 ºC ± 2 ºC) at a pH of 8.0. This is the natural value for the anaerobic sludge inoculated in the digester.

The AD lab unit was inoculated with 500 mL of anaerobic sludge that was obtained from an industrial scale thermophilic digester. The redox potential was always below -350 mV. The hOFMSW used in the AD assays is the same used in the industrial scale digester.

Figure 3.1 shows a flowsheet the AD lab unit used in the present work.

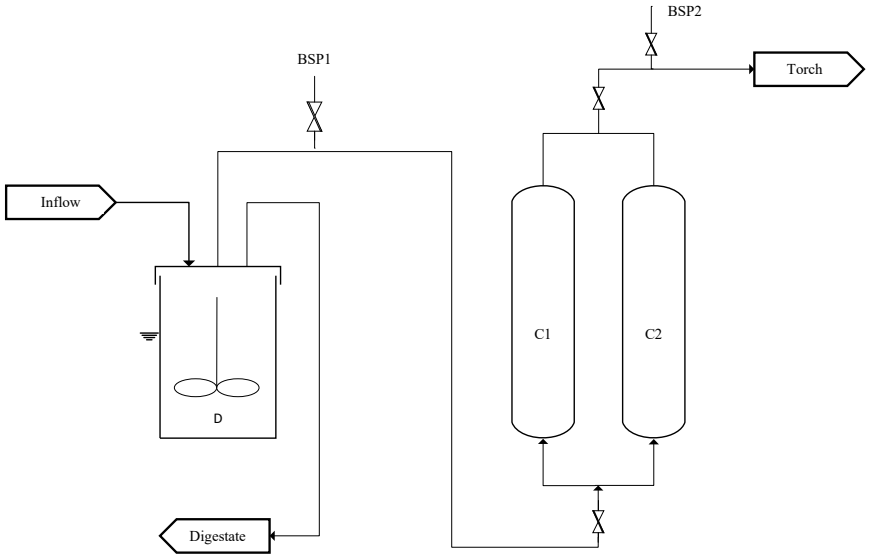

Figure 3.1: Completely mixed AD lab scale unit. Acronyms: D - Digester; BSP# - Biogas sampling point; C# - Water columns.

The biogas line includes two water columns with a total volume of 6720 mL (C1 and C2 in Figure 3.1) used for biogas volume measurement.

The anaerobic digester operation started with the hOFMSW at an inflow of 0.1 L/d, an hydraulic retention time (HRT) of 21 d and an Organic Load Rate (OLR) of 2.16 g SV/(L.d), until the biogas production achieved stability.

The feeding condition was like the industrial scale digester in order to simulate the real operational conditions at the industrial plant.

MCW pre-treated under Pre1, Pre2 and Pre3 conditions and untreated MCW was then co-digested with the hOFMSW at an OLR of 2.48 g VS/(L.d), representing an OLR increase of 15%.

The efficiency of the AcoD process was assessed in terms of biogas and methane yields, removal percentages of TS, VS, tCOD, and sCOD. TKN, NH_4-N, o-N and VFAs were considered as indicators of the process stability. All the analyses were performed at least in duplicate.

Biogas and methane efficiencies were calculated according to Eq. 3.2:

$$\eta_{\alpha} = \left(\frac{V_{\alpha}}{OLR \times V_{inflow}}\right), \qquad (Eq\ 3.2)$$

where α stands for biogas or methane, V_α is the volume of α produced (L), OLR is the Organic Load Rate (gVS/ L.d) and V_{inflow} is the volume of substrate fed per day (L/d).

The removal efficiencies of VS, TS, tCOD and sCOD were assessed by Eq. 3.3:

$$\eta_i\ removal\ (\%) = \left(\frac{C_{i,inflow} - C_{i,digestate}}{C_{i,inflow}}\right) \times 100, \qquad (Eq\ 3.3)$$

where C_i stands for the concentration of solids (g/L) or COD ($mg/O_2.L$) either in the flow or in the digestate.

The biogas Low Heating Value (LHV) was calculated according to the Eq. reported by IPCC (2006) (Eq. 3.4)

$$LHV(MJ/m^3) = \sum_{i=1}^{n} HHV_i\ x_i - (0.212\ H - 0.0245\ M - 0.008\ Y), \qquad (Eq.\ 3.4)$$

where HHV_i is the High Heating Value of the component i (MJ/m^3), x_i is the volume fraction (% v/v) of the component i in the biogas stream, and H, M and Y are the volume percentages of H_2, moisture and O_2, respectively.

3.2.5.1 Analytic Methods for AD Efficiency Assessment

The biogas composition (CH_4, CO_2, O_2, N_2, H_2S) was determined by gas chromatography (GC), according to the standard ASTM D 1946, using a gas chromatograph (Varian 430-GC) equipped with a split injector with He (63.5 mL/min), at 80 ºC, and thermal conductivity detector (TCD), operating at 120 ºC. A fused silica column (Select Permanent Gases/CO_2 HR-molsieve 5A/Borabound Q tandem #CP7430) was used. H_2S concentration was determined by a GC Varian CP-3800 equipped with a split injector 1:100 at 60 ºC and Pulsed Flame Photometric Detector (PFPD) at 200 ºC. A CP-SIL 5CB 30m x 0.32mm x 4 µm column, operating at 40 ºC, in the presence of He, was used. At least, duplicate samples were analysed.

TS, Ashes, VS, tCOD, sCOD, TKN, NH_4–N, o-N, VFAs and EA were performed according to the same methodologies described in section 3.2.2.

3.3 Results and Discussion

3.3.1 Pre-treatments

3.3.1.1 Pre-treatments Screening

Lignin, cellulose, hemicellulose and monomeric sugars solubilisations as well as inhibitors production obtained in the screening pre-treatments phase are reported in Figures 3.2, 3.3 and 3.4.

In this first set of the pre-treatments, no lignin removal occurred, and cellulose removal never exceeded 11.3% (room temperature, H_2O_2/biomass ratio of 0.5, 2% MCW w/v, pH of 9.8). Hemicellulose solubilisation preferentially occurred with microwave irradiation pre-treatment catalysed by NaOH, with a maximum percentage of 34.7% in the presence of 20% NaOH. Slight hemicellulose solubilisation (3.94%) was observed with chemical pre-treatment at room temperature, a H_2O_2/ biomass ratio of 0.125, 2% MCW w/v and pH of 9.8.

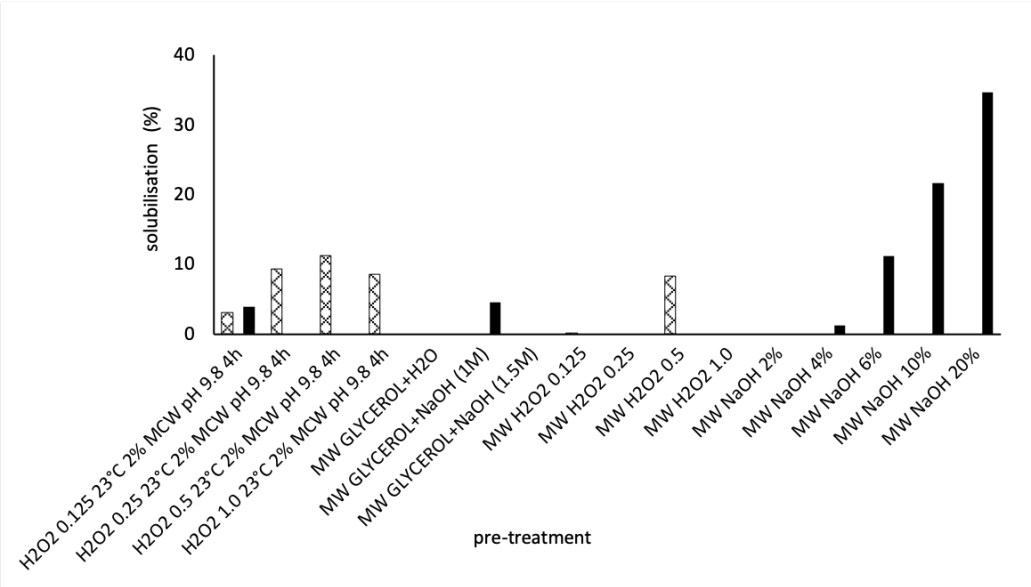

Figure 3.2: Cellulose, lignin and hemicellulose solubilisation of MCW in the pre-treatment screening phase. Checkerboard and solid black bars represent cellulose and hemicellulose solubilisation, respectively.

Microwave irradiation pre-treatments catalysed by NaOH, for all the concentrations tested, showed no delignification, no cellulose solubilisation and moderate hemicellulose removal.

Previous results obtained by Chen et al. (2013) on corn stover after microwave irradiation pre-treatment catalysed by NaOH/corn stover ratio of 0.077, at

95 ºC, during 30 minutes of reaction time, produced approximately 65% lignin solubilisation.

In the present study, higher temperature (160 ºC) and similar NaOH/biomass ratio (0.1) did not promote a significant lignin solubility. This difference may be related with two factors: the residence time that, in the present study, was 3 times lower than in Chen's *et al*. assays (10 *vs* 30 minutes), and to the higher resistance offered by cob to hydrolysis than by corn stover.

No lignin or cellulose removals were detected with MW pre-treatment catalysed by glycerol either in presence or absence of alkaline water. Very low hemicellulose solubilisation (4.59%) was detected with MW catalysed by glycerol and NaOH (1M). These results are apparently in contrast with the work of Diaz et al. (2015) that reported 29.5% and 22.6% delignification after having immersed corn straw in aqueous glycerol solution (95% v/v) and in an alkaline glycerol solution (95% v/v glycerol-NaOH 1.4 M), respectively, during 16 hours, before MW irradiation. Moretti De Souza et al. (2014), on the other hand, obtained 15.8% lignin removal on sugar cane bagasse after having pre-treated the biomass with pure glycerol during 24 h, before submitting it to microwave irradiation for 5 minutes, at 2450 mHz. Comparing all these results, it seems that residence time of the chemical pre-treatment before microwave irradiatio, is more effective for lignin solubilisation than MW pre-treatment itself.

H_2O_2 pre-treatment did not allow any lignin solubilisation. Only slight cellulose and hemicellulose solubilisations were observed (8.12% and 0.98% at room temperature, 2.9% and 0% with MW, on average respectively) (Figure 3.2). This result is confirmed by literature, where very little lignin was solubilized below pH of 11, with 4 hours of reaction time, whereas 30% of the lignin was solubilized at pH of 13 (Gould, 1985).

The highest cellulose removal (11.3%) was observed after the pre-treatment performed at room temperature with a H_2O_2/biomass ratio of 0.5 w/v, pH of 9.8 and 2% of MCW w/v.

Figure 3.3 shows the experimental data of the solubilisation of monomeric sugars after the pre-treatment screening phase.

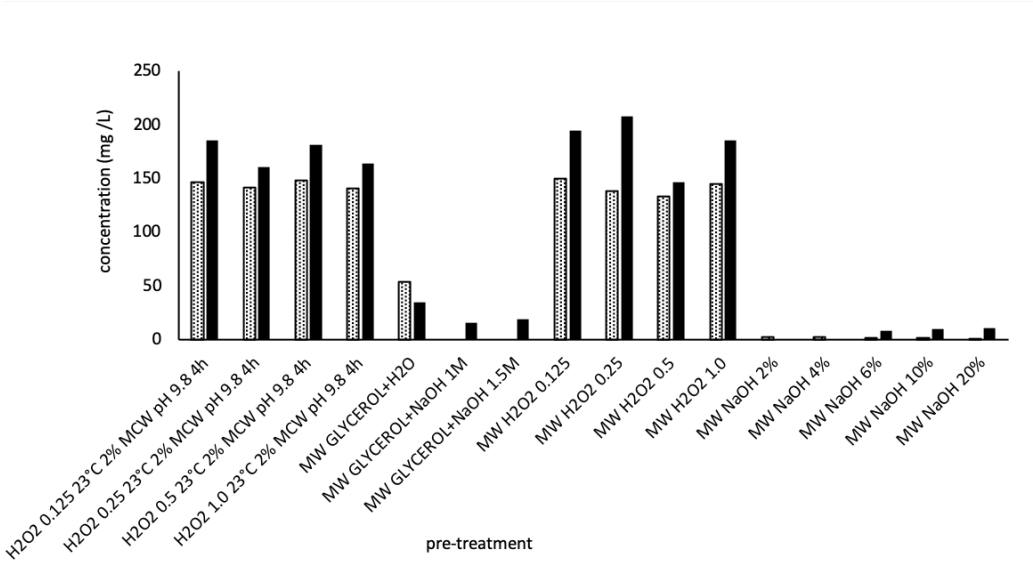

Figure 3.3: Concentration of monomeric sugars in the liquid phase resulting from the pre-treatment screening phase. Dotted and solid black bars stand for glucose and fructose concentrations (mg/L) in the liquid phase, respectively.

Glucose and fructose were detected in all samples, whereas arabinose or xylose were never detected in any of the pre-treatment's eluates. MCW-assisted pre-treatments produced significant glucose and fructose solubilisation, with average concentrations of 142 mg/L, glucose and 183 mg/L fructose only when catalysed by H_2O_2. The ANOVA ($p<0.05$) shows that no significant differences were detected between glucose and fructose solubilisation, either with or without microwave irradiation.

MCW-assisted pre-treatments catalysed with NaOH produced very low glucose (1.44 mg/L) and fructose (5.66 mg/L) solubilisation, when compared with the MCW catalysed by H_2O_2 at any NaOH load. This is in agreement with the work of Boonsombuti and Luengnaruemitchai (2013) which did not found any sugar release from corncob after MW-assisted pre-treatment catalysed by 0.75 - 3% w/v NaOH, at 120 ºC, during 30 minutes. Similar results were obtained by Chen et al. (2013) that found 95% glucan recovery from the corn stover solid phase, after MW pre-treatment, for all temperatures (74 ºC – 130 ºC) and times (30 - 102 minutes) tested.

Microwave assisted pre-treatment catalysed by glycerol showed low solubilisation rates of sugars. In the presence of water, glucose and fructose solubilisations were 53.8 mg/L and 34.5 mg/L, respectively, while in the presence of alkaline water (NaOH 1.0M and NaOH 1.5M) this pre-treatment produced, for both cases, low sugar yields (no glucose solubilisation was registered, and

fructose solubilisation was lower than 20 mg/L). These results are in agreement to those obtained by Diaz et al. (2015). These authors showed that polysaccharides were not significantly degraded during the MCW pre-treatment catalysed by glycerol in either the presence or absence of NaOH.

Room temperature chemical pre-treatment catalysed by H_2O_2, with 4 hours of reaction time, showed interesting concentrations of glucose and fructose, with the highest glucose and fructose concentrations of 148 mg/L (0.5 H_2O_2/biomass ratio) and 186 mg/L (0.125 H_2O_2/biomass ratio), respectively.

Based on the results obtained, it is possible to conclude that microwave assisted pre-treatment catalysed by H_2O_2 do not carry, under the conditions applied, any significant improvements in terms of sugar solubilisation when compared with the pre-treatments carried out at room temperature in the presence of H_2O_2.

In all the pre-treated samples analysed, neither furfurals nor 5-HMF have been detected (DL furfural: <3.5 mg/L; DL 5-HMF: <3.9 mg/L). Literature data suggest that furfural concentrations higher than 20 mM (1.92 g/L) can strongly inhibit *Methanococcus deltae* growth (Belay and Voskuilen, 1997). On the other hand, Pekařová et al. (2017) found that concentrations of furfural below 1.0 g/L does not produce any significant inhibition, whereas HMF concentrations higher than 0.2 g/L can cause noticeable inhibition on methanogens.

The experimental results obtained in this pre-treatment phase are quite below the concentrations that can cause inhibition of AD process.

p-Coumaric acid (p-CA) and Ferulic Acid (FA) were the main phenolic compounds produced during pre-treatments, followed by minor concentrations of Caffeic (CA), Syringinc (SA), Vanillin (VA), Vanillic (VnA) and Chlorogenic (Cl) acids. The production of phenolic compounds was higher in the samples pre-treated with MW irradiation in the presence of NaOH, with an average of 108 mg/L p-CA and 54.3 mg/L FA. The highest concentrations were detected in the samples pre-treated with 20% NaOH (215 mg/L p-CA, 105 mg/L FA, 7.9 mg/L VA, 5.7 mg/L VnA, and 2.5 mg/L SA). These results show that NaOH is a catalyst that promotes phenolic compound formation from corncob. This evidence is confirmed by Torre et al. (2008).

These authors have reported that chemical pre-treatment performed at room temperature, catalysed with NaOH, with 1 h of reaction time, produced FA and p-CA in high concentrations, which were above than those obtained in this

work with 10 minutes MW pre-treatment at similar NaOH/biomass ratios. Hence, reaction time seems to be more important than temperature to produce phenolic compounds. Figure 3.4 shows the concentrations of the phenolic compounds detected in the liquid fractions after initial screening pre-treatment phase.

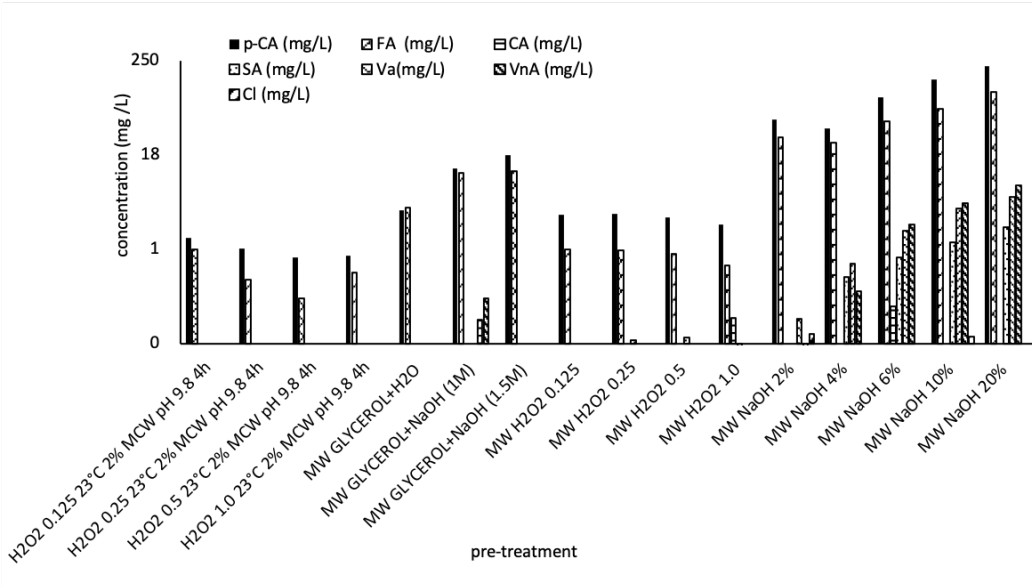

Figure 3.4: Concentration of phenolic compounds in the liquid phase resulting from the pre-treatment screening phase.

The effect of NaOH on phenolic compound production is significant, although less intense, in MW pre-treatments catalysed by glycerol with alkaline water (1.0 M and 1.5 M NaOH). During these pre-treatments, average concentrations of p-CA and FA of 15.3 mg/L and 11.5 mg/L, respectively were detected (Figure 3.4). In the presence of glycerol in water solution, the concentrations of p-CA and FA were lower (3.9 mg/L p-CA and 4.3 mg/L FA) than in the presence of alkaline water. Calabró et al. (2015) tested the effects of NaOH pre-treatment on AD of tomato processing wastes at room temperature and found that NaOH pre-treatment did not affected the methane production with NaOH concentrations within the range of 1-5% w/w.

During all the pre-treatments catalysed by H_2O_2 (MW assisted and at room temperature), phenolic compounds were always below 5 mg/L for all compounds analysed. The lowest concentrations of phenolic compounds were found in the pre-treatment at room temperature, 0.5 H_2O_2 MCW w/w (1.1 mg/L p-CA and 0.3 mg/L FA) (Figure 3.4).

Regarding the inhibitory effect of phenolic compounds on AD, literature data pointed out that during AcoD of olive mill wastewater with wine distillery wastewater by using a cuttle manure inoculum, concentrations of p-CA higher than 50 mg/L can strongly inhibit methanogenesis (Akassou et al., 2010). On the other hand, Mousa and Forster (1999) stated that Gallic acid concentration below 20 mg/L does not cause inhibition, whereas 50 mg/L Gallic acid can cause 15% decrease of methane content in the biogas. Finally, Hernandez and Edyvean (2008) observed that 1.0 g/L of Caffeic acid and Gallic acid can cause significant inhibition of the AD process.

On the basis of the results obtained, the best balance between lignin, cellulose, hemicellulose and sugars solubilisations, as well as low production of inhibitors in the pre-treatment screening phase, was obtained in the pre-treatment performed at room temperature with a H_2O_2 biomass ratio of 0.5 w/v, 2% MCW w/v, pH of 9.8, during 4 h (Pre1). Pre1 allowed i) lignin, cellulose and hemicellulose solubilisation of 11.3%, <1.0%, <1.0% respectively, ii) concentrations of 148 mg/L glucose and 182 mg/L fructose, iii) concentration of inhibitors <3.5 mg/L furfural and <3.9 mg/L 5-HMF, and 1.1 mg/L of p-CA and 0.3 mg/L FA. Hence, the most favourable pre-treatment for AD is catalysed by H_2O_2. This low inhibitor production with the use of H_2O_2 as catalyst is validated by data already reported in the literature (Saha and Cotta, 2007).

3.3.1.2 Optimisation of the Pre-treatment Pre1

Pre1 was then optimised according to the conditions reported in Table 3.4. In detail, a different pH value (11.5), solid concentration (10% MCW w/v) and reaction times (4h, 1, 2 and 3 days) at different H_2O_2/MCW ratios were tested. The solubility of lignin, cellulose, hemicellulose and monomeric sugars, as well as the production of inhibitors during this optimisation step are reported in Figures 3.5, 3.6, and 3.7.

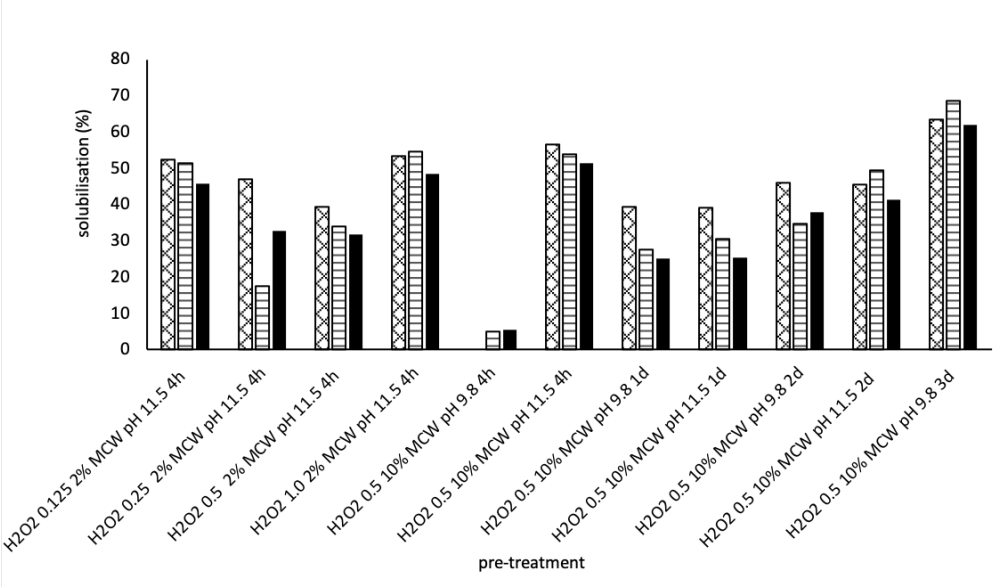

Figure 3.5: Cellulose, lignin and hemicellulose solubilisation of MCW in the pre-treatment optimisation phase. Checkerboard, horizontal lines and solid black bars represent cellulose, lignin and hemicellulose solubilisation, respectively.

Considering lignin, cellulose and hemicellulose solubilisation, the results obtained in the pre-treatment optimisation show average solubilisation percentages higher than those obtained through Pre1 in almost the assays performed.

At a reaction time of 4 h, increasing pH from 9.8 to 11.5 allowed average solubilisation percentages of 36.4% lignin, 45.8% cellulose and 35.8% hemicellulose, respectively. The highest lignin, cellulose and hemicellulose solubilisations (53.9%, 56.6% and 51.5%, respectively) were obtained at a H_2O_2/biomass ratio of 1.0, 2.0% MCW w/v and pH of 11.5. This indicates that at 4h reaction time, pH has a key role in depolymerizing MCW and disrupting lignocellulosic structure. These data are in agreement with Gould (1985), who achieved 50% lignin solubilisation, after 4h of pre-treatment, at 2% MCW w/v and 0.5 H_2O_2/biomass ratio, at pH of 11.5 and at room temperature. The very low cellulose, lignin and hemicellulose solubilisation values (0.0% w/w , 5.0% and 5.6% w/w, respectively) observed with a H_2O_2/biomass ratio of 0.5, 10% MCW w/v, pH of 9.8 and 4 h of reaction time (Pre3), can be due to the low pH value used during this pre-treatment.

The increase of solid concentration from 2% MCW w/v to 10% MCW w/v, at a pH of 11.5, with 0.5 H_2O_2/biomass ratio, increased the lignin, cellulose and

hemicellulose solubilisation (37%, 30% and 38%, respectively) (Figure 3.5). Therefore, keeping constant both pH and reaction time, the solid concentration has an important role in MCW depolymerisation.

No significant differences ($p<0.05$) were observed between the percentages of lignin, cellulose and hemicellulose solubilisations obtained at pH of 9.8 and 11.5, after 1 and 2 days of pre-treatment. This allows to conclude that, at reaction times of 1 and 2 days, a less severe pre-treatment (pH of 9.8) achieved levels of solubilisation comparable to those of a more severe environment (pH of 11.5), offering the chance to save chemicals and reducing costs related to the pre-treatments. The key role of the reaction time was already highlighted by Banerjee et al. (2011).

The best solubilisation percentages of lignin, cellulose and hemicellulose (68.6%, 63.4% and 61.9% respectively) occurred in the pre-treatment with the ratio of 0.5 H_2O_2/MCW w/w, pH of 9.8, 10% MCW w/v and a reaction time of 3 days (Pre2).

Figure 3.6 shows the solubility of sugars during the optimisation of Pre1.

Keeping constant the reaction time (4h) and the solid concentration (2% w/v), the solubility of sugars did not show any significant changes (ANOVA, $p<0.05$), when the pH was increased from 9.8 to 11.5.

On the other hand, fructose solubility increased slightly from 131 mg/L to 173 mg/L by comparison with Pre1. This evidence seems to be in contrast with the work of Banerjee et al. (2012), in which the pH control at values equal or higher than 11.5 is considered a key factor for glucose conversion and for the oxidative reaction taking place.

If MCW concentration is raised from 2% w/v to 10% w/v, keeping unchanged the pH at 11.5, reaction time at 4 h and H_2O_2/biomass ratio at 0.5, glucose and fructose solubilisations increase by 184% (383 mg/L glucose) and 218% (358 mg/L fructose). This trend is confirmed by Banerjee et al. (2011), who found higher monomeric glucose yield increasing the solid content up to 10%.

At 10% MCW w/v, with 4h reaction time and pH of 9.8 it was observed an unexpected monomeric sugar concentration in the liquid phase higher than those observed at similar conditions with pH of 11.5, showing values of 636 mg/L glucose and 710 mg/L fructose. These concentrations were always lower than those observed at higher reaction times of 1, 2 and 3 days.

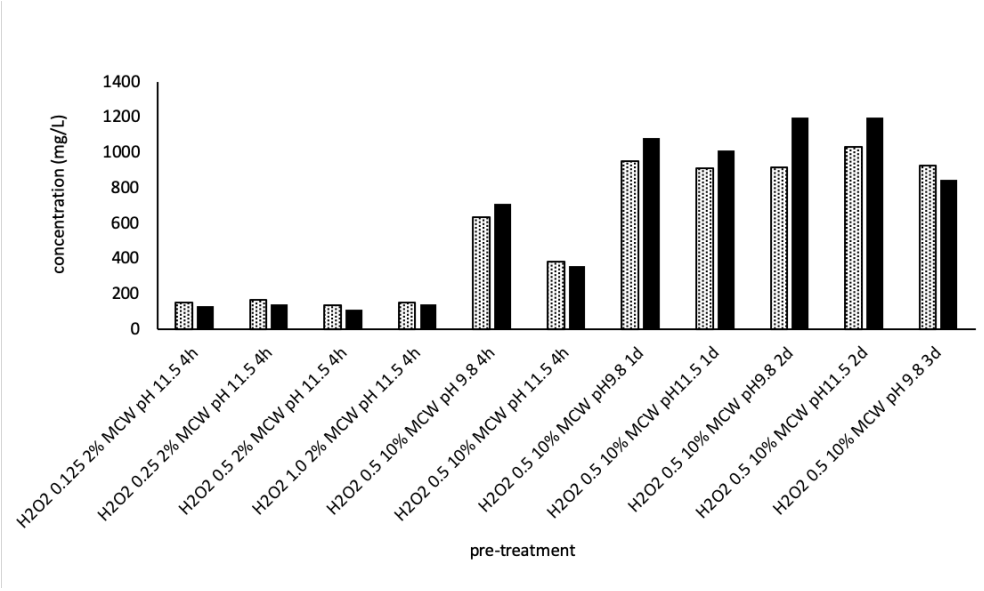

Figure 3.6. Concentration of monomeric sugars in the liquid phase resulting from of the pre-treatment optimisation phase. Dotted and solid black bars stand for Glucose and Fructose concentrations (mg/L) in the liquid phase, respectively.

Significantly higher sugar solubilisation was obtained at both pH values of 9.8 and 11.5 by increasing the reaction time from 4 hours to 1, 2 and 3 days (Figure 3.6).

This trend occurred at both pH values tested with the concentration of sugars being always above 800 mg/L after 2 days of pre-treatment.

ANOVA ($p<0.05$) showed no significant differences between glucose and fructose solubilisation when pH varied between 9.8 and 11.5, for reaction times of 1 and 2 days, keeping constant H_2O_2/biomass ratio (0.5) and solid concentration (10% w/v).

The suggestion that reaction time has a key role in the efficiency of sugar conversions is in full agreement with the literature (Banerjee et al., 2011; Saha and Cotta, 2007), thus reinforcing the idea that for longer reaction times it is possible to achieve higher sugar concentrations even at a lower pH (9.8).

Figure 3.7 shows the concentration of phenolic compounds detected in the liquid fraction during the pre-treatment optimisation phase.

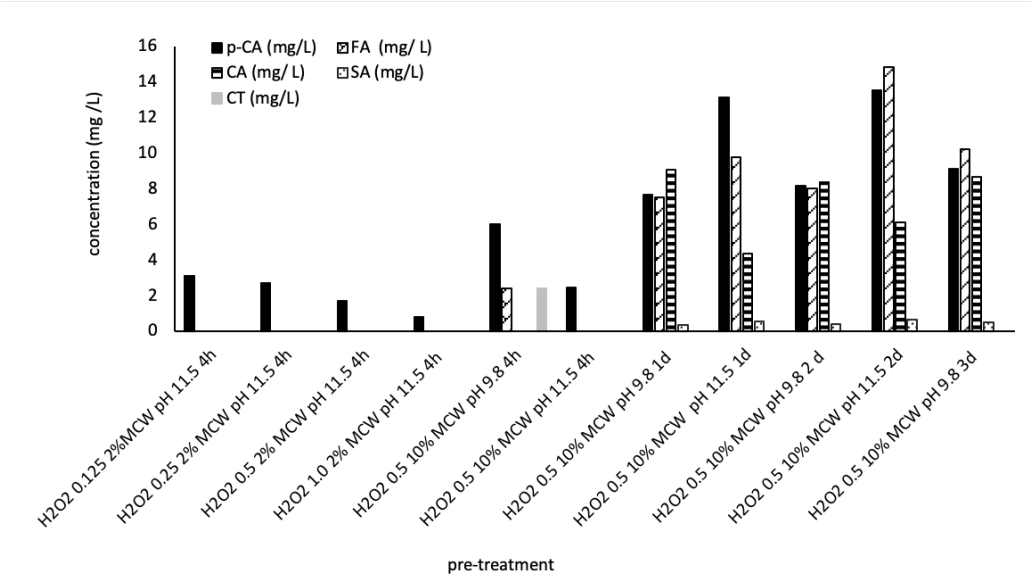

Figure 3.7: Phenolic compounds concentration in the liquid phase resulting from the pre-treatment optimisation phase.

Furfural and 5-HMF were not detected in all the pre-treated samples (DL furfural <3.5 mg/L and DL 5-HMF <3.9 mg/L).

The lowest concentrations of phenolic compounds occurred in the pre-treatments with a reaction time of 4h in most of the cases.

The p-Coumaric acid concentration slightly increased as solid concentration increased from 2% w/v to 10% w/v, showing value of 6 mg/L p-Coumaric acid, 2.4 mg/L Ferulic acid, 3.5 mg/L Caffeic acid and 2.4 mg/L Protocatechuic (CT) acid were produced during the pre-treatment characterised by ratio of 0.5 H_2O_2/MCW w/w, pH of 9.8 and 10% MCW w/v (Pre3) (Figure 3.7).

The lowest inhibitor concentrations obtained for H_2O_2 pre-treatments, at a reaction time of 4 hours, were of 3.1 mg/L p-CA (0.125 H_2O_2/biomass, 4h, 2 MCW % w/v – Figure 3.7) and 1.34 mg/L FA (0.125 H_2O_2/biomass, 4h, 2% MCW w/v - Figure 3.3) for both pH and solid concentration tested.

Increasing the reaction times to 1, 2 or 3 days and maintaining unchanged the solid concentration at 10% w/v, H_2O_2/biomass ratio at 0.5 and pH at 9.8, the phenolic compounds increased approximately two-fold when compared to the pre-treatment carried out with 4 h reaction time under the same conditions. This pre-treatment produced 8.3 mg/L p-CA, 8.6 mg/L FA, 8.5 mg/L CA and 0.4 mg/L SA.

Reaction times of 1 and 2 days, at pH 11.5, produced the highest inhibitor concentrations (14.0 mg/L p-CA, 12.3 mg/L FA, 5.22 mg/L CA and 0.6 mg/L SA).

All the concentrations of inhibitors obtained in the pre-treatment optimisation phase are below the inhibition thresholds reported in literature for AD process (Akassou et al., 2010; Hernandez and Edyvean, 2008; Pekařová et al., 2017).

The best balance between lignin, cellulose, hemicellulose and sugar solubilisations, and the production of inhibitors in the optimisation phase, was obtained at room temperature in the pre-treatment with a H_2O_2/MCW w/w ratio of 0.5, pH of 9.8, 10% MCW w/v and reaction time of 3 d (Pre2).

This pre-treatment allowed: a) lignin, cellulose and hemicellulose solubilisations of 68.6%, 63.4%, and 61.9%, respectively, b) concentrations of sugars of 928 mg/L glucose and 846 mg/L fructose, b) concentration of inhibitors <3.5 mg/L for furfural, <3.9 mg/L for 5-HMF, 9.12 mg/L for p-CA, 10.2 mg/L for FA.

The results obtained a H_2O_2/MCW w/w ratio of 0.5, pH of 9.8, 10% MCW w/v and reaction time of 4 d (Pre3) provided interesting monomeric sugar solubilisation and relatively low inhibitor compound concentrations, suggesting the potential of this pre-treatment for AcoD.

3.3.2 Co-digestion Assays

3.3.2.1 Control Parameters of AD Process

Averages and standard deviations of pH and redox potential in AD and AcoD experiments are reported in Table 3.5. AcoD promoted a decrease of redox potential, addressing this parameter at values lower than <300 mV; this is considered the redox potential value below which the AD process starts to work properly giving high biogas productions (Mauky et al., 2017).

On the other hand, the slight decrease of pH during AcoD is probably due to the presence of easily biodegradable sugars derived from MCW in the substrate that can favour the VFAs accumulation (Li et al., 2015). The degradation of solids (TS and VS) and removal of tCOD and sCOD during AD and AcoD experiments are reported in Table 3.6.

TS highest removals were observed in the AcoD of OFMSW+Pre3 and OFMSW+MCW, with average removal percentages of 56.5% and 55.8%, respectively, while VS removal showed a decrease during AcoD, changing from 67.7% (hOFMSW) to 58.6% (hOFMSW+Pre2).

Table 3.5: pH and Redox Potential in the AD and AcoD assays (average and standard deviation)

AD and AcoD assays	pH	Redox Potential (mV)
hOFMSW	8.26 ± 0.06	-397 ± 11.7
hOFMSW+Pre1	8.12 ± 0.08	-461 ± 22.5
hOFMSW+Pre2	8.18 ± 0.05	-460 ± 14.9
hOFMSW+Pre3	8.16 ± 0.06	-409 ± 6.41
hOFMSW+MCW	8.16 ± 0.07	-430 ± 6.33

The highest tCOD removal was observed during AD with standalone OFMSW (80.1%) and removals percentages higher than 73% were observed in most of the other AcoD assays performed (OFMSW+Pre2, OFMSW+Pre3 and OFMSW+MCW). The percentages of tCOD removal is in good agreement with the values present in literature for AD of commercial food (Lopez et al., 2016). sCOD showed a clear decreasing trend with AcoD ranging from 74.4% with hOFMSW+MCW to 51.1% with hOFMSW+Pre2.

Table 3.6 :Removal of TS, VS, tCOD and sCOD during the AD and AcoD assays (average and standard deviation).

AD and AcoD assays	TS	VS	tCOD	SCOD
	Removal (% w/w)			
hOFMSW	48.4 ± 3.8	67.7 ± 2.9	80.1± 1.8	72.3 ± 7.4
hOFMSW+Pre1	52.9 ± 3.0	63.3 ± 3.5	60.9 ± 3.9	66.9 ± 6.4
hOFMSW+Pre2	46.1 ± 4.1	58.6 ± 3.1	77.3 ± 7.6	51.1 ± 13.4
hOFMSW+Pre3	56.5 ± 1.7	63.1 ± 1.9	73.3 ± 4.2	70.6 ± 3.2
hOFMSW+MCW	55.8 ± 2.4	65.5 ± 3.5	74.6 ± 5.13	74.4 ± 4.1

The comparison between the ratio of NH_4-N/TNK and o-N/TNK during AD and AcoD experiments showed a reduction of o-N, demonstrating that good protein degradation took place during the AD with hOFMSW, AcoD with hOFMSW+Pre1 and with hOFMSW+Pre2.

o-N reduction was very low using untreated MCW as co-substrate and close to zero during AcoD with hOFMSW+Pre2 (Figure 3.8).

The higher degree of protein degradation during AD and AcoD experiments with hOFMSW+Pre1 and hOFMSW+Pre3 could contribute to the stability of the AcoD process (Kim et al., 2011).

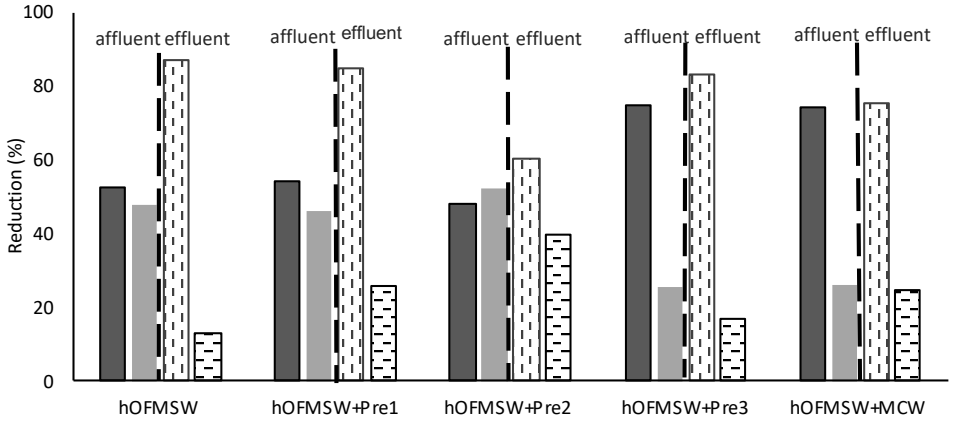

Figure 3.8: Comparison of NH_4-N and o-N contents over TKN in the substrates and in the effluents during AD and AcoD experiments. Dark grey and vertical dashed bars stand for NH_4-N-N/TNK in the affluent and in the effluent, respectively; light grey and horizontal dashed bars stand for o-NH_4-N/TNK in the affluent and in the effluent, respectively.

EA performed on the three substrates used showed that the C:N ratio increased with AcoD from a value of 9.46 in the AD assay with hOFMSW, to 21.21 in the AcoD assays with hOFMSW+Pre3 (Figure 3.9). This value of C:N ratio is close to the optimal value reported in literature for AD (25) (X. Wang et al., 2012).

It must be noticed that, even if the C:N ratios in most of the AcoD assays performed were far from the optimal ratio of 25, biogas and methane yields increased significantly in AcoD experiments, confirming the idea that MCW can correct the C:N ratio of a C-poor and N-rich waste, as it is hOFMSW, and improve AD efficiency.

Aiming to assess the process stability, NH_4-N and VFAs were quantified in the digestate (Table 3.7).

NH_4-N concentrations detected in the digestate were close to the threshold concentration responsible for 100% inhibition (2500 mg/L) (Masoud Kayhanian, 1994) and lower than the concentration that, according to El-Hadj et al.(2009), cause 50% of inhibition of AD (5600 mg/L). The NH_4-N concentration during co-AD of hOFMSW+MCW (2544 mg/L) exceeded the threshold for AD reported by Masoud Kayhanian (1994) (Table 3.7).

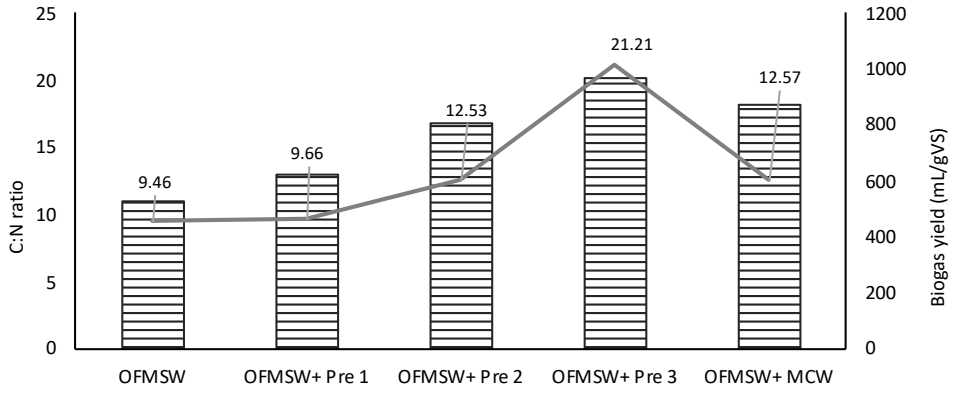

Figure 3.9: C:N ratios and biogas yields in the AD and AcoD experiments. Bars represent the biogas yields, line the C:N ratio observed in the different AcoD tested.

Excessive concentration of NH_4-N in the medium, that cause ammonia accumulation, can inhibit acetotrophic methanogens involved in the conversion of acetate into CH_4. If it occurs, the acetate produced during the acidogenesis phase accumulates in the medium, lowering the buffer capacity and pH, and inhibiting biogas production (Siegrist et al., 2002). This situation seems to occur during AcoD with hOFMSW+MCW and hOFMSW+Pre3.

The concentrations of all the VFAs in the digestate increased, on average, during the co-digestion with Pre1 and Pre2. On the other hand, during AcoD of hOFMSW+ Pre2, 876 mg/L Propionic acid, 412 mg/L Butyric acid and 3132 tVFA concentrations were observed (Table 3.7). It is seen a decrease in Propionic and Butyric acids concentrations during AcoD with hOFMSW+Pre3 and hOFMSW+MCW, when compared to AD of standalone hOFMSW.

The addition of pre-treated MCW produced an accumulation of the Acetic acid quantified, achieving the highest concentrations during AcoD of hOFMSW + MCW with 2512 mg/L and 2154 mg/L Acetic acid during hOFMSW+Pre3 (Table 3.7).

Wang et al. (2009) reported that Acetic acid and Butyric acid concentrations of 2400 and 1800 mg/L, respectively, resulted in no significant inhibition of the activity of the methanogens, while a PA concentration of 900 mg/L resulted in significant inhibition of these bacteria.

Similary Drosg (2013) defined the Acetic acid and Propionic acid limits for the process stability at 4000 mg/L and 1000 mg/L, respectively, and stated that

tVFAs concentrations above 4000 mg/L, and acetic acid/propionic acid ratio lower than 2 are indicators of process instability.

The two most favourable AcoD conditions, from the point of view of biogas and methane yields (OFMSW+MCW and hOFMSW+Pre3) (Table 3.8) can be affected by some inhibition of the AD process due to $N\text{-}NH_4$ and Acetic acid accumulations. The absence in the digestate of these AcoD assays of Propionic and Butyric acids limits the instability.

Nevertheless, according to Angelidaki et al. (1993) it seems difficult to define VFA levels to indicate the state of an AD process, as different systems have their own levels of VFAs that can be considered 'normal' for the reactor. The conditions that cause instability in one reactor may not cause problems in another reactor (Franke-Whittle et al., 2014) .

3.4 Biogas Production and Yields

The co-digestion of MCW with the hOFMSW allowed a significant increase in daily biogas production when compared to the AD performed with the hOFMSW alone (Table 3.8).

The methane content in biogas streams did not showed any significant difference (ANOVA, $p<0.05$) during the AD of hOFMSW alone and the AcoD's of hOFMSW+Pre1 and hOFMSW+Pre2, with an average value of 66.5% v/v. A slight decrease in methane content was observed in the biogas streams obtained during AcoD of hOFMSW+Pre3 (63.1% v/v) and hOFMSW+MCW (60.1% v/v). During these two latter assays, it was observed the most favourable average daily biogas production (4,830 mL/d and 5,017 mL/d, respectively) (Table 3.8).

The co-digestion of OFMSW+Pre3 increased biogas and methane yields by 65% and 48%, and co- digestion of hOFMSW with non-pre-treated MCW by 84% and 57%, respectively, when compared to the hOFMSW alone (Figure 3.10). Despite the highest yield and similar biogas volume produced during these two co-digestion assays, the biogas stream obtained during co-AD of OFMSW+MCW has a LHV on average 4% lower than the LHV obtained in the co-AD of OFMSW+Pre3 (Figure 3.8). Regarding the contaminant's concentrations, all the AcoD assays performed provided a reduction of the H_2S concentrations in all the AcoD, when compared with the AD of standalone hOFMSW. The same trend was observed for H_2 and CO.

The H_2S concentration observed is in agreement with the values reported in literature (0.005-2%) for AcoD in presence of OFMSW (Ryckebosch et al., 2011).

Table 3.7: NH_4-N and VFAs concentrations (mg/L) quantified in the digestate (average and standard deviation) and limit concentrations cited in literature.

Parameters	hOFMSW	hOFMSW+ Pre1	hOFMSW+ Pre2	hOFMSW+ Pre3	hOFMSW+ MCW	Threshold	Reference
	mg/L						
NH_4-N	211 ± 306	1952 ± 87.6	2171 ± 218	2097	2544	2500 5600	(Masoud Kayhanian, 1994) (El-Hadj et al., 2009)
AA	243 ± 44.8	719 ± 70	1844 ± 62.9	2154	2512	4000	(Drosg, 2013; Mauky et al., 2017)
PA	19.5 ± 12.0	67.3 ± 6.7	876 ± 33.2	<10	<10	900	(Wang et al., 2009)
BA	69.0 ± 39.8	106 ± 6.8	412 ± 7.8	51.0	<11.5	1800	
tVFAs	289	834	3132	2205	2512	4000	(Drosg, 2013)
AA/PA ratio	10.3	10.7	2.1	>>	>>	<2.0	

Table 3.8: Biogas composition in each AD experiment (STP) (average ± standard deviation).

AD and AcoD assay	CH_4	CO_2	O_2	N_2	H_2S	CO	H_2	Biogas	LHV
	% v/v					ppm		mL/d	MJ/m^3
hOFMSW	66.1 ± 6.5	32.4 ± 6.9	0.0	0.8 ± 0.3	970 ± 215	109 ± 34	155 ± 62	2389	22.4
hOFMSW+Pre1	65.5 ± 0.4	32.6 ± 0.2	0.0	1.2 ± 0.3	737 ± 81.3	76.0 ± 21	70.0 ± 15	3787	22.5
hOFMSW+Pre2	66.8 ± 1.7	32.2 ± 1.6	0.0	0.5 ± 0.3	722 ± 106	5.50 ± 1.3	51.0 ± 12	3941	22.6
hOFMSW+Pre3	63.0 ± 1.3	36.0 ± 1.3	0.0	-	783 ± 50.5	10.0 ± 2.4	115 ± 11	4830	21.3
hOFMSW+MCW	60.3 ± 0.9	39.6 ± 0.9	0.0	-	820 ± 28.3	7.00 ± 2.5	90.0 ± 5.6	5017	20.4

In the AcoD of hOFMSW+MCW and hOFMSW+Pre3 biogas stream, the H_2 and CO concentrations found were lower than the threshold values considered critical for automotive fuel and for grid injection, respectively (Hoyer et al., 2016).

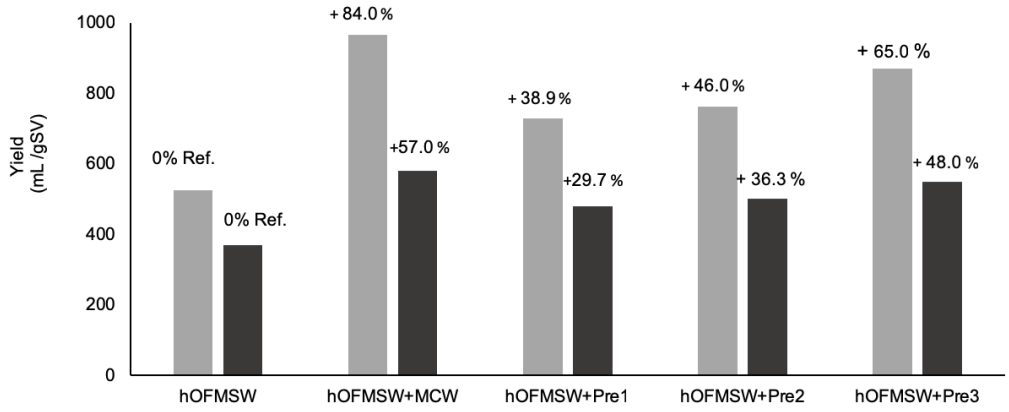

Figure 3.10: Variation of biogas and methane yields in AcoD assays (hOFMSW+MCW, hOFMSW+Pre1, hOFMSW+Pre2 and hOFMSW+Pre3) relatively to AD of hOFMSW.

The results of biogas and methane yields were compared with other AcoD assays performed with maize residues and food wastes reported in literature (Table 3.9).The data reported in literature shows similar biogas and methane yields (Owamah and Izinyon, 2015; Amon et al., 2006; Li et al., 2015) to the results obtained in the present work, but with HRTs quite higher (44, 45 and 42 d) in the mesophilic conditions. Lower yields were obtained in the co-digestion of maize stalk with swine manure under thermophilic conditions with 35 d HRT (T. Zhang et al., 2015) and at mesophilic conditions in presence of maize silage with an HRT of 101 days (Hutňan, 2016).

3.1 Conclusions

The results showed that the chemical pre-treatment catalysed by H_2O_2, at pH of 9.8, 4h of reaction time, and at room temperature (Pre3) is a promising and low energy demanding pre-treatment applicable to MCW to allow its AcoD with hOFMSW. The reaction time of Pre2 produced inhibitors that affected the efficiency of AcoD process. The co-digestion of OFMSW with pre-treated MCW under Pre3 increased the biogas yield by 65% and CH_4 yield by 48%, when compared with the results obtained using OFMSW alone

Table 3.9 Experimental data available in literature on co-AD assays in the presence of maize wastes performed under similar AD conditions to the present study.

Feedstock	Conditions	Biogas yield	Methane yield	Reference
		mL/gSV		
75% w/w Food Waste (FW) 25% w/w Maize Husk (MH)	Continuous flow; OLR= 3.5 g SV/ L.d 37 ºC ± 1 ºC pH=6.8; C:N 23.4 HRT=44 days	700	446	(Owamah and Izinyon, 2015)
54% Dairy Manure, 33% Corn Stover, 13%Tomato Residues	Solid State AD; 35 ºC ± 1 ºC HRT=45 days	-	415	(Y. Li et al., 2015)
70% ratio/TS Swine Manure (SM) 30% ratio/TS Maize Stalk (MS)	55 ºC ± 2 ºC HRT=35 days pH= 8	203	64.6	(T. Zhang et al., 2015)
35% w/w Maize Silage Anaerobic Stabilized Sludge	Batch; 35 ºC ± 1 ºC HRT=101 days pH= corrected	569	310	(Hutňan, 2016)
31% w/w Maize Silage 15% w/w Corn 54%w/wPig Manure (PM)	Batch; 38 ºC ± 1 ºC HRT=42 days pH= corrected	639	439	(Amon et al., 2006)

The co-digestion of hOFMSW with non-pre-treated MCW increased biogas and CH_4 yields by 84% and 57%, respectively. Despite the higher yields, the LHV of the biogas obtained in the AcoD of hOFMSW with non-pre-treated MCW were on average 4% lower than the LHV obtained with AcoD of hOFMSW+Pre3. Moreover, Pre3 favoured the stability of the AcoD process, providing reduced Acetic acid and N-NH_4 accumulations when compared to non-treated MCW. From these results, one can conclude that a pre-treatment is recommended before submitting MCW to AD, and that co-digestion of hOFMSW with pre-treated MCW allows a significant enhancement of biogas and methane yields.

4

H_2S Removal from Biogas using the ACs produced from Maize Cob Waste and Liquid Digestate

4.1 Introduction

Biogas produced in AD may contain from less than 500 ppmv to more than 5000 ppmv of H_2S depending on the substrate used and operational conditions of the bio-reactor (Abatzoglou and Boivin, 2009; Awe et al., 2017; Ryckebosch et al., 2011).

Both the direct combustion of biogas and its upgrading to bioCH_4 (CH_4>97% v/v) usually require a previous H_2S removal step to prevent equipment damage and environmental poisoning issues related to the emission of sulphur compounds.

Among the different techniques that can be used for H_2S removal from biogas stream, such as physical/chemical absorption, iron chloride precipitation, metal oxide/hydroxide adsorption, membrane permeation, biological methods, physical adsorption, among others (Abatzoglou and Boivin, 2009; Awe et al., 2017; Muñoz et al., 2015; Ryckebosch et al., 2011), adsorption onto activated carbons, namely lignocellulosic-derived ACs, is considered a safe, sustainable, reliable, highly efficient, and in most cases an environmentally sound technique (Kwaśny and Balcerzak, 2016; Mohamad Nor et al., 2013).

On the other hand, maize is one of the most important crops worldwide with a total production, in 2018, of around 1060 million tons (IGC - International

Grain Council, 2018). For 1 kg of dry corn grains, about 150 g cobs are generated (Zhang et al., 2012), which would have resulted, by the end of 2018, in approximately 159 million tons of corn cobs. The cobs are usually left in the field as part of the corn stover for soil conditioning. This lignocellulosic bio-waste can be considered a good precursor for ACs with relatively high surface area, due to its high carbon content (around 45% w/w) and low percentage of ashes (about 2% w/w) (Bagheri and Abedi, 2009; Flores et al., 2017; Tsai et al., 2001).

The mechanisms underlying H_2S adsorption onto ACs are highly dependent on the adsorbent characteristics (porosity and surface chemistry) and on the operating conditions, such as relative humidity, H_2S concentration, O_2 concentration, presence of other contaminants in biogas stream, and temperature (Bandosz, 1999; Chen et al., 2010; Le Leuch et al., 2003; Seredych and Bandosz, 2008; Sitthikhankaew et al., 2014).

Concerning the ACs used in biogas conditioning, it is usually considered that their surface chemistry is more important than the textural properties in H_2S adsorption; additionally, the complexity of the involved chemical mechanisms may be significant (Adib et al., 2000a, 1999a; Bandosz, 1999). Regarding the operating conditions of the adsorption system, the presence of oxygen and water is considered critical to the mechanisms that are usually associated with H_2S removal onto carbonaceous materials, namely dissociative adsorption and oxidation.

There are three main groups of ACs for gas stream desulphurisation: unmodified ACs (virgin carbons), impregnated ACs, and/or surface-modified ACs. The role of virgin carbons on H_2S removal, at ambient temperature, was widely studied (Adib et al., 2000a, 1999b, 1999a; Bandosz, 2002, 1999; Klein and Henning, 1984; Xiao et al., 2008). It was found that under dry conditions and without added oxygen, hydrogen sulphide can also be oxidized in activated carbon, being subjected to chemisorption. This oxidation capacity was associated with the presence of oxygen functional groups in the carbon surface (Adib et al., 2000a; Bouzaza et al., 2004; Feng et al., 2005; Le Leuch et al., 2003). Other authors stated that in the absence of oxygen and under dry conditions, the micropore filling theory (physisorption) should be assumed (Bagreev et al., 1999; Guo et al., 2007; Menezes et al., 2018).

Several chemical agents may be used to produce impregnated ACs, such as Na_2CO_3, NaOH, KOH, metallic oxides, KI, $KMnO_4$, among others, which will

promote the oxidation of H_2S to elemental sulphur (S), depending on the type of agent and operating parameters. However, side reaction products can also be formed, such as SO_2, SO_3, and/or H_2SO_4. Alkaline impregnated ACs also lead to the formation of metallic sulphides and/or metallic sulphates. The advantages of impregnated activated carbons compared to virgin carbons are their high efficiency and fast reaction kinetics, since they would catalyse the H_2S dissociation and oxidation step through a chemisorption process (Bagreev and Bandosz, 2005; Castrillon et al., 2016; Dalai et al., 2008; Sitthikhankaew et al., 2014; Xiao et al., 2008).

ACs can also be submitted to surface chemical treatments in order to promote functionalization and introduce heteroatoms that enhance H_2S removal. Nitrogen-containing ACs, such as those modified by urea, amines, or ammonia treatments were widely studied, demonstrating their catalytic role in H_2S dissociation and oxidation, mainly due to the increase of basic sites on carbon surface (Adib et al., 2000b; Bagreev et al., 2004; Bashkova et al., 2002; Seredych and Bandosz, 2008). Feng et al. (2005) reported an increase of H_2S removal with oxidized fibres of ACs due to an increase of the surface oxygen functionalities after the oxidation treatment with oxygen. On the other hand, Adib et al. (2000a) observed that when ACs were oxidized with nitric acid and ammonium persulfate, there is a significant increase in the number of acidic oxygenated groups affecting negatively the H_2S dissociation.

ACs derived from MCW for H_2S removal from biogas have not been much studied. To authors' knowledge, it is only available in literature the work of Kaźmierczak et al. (2013), in which these authors have obtained MCW-derived ACs from both physical activation with CO_2 and chemical activation with KOH. Although KOH activated carbon presented the highest surface area, its H_2S removal capacity was lower than that obtained with the physically activated carbon. This better result for the physically activated carbon was attributed to its surface chemistry that was richer in basic groups, contributing for a higher H_2S removal.

In this context, the aim of the Tasks 3 and 4 was to assess the H_2S removal capacity of MCW-derived ACs from real biogas produced in a lab-scale bioreactor. A first set of ACs was physically activated with CO_2 and a second set

was obtained from the impregnation of MCW with anaerobic Liquid Digestate (LD). LD was obtained from the same industrial AD plant located in Lisbon area. LD was used because it is an ammonia-containing material rich in minerals, such as K, which may have a catalytic activity in H_2S removal.

4.2 Materials and Methods

4.2.1 Precursor and Impregnation Agents: Maize Cob Waste and Liquid Digestate

The MCW collected in a farm located at Coruche municipality (Lisbon surroundings, Portugal) presented an initial moisture content of 20% w/w and was air-dried to a final moisture content of 9.3% w/w by contact with air at ambient temperature. The air-dried MCW was then milled to a particle size of 2-4 mm (Retsch SM 2000 grinder).

LD was used as both a precursor and impregnation agent to produce ACs. Both MCW and LD were submitted to the following characterizations:

(i) Elemental analysis (EA) – it included the quantification of C, H, N, and S (Thermo Finnigan-CE Instruments Flash EA 1112 CHNS analyser);

(ii) Proximate analysis – it included the quantification of moisture content (EN 14774- 1), volatile matter (EN 15148) and ashes (EN 14775) (CEM MAS 7000 microwave furnace);

(iii) Thermogravimetric analysis (TGA) – it included the quantification of mass loss between room temperature and 850 °C, with a heating rate of 5 °C/min, under argon atmosphere (Setaram Labsys EVO equipment);

(iv) Mineral content – it was performed according to the European Standard EN 15290 on samples previously digested (3 cm^3 H_2O_2 30% v/v + 8 cm^3 HNO_3 65% v/v + 2 cm^3 HF 40% v/v) in a microwave station (Milestone Ethos 1600 Microwave Labstation) followed by neutralization (20 cm^3 H_3BO_3 4% w/v); the acidic solutions were analysed by Inductively Coupled Plasma – Atomic Emission Spectroscopy (ICP-AES) (Horiba Jobin-Yvon equipment) for the quantification of 16 chemical elements.

4.2.2 Preparation and Characterisation of Activated Carbons

A first set of MCW-derived ACs was obtained from physical activation of MCW with CO_2. The physical activation was performed in a quartz reactor placed in a bench-scale vertical furnace, temperature-controlled by a PID programmable controller (RKC, REX-P96). The temperature inside the furnace was measured by a thermocouple connected to the PID controller.

The MCW was heated up to 500 °C, at a heating rate of 10 °C/min, and kept for 1h at this temperature, under N_2 atmosphere (150 cm^3/min). After this stage, the carbonized material was submitted to another heating step up to 800 °C, at a heating rate of 5 °C/min. When the target temperature was achieved, the N_2 flow was switched to CO_2 flow (150 cm^3/min). CO_2 was used as the physical activation agent of these MCW-derived ACs. Two and three hours of activation time with CO_2 were used to produce the activated carbon samples named as MCW(PA)2h and MCW(PA)3h, respectively. After activation, the produced ACs were cooled down to room temperature under N_2 flow (150 cm^3/min). In the codes of ACs, PA stands for Physical Activation.

The second set of ACs resulted from the impregnation of MCW with the LD. Both raw MCW and previously carbonized MCW (CAR-MCW) were impregnated. The previous carbonization procedure was performed as follows: 2h of carbonization time, at 450 °C, under atmospheric pressure and in the absence of air by inserting the sample in a closed and air-tight vessel. The impregnation step was performed at a L/S ratio of 30.1 cm^3_{LD}/g_{MCW}, allowing an impregnation weight ratio of 1:1. The impregnation was performed at 50 °C, for 48 hours, under constant stirring. Afterwards, the impregnated samples were oven-dried at 95 °C, for 24 h. The dried samples were subsequently carbonized at 800 °C (heating rate of 5 °C/min), under N_2 flow (150 cm^3/min), for 2 h. Under this procedure, two ACs were obtained: MCW(LD), in which raw MCW was used as feedstock, and CAR-MCW(LD), in which previously carbonized MCW were used as feedstock.

Figure 4.1 summarizes the methodology used in the preparation of biomass-derived ACs.

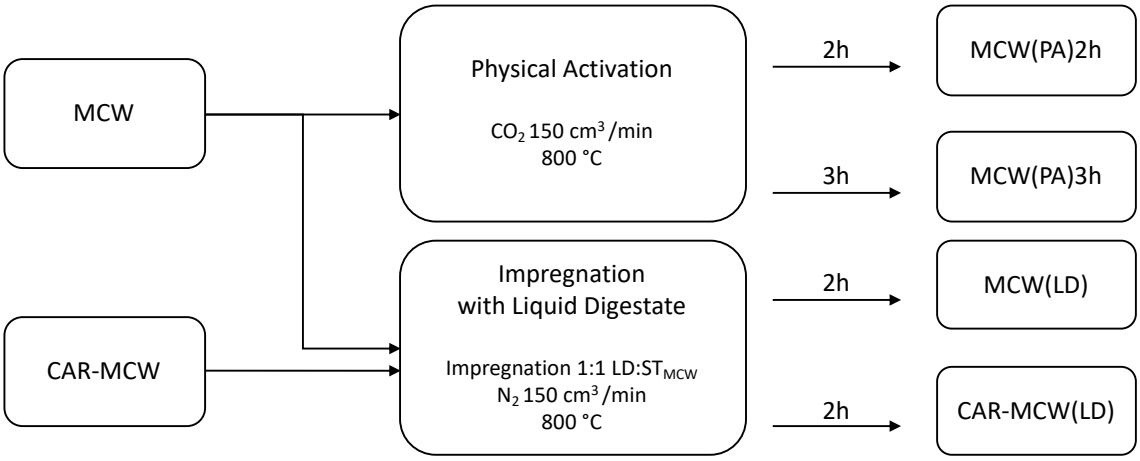

Figure 4.1: Methodology used to produce different ACs from MCW, carbonized MCW (CAR-MCW) and anaerobic liquid digestate (LD).

For comparison purposes, a Commercial Activated Carbon (CAC) specifically designed for biogas purification was also used in the H_2S removal assays. CAC is a non-impregnated steam activated catalytic carbon.

The samples of ACs were submitted to the following characterizations:

(i) EA – it was determined as described above for precursors;

(ii) Proximate analysis – it included the same parameters as described above for precursors, but following the ASTM D1762 standard, which is specifically designed for wood charcoal;

(iii) Apparent density – it was determined through a gravimetric method according to ASTM 2854 standard;

(iv) TGA – it was determined as described above for precursors;

(v) X-ray powder diffraction (XRPD) by using a benchtop X-Ray diffractometer (RIGAKU, model MiniFlex II), with Cu X-ray tube (30 kV / 15 mA); the diffractograms were obtained by continuous scanning from 15° to 80° (2θ) with a step size of 0.01° (2θ) and scan speed of 2°/min. A tentative identification of XRD peaks by matching with ICDD database of XRD software (Windows Qualitative Analysis version 6.0 - Rigaku Corporation Database: ICDD PDF-2 Release 2007) was performed;

(vi) pH at the point of zero charge (pHpzc) – it was determined according to the following methodology: 0.1 M NaCl solutions with initial pH values between 2.0 and 12.0 were prepared (pH adjustment was performed with solutions of NaOH or HCl with concentrations of 0.01 to 1M). 0.1 g of ACs was added to 20 cm^3 of each 0.1 M NaCl solution; the mixtures were stirred for 24 h and the

final pH was measured; pH_{PZC} value corresponds to the plateau of the curve pH_{final} *vs* $pH_{initial}$;

(vii) Textural properties – they were evaluated from the adsorption--desorption isotherms of N_2 at 77 K (ASAP 2010 Micromeritics equipment); all samples were previously outgassed overnight, under vacuum, at 150 °C; the data of isotherms were used to calculate the apparent surface area through the BET equation (S_{BET}); total pore volume (V_{total}) was determined by the amount of N_2 adsorbed at the relative pressure of $P/Po = 0.95$; micropore volume (V_{micro}) was quantified by the t-plot method; mesopore volume (V_{meso}) was determined by the difference between V_{total} and V_{micro};

(viii) Surface elemental composition and morphology – they were analysed by Scanning Electron Microscopy with Energy Dispersive Spectroscopy (SEM-EDS) using a JEOL 7001F analytical FEG-SEM with Oxford model INCA 250 PREMIUM EBSD (electron backscatter diffraction) and energy dispersive X-ray spectrometer light elements detector attachments.

4.2.3 H_2S Removal Assays

4.2.3.1 Biogas Samples

The H_2S removal assays were carried out using real biogas samples produced in a 2.1 dm^3 lab-scale stirred bioreactor (New Brunswick Scientific, BIOFLO 1000), equipped with controlling systems for temperature, pH and redox potential.

The bioreactor was operated under thermophilic conditions (50 ± 1 °C), at a constant pH of 8. The bioreactor was fed each 48 h with a biologically hydrolysed sample of OFMSW. The operating conditions used mimicked those of the industrial-scale AD plant from which the real LD was collected. The average biogas production was of 4 dm^3/day. Biogas samples were stored in Tedlar bags (SKC) with polypropylene fitting, to be subsequently used in the H_2S removal assays.

The biogas composition was determined by a multichannel biogas analyser (Gas Data, model GFM410), equipped with non-dispersive infra-red spectroscopy detector for CH_4 and CO_2 (quantification limit: 0.1% v/v for both

gases), and electrochemical detectors for H_2S, O_2, CO and H_2 (quantification limits: 1 ppmv for H_2S, CO and H_2, and 0.1% v/v for O_2). The data obtained from the analyser was processed with Gas Data SiteMan v6 software. Water vapour and ammonia (NH_3) concentrations were determined with GASTEC Detector Tubes (6 WV tube for water vapour; 3M Ammonia tube for NH_3), coupled to a GASTEC GV-100S gas sampling pump. Table 4.1 shows the variation intervals of each gas present in biogas samples.

Table 4.1: Variation intervals of each gas present in biogas samples used in H2S removal assays.

Gas compound	Unit	Concentration interval
CH_4	% v/v	49.0 – 52.9
CO_2		47.0 – 50.9
O_2		< 0.1
H_2O		0.0013
H_2S	ppmv	1100 – 1800
H_2		102 – 217
CO		7 – 23
NH_3		3 – 32

4.2.3.2 Experimental Setup used in H_2S Breakthrough Assays

To assess the H_2S uptake capacity of ACs, dynamic H_2S breakthrough assays were performed in the following experimental setup: a stainless steel (AISI 304) column (internal diameter: 15 mm; length: 230 mm), with vertical configuration, was filled up with 0.5 g of each activated carbon. The particle size of ACs were set to 1 mm < Ø < 3 mm. A stainless-steel mesh (0.5 mm) was used to support the ACs in the column; the empty volume was packed with glass spheres to promote an adequate biogas distribution. The glass spheres were tested alone for H_2S adsorption, but no significant removal was detected.

Figure 4.2 reports a diagram on the experimental setup used.

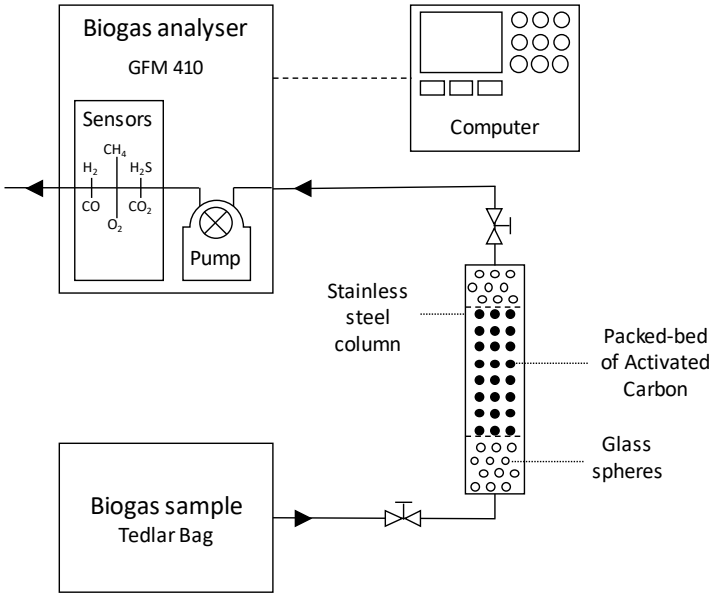

Figure 4.2: Experimental setup used in H_2S breakthrough assays.

The Tedlar bags filled up with biogas were connected to the column inlet, at the bottom of the column, while the biogas analyser was connected to the outlet, at the top of the column. The assays were performed at room temperature (25 °C) and atmospheric pressure. A biogas flow of 400 cm^3/min, with a linear velocity of 3.78 cm/s was used.

Table 4.2 presents the main experimental conditions used in H_2S removal assays. All the assays were performed in duplicates.

Table 4.2: Experimental conditions used in the dynamic H_2S breakthrough assays.

Parameter	Unit	Value
T	°C	Room temperature (25 °C)
P	atm	1
F	cm^3/min	400 [1]
v	cm/s	3.78
m	g	0.5
Mean particle diameter (ø)	mm	$1 \leq ø \leq 3$

4.2.3.3 Assessment of H_2S Breakthrough Capacity

The H_2S uptake capacity of ACs, q_{H_2S} (mg/g), was calculated according to Equation 4.1 (Gutiérrez Ortiz et al., 2014):

$$q_{H_2S} = \frac{F \times M_w}{m \times V_M} \times \left[C_0 \times t_{br} - \int_0^{t_{br}} C_t \, dt \right], \qquad (Eq.4.1)$$

where F is the gas flow rate (m^3/s), m is the weight of activated carbon used (g), M_w is the molecular weight of H_2S (34000 mg/mol), V_M is the molar volume (22400 cm^3/mol), C_0 is the H_2S concentration in the inlet biogas flow (ppmv), C_t is the H_2S concentration in the outlet biogas flow (ppmv) at time t, and t_{br} is the time (s) at which H_2S breakthroughs the column. 50 ppmv H_2S was chosen as a breakthrough concentration since it is the concentration defined by the ASTM D 6646-03 standard (Determination of the Accelerated Hydrogen Sulfide Breakthrough Capacity of Granular and Pelletized Activated Carbon), as well as in several published works dealing with H_2S removal (Bagreev and Bandosz, 2005; Bandosz, 1999; Chen et al., 2010; Yan et al., 2002).

4.3 Results and Discussion

4.3.1 Characterization of Maize Cob Waste and Liquid Digestate

MCW showed a high percentage of volatile matter (80.1% w/w), high content of fixed carbon (9.10% w/w) and low ash-content (1.50% w/w) (

Table 4.3). These characteristics fit well the properties usually desired for precursors of ACs with high surface area. TGA analysis of MCW (Figure. A.1) confirmed the high volatile content of this precursor, with the major weight loss being observed between 230–340 °C, which is mainly associated with the degradation of cellulose and hemicellulose. Above 340 °C and up to ca. 500 °C, there is a slow degradation of the sample, mainly associated with lignin decomposition. At 850 °C, about 38% w/w of carbonaceous residue remains in the sample.

The LD sample submitted to proximate and elemental analyses was previously dried up to a moisture content of around 3.30% w/w, at 65 ºC, during 48 h. The dried LD is characterized by high ash (51.4% w/w) and low fixed carbon (0.80% w/w) contents. The volatile matter is present in high percentage (44.5% w/w), due to the relatively incomplete biological oxidation of organic substrates during AD. TGA analysis of the dried LD (Figure. A.2) confirmed that there are lignocellulosic components that were not completely degraded during AD, being observed a steady degradation from 222 ºC up to 850 ºC. At this latter temperature, around 60% w/w of carbonaceous residue remained in the sample, which should be composed by a significant fraction of minerals.

The dried LD is also characterized by a concentration of N (3.63% w/w) (

Table 4.3) that, if properly impregnated in ACs, may introduce nitrogen-containing groups on their surfaces, enhancing H_2S removal capacity, as mentioned above.

Regarding the mineral composition (Table 4.4), MCW is composed by K (7632 mg/kg), Mg (2970 mg/kg), Al (2731 mg/kg), Si (2506 mg/kg), Zn (1537 mg/ kg), and Ca (1012 m/kg) as major elements, with concentrations in agreement with literature (Raveendran et al., 1995; Yu et al., 2010)

Table 4.3: Proximate and elemental analysis of the precursors/impregnation samples.

Parameter	Unit	Precursors/impregnation samples	
		MCW [1]	LD [2]
Proximate analysis			
Moisture	% w/w	9.30	3.30
Volatile matter		80.1	44.5
Fixed carbon		9.10	0.80
Ashes		1.50	51.4
Elemental analysis			
C	% w/w	41.7	31.1
H		5.60	3.99
N		0.10	3.63
S		<0.03	1.60
O [3]		51.1	8.28

[1]After drying to 9.30% w/w moisture content; [2] After drying to 3.30% w/w moisture content; [3] Calculated as follows: O = 100 – (C + H + N + S + Ashes)

Table 4.4: Mineral content of the precursors/impregnation samples.

Chemical element	Unit	MCW	LD
K	mg/kg db	7632	59579
Mg		2970	3055
Al		2731	3140
Si		2506	1840
Zn		1537	1100
Ca		1012	3771
Na		342	2753
Fe		86.0	1406
Cr		5.00	10.0
Mn		4.00	39.0
Se		<0.490	45.0
Ni		<0.390	6.00
Cu		<0.370	21.0
Pb		<0.050	11.0
Sn		<0.040	9.00
Cd		<0.040	<0.040

db: dry basis

LD is characterized by having high concentrations of chemical elements that can have catalytic effect on H_2S oxidation, such as K (59579 mg/kg), Ca (3771 mg/kg), Al (3140 mg/kg), Mg (3055 mg/kg), Na (2753 mg/kg), and Fe (1406 mg/kg) (Table 4.4). It should be mentioned that sylvite (KCl) was identified in the XRPD diffractogram of the dried LD (Figure. B.1), indicating that K, the major element present in the highest concentration in this biomass, is mainly in the form of chloride.

4.3.2 Characterization of Activated Carbons

Table 4.5 shows the results of proximate and elemental analyses, as well as pH_{PZC} for all ACs. CAC is characterized by high ash-content (28.6% w/w). Also, this activated carbon presented a considerable S-content when compared to the biomass-derived ACs, which may be related to the precursor used in its production (mineral coal). It also shows a very strong alkaline behaviour with a pH_{PZC} of 11.9.

The impregnated activated carbons MCW(LD) and CAR-MCW(LD) also presented very high content of ashes with percentages of 34.2% w/w and 24.7%

w/w, respectively, showing that the impregnation with LD increased significantly the mineral fraction of these ACs. As registered for CAC, both impregnated carbons presented a very high pH_{PZC} value (11.8 for both ACs).

Both physically ACs (MCW(PA)2h and MCW(PA)3h) showed a good conversion of the initial volatile matter, providing final carbon materials with high fixed carbon-content. Although MCW(PA)2h was submitted to an activation time with CO_2 lower than for MCW(PA)3h, it is characterized by a higher fixed carbon content (85.4% w/w) and lower oxygen content (11.7% w/w) than the latter. This suggests that a further increase of the activation time with CO_2 can promote the incorporation of more oxygen-containing groups at the surface of carbon materials. Effectively, MCW(PA)3h presents an oxygen content (20.5% w/w) higher than that calculated for MCW(PA)2h (11.7% w/w). As expected, all the four biomass-derived ACs show higher amounts of heteroatoms than CAC, except for S.

Both physically ACs showed pH_{PZC} values in the alkaline range, although with a lower alkaline character than the others biomass-derived ACs and CAC.

N-content in the impregnated ACs was low when compared to the physically ACs, indicating that the incorporation of nitrogen from raw LD (

Table 4.3) in the resulting ACs was not very successful. Probably, some loss of N has occurred during the carbonization of the impregnated activated carbons.

Regarding the thermal stability of ACs, TGA analysis (Figures A 3 - A 7) showed that all samples are quite stable up to 850 ºC, presenting mass losses lower than 10% w/w. The only exception is MCW(LD) that is thermally stable up to 600 ºC, but above this temperature it slowly degrades up to 850 ºC with a total mass loss of around 20% w/w (Figure A 6).

CAC was submitted to the mineral analysis, in order to elucidate about the chemical elements constituting this activated carbon that may be involved in H_2S removal. Very high concentrations of Ca (26961 mg/kg db), Al (19752 mg/kg db) and Fe (14443 mg/kg db) were determined. These elements are known for their catalytic behaviour on H_2S (Bagreev and Bandosz, 2005; Castrillon et al., 2016; Kwaśny and Balcerzak, 2016; X. Zhang et al., 2015). K, Mg and Si were quantified in lower concentrations (1708, 3345 and 5525 mg/kg db, respectively) than those chemical elements

Table 4.5: Proximate analysis, elemental analysis and pHPZC of ACs.

Parameter		ACs				
		CAC	MCW(PA)2h	MCW(PA)3h	MCW (LD)	CAR-MCW(LD)
Proximate analysis						
Moisture	% w/w ap	1.00	5.40	4.60	3.10	1.00
Volatile matter		5.30	6.50	6.80	7.10	4.50
Fixed carbon		65.1	85.4	83.6	55.6	69.8
Ashes		28.6	2.70	5.00	34.2	24.7
Elemental analysis						
C	% w/w ap	65.5	83.8	71.8	43.2	47.3
H		0.40	1.10	1.10	0.50	0.20
N		0.50	0.70	1.60	1.10	1.10
S		1.40	<0.03	<0.03	<0.03	<0.03
O [1]		3.60	11.7	20.5	21.0	26.7
pH_{PZC}		11.9	9.70	9.60	11.8	11.8

[1] Calculated as follows: O = 100 – (C + H + N + S + Ashes); CAC: commercial activated carbon; MCW(PA)2h and MCW(PA)3h: maize cob waste physically activated during 2 and 3 h, respectively; MCW(LD): maize cob waste impregnated and activated with liquid digestate; CAR-MCW(LD): previously carbonized maize cob waste impregnated and activated with liquid digestate; ap: as-produced basis

XRPD analysis was performed on the ACs that presented the higher ash content, namely CAC, MCW(LD) and CAR-MCW(LD), in order to elucidate about the crystalline mineral phases in their composition (Figures B 2, B 3 and B 4). Only quartz (SiO_2) was identified in the XRDP pattern of CAC; quartz, sylvite (KCl) and halite (NaCl) were identified in both impregnated ACs (MCW(LD) and CAR-MCW(LD)). The chloride species of K that was found in LD (Figure B 4) was retained in the impregnated ACs.

4.3.2.1 Textural Characterization

Table 4.6 reports the textural properties of the ACs based on N_2 adsorption-desorption isotherms. MCW(PA)2h and MCW(PA)3h developed the highest S_{BET} areas, with values of 630 m^2/g and 820 m^2/g, respectively. Both ACs presented N_2 isotherms that can be associated to type I(a) isotherms, according to IUPAC classification (Figures C 1 and C 2); this means that these ACs are essentially microporous materials having mainly narrow micropores (width < 1 nm) (Thommes et al., 2015). As expected, sample MCW(PA)3h presented a higher surface area, as it was subjected to a higher activation time.

Impregnated ACs presented very low S_{BET} values (38.0 m^2/g for MCW(LD) and 8.0 m^2/g for CAR-MCW(LD)), with very low porosity, mainly in the range of meso and microporosity (Figures C 3 and C4). In fact, the porous properties of these carbons resemble more to chars not activated (Sun et al., 2017, 2016).

Some authors reported sewage sludge-derived carbons with textural properties very similar to the impregnated carbons prepared in the present work, being a similar feature also the very high ash-content (Ansari et al., 2005; Wallace et al., 2014; X. Xu et al., 2014; Yuan and Bandosz, 2007).

Table 4.6: Textural parameters of ACs obtained from N2 adsorption-desorption isotherms.

Parameter	Unit	ACs				
		CAC	MCW(PA)2h	MCW(PA)3h	MCW(LD)	CAR-MCW(LD)
S_{BET}	m^2/g	459	630	820	38.0	8.0
V_{total}	cm^3/g	0.40	0.25	0.35	0.02	n. q.
V_{micro}		0.10	0.21	0.32	0.01	0.01
V_{meso}		0.30	0.04	0.03	0.01	n. q.

n. q. – not quantifiable

Despite of the good properties of MCW as precursor for ACs, probably it occurred a structural collapse during carbonization/activation, due to the catalytic effect of the alkali and alkaline earth metals that were present in very high concentrations in the LD.

Concerning CAC, its N_2 isotherm is of type II, which is typically of non-porous or macroporous materials; however, the presence of a relatively large H3 type hysteresis (Figure C 5) indicates that this carbon presents mesoporosity, with large slit-like mesopores.

4.3.3 Surface Elemental Composition and Morphology

The SEM analysis of MCW(PA)2h and MCW(PA)3h (Figures 4.3 and 4.4) showed a homogeneous and well-developed porous structure, confirming the results obtained with the N_2 isotherms at 77K. The EDS analysis performed on these samples did not show the presence of significant mineral aggregates.

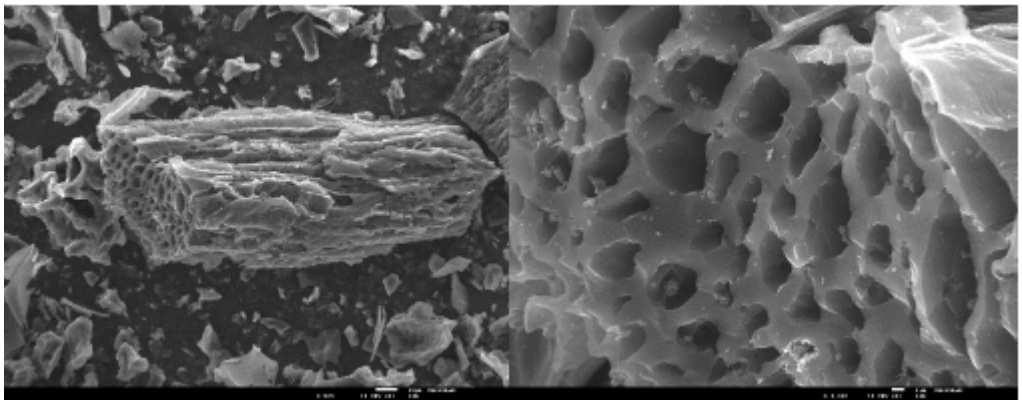

Figure 4.3a) Figure 4.3b)

Figure 4.3: SEM images of MCW(PA)2h sample with magnifications of 500x (a) and 3000x (b).

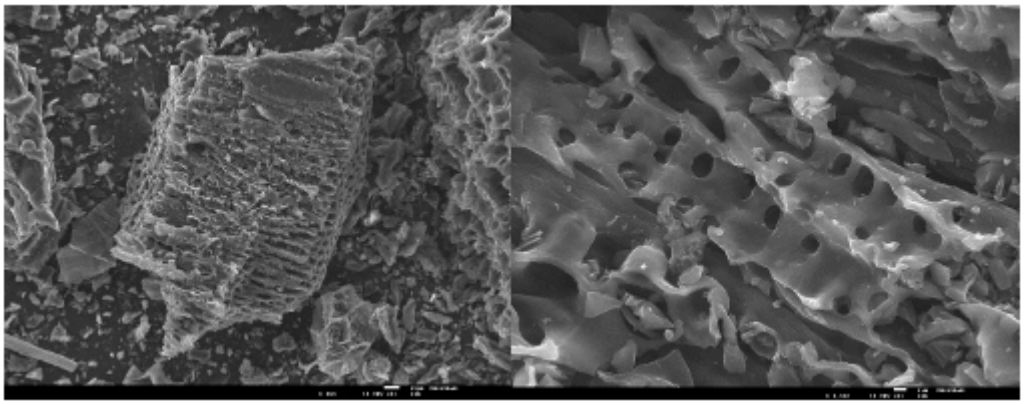

Figure 4.4a) Figure 4.4b)

Figure 4.4: SEM images of MCW(PA)3h sample with magnifications of 350x (a) and 3000x (b).

On the other hand, the SEM analysis of MCW(LD) and CAR-MCW(LD) (Figures 4.5 and 4.6) showed particles with very heterogeneous surface, a poorly porous structure and the presence of inorganic matter (brighter areas). The EDS spectra obtained for both carbons indicated the presence of C, Cl, K, Na and Ca, pointing out that these ACs are a mixture of scattered carbon particles enriched with mineral aggregates. These results were confirmed by XRPD diffractograms (Figures B. 2 and B 3) that showed K and Na chlorides as diffractable mineral species over the surface of these ACs. In addition, the EDS spectra of the selected

particles of CAR-MCW(LD) also detected oxygen and phosphorus, which may indicate the presence of some oxides and phosphates.

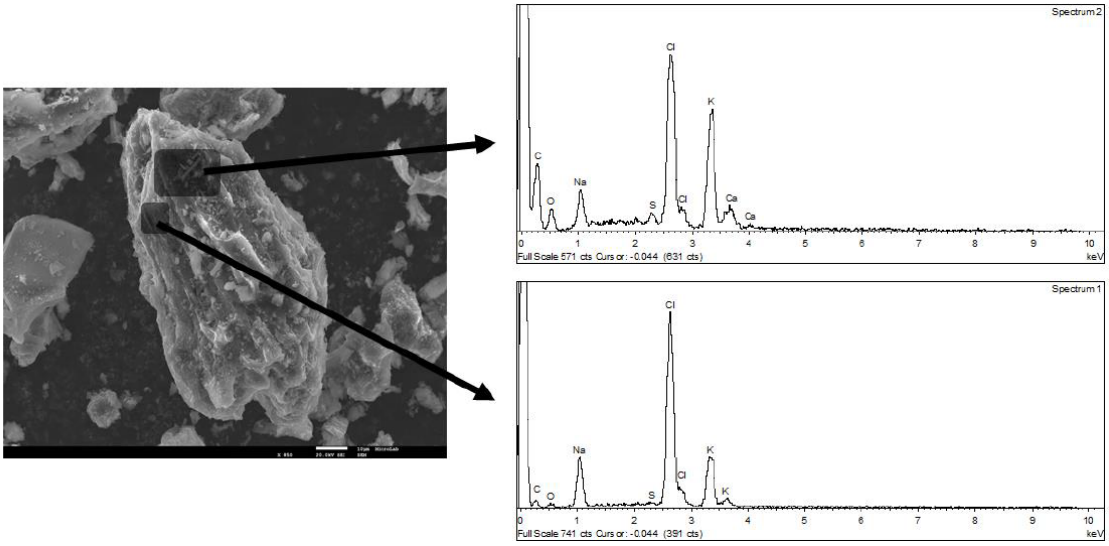

Figure 4.5: SEM image of MCW(LD) with magnification of 850x and EDS spectra of the selected zones.

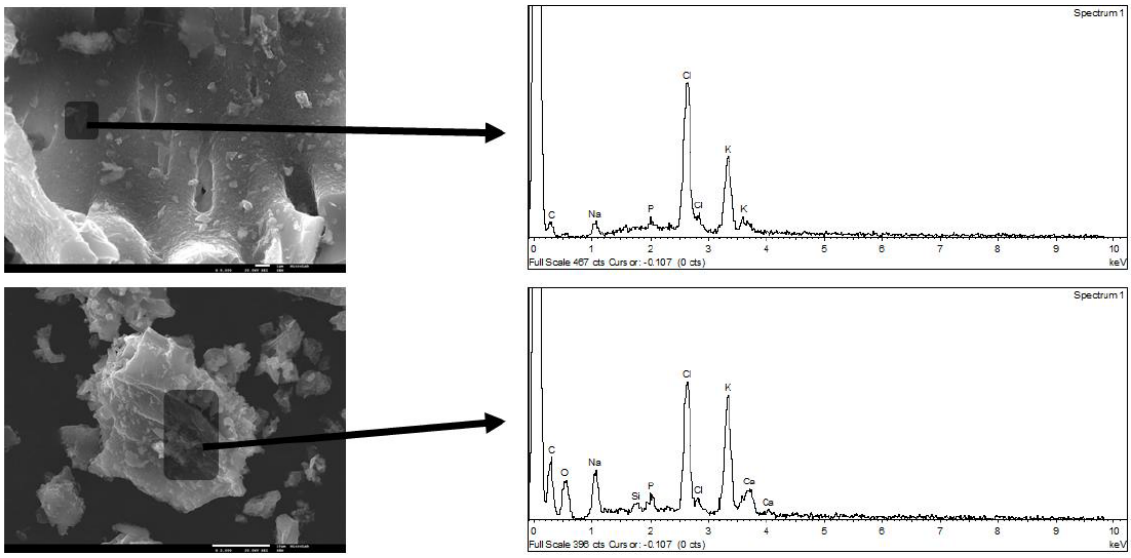

Figure 4.6: SEM image of CAR-MCW(LD) with magnification of 5000x (a) and 2000x (b), and EDS spectra of the selected zones

The particles of CAC showed heterogeneous morphology with rough surface, also typical of mineral rich materials (Figure 4.7). The EDS spectra of selected zones in the CAC particles was characterized by carbonaceous particles enriched with Fe, Mg, Ca, Al, Si, and O.

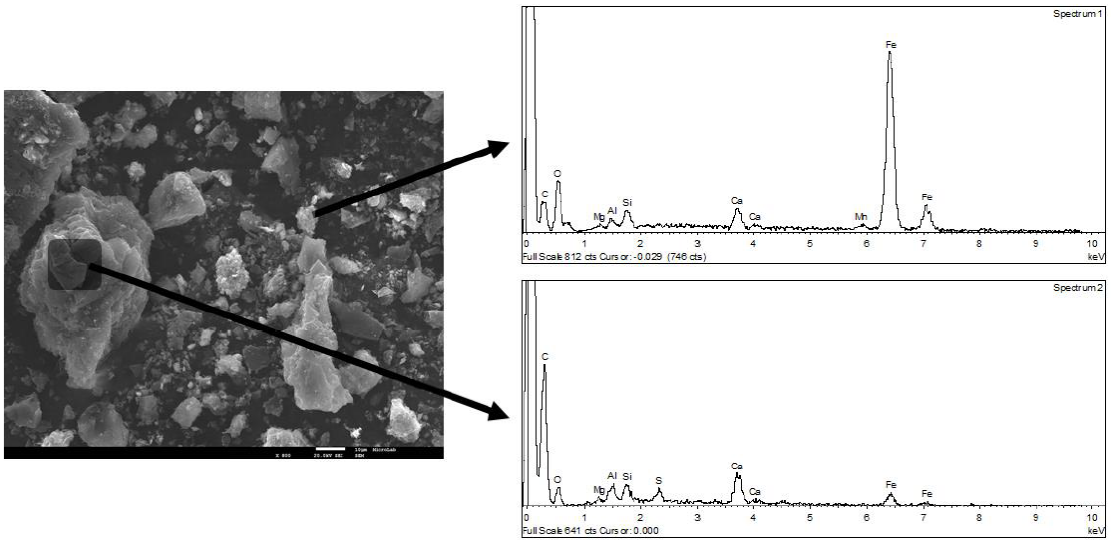

Figure 4.7: SEM image of CAC with magnification of 800x and EDS spectra of the selected zones.

4.3.4 H_2S Dynamic Breakthrough Assays

Figures 4.8 and 4.9 show the H_2S breakthrough curves obtained in the dynamic removal assays for all ACs. For the impregnated ACs (MCW(LD) and CAR-MCW(LD)) and for CAC, it can be observed that after an initial sharped increase of the breakthrough curves, a plateau is generically achieved. The configuration of all curves where a pseudo-steady state is observed without the saturation of ACs ($C_{out} < C_{in}$), points out for catalytic reactions in H_2S removal through dissociative adsorption and oxidation (Ayiania et al., 2019; Bak et al., 2019; Meeyoo et al., 1997; Sitthikhankaew et al., 2014). The products of the catalytic reactions (such as elemental sulphur) are retained on carbons' surface. To determine the saturation capacity of these ACs, much longer assays should be performed; however, the total time of the present experiments (between 400 –

1700 s) were controlled by the availability of biogas samples as the present work was based on the use of real biogas and not on pure H_2S.

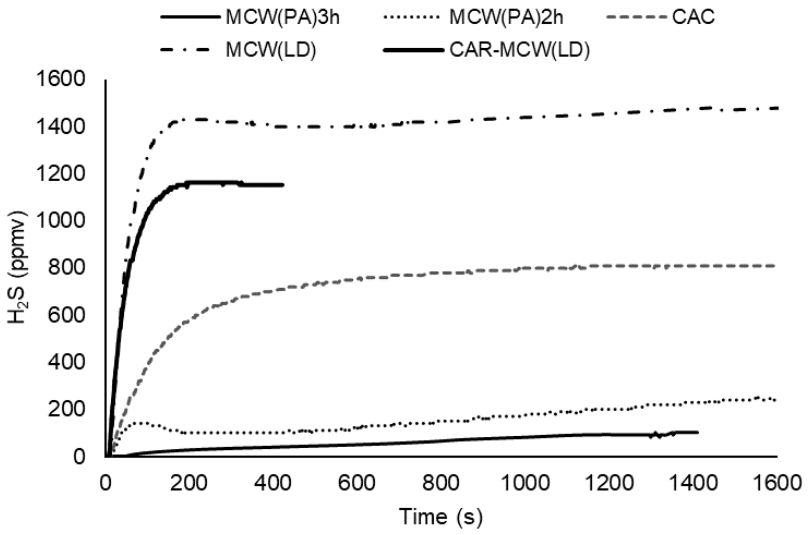

Figure 4.8: H_2S breakthrough curves obtained for ACs.

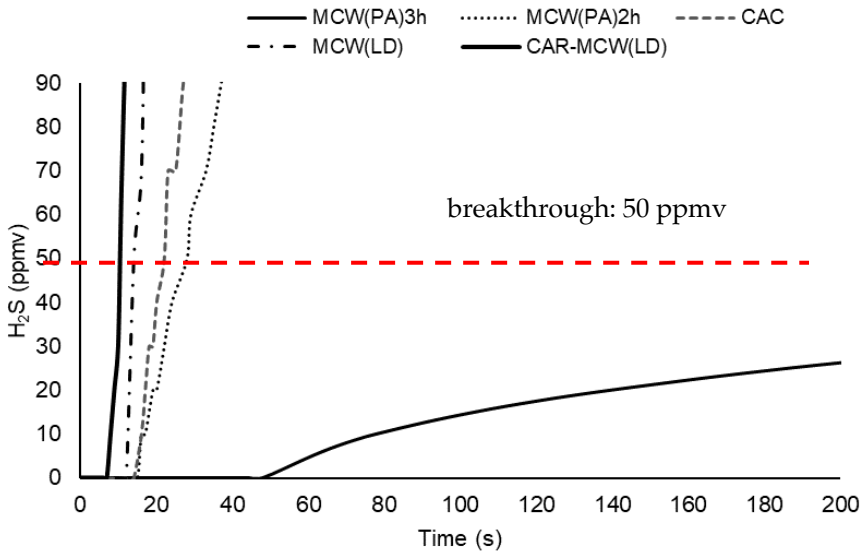

Figure 4.9: Detail of H_2S breakthrough curves up to 200 s with indication of the breakthrough concentration (50 ppmv).

Physically ACs, namely MCW(PA)2h and MCW(PA)3h, presented the best performance from all the materials. At the end of H_2S removal assays, the sample MCW(PA)2h was still removing 78% of the H_2S inlet concentration and sample

MCW(PA)3h was still removing 92%. The latter activated carbon presented an uptake capacity of 15.5 mg/g activated carbon at the breakthrough concentration (50 ppmv) (Table 4.7), which is a value much higher than those registered for the other ACs. Although the adsorption capacity for MCW(PA)2h at the breakthrough point was much lower (0.65 mg/g), this activated carbon performed quite well after 150 s of assay, as mentioned above.

Table 4.7: H2S adsorption capacity (qH2S) and time of breakthrough (tbr) for the breakthrough concentration of 50 ppmv.

Parameter	Unit	CAC	MCW(PA)2h	MCW(PA)3h	MCW(LD)	CAR-MCW(LD)
q_{H2S}	mg/g	0.51	0.65	15.5	0.47	0.25
t_{br}	s	22	28	629	14	11

MCW(PA)3h showed a much higher H_2S uptake capacity than MCW(PA)2h due to its higher surface area, higher microporosity (namely the super-micropores), and higher oxygen content.

Regarding the other ACs, CAC was still removing about 30% of the inlet H_2S concentration at the end of the assays; MCW(LD) and CAR-MCW(LD) were able to remove only 16% and 5%, respectively, which indicates that these ACs were probably near their saturation.

The removal of other gases from the biogas stream, such as CO_2 and CH_4, was also monitored. No retention of CH_4 was observed during the assays. For CO_2, a small retention was registered in the beginning of the assays (<100 s), particularly for the microporous ACs, MCW(PA)2h and MCW(PA)3h. From that point onwards, the outlet CO_2 concentration attained the inlet concentration. This indicates that these ACs may also present some potential for CO_2 removal.

4.3.4.1 H_2S Removal Conditions and Mechanisms

It should be highlighted that the H_2S removal experiments were performed on real biogas samples with other gases present besides H_2S, including CH_4, CO_2, H_2 and CO. Additionally, CH_4 and CO_2 were present in much higher concentrations than H_2S which may have influenced the removal kinetic of H_2S. The biogas stream and ACs were also characterised by very low moisture concentrations;

the oxygen content in biogas was likewise very low (<0.1% v/v). Globally, the conditions for H_2S removal were not the best, but were like those registered in a real case-study of an AD plant at industrial-scale.

Some facts must be kept in mind when looking into breakthrough capacities of the ACs tested in the present work. Most of the studies available in literature is performed with pure H_2S streams and in the presence of optimized moisture and oxygen concentrations. If the biogas is intended to be upgraded to bio-methane (CH_4>97% v/v) directly in an AD plant, most of the upgrading technologies requires a biogas stream free of H_2S, but also free of water and oxygen; otherwise, process contamination will occur. The lack of moisture (both in biogas and ACs) and oxygen (in biogas stream) as it was tested in the present work, will significantly affect the performance of the catalytic H_2S removal by ACs (Le Leuch et al., 2003; Sigot et al., 2016; Sitthikhankaew et al., 2014; Xiao et al., 2008; X. Zhang et al., 2015). Therefore, the H_2S removal conditions studied in the present work were not optimized, but closer to real conditions.

In this work, among the biomass-derived carbons produced, the physically ACs behaved much better than the impregnated ones, which may indicate that the textural properties, such as surface area and microporosity, were more important than the mineral content for H_2S removal. Besides oxygen content, surface area and micropore volume were much higher in MCW(PA)2h and MCW(PA)3h (Table 4.6), particularly in the latter one.

H_2S oxidation is unlikely to happen in very small micropores, being more probable to occur in micropores with sizes above 0.7 nm, which will act as nano-reactors for H_2S dissociation and oxidation (Adib et al., 1999b; Chen et al., 2010; Gonçalves et al., 2018; Hervy et al., 2018; Kante et al., 2012; Seredych and Bandosz, 2008). The micropore size distribution of these two physically ACs was calculated using the Density Functional Theory (DFT) adsorption model for carbon slit-shaped pores (Figure 4.10). Based on these calculations, the sample MCW(PA)3h showed the highest volume of micropores with sizes between 0.7–1.8 nm, which may have played an important role in H_2S removal. Other authors have also indicated the importance of mesoporosity to a higher diffusion rate of H_2S to the active sites and deposition of oxidation products (Dalai et al., 2008; Nowicki et al., 2014). The activated carbon MCW(PA)3h also presented a slightly

higher mesopore volume than the other biomass-derived activated carbons (Table 4.6).

Additionally, the surface chemistry is important for H_2S oxidation, due to the catalytic reactions involved. The sample MCW(PA)3h presented a higher oxygen content than MCW(PA)2h (Table 4.5).

It is known that oxygen groups present in the surface of activated carbons can act as catalysts in H_2S oxidation-reaction (Adib et al., 2000a; Bouzaza et al., 2004; Feng et al., 2005; Le Leuch et al., 2003). Thus, the better performance of MCW(PA)3h can be also related to its better surface chemistry properties.

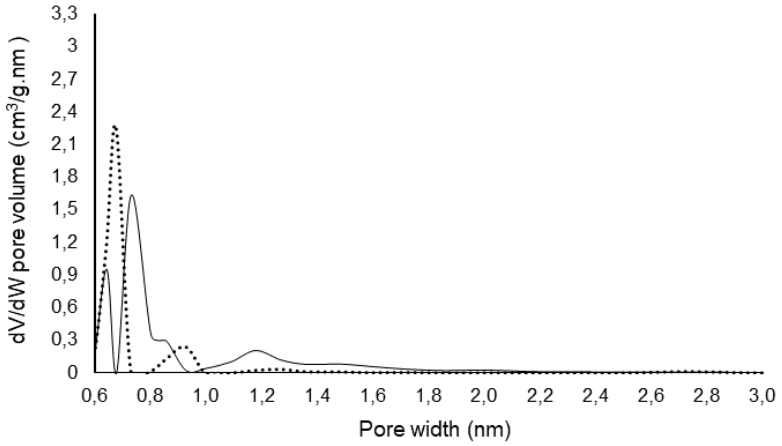

Figure 4.10: Micropore size distribution (DFT adsorption model for carbon slit-shaped pores) of MCW(PA)2h (dashed line) and MCW(PA)3h (solid line).

Regarding CAC, both textural properties (high mesopore content) and high catalytic mineral content (Fe, Al, Ca, K) may have been important for its performance.

Despite of their strong alkaline behaviour and the presence of mineral species (namely K, Na, and Ca) and oxygen in their surface, the impregnated ACs (MCW(LD) and CAR-MCW(LD)) have presented the lower breakthrough capacities among all the tested ACs (Table 4.7). Their poor textural properties, with almost no microporosity, may have been the most important feature on their performance. Nevertheless, their H_2S breakthrough capacities are comparable with the ones obtained in previous works (Gutiérrez Ortiz et al., 2014; Shang et al., 2016, 2013; Yuan and Bandosz, 2007), in which the authors used sewage sludge and digestate-derived biochars or ACs in H_2S removal assays.

4.4 Conclusions

The physically ACs performed better in H_2S removal assays than ACs impregnated with an anaerobic liquid digestate, with uptake capacities, q_{H2S}, of 15.5 and 0.65 mg/g for MCW(PA)3h and MCW(PA)2h, respectively; the uptake capacities for MCW(LD) and CAR-MCW(LD) were 0.47 and 0.25 mg/g, respectively. Thus, textural properties, such as surface area and microporosity, seemed to be more important than mineral content in H_2S removal from real biogas samples. Effectively, both surface area (S_{BET}) and micropore volume (V_{micro}) were much higher in MCW(PA)3h (S_{BET} = 820 m^2/g and V_{micro} = 0.32 cm^3/g) and MCW(PA)2h (S_{BET} = 630 m^2/g and V_{micro} = 0.21 cm^3/g) than in impregnated ACs (S_{BET} = 38.0 m^2/g and V_{micro} = 0.01 cm^3/g for MCW(LD); S_{BET} = 8.0 m^2/g and V_{micro} = 0.01 cm^3/g for CAR-MCW(LD)).

The highest volume of micropores, with sizes between 0.7–1.8 nm, that were registered for MCW(PA)3h may have played an important role in H_2S removal. Also, its higher oxygen content may have been involved in the catalytic oxidation reaction of H_2S, indicating that its better performance on H_2S removal is also due probably to the better surface chemistry properties.

Finally, MCW(PA)3h showed a higher H_2S adsorption capacity (15.5 mg/g) than the commercial activated carbon (0.51 mg/g), which means that this new biomass-derived activated carbon suits better at non-optimized conditions of H_2S removal, namely in what concerns moisture and oxygen deficiencies.

5

CO_2 Separation from Biogas Using the ACs Produced from Maize Cob Waste

5.1 Introduction

Biogas is a mixture made of approximately 60-70% v/v of CH_4 in CO_2, over some minor amounts of contaminants. After having removed the trace contaminants, the biogas purification process consists essentially in CO_2 separation from CH_4.

Among the several technologies available for removing CO_2 from biogas streams, Pressure Swing Adsorption (PSA) is an adsorption-based process that is attracting increasing interest for its low energy requirements and limited initial capital investment in comparison with other separation technologies (D.M. Ruthven et al., 1994 and Bauer et al., 2013). Moreover, PSA can process high throughputs and produce high-purity CH_4 (Esteves and Mota, 2007).

In a PSA unit for biogas upgrading, an adsorbent is submitted to cyclic pressure changes to selectively adsorb and desorb CO_2. The final product of interest is a stream enriched in CH_4 (> 97% v/v). The efficiency of adsorption of CO_2 depends, among other factors, specifically on the textural properties of the adsorbent material employed, on its working capacity, CO_2 selectivity and on its capability to be regenerated. Thus, the choice of the adsorbent plays a crucial role in the PSA process efficiency.

Common adsorbents used in PSA units are Carbon Molecular Sieves (CMS), activated carbons (AC), natural and synthetic zeolites (Grande, 2011; Yang, 1987). Metal Organic Framework (MOF) is gaining consensus as a potential alternative adsorbent (Schell et al., 2013) with promising results (Casas et al., 2013) for PSA application, although the present high costs still cut off this material from commercial scale-up application (Férey, 2016).

The choice of the best adsorbent for CO_2 separation depends largely on its cost and the operating conditions applied. Pellerano et al., 2009 observed that ACs can provide higher adsorption capacities than some zeolites at pressures higher than 2.5 bar and Siriwardane et al. (2001) demonstrated that ACs can provide better performances than CMS, when $CO2$ partial pressure is higher than 1.7 bar. Thus, ACs can be considered suitable candidates for biogas upgrading, since the typical CO_2 partial pressure used during the upgrading process commonly ranges from 1.8 bar to 4 bar (Grande, 2011).

The ACs used in PSA units are generally produced by thermal activation of relatively dense form of carbon precursors, such as bituminous coal, due to its high physical strength (Ruthven et al., 1994). The use of agricultural residues as precursors to produce carbon adsorbent materials can be considered one of the main challenges in the manufacture of activated carbons, since these precursors are cheap, available in large amounts and are environmentally friend.

Few studies are present in literature about the preparation of biomass based ACs for biogas upgrading purposes. The most used precursors are coconuts shells (Vilella Costa et al., 2017), cherry stones (Álvarez-Gutiérrez et al., 2014 and 2016), pine sawdust (Durán et al., 2018), date seeds (Ogungbenro et al., 2018) and MCW (Song et al., 2013). All these authors agree on the high potential of these materials as precursors of the adsorbent media for biogas upgrading and CO_2 separation.

Among the available biomass, MCW, is particularly appealing and may be a source of substantial economic rewards, being actually left unused on soil. To the author knowledge, no study is present in literature about the use of AC produced from MCW for biogas upgrading with PSA.

Chapter 5 aims to assess the suitability of two of the activated carbons produced from MCW (MCW(PA)2h and MCW(PA)3h) that showed the best properties as potential adsorbents for CO_2 separation from a biogas stream. This gives the basis for future design and modelling works of a PSA cycle based on

the use of renewable adsorbents. This Section represents the development of the **Task 5** of this work.

5.2 Experimental

5.2.1 Materials

The physical activated MCW(PA)2h and MCW(PA)3h were selected as potential candidates' adsorbents for CO_2 separation from a biogas stream due to their favorable textural properties (Table 4.6) and on their good thermal stability (Figures A 4 and A 5) when compared to the others produced ACs. Furthermore, their apparent good mechanical strength and low dusting made them potential candidates for PSA application.

Prior to each adsorption equilibrium experiment, the carbon samples were pre-treated by degassing in vacuum for at least 3 h, at 423.15 K[1]. Approximately 0.6 g of MCW(PA)2h and 0.8 g (MCW(PA)3h of each sample were used in the adsorption equilibrium experiments.

In a first step, CO_2 and CH_4 adsorption equilibrium measurements on MCW(PA)2h and MCW(PA)3h were performed at 303.15 K. The adsorbent that provided the overall higher adsorption capacity, selectivity towards CO_2 and working capacity, was then submitted to the adsorption equilibrium measurements at 323.15 K and 353.15 K. In a second step, fixed-bed experiments were performed to analyse the kinetics and dynamic behavior of the sample MCW(PA)3h upon its packing into a column. For this purpose, approximately 18 g of MCW(PA)3h were produced in different batches according to the same methodology described in Figure 4.1. Prior to column packaging, the MCW(PA)3h was sieved (> 1 mm) and homogenized using a procedure based on Allman and Lawrence (1972) technique.

[1] In the present Chapter 5, the Kelvin (K) was chosen as unit of measurement for temperature, since it is the most commonly used in the area of gas separation.

All gases used were provided by Air Liquide and Praxair (Portugal): CO_2 N48, CH_4 N35, and Helium at 25.2 mg/(N m^3).

5.2.2 Experimental Apparatuses

5.2.2.1 Volumetric Unit

The adsorption equilibrium measurements were performed in a volumetric experimental apparatus built with stainless steel tubing (Swagelok Company, USA) and a set of solenoid valves (ASCO Numatics, USA) that are controlled through a LabVIEW-based (National Instruments Corp., USA) software developed in-house. The unit was built in-house and is fully described in Ribeiro et al. (2015). The general scheme of the volumetric unit used in this work is reported in Figure 5.1.

The unit allows the simultaneous equilibrium measurements of two adsorbent samples up to an operation pressure of 20 bar that can be controlled by two pressure transducers (Omega Eng. Inc., USA). An oven (Nabertherm B170 GmbH, Germany) controls the temperature of the adsorption cells over the range of 303–1373 K. The apparatus includes a stainless-steel calibrated volume (Hoke, USA), v_{cal}, used in the determination of the volumes in the unit.

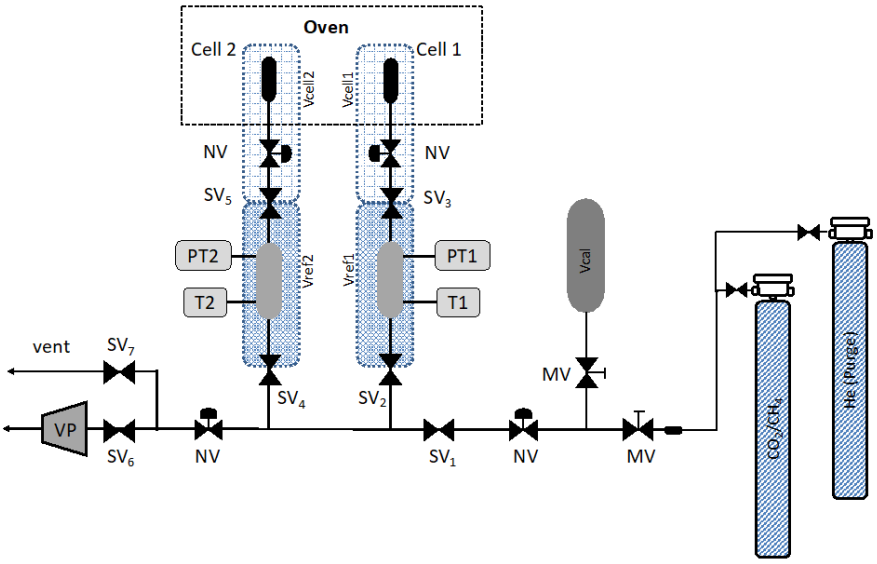

Figure 5.1: Schematic of the volumetric unit (vcal, calibration volume; vref1 and vref2, reference volumes; vcell and vcell2, cell volumes; PT, pressure transducer; T, Pt100 temperature sensor; SV, solenoid valve; NV, needle valve; MV, manual valve; VP, vacuum pump). Adapted from Ribeiro et al. (2015).

The gas is admitted into the apparatus through a single feed line, which is then divided into two parallel lines connected to the two adsorption cells (Cell 1 and Cell 2). Each independent gas line connects to a previously calibrated reference volume (v_{ref1} and v_{ref2}) linked to the respective adsorption cell.

The volumes v_{ref1} and v_{ref2} are confined between valves SV_2 and SV_3, and SV_4 and SV_5, respectively; v_{cell1} and v_{cell2} correspond to the volumes after SV_3 and SV_5, respectively. The temperature of the reference volumes is measured using four-wire Pt-100 probes (RS Amidata, Spain). The temperature of the adsorber cells is controlled by the oven (Figure 5.1). This oven allows the *in situ* degasification of the adsorbent samples. The mass of the activated sample inside each Cell was corrected weighting the mass of the adsorbent before and after the degasification procedure at net of the tare of the Cell and connecting fittings. A vacuum pump (model RV3, Edwards Ltd., USA) is connected to the volumetric unit to allow the degassing and regeneration of the adsorbent samples under vacuum.

5.2.2.2 Fixed- bed Unit

The experimental apparatus used in this work for the fixed bed experiments is an adaptation of the apparatus built in-house and fully described in Ribeiro et al. (2017). This unit permits a flexible operation in terms of feed composition, flow rates, pressure and temperature. The one-column adsorption unit is composed by three main parts: the gas feed/eluent section, the separation section, and the pressure control/product outlet section. The scheme of this unit is presented in Figure 5.2.

The unit is made of 316 stainless steel tubing with outer diameter of 1/8 in. (Swagelok Company, USA). In the gas feed/eluent section, the gaseous feed mixture is admitted into the unit by means of two mass flow controllers (MFC1 and MFC2) with operating ranges of 0–100 sccm (accuracy ±0.8% of reading (Rd) + 0.2% of full scale (FS); Alicat Scientific, The Netherlands), and 0–2 slpm (accuracy of ±0.5% Rd + 0.1% FS; Bronkhorst High-Tech B.V.), respectively. The purge stream (Helium) is controlled by MFC3 with an operating range of 0–5 slpm (accuracy of ±0.5% Rd + 0.1% FS; Bronkhorst High-Tech B.V.). The column pressure is controlled by a backpressure regulator (BPR1 and BPR2) in the range of 2–10 bar (accuracy of ±0.5% FS; Bronkhorst High-Tech B.V., The Netherlands).

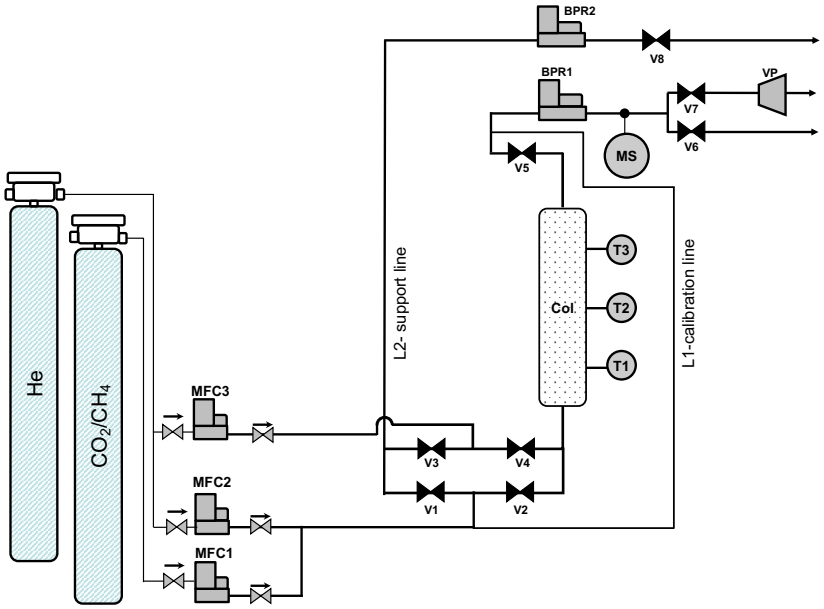

Figure 5.2: Schematic of the adsorption unit (Col: Column; MFC: Mass Flow Controller; BPR: Back Pressure Regulator; PT: Pressure Transducer; V: solenoid valve; T: Pt100 Temperature Sensor; VP: Vacuum Pump; MS: Mass Spectrometer).

The adsorption unit is composed by one column (Col), through which the gas flux is controlled using 8 on-off solenoid valves from ASCO Valve Inc. (USA). The unit is supported with a second line vented to the atmosphere (L2-support line, Figure 5.2). This line has the function of improving the mixing of the feed mixture before each dynamic assay and allows a more efficient switch between the feed and the purge steps. The temperature is measured at three different positions (top, middle and bottom) inside the column using four-wire Pt100 probes (RS Amidata S.A., Spain). The column temperature is controlled using an external electric resistance coiled around the bed and connected to a PID controller (model E5CN-R2MT-500, Omron Corporation).

The gas composition is measured online by mass spectrometry (MS) using a Dymaxion DM100 quadrupole mass spectrometer from Ametek Process Instruments (USA). The MS is operated by the commercial software Dycor System 2000. The gas composition of the exit stream is analysed using a real-time gas stream composition quantification algorithm, fully detailed elsewhere(I. A. A. C. Esteves et al., 2016). The complete apparatus is controlled by an in-house developed software built in Labview®. The program can be operated in manual or automatic modes and monitors the experiments and records all the data (i.e., time, temperatures, flowrates, pressures) acquired during each experiment.

5.2.3 Experimental Methodology

5.2.3.1 Volumetric Unit

The experimental measurements of the adsorption equilibrium isotherms follows the typical methodology applied to a volumetric apparatus (Pakseresht et al., 2002 and Policicchio et al., 2013). According to Figure 5.1, the experimental procedure consists in the addition of static pressure steps to the reference volumes (v_{ref1} and v_{ref2}). After pressure and temperature equilibration, the gas supplied is expanded to the cell containing the adsorbent (v_{cell1} and v_{cell2}). After this step, the system pressure is monitored until the adsorption equilibrium is reached, which is assumed to occur when the rate change of the pressure approaches zero under isothermal conditions, i.e., the pressure variation is lower than 0.01 bar, which is the accuracy of the pressure transducers employed (0.05% of their full scale), over a minimum period of time of 45–60 min. Then, the adsorption cells are once again isolated from the reference volumes, by closing valves SV_3 and SV_5, and the method is repeated until enough experimental points to generate the adsorption isotherm are obtained. When the desired pressure is reached, a similar procedure is repeated, but by stepwise depressurization of the reference volumes and subsequent contact with the adsorption cells. This allows the measurement of the desorption equilibrium isotherms. In order to reduce the accumulated error of the measurements, a maximum of 15 experimental points per isotherm is recorded (Ribeiro et al., 2015).

5.2.3.2 Fixed-bed Unit

In order to describe the adsorption kinetics of CO_2 and CH_4 in the selected activated carbon, diluted breakthrough experiments at three different temperatures (303 K, 323 K and 353 K) with molar fraction of 1% v/v in Helium were performed. Helium (He) was used as inert carrier gas.

Preliminary essays were performed with He to assess the proper operation of the experimental setup. The pressure drop across the column was evaluated using the pressure transducer assembled in the experimental apparatus. The measurements showed that, at the low flow rates studied in this work, the pressure drop was smaller than the accuracy of the pressure transducer used (6.9 mbar) and could, therefore, be neglected.

During the experimental runs, the total pressure was fixed at 4 bar and the gas interstitial velocity (u) was set at 0.01 m/s. A total of 12 fixed-bed experiments were performed. To assess the reproducibility of the data results some of the assays were repeated.

Table 5.1 reports the experimental system properties used and Table 5.2 reports the operation conditions applied during the dynamic assays.

Appendix D reports the methodology used to determine the bulk density, ρ_b (g/cm^3), density of the carbon matrix, ρ_S (g/cm^3), dry particle density, ρ_p (g/cm^3), as well as the calculation of the void fraction of packing, ε_b, the internal or intraparticle porosity, ε_p, and the total void, ε. The adsorbent mean particle radius, R_p, was assumed to be equal to half of the average value of the mesh used to sieve the ACs particles. Prior of the dynamic assays, the adsorbent bed was degassed in vacuum and at the temperature of 353-358 K for several hours.

Before each dynamic assay, the system was properly prepared according to the following method: (i) warm-up of the MS system for 1 hour, (ii) electronic stabilization of the instruments (MFC's, BPR, power supplies) for approximately 30 minutes, and (iii) stabilization of the MS signal using its System 2000 software followed by calibration for the gas mixtures to use.

This latter feature allows in real-time the quantification of the column exit stream. The algorithm obtained provides trend screens for data acquisition, input, and calculation of the gaseous composition of the exit stream. The details of the configuration files used for the composition analysis are reported elsewhere (Esteves, 2005; (I. A. A. C. Esteves et al., 2016).

Table 5.1: Characteristics of the experimental system used in the fixed-bed experiments with the carbon sample MCW(PA)3h.

MCW(PA)3h Properties	Unit	Value
Specific Pore Volume (W_s)	cm^3/g^3	0.35
BET surface area (A)	m^2/g	886
Particle density (ρ_p)	g/cm^3	0.40
Carbon matrix density (ρ_c)	g/cm^3	1.77
Intraparticle void fraction (ε_p)	-	0.77
Total Voidage (ε)	-	0.90
Mean pore radius (r_p)	Å	7.80
Tortuosity (τ) (*)	-	4.00
Mean particle radius (R_p)	mm	0.75
Column Properties		
Bed length (L)	cm	18.0
Bed Diameter (D)	cm	2.10
Adsorbent weight	g	14.4
Bed porosity (ε_b)	-	0.47
Bulk density (ρ_b)	g/cm^3	0.21

(*) The tortuosity factor, τ, was assumed to be 4.0, which is a typical value for activated carbon (D. M. Ruthven, 1984 and Costa et al., 1985).

Briefly, for diluted working conditions, the MS calibration was performed firstly by feeding a diluted mixture of 1% v/v of CO_2 or CH_4 than 0.5 % v/v of CO_2 or CH_4 in He to the MS, which is verified by the respective MFC. This is performed through the bypass line L1 (Table 5.2) and guarantees that the adsorbent is not contaminated by the diluted mixture prior to the experiment. Afterwards, the dilute mixture is fed firstly to the L2-support line to allow the complete mixing of the gases (adsorbate and eluent), when the column is simultaneously fed with the inert gas (Table 5.2). The pressure inside the system is stabilized at 4 bar, through the backpressure regulators BPR1 and BPR2

Table 5.2. Experimental conditions applied in the breakthrough runs for CO2/He and CH4/He diluted mixtures.

Adsorbate	T	F	y_i, Adsorbate	y_{He}, Eluent	u	P_{tot}
	K	cm^3/min	%		m/s	bar
CO_2	303.35	104.2	1.04	98.96	0.01	4.01
	323.35	104.5	1.04	98.96		4.00
	353.25	103.7	1.05	98.95		4.02
	303.35	102.4	0.52	99.47		4.01
	323.35	104.9	0.51	99.48		4.00
	353.25	105.1	0.53	99.46		4.00
CH_4	303.95	104.5	1.03	98.97		4.01
	323.05	104.6	1.04	98.96		4.00
	353.05	105.6	1.04	98.96		4.00
	303.95	105.11	0.53	99.49		4.01
	323.05	104.64	0.54	99.48		4.01
	353.05	105.61	0.52	99.48		4.02

The gaseous flows were then switched closing valves V1 and V4 and opening valves V3 and V2, and the diluted mixture flows through the column. The system is continuously fed at constant flowrate and (T, P) conditions until breakthrough of the more adsorbable component occurs, and up to the saturation of the adsorbent bed. The concentration profiles of the gases at the exit of the column is continuously quantified by the MS analysis during the dynamic assay. When the inlet and outlet compositions are equalized, the feed mixture is switched back to the support line L2 (closing valves V2 and V3, and opening valves V1 and V4) and the inert gas (He) enters the column to purge the system. Finally, the purge with the eluent is stopped when the MS signal detects only pure He exiting the column. This indicates that the adsorbent bed is fully regenerated and clean of any adsorbate.

5.2.4 Theoretical Analysis

5.2.4.1 Adsorption Equilibria

5.2.4.1.1 Sips Model

The experimental adsorption equilibria data obtained at different temperatures can be accurately fitted to the Sips model (Do, 1998) to provide an accurate representation of the adsorption equilibria when there is no need to obtain a gen-

eral equation that allows the extrapolation to other adsorbates, or to a substantially different temperature range as allowed by the Adsorption Potential Theory (APT) (Esteves et al., 2008).

The advantages of the Sips model are its ability to fit well the experimental data, its mathematical simplicity, and its straightforward extension to multicomponent adsorption. For these reasons, the Sips model is predominantly used in the modelling and design of adsorbers and cyclic gas separation processes for concentrated mixtures (Yang, 1987).

The Sips isotherm model is given by (Do, 1998) as follows,

$$q = \frac{q_s (bP)^{1/n}}{1 + (bP)^{1/n}}, \qquad (Eq.\ 5.1)$$

$$b = b_0 \exp\left[\frac{Q}{RT_0}\left(\frac{T_0}{T} - 1\right)\right], \qquad (Eq.\ 5.2)$$

$$\frac{1}{n} = \frac{1}{n_0} + \alpha\left[\left(1 - \frac{T_0}{T}\right)\right], \qquad (Eq.\ 5.3)$$

$$q_s = q_{s0} \exp\left[\chi\left(1 - \frac{T_0}{T}\right)\right], \qquad (Eq.\ 5.4)$$

where q is the amount adsorbed (mol/kg), q_s is the maximum adsorbed amount at saturation (mol/kg), q_{s0} is the saturation capacity at reference temperature T_0, b is the adsorption affinity constant (bar^{-1}) that measures how strong an adsorbate molecule is attracted onto the solid surface, b_0 is the affinity constant at the reference temperature (T_0), n is the parameter that characterizes the adsorbate/adsorbent interaction (the further from the unit its value is, the highest is the heterogeneity of the system adsorbent/adsorbate), n_0 is the parameter n at the reference temperature T_0; α is a constant parameter; Q is the adsorption heat or the isosteric heat of adsorption at half loading (kJ/mol); $\gamma = Q/R_g T_0$ is the heat coefficient; and χ is a constant parameter.

The temperature dependence of each parameter in the Sips model was determined by a global fitting of the adsorption isotherms obtained experimentally at all the temperatures studied. For this purpose, the Solver of Microsoft Office Excel was used. The goodness of the fit is evaluated based on the regression sum of squares due to error (RSS) defined as

$$\mathrm{RSS} = \sum_{i=1}^{i=n} \left(Y_{i,exp} - Y_{i,pred}\right)^2, \qquad (Eq.\ 5.5)$$

where Y is the specific variable, subscripts *exp* and *pred* correspond to the experimental and predicted values, respectively. The Fit Standard Error (FSE) is determined as

$$FSE = \sqrt{\frac{RSS}{DOF}}, \qquad (Eq.\ 5.6)$$

where *DOF* is the degree of freedom defined as $(N - m)$, the difference between the number of data points N and the number of coefficients fitted m. The average relative error (ARE) is defined as

$$\text{ARE}\ (\%) = \frac{100}{\sum N} \sum \left(\sum_{i=1}^{i=N} \frac{|q_{i,pred} - q_{i,exp}|}{q_{i,exp}} \right), \qquad (Eq.\ 5.7)$$

where $i = 1, \ldots, N$ is the adsorbate species.

5.2.4.1.2 Isosteric Heat of Adsorption

The isosteric heat of adsorption represents the energy difference between the state of the system before and after the adsorption of a differential amount of adsorbate on the adsorbent surface (Lyubchik ert al., 2011). It can also be defined as the ratio of the infinitesimal change in the adsorbate enthalpy to the infinitesimal change in the amount adsorbed (Do, 1998).

The knowledge of the isosteric heat of adsorption is essential for the characterization of any gas-phase adsorption process, and the correlations that describe the correct temperature dependence over a relatively wide range of pressure are essential for designing and operating a gas-phase adsorption process (Esteves et al., 2008). The isosteric heat of adsorption is usually estimated from the temperature dependence of the adsorption isotherm (Builes et al., 2013 and Karavias and Myers, 1991).

It must be noticed that the assumption of a constant heat of adsorption, over a relatively large temperature interval, introduces in practice only small errors in the pressure and loading estimations (Shen et al., 2000). This is why the assumption of a temperature-invariant heat of adsorption is frequently adopted (Sircar and Cao, 2002).

For any given isotherm model, the isosteric heat of adsorption ($-\Delta H$) (kJ/mol) can be estimated using the van't Hoff equation (Do, 1998). This equation is based on some simplifying assumptions: the adsorbed molar volume is neglected and ideal behavior for the bulk gas phase is assumed (Holland et al.,

2001). These assumptions, in most cases, have negligible impact on the estimated value of the isosteric heat.

Applying the van't Hoff equation to the Sips isothermal model, the isosteric heat of adsorption in terms of the adsorbed amount q (mol/kg) can be written as follows (Do, 1998):

$$(-\Delta H) = Q - (\alpha R T_0) n^2 ln\left(\frac{q}{q_s - q}\right), \qquad (Eq.\ 5.8)$$

or alternatively in terms of fractional loading $\theta = q/q_s$,

$$(-\Delta H) = Q - (\alpha R T_0)\, n^2 ln\left(\frac{\theta}{1-\theta}\right). \qquad (Eq.\ 5.9)$$

The heat of adsorption, Q, equals (- ΔH) when q/q_s is 0.5.

5.2.4.2 Adsorption Potential Theory (APT)

One of the most widely used theories to describe physical adsorption of gases and vapours onto microporous adsorbents is the Adsorption Potential Theory (APT), developed by Dubinin (1960, 1975) and reviewed by Tien (1994). The APT has been widely used for correlating adsorption equilibria data on microporous carbons (Yang, 1987; Holland et al., 2001 and Rouquerol et al., 1999).

This theory assumes that (i) the adsorbed phase is considered to behave as a liquid, (ii) the adsorbate progressively fills the pore volume and (iii) only the unoccupied volume remains available for adsorption. The difference in free energy between the adsorbed phase and the saturated liquid sorbate, determined from the ratio of the adsorbate saturated vapor pressure and the equilibrium pressure, is referred to as the adsorption potential, ϕ.

The APT states that for a given gas–solid system the specific volume of the adsorbed phase, W, is a function of ϕ (Eq. 5.10):

$$W = qV_{m=}W(\phi), \qquad (Eq.\ 5.10)$$

where q is the total amount of gas adsorbed at equilibrium and $V_m\ (T)$ is the molar volume of the adsorbed phase at temperature T. The adsorption potential is defined as

$$\phi = RT \ln\left(\frac{P_s}{P}\right), \qquad (Eq.\ 5.11)$$

where P is the equilibrium pressure at temperature T, $P_s(T)$ is the saturated vapor pressure of the adsorbate, and R is the ideal gas constant. In order to correct the non-ideal gas behavior, at high pressure, P and P_s should be replaced by the corresponding fugacities, f and f_s.

The functional relationship between ϕ and W is typical of a given gas–solid system and it is known as the characteristic curve. The characteristic curve is temperature independent, thus the adsorption equilibrium measurements performed at one temperature should be sufficient to describe the adsorption equilibria at all temperatures for the same gas–solid system (Yang, 1987 and Agarwal and Schwarz, 1988). Therefore, the APT allows the prediction of single-component adsorption equilibria from a limited set of experimental measurements. Additionally, in many cases, the theory can be generalized if an affinity coefficient or scaling divisor, β, is used as a shifting factor to bring the characteristic curves of all adsorbates on the same adsorbent into a single curve (Yang, 1987 and S.D. Mehta, 1985). Under this assumption, Eq. 5.10 is replaced by

$$W = qV_{m=}\mathrm{W}(\phi') \qquad (Eq.\ 5.12)$$

with

$$\phi' = \left(\frac{\phi}{\beta}\right) \qquad (Eq.\ 5.13)$$

Eq. 5.13 becomes characteristic of a given adsorbent and it is potentially applicable to all adsorbates. Several works have corroborated the applicability of the APT theory (Chang and Talu, 1996; Camacho et al., 2015; Holland et al., 2001; Mota and Rodrigo, 2000).Wood (2001, 1992) has published an extensive compilation of experimental β values for gases and vapours on activated carbon. He showed that β is highly correlated to the molecular parachor, according to

$$\beta = 8.27 \times 10^{-3}\ (parachor)^{0.90}, \qquad (Eq.\ 5.14)$$

where, in absence of an experimental β value, the parachor can be estimated using the following correlation based on the critical volume, V_c (cm^3/mol),

$$parachor = 8.0 + 0.707\ V_c. \qquad (Eq.\ 5.15)$$

Whenever the conditions are below the critical temperature, T_c, of the adsorbate, V_m is assumed equal to the molar volume of the saturated liquid at system temperature, which can be estimated from the modified Rackett equation

$$V_m = \frac{RT_c}{P_c} Z_{RA} \left[1 + \left(1 - \frac{T}{T_C}\right)\right]^{\frac{2}{7}}, \qquad (Eq.\ 5.16)$$

where P_c is the adsorbate critical pressure and Z_{RA} is its Rackett compressibility factor. The constants in Eq. 5.16 can be obtained from the online NIST Database, Vidal (1997) and from Spencer and Danner (1972). The saturated vapor pressure, P_s, is estimated using the Wagner equation:

$$ln\left(\frac{P_s}{P_c}\right) = \frac{Ax + Bx^{1.5} + Cx^3 + Dx^6}{1-x},\ x = 1 - \frac{T}{T_c}, \qquad (Eq.\ 5.17)$$

with adsorbate-specific constants A, B, C, and D taken from the literature (Dubinin, 1975; Forero and Velásquez, 2011; Reid et al., 2009).

Above T_c the adsorbed phase is not well defined, and this has led to the proposal of different approximations for V_m. Likewise, under these conditions, the concept of vapor pressure doesn't exist, and P_s is a pseudo-vapor pressure. Following the suggestions given by Agarwal and Schwarz (1988), P_s and V_m at temperatures above T_c were estimated as

$$P_s = \left(\frac{T}{T_c}\right)^2 P_c, \quad V_m = V_b\, exp[\,\Omega(T - T_b)], \quad \Omega = \ln\frac{V_c/V_b}{(T_c - T_b)}, \qquad (Eq.\ 5.18)$$

with T_b and V_b the temperature and molar volume of the liquid adsorbate at the normal boiling point, respectively, and Ω an estimate of the thermal expansion coefficient of the adsorbate in a superheated liquid state (Ozawa et al., 1976).

To obtain a workable isotherm model for process simulation, the experimental characteristic curve is fitted to the modified Dubinin–Astakhov (D–A) equation (Dubinin, 1975; Dubinin and Astakhov, 1970; Ozawa et al., 1976)

$$W = W_s\ \exp(-\gamma\phi'^{\,n}), \qquad (Eq.\ 5.19)$$

where W/W_s is the fractional filling of the specific (micro)pore volume of the carbon, W_s, accessible to the adsorbate, γ is a parameter function of the characteristic energy for the solid-fluid system, and n is a parameter related to the pore size distribution. The values of these parameters are determined from the linear fitting of $ln[ln(W_s/W)]$ versus $ln\ \phi'$. Alternatively, $ln(W_s/W)$ can be expressed as a polynomial expansion in ϕ, where a third-order polynomial expansion usually suffices:

$$\ln(W_s/W) = a_1\phi' + a_2\phi'^2 + a_3\phi'^3. \qquad (Eq.\ 5.20)$$

5.2.4.3 Dynamic assays and Kinetics

The breakthrough experiments were modelled by means of computational simulation to understand the adsorption kinetics of the solid-fluid system studied. For this purpose, a trace system of an adsorbate component (CO_2 or CH_4), diluted in a non-adsorbing (or weakly adsorbing) carrier or eluent gas (He) was considered, where the velocity changes across the mass transfer zone were assumed negligible and the temperature was considered constant (isothermal trace system).

In a real trace isothermal system, the outlet response is dispersed as a result of the combined effects of axial dispersion and of the mass transfer resistance, that is due to the intraparticle diffusion and to the external film mass transfer resistance. The flow rate was considered high enough to assume negligible film mass transfer resistance.

The mathematical model built for the simulations is based on the following assumptions: (i) ideal gas behaviour, (ii) homogeneous bed porosity, (iii) mass, heat and momentum transport in the radial dimension is neglected, (iv) the axial dispersed plug-flow and Linear Driving Force (LDF) approximation for lumped solid-diffusion mass transfer are considered to provide a realistic representation of the chromatographic column (Yang, 1987). Furthermore, the average particle diameter, bulk porosity and tortuosity of the packaged bed are assumed constant and independent of temperature.

The mathematical model applied uses the individual component mass balance equations, coupled with boundary and initial conditions. The differential material balance to the *i* component is expressed as

$$\frac{\partial C_i}{\partial t} + \left(\frac{1-\varepsilon_b}{\varepsilon_b}\right)\frac{\partial q_i}{\partial t} = \frac{u}{L}\left(\frac{1}{Pe_i}\frac{\partial^2 C_i}{\partial x^2} - \frac{\partial C_i}{\partial x}\right), 0 < x < 1 \qquad (Eq.\ 5.21)$$

where C_i and q_i are the concentrations in the gas phase and in the adsorbed phase of component *i*, respectively; $Pe_i = uL/D_{iL}$, the Péclet number, u is the interstitial velocity, D_{iL} the axial dispersion coefficient, L is the column length, and $x = z/L$ is the dimensionless axial coordinate with z the axial coordinate along the column.

The lumped solid-diffusion LDF model is described by

$$\frac{\partial \mathrm{q}_i}{\partial \mathrm{t}} = k_{LDF,i}(q_i^* - q_i) \qquad (Eq.5.22)$$

where $k_{LDF,i}$is the LDF constant for component i and the equilibrium loading, q_i, is governed by a linear isotherm,

$$q_i^* = K_i C_i \qquad (Eq.5.23)$$

where K_i is the Henry constant. Under linear adsorption conditions, the dispersed plug-flow model with lumped solid-diffusion LDF is well approximated by an equilibrium dispersed plug-flow model (Ruthven et al., 1994 and Guiochon et al., 2005; Ribeiro et al., 2017). Therefore, Eq. 5.22 can be rewritten as

$$\left(1 + \frac{1-\varepsilon_b}{\varepsilon_b} K_i\right) \frac{\partial \mathrm{C}_i}{\partial \mathrm{t}} = \frac{u}{L}\left(\frac{1}{Pe_{,i}} \frac{\partial^2 C_i}{\partial x^2} - \frac{\partial C_i}{\partial x}\right), \quad 0 < x < 1 \qquad (Eq.5.24)$$

The applicable boundary conditions are

$$\frac{\partial \mathrm{C}_i}{\partial x} = 0, \qquad x = 1 \qquad (Eq.5.25)$$

and

$$C_i - C_i^{in} = \frac{1}{\mathrm{Pe}_i} \frac{\partial C_i}{\partial x}, \qquad x = 0 \qquad (Eq.5.26)$$

The initial condition applied are

$$C_i\ (\mathrm{t}=0) = 0 \quad \text{for } y_i \neq \text{carrier gas} \qquad (Eq.5.27)$$

and

$$\mathrm{q}_i\ (\mathrm{t}=0) = 0. \qquad (Eq.5.28)$$

When a fluid flows through a packed bed there is the tendency for axial mixing to occur, that has the effect to reduce the efficiency of adsorption. In the axial dispersed plug flow model used in this work, the effects of all mechanisms which can contribute to the axial mixing are lumped together into a single axial dispersion coefficient, D_{iL} (m^2/s), whose value is calculated from the Péclet Number estimation, obtained by fitting the breakthrough experiments at diluted conditions (CO_2/He and CH_4/He both at 0.5/99.5% v/v and 1/99% v/v) in gProms (Process Systems Enterprise Limited, UK) simulator package.

5.3 Results and Discussion

5.3.1 Selection of the Adsorbent

Among the materials produced MCW(PA)2h and MCW(PA)3h, the selection of the best candidate adsorbent for selective CO_2 capture from biogas streams was based on the following parameters: (i) specific BET surface area, (ii) pore size distribution (PSD), (iii) CO_2/CH_4 ideal selectivity, and (iv) adsorbent working capacity (*i.e.*, the difference in CO_2 capacity between adsorption and regeneration conditions) (Chue et al., 1995). The adsorption kinetics and the tolerance of the adsorbents against water, pressure cycling, and energy requirements for regeneration were not taken into consideration in this preliminary screening.

As mentioned in Chapter 4, the textural characterization, namely the BET analysis obtained from the N_2 adsorption at 77 K, showed higher specific surface area and microporous volume for the MCW(PA)3h sample in comparison with those obtained for the activated carbon MCW(PA)2h (Table 4.6). This suggests that AC MCW(PA)3h should have more potential for the target application.

The single component adsorption equilibria of CO_2 and CH_4 in the activated carbons MCW(PA)2h and MCW(PA)3h are presented in Figure 5.3. The respective Tables 5.3 and 5.4 show the experimental values of the adsorbed amounts obtained. The adsorption isotherms predicted from the Sips model are in excellent agreement with the experimental data obtained. As verified in Table 5.4 the sample MCW(PA)3h provides higher CO_2 uptakes relative to the activated carbon MCW(PA)2h, within the operating pressure ranges studied.

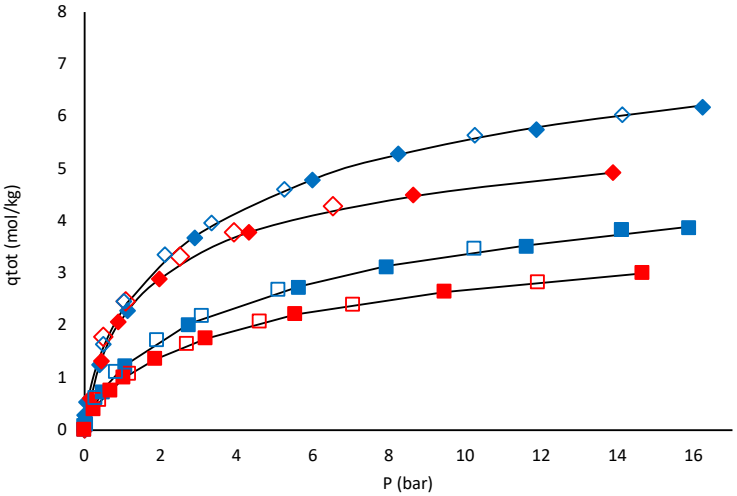

Figure 5.3: Single-component adsorption isotherms of CO_2 (diamonds) and CH_4 (squares) at 303.15 K in samples MCW(PA)2h (red symbols) and MCW(PA)3h (blue symbols). Closed symbols denote adsorption data and open symbols denote desorption experimental data points for CO_2 and CH4, whereas the lines are the predictions of the Sips isotherm model. The individual average errors (ARE) are 5.33% for MCW(PA)3h and 5.23% for MCW(PA)2h.

Table 5.3: Experimental CO_2 and CH_4 adsorption equilibria data of MCW(PA)2h at 303.15 K.

CO_2		CH_4	
P bar	q mol/kg	P bar	q mol/kg
0.32	1.06	0.48	0.53
0.80	1.99	1.04	0.10
2.91	3.58	3.06	1.89
5.89	4.43	6.15	2.54
8.22	4.80	8.33	2.82
12.10	5.21	12.14	3.17
15.95	5.48	15.94	3.41
13.87	5.50	13.86	3.32
10.13	5.21	10.22	3.04
5.00	4.46	4.80	2.34
2.38	3.53	2.19	1.65
0.93	2.34	0.90	0.10

Table 5.4: Experimental CO_2 and CH_4 adsorption equilibria data of MCW(PA)3h at 303.15 K.

CO_2		CH_4	
P	q	P	q
bar	mol/kg	bar	mol/kg
1.05	1.25	0.50	0.72
1.75	2.30	1.10	1.20
3.78	3.69	2.77	1.98
6.85	4.77	5.64	2.70
8.81	5.27	7.94	3.09
12.50	5.75	11.61	3.51
16.94	6.18	15.88	3.86
13.76	6.04	14.13	3.81
9.55	5.62	10.27	3.45
4.13	4.59	5.08	2.68
2.78	3.97	3.07	2.16
1.64	3.34	1.91	1.72
0.50	2.46	0.84	1.10
0.02	1.63	0.32	0.61

In cyclic processes such as PSA, the difference in the uptake capacity between adsorption and regeneration conditions is of extreme importance, apart from a high CO_2 uptake at higher pressures. Specifically, when considering applications of CO_2 separation from biogas streams using pressure-swing cyclic processes, the feed total pressures are between 6-10 bar (Augelletti et al., 2017 and Lestinsky et al., 2014) and the affluent stream compositions is mainly composed by 30-40% v/v CO_2 in CH_4. The respective regeneration pressures are typically sub-atmospheric (Grande, 2011; D. Ruthven et al., 1994). With this target application in mind, one can conclude that the adsorbent sample MCW(PA)3h shows superior CO_2 working capacities of about 11%, at a CO_2 partial pressure of P_{CO2} = 1.8 bar; and of 18% at P_{CO2} = 4.0 bar, in comparison with MCW(PA)2h (Figure 5.4).

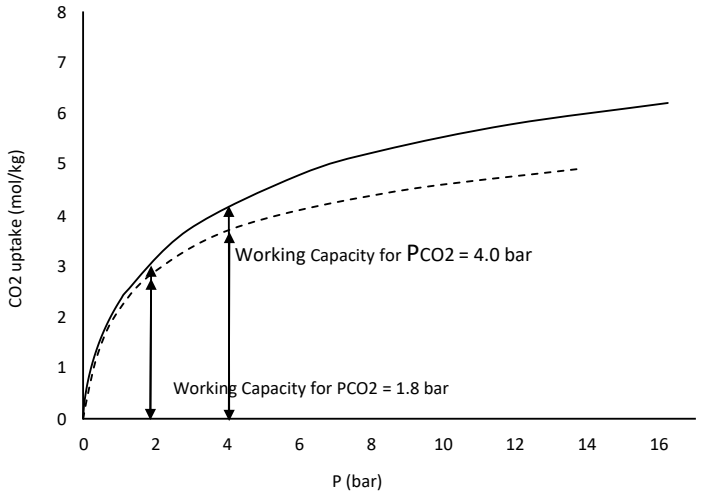

Figure 5.4: CO2 working capacities at 303.15 K of samples MCW(PA)2h (dashed line) and MCW(PA)3h (solid line).

The CO_2 ideal selectivities, α_{CO_2/CH_4}, is MCW(PA)2h and MCW(PA)3h carbons was expressed as calculated from the single components experimental equilibrium measurements performed at 303.15 K on accurately fitted with Sips isothermal model using with the Eq. 5.33

$$\alpha_{CO_2/CH_4} = {q(CO_2)_{P,T}}\Big/{q(CH_4)_{P,T}}\,, \qquad (Eq\ 5.29)$$

where q_i is the Sips predicted amount adsorbed (mol/kg) at the equilibrium of component *i*.

The results obtained showed that, at P_{CO2} between 1.8 and 4.0 bar, the two tested adsorbents provided similar CO_2/CH_4 ideal selectivities, with values ranging from 1.62 -1.71 for MCW(PA)3h to 1.69 - 1.88 for MCW(PA)2h. Sample MCW(PA)3h shows higher selectivity values. The results obtained are in agreement with selectivities provided in literature by similar renewable adsorbents (Peredo-Mancilla et al., 2018; Álvarez-Gutiérrez et al., 2014 and Álvarez-Gutiérrez et al., 2016) .

From Figure 5.5 it can be concluded that sample MCW(PA)3h is the most suitable candidate as adsorbent for CO_2 separation in CH_4 enriched streams. This activated carbon presents the higher specific surface area (BET), microporous volume, more favourable pore size distribution towards CO_2 and higher working

capacity in comparison with the analogue properties obtained for sample MCW(PA)2h.

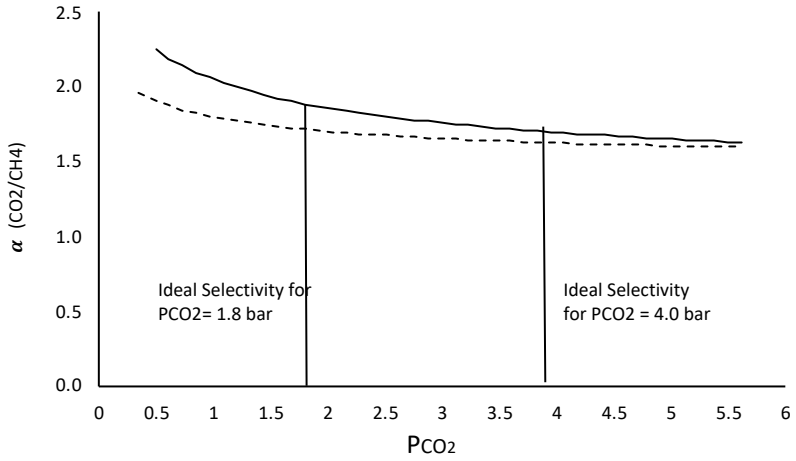

Figure 5.5: Ideal CO_2/CH_4 selectivity as a function of the CO_2 partial pressure at 303.15 K of the activated carbons MCW(PA)2h (dashed line) and MCW(PA)3h (solid line).

5.3.2 Single- Component Adsorption Equilibria

5.3.2.1 Analysis Using Sips Model

The experimental adsorption equilibrium data of CO_2 and CH_4 in sample MWC(PA)3h, measured at 303 K, 323K and 353 K, and up to 16 bar, were fitted to the Sips adsorption isotherm model.

Tables 5.4 and 5.5 report the experimental data points obtained and Figures 5.6 and 5.7 present the predicted fittings and their comparison with the experimental results.

The fitting of the isotherm data obtained at multiple temperatures allowed to obtain optimal values of the parameters characterizing the adsorption isotherm model applied.

As a first approximation, the fitting parameters q_s, n and b, were considered temperature independent in order to obtain initial guess values for these parameters. Their dependencies of temperature were then incorporated into the isotherm model to obtain a global equation able to describe the adsorbent-adsorbate system at all ranges of temperature. Figures 5.6 and 5.7 represent the global fittings of the experimental data by using the Sips model.

Table 5.5: Experimental CO_2 and CH_4 adsorption equilibrium data of MCW(PA)3h at 323 K and 353 K.

T=323 K				T=353 K			
CO_2		CH_4		CO_2		CH_4	
P bar	q mol/kg	P bar	q mol/kg	P bar	Q mol/kg	P bar	Q mol/kg
0.01	0.00	0.02	0.00	0.02	0.00	0.00	0.00
0.32	0.92	0.57	0.57	0.43	0.62	0.54	0.36
0.91	1.82	1.25	0.96	1.03	1.25	1.57	0.81
2.70	3.12	2.91	1.63	2.60	2.28	3.12	1.28
5.88	4.23	5.68	2.19	5.59	3.34	5.81	1.88
7.97	4.73	7.83	2.65	7.83	3.84	8.10	2.23
11.80	5.30	11.70	3.11	11.43	4.52	11.82	2.69
15.94	5.74	15.66	3.46	15.67	5.05	15.86	3.06
14.00	5.62	13.85	3.29	14.17	4.88	13.91	2.90
10.26	5.14	10.18	2.92	10.23	4.36	10.23	2.52
5.18	4.24	5.07	2.12	4.97	3.26	5.06	1.68
3.58	3.71	2.82	1.56	3.34	2.73	3.03	1.26
1.86	2.84	1.82	1.20	2.23	2.24	1.85	0.92
0.98	2.11	0.80	0.67	1.14	1.56	0.67	0.43
0.45	1.33	0.28	0.26	0.43	0.00	0.20	0.14

Table 5.6 lists the optimal isotherm parameters obtained by simultaneously fitting all the adsorption equilibrium data at multiple temperatures for each adsorbate.

As shown in Figures 5.6 and 5.7, the Sips model predictions are in excellent agreement with the experimental data. The average relative errors (ARE) found for the temperature-dependent fitting are lower than 10%. This demonstrates that Sips model can be confidently employed to accurately correlate the adsorption equilibria of the two adsorbates. The multicomponent form of the Sips model can be used to describe the adsorption/desorption behaviour of the biogas fed to an upgrading process, such as PSA.

The amounts adsorbed at saturation conditions are 8.32 mol/kg and 5.65 mol/kg for CO_2 and CH_4, respectively. The carbon adsorbent is sufficiently selective to CO_2 for making it a good candidate for biogas purification.

The adsorption isotherms (Figures 5.6 and 5.7) show that, at the same (P, T) operating conditions, the amount of CO_2 adsorbed is significantly higher than the adsorbed quantity of CH_4.

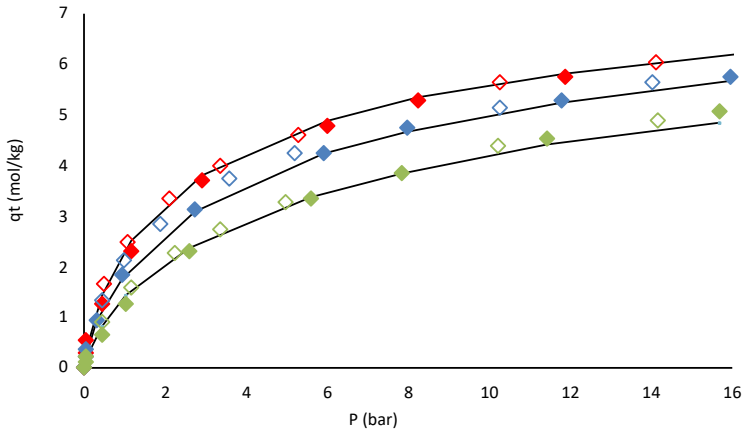

Figure 5.6: Absolute adsorption-desorption isotherms of CO_2 on MCW(PA)3h at 303.15 K (red), 323.15 K (blue) and 353.15 K (green). Closed symbols denote adsorption data and open symbols denote desorption data. The solid line represents the global predictions obtained with the Sips model. The FSE is 0.13 and the ARE is 6.61%.

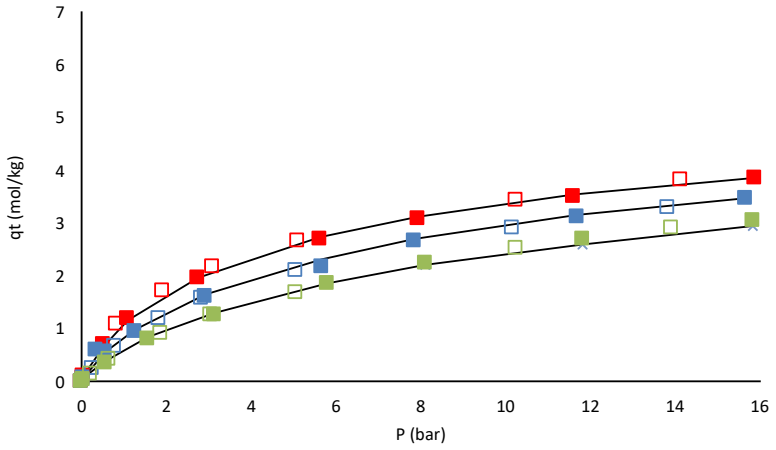

Figure 5.7: Absolute adsorption-desorption isotherms of CH_4 on MCW(PA)3h at 303.15 K (red), 323.15 K (blue) and 353.15 K (green). Closed symbols denote adsorption data and open symbols denote desorption data. The solid line represents the global fittings obtained with the Sips model. The FSE is 0.06 and the ARE is 8.10%.

Table 5.6: Temperature-dependent parameters obtained by fitting the Sips Isotherm model to the experimental adsorption equilibrium data (T0= 303.15 K).

Parameter	Unit	Sips Model	
		CO_2	CH_4
q_{s0}	mol/kg	8.32	5.65
b_0	1/bar	0.27	0.17
α	-	0.10	0.10
n_0	-	1.39	1.25
Q	KJ/mol	17.1	15.4
FSE	-	0.13	0.07
ARE	%	6.61	8.10

This phenomenon can be ascribed to the large quadrupole moment of CO_2 compared to CH_4 (CH_4 does not have a quadrupole moment), that is able to strong interact with the heterogeneous surface of the adsorbent. This property leads to a higher affinity of the adsorbent surface for CO_2 which results in an increased uptake (Arefi Pour et al., 2015). Moreover, this mechanism is favoured by the higher heterogeneity provided by CO_2/adsorbent than CH_4/adsorbent system, as shown by the higher value obtained for the parameter n during the fitting with the Sips model (Table 5.6). This heterogeneity is introduced by the presence of a network of (micro-meso) pores within the adsorbent, as well as by a distribution of chemically distinct adsorption sites within the pores.

Figure 5.8 shows the variation of the Q_{st} with pressure for each of the two adsorbates studied, as determined from the temperature-dependent Sips isotherm model; the selected temperatures for plotting the results are those at which the adsorption equilibria were measured. In the Henry's law region ($\lim \theta \rightarrow 0$), the isosteric heat of adsorption for CO_2, calculated from the Sips isotherm model, is 21.5 kJ/mol, decreasing with increased loading until levelling off at an average plateau of 17.1 kJ/mol at higher pressures. The values of Q_{st} obtained from the Sips fittings are in agreement with the values referred by literature, being sometimes slightly lower than those reported for activated carbons produced from renewable biomasses (Álvarez-Gutiérrez et al., 2016; Durán et al., 2018), sometimes slightly higher (Kacem et al., 2015), as listed in Table 5.7. Regarding CH_4, a value heat of adsorption of 17.4 kJ/mol is estimated in the Henry's law limit, and then it decreases to 15.5 kJ/mol as pressure and loading increase. From Figure 5.8 it is

also concluded that the variation of Q_{st} with temperature for CO_2 and CH_4 is quite small over the temperature range analysed in this study. This corroborates the usual simplifying assumption regarding the temperature invariance of Q_{st} over a broad temperature range (Esteves et al., 2008). When the value of Q_{st} slightly decreases with increasing loading, showing that the carbon is energetically heterogeneous for the adsorption of CO_2 and CH_4 (Esteves, 2005; Shen et al., 2000; Sircar and Cao, 2001), with a tendency to show a balance between the strength of cooperative gas–gas interactions and the degree of heterogeneity of gas–solid interactions (Dunne et al., 1996). This behaviour is typical of most amorphous adsorbents, such as activated carbon. At low pressures, the high-energy adsorption sites are preferentially filled; at higher pressures, the low-energy sites are preferentially filled.

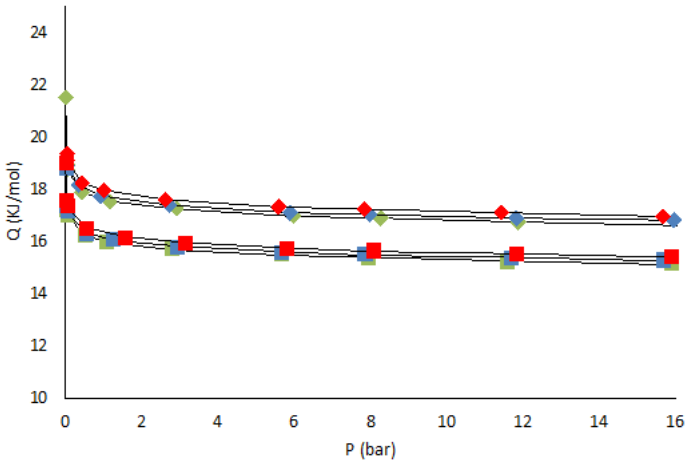

Figure 5.8. Isosteric heats of adsorption predicted by the Sips model as a function of pressure for CO_2 (diamonds) and CH_4 (squares) at 303.15 K (red), 323.15 K (blue), and 353.15 K (green).

From an engineering point of view, the heat of adsorption is a measure of the energy required to regenerate an adsorbent as it provides an indication of the temperature variations that might be expected on the bed during adsorption (and desorption) under adiabatic conditions. Therefore, although high adsorption energies are associated with high selectivity, it is generally desirable for the strongly adsorbed component as CO_2 to have a relatively low adsorption enthalpy in order to reduce the regeneration requirements. The relatively low Q_{st} provided by MCW(PA)3h is a favourable feature of this AC to be tested in cyclic separation processes.

The Table 5.7 shows the comparison of the CO_2 adsorption capacities observed in the range of CO_2 partial pressure of interest for biogas purification (approx. P_{CO2} of 1.8-4.0 bar) and the isothermal parameters obtained from the fitting with the Sips and Toth isotherm models of similar activated carbons produced both from renewable and coal-based precursors. The sample MCW(PA)3h used in this work provided higher adsorption capacities than the ones reported for coal-based ACs (Esteves et al., 2008) and the most of the bio-based ACs, with the only exception of the ACs produced from Babassu coconuts shell (Vilella et al., 2017).

The coal based ACs showed higher uptakes at higher loadings, as suggested by the predicted values of the CO_2 adsorbed amounts at saturation (q_{s0}). In the range of the partial pressures of interest for the biogas upgrading, sample MCW(PA)3h provided higher CO_2 uptakes than the ones reported for coal-based commercial ACs and similar uptakes to the ones reported for the bio-based ACs; the Babassu coconuts shell ACs are the exception that provided better performance both in terms of working capacities, as in terms of CO_2 selectivity (Vilella et al., 2017).

Table 5.7: Comparison of different activated carbons suitable for the removal of CO_2 in biogas upgrading applications.

Adsorbent	Activation	BET	Total Pore volume	Micropore volume	T	Q_{st} [a]	n_o	q_{so}	b_o	q (aprox)	α CO_2/CH_4	Ref.
		m^2/g	cm^3/g	cm^3/g	K	kJ/mol	-	mol/kg	1/bar	mol/kg		
Cherry stone	Physical /CO_2	1045	0.48	0.40	303 323	19.12	1.34	10.88	0.10	3.1-4.4 2.5-3.7	-	(Álvarez-Gutiérrez et al., 2016)
CS [b]	Physical /CO_2	1452	0.65	0.60	293	-	0.552[c]	14.67	0.401	3.8-5.2	2.5-3.5	(Vilella et al., 2017)
BABASSU CS		809	0.39	0.32			0.743[c]	10.49	0.343	3.2-4.5	4.0-3.8	
CS	Physical / H_2O	1087		0.44	298	14.28	-	-	-	1.7-2.4	-	(Kacem et al., 2015)
Date Seed	Physical /CO_2	627		0.23	303	18.79	-	-	-	0.00016[d]	-	(Ogungbenro et al., 2018)
Pine Saw-dust	Physical /CO_2	788		0.34	303 323	24.20	-	-	-	3.2-4.2 2.5-3.3	- -	(Durán et al., 2018)
Coal based AC	-	1342	0.85	0.77	310 323	19.58	1.25	20.6	0.036	1.8-3.0 1.3-2.4	- -	(Esteves et al., 2008)
Norit R2030 AC	-	942			303					0.8-1.4	-	(Plaza et al., 2010)
MCW(PA)3h	Physical/CO_2	886	0.38	0.35	303 323	17.14	1.39	8.32	0.27	3.1-4.3 2.5-3.7	1.62-1.71	This work

[a] Q_{st}: Isosteric heat of adsorption for CO_2.

[b] CS: Coconuts shell.

[c] value of parameter *t* from Toth isothermal model.

[d] measured at 1 bar

5.3.2.2 Analysis Using the Adsorption Potential Theory

The Adsorption Potential Theory (APT) was applied in this work to the adsorption equilibrium data of CO_2 and CH_4. The (micro)pore volume of MCW(PA)3h was estimated through the APT, along with the predicted adsorption isotherms. The results were consequently compared with the experimental data.

The molar volume V_m above the critical temperature of the adsorbate was calculated using Eq. 5.21. For this purpose, a value for the thermal expansion coefficient, Ω, was assumed. The first calculations were performed employing the values reported by Ozawa et al. (1976), which were subsequently fine-tuned to obtain a prediction of the characteristic curve for each adsorbate. The final Ω values are listed in Table 5.8.

Table 5.8: Affinity coefficients (β) and thermal expansion coefficients (Ω) estimated for CO_2 and CH_4 on MWC(PA)3h.

Parameter	Unit	CO_2	CH_4	Ref.
Parachor[a]		91.2	73.2	(Wood, 2001)
β_{calc}[a]		0.4006	0.4160	
β_{exp}[b]		0.4006	0.3940	
Ω_{calc}	K^{-1}	0.0025		(Ozawa et al., 1976)
Ω_{exp}	K^{-1}	0.003	0.003	

[a]From Equation 5.14 and 5.15 and listed in (Wood, 2001)

[b]From Equation 5.14 and 5.15.

A generalized version of the APT was employed to collapse all the characteristic curves into a single master curve. For this purpose, the adsorption potential for each adsorbate was scaled by the respective affinity coefficient, β. The β values employed as first guesses were determined from Eqs. 5.14 and 5.15. These initial estimates were subsequently fine-tuned in order to obtain a better superposing of the adsorption data for the different gases on the same adsorbent into a single characteristic curve. The β values, first calculated (β_{calc}) and lastly modified (β_{exp}), are listed in Table 5.8.

Figure 5.9 displays the single temperature-independent characteristic curve obtained for the adsorption of all the adsorbates on MCW(PA)3h, showing that a single curve was successfully obtained. The solid line corresponds to the fitting of the Dubinin-Astakhov (DA) model. The parameters found for the curve fitting

predicted from the Dubinin–Astakhov (D–A) isotherm model (Eq. 5.13) to the experimental data are:

$$W_s = 0.313 \text{ cm}^3/\text{g}$$

$$\gamma = 9.80 \times 10^{-10} (\text{J/mol})^n$$

$$n = 2.08 \ (R^2 = 0.9792)$$

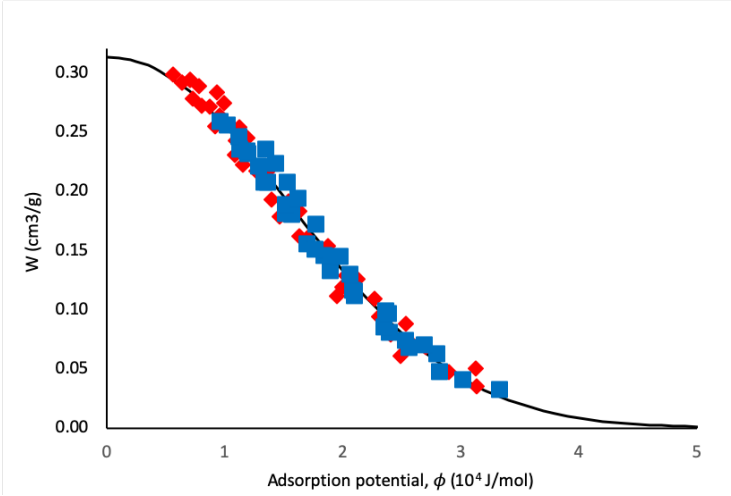

Figure 5.9a)

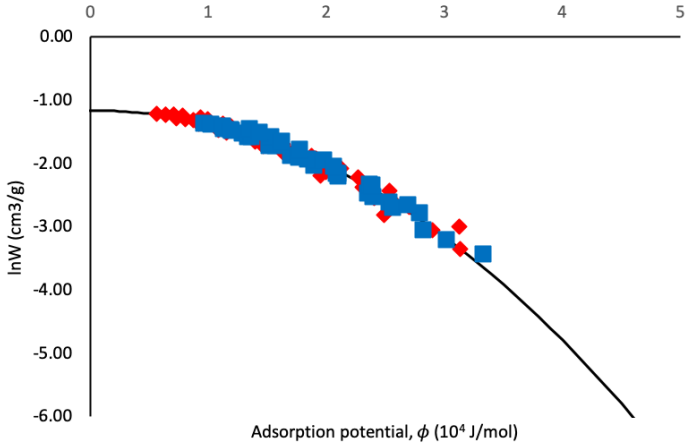

Figure 5.9b)

Figure 5.9: a) Characteristic curve obtained by collapsing the experimental data of CO_2 (diamonds) and CH_4 (squares) into a single curve; the solid line represents the fitting with the D–A isotherm model; b) Plot of the characteristic curve in log scale.

The value of Ws (0.313 cm^3/g) obtained is in good agreement with the pore volume of the sample MCW(PA)3h obtained by the textural analysis of the solid (0.35 cm^3/g in Table 5.1).

The difference between the pore volumes can be relative to the presence of mesopores. Moreover, the determined values are within the range of data available in the literature (Durán et al., 2018; Ogungbenro et al., 2018; Vilella et al., 2017).

Figures 5.10 and 5.11 show the D–A isotherm model predictions at 303.15 K, 323.15K and 353.15 K and their comparison with the experimental adsorption equilibria of CO_2 and CH_4 on the activated carbon MCW(PA)3h. The results obtained show a good agreement between the D–A model predictions and the experimental data, being the ARE error of the fittings of the measured isotherms of 9.08% and 8.85% for CO_2 and CH_4, respectively (Figures 5.10 and 5.11).

Although the D-A isotherm model is thermodynamically inconsistent when the pressure is approaching zero (Henry law's limit), it can be applied to predict adsorption/desorption of the various adsorbates over a broad range of experimental conditions (Do, 1998). The small scattering of the data points demonstrates that the adsorption data for the various adsorbates have been successfully correlated as a single temperature-independent characteristic curve. This fact corroborates the applicability of the adsorption potential theory to the carbon analysed. All the adsorption isotherms are classified as Type I (monotonically concave isotherm) in the IUPAC classification, which is typically characteristic of a microporous adsorbent (Sing, 1985; Thommes et al., 2015). Given that physical adsorption is an exothermic process, it is favoured at lower temperatures and the slope of its curvature decreases with increasing temperature.

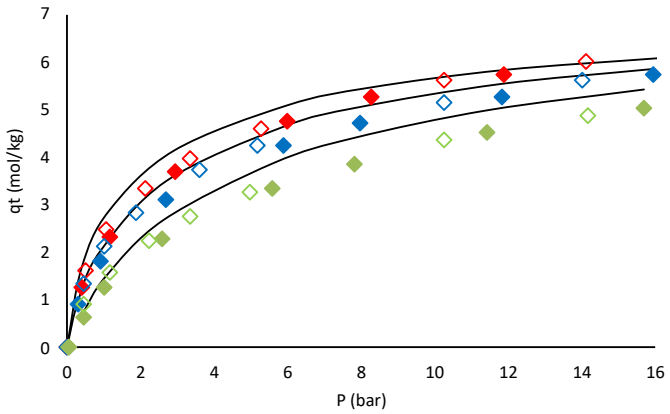

Figure 5.10: Absolute adsorption isotherms of CO_2 on MCW(PA)3h at 303.15 K (red), 323.15 K (blue), and 353.15 K (green). The solid lines represent the predictions with the D–A isotherm model. Closed and open symbols denote adsorption and desorption data, respectively.

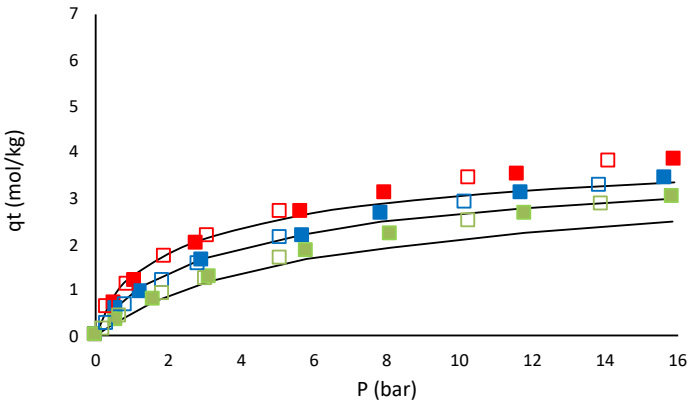

Figure 5.11. Absolute adsorption isotherms of CH_4 on MCW(PA)3h at 303.15 K (red), 323.15 K (blue), and 353.15 K (green). The solid lines represent the predictions with the D–A isotherm model. Closed and open symbols denote adsorption and desorption data, respectively.

5.3.3 Fixed-Bed Experiments

5.3.3.1 Fixed-Bed Experiments Results

The fixed-bed experiments for trace amounts of CO_2 and CH_4 diluted in He were performed according with the operating characteristics and conditions

listed in Tables 5.1 and 5.2, to study the system kinetics and provide the basis for future modelling works of a PSA cycle. At these conditions, thermal effects in the adsorbent bed due to adsorption are neglected and an isothermal behaviour is ensured. Moreover, the temperature difference between the adsorbent and the ambient fluid when sorption takes place was negligible (<0.5 K). The results obtained were mathematically modelled in gProms and the respective equations and boundaries are described in Section 5.2.4.3.

The CO_2 and CH_4 adsorption capacities on the activated carbon MCW(PA)3h, as well as the Henry's constants, were predicted from the breakthrough times (t_s) at which the adsorbate starts exiting the column. At these diluted conditions, the possible mass transfer resistances are diffusivity film mass transfer and axial dispersion. The flow rate employed was considered high enough to assume negligible film mass transfer resistance. The LDF (Eq. 5.22) and Henry's coefficients (Eq. 5.23) determined from the modelling of the experimental breakthrough curves are reported in Table 5.9.

Table 5.9: Breakthrough times (t_s), Henry's Constants (Ki) calculated from the results of the dynamic assays and the adsorbent amount adsorbed (q_i) obtained experimentally.

Adsorbate	T	t_s	q_{exp}	K_i	T	t	q_{exp}	K_i
	K	s	mol/kg	-	K	s		-
	1.0% v/v				0.5% v/v			
CO_2	303.35	2441	0.528	128	303.65	2449	0.263	126
	323.35	1578	0.324	83.1	322.65	2110	0.214	111
	353.25	947	0.179	50.0	354.55	1106	0.105	58.7
CH_4	303.95	565	0.113	27.8	303.85	542	0.057	28.7
	323.05	358	0.073	18.9	322.80	391	0.039	20.6
	353.05	237	0.044	12.6	353.05	222	0.021	11.8

Figures 5.12 and 5.13 show the modelling results obtained from the diluted CO_2/He and CH_4/He breakthrough simulations, and their comparison with the respective experimental data.

As one can see, the model predictions show a very good agreement with the experimental results, demonstrating that the axial dispersed plug-flow model and LDF approximation for lumped solid-diffusion mass transfer can be successfully employed to the studied system.

The time elapsed between the CH_4 and the CO_2 breakthroughs is indicative of the separating capacity of the adsorbent bed under transient conditions. Also, as the temperature increases, the adsorbate breakthrough occurs earlier, as expected. This is a consequence of the higher loading and adsorption effect at lower temperatures. When the solid reaches saturation at the run conditions, the equilibrium capacity is attained, and all the breakthrough curves tend to the inlet concentration of the adsorbate at each experiment.

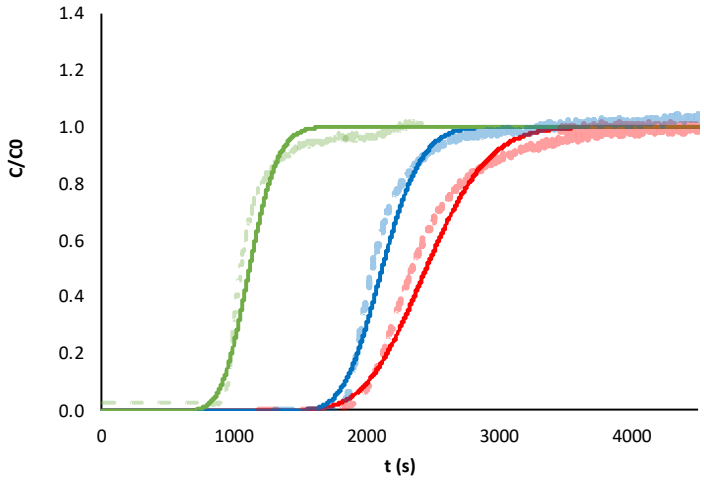

Figure 5.12a)

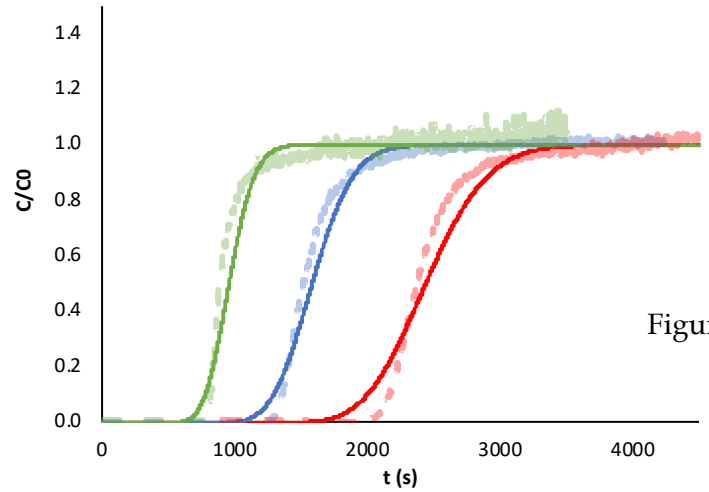

Figure 5.12b)

Figure 5.12: Breakthrough simulations and their comparison with the experimental data for the diluted mixture of a) 0.5/99.5% v/v and b) 1.0/99.0% v/v CO_2/He at 303.35 K (red), 323.25 K (blue) and 353.35 K (green). Dashed lines represent the experimental CO_2 composition profile at the bed exit stream, whereas the solid lines denote the predicted CO_2 composition history.

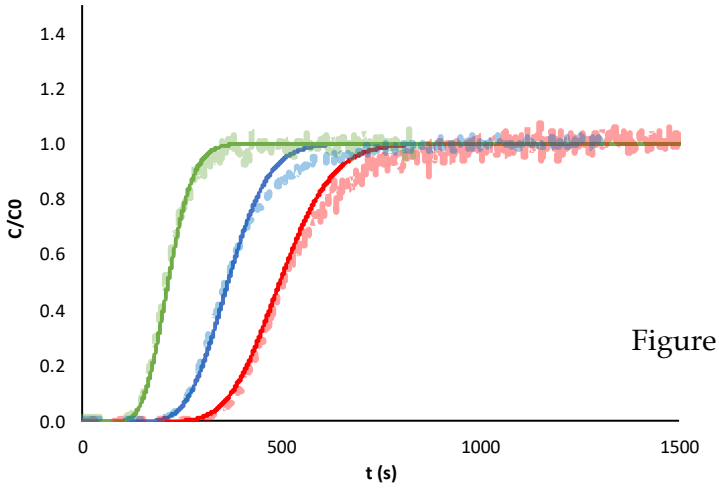

Figure 5.13a)

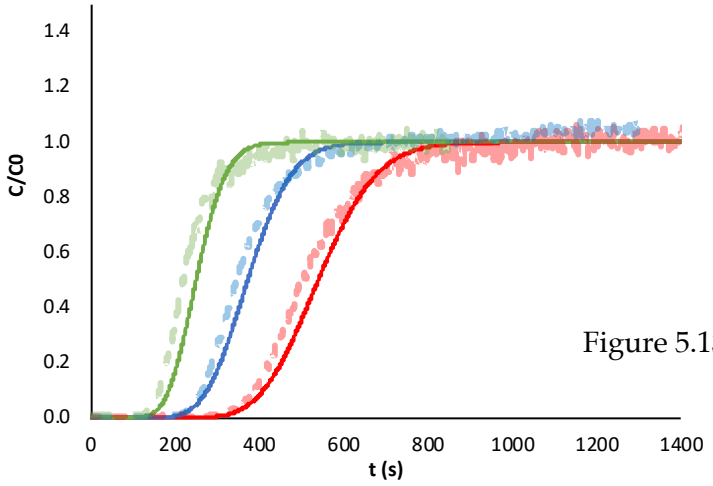

Figure 5.13b)

Figure 5.13: Breakthrough simulations and their comparison with the experimental data for the diluted mixture of a) 0.5/99.5% v/v a) and b) 1.0/99.0% v/v CH_4/He at 303.35 K (red), 323.25 K (blue) and 353.35 K (green). Solid lines are the experimental CH_4 composition profile at the exit stream of the bed, whereas the dashed lines denote the predicted CH_4 composition history.

The LDF coefficients, the Péclet numbers obtained from the breakthrough analysis and the diffusivity coefficients (D_i) calculated on the basis of the LDF coefficients ($D_i = k_i \tau {R_p}^2/15\ \varepsilon_p$) are reported in Table 5.10.

Table 5.10: LDF coefficients (k_i), Péclet numbers (Pe_i), the axial dispersion coefficients (D_{iL}) and the Diffusivity coefficient (D_i) obtained from the fitting of the diluted CO_2 and CH_4 (0.5% v/v and 1% v/v in He) breakthrough experimental curves.

Adsorbate	T K	k_i 1/s	Pe -	$10^{-5}\,D_{iL}$ m^2/s		$10^{-8}D_i$ m^2/s
				0.5% v/v	1.0% v/v	
CO_2	303.35	0.07	184	1.025	1.043	1.363
	323.35	0.10		1.050	1.045	1.948
	353.25	0.15		1.052	1.048	2.922
CH_4	303.95	0.12		1.052	1.046	2.337
	323.05	0.14		1.047	1.047	2.727
	353.05	0.20		1.057	1.056	3.896

Figure 5.14 reports the temperature dependence of CO_2 and CH_4 diffusivities in MCW(PA)3h AC and shows that the diffusivity increases with increasing temperature.

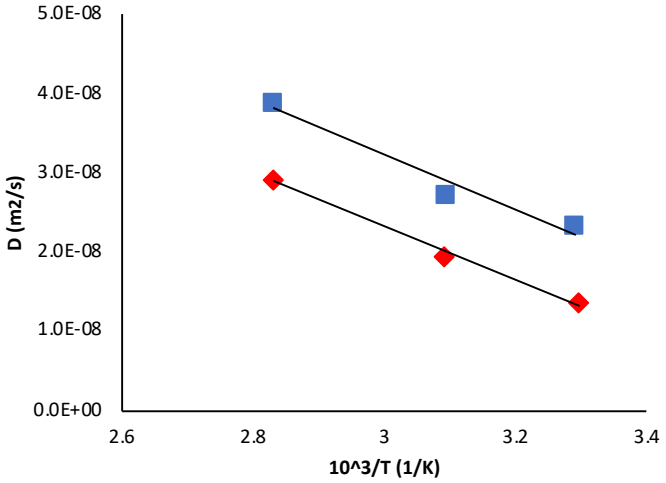

Figure 5.14: Correlation of diffusivity coefficients of CO_2 and CH_4 against the average experimental temperatures of 303.15 K, 323,5 K and 353.15 K. Diamonds and squares correspond to CO_2 and CH_4, respectively.

The diffusion mechanism is an activated process,

$$D = D_0\, e^{-E/RT} \qquad (Eq.5.30)$$

where E is the diffusional activation energy, generally smaller than the heat of adsorption, and D_0 is a parameter.

reports the calculated values for the adsorption activation energy and for the parameter D_0.

Table 5.11: Adsorption activation energy and *Do* calculated for CO_2 and CH_4

		CO_2	CH_4
D_{0i}	m^2/s	2.99E-06	1.04E-6
E	KJ/mol	13.4	9.4

5.4 Conclusions

Among the produced activated carbons from Maize Cob Waste, MCW(PA)3h can be considered the most suitable candidate for CO_2 separation due to its higher specific surface area (BET), higher microporous volume, more favourable pore size distribution and higher working capacity, when compared to others AC studied.

The study of the adsorption equilibrium measurements of CO_2 and CH_4 on MCW(PA)3h activated carbon showed that the Sips isotherm model can be confidently employed to accurately correlate the adsorption equilibria of the two adsorbates. The MCW(PA)3h carbon adsorbent demonstrated to be sufficiently selective to CO_2 for making it a good candidate for biogas purification.

Moreover, the experimental adsorption equilibrium data were successfully correlated using the APT in the form of a characteristic curve. The existence of little scatter in the characteristic curve data demonstrates that the isotherms of CO_2 and CH_4 were successfully correlated as a single temperature independent curve. This corroborates the applicability of the APT to the carbon under study. The regressed value of W_s is in good agreement with the total pore volume determined from the N_2 adsorption at 77 K. In the range of the partial pressures typical for biogas upgrading units, MCW(PA)3h showed higher CO_2 uptakes than the ones reported for coal-based commercial ACs and similar uptakes to the ones reported for the bio-based ACs. Finally, the axial dispersed plug-flow and Linear Driving Force (LDF) approximation for lumped solid-diffusion mass transfer model used for the prediction of the dynamic behaviour of the adsorbate-adsorbent system, provided a good agreement with the laboratory experiments, demonstrating its applicability to the system.

6

Life Cycle Assessment of a biorefinery for bioCH_4 production from the Anaerobic co-Digestion of the Organic Fraction of Municipal Solid Wastes and Maize Cob Wastes

6.1 Introduction

The key targets of the European Union 2030 climate action point out for a reduction by 40% of the emissions of greenhouse gases (GHG) and for an increase of the total renewable energy consumption up to at least 32% by 2030, relatively to the values of 1990 (European Commission, 2019).

Anaerobic Digestion (AD) offers the opportunity to produce biogas from organic waste (Liu et al., 2015). Biogas can be upgraded to a higher methane content (>97% v/v) to produce bioCH_4. When it achieves the quality of NG, bioCH_4 is suitable for grid injection, or to be used as transportation fuel (EBA, 2015).

The bioCH_4 potential is estimated to increase from 300 x 10^6 Nm^3/y in 2010, up to 18000 x 10^6 Nm^3/y in 2030 (EBA, 2015), suggesting that bioCH_4 is a consolidated marked, with a positive trend that will continue in the near future (URL2, 2016). Therefore, opportunities for integrating bioCH_4, particularly in Europe and USA, are rising due to the spread of infrastructures for compressed natural gas (CNG) for fuel stations and new technologies for vehicles. The introduction of the European quality standard for bioCH_4 injection in NG networks, as well

as for its use as transport fuel will contribute to its full integration in traditional markets.

Under this framework, the maximization of the environmental benefits derived from the biogas production and/or from the biogas upgrading process to bioCH_4 is a priority.

The use of Life Cycle Assessment (LCA) methodology allows to quantitatively analyse the life cycle of biogas and bioCH_4 within the context of the environmental impacts, providing a useful support for strategic future decisions (Goedkoop and Huijbregts, 2013).

This work comprises the LCA of a biorefinery that it is not yet implemented, but that was hypothesised for an existing Portuguese AD full-scale plant, currently processing 40000 t/y OFMSW. It is assumed that the biorefinery would include (i) an AcoD using MCW as co-substrate; (ii) a H_2S removal unit from biogas stream based on the use of activated carbons produced from MCW, and (iii) an upgrading process to bioCH_4 based on PSA technology.

This LCA is highly reliable because most of the input data have been collected at the AD full-scale plant and the scenarios analysed were developed based on the upscaling of the laboratory results obtained by the authors in previous published works (Surra et al., 2019, 2018b). Supplementary data were retrieved from peer reviewed papers and scientific reports.

6.2 Goal and Scope

The main aim of this study is a reliable assessment of the environmental benefits generated from different uses of biogas. The following three biogas production configurations were considered: (i) AD of standalone hOFMSW (named as hOFMSW) (ii) AcoD of hOFMSW with pre-treated MCW (named as hOFMSW+Pre3), and (iii) AcoD of hOFMSW with non-pre-treated MCW (named as hOFMSW+MCW). The detailed description of the pre-treatment Pre3 to which MCW was submitted before AcoD was reported elsewhere (Surra et al., 2018a, 2018b). In summary, this pre-treatment comprises a room temperature chemical pre-treatment at pH of 9.8 in presence of hydrogen peroxide in a ratio of 0.5 with MCW (wH_2O_2/wMCW). The most environmentally favourable configuration for the biogas production through AcoD was considered for the next step of the LCA, in which the biogas upgrading to bioCH_4 was assessed. The base scenario, to

which all the other upgrading scenarios were compared to, included the conversion of biogas into electricity and heat (CHP).

Within the main aim, this study also intends to evaluate the environmental benefits generated from the substitution of a commercial activated carbon (CAC) used in H_2S removal from biogas by activated carbons produced from MCW (MCW(PA)3h). This is the biogas preconditioning process that was located before the upgrading process to bioCH_4. The physic-chemical characterization and adsorption capacities of these ACs, as well as the production methodology of MCW(PA)3h were reported elsewhere (Surra et al., 2019).

The plant performances for each scenario have been compared to each other in a LCA perspective using the same functional unit: **1 m^3 biogas (STP)**. This approach allowed to compare the overall environmental sustainability of the bioCH_4 production with the direct electricity and heat production from biogas, through the quantification of the associated environmental impacts.

In defining the scope of this study, the base scenario (hOFMSW) refers to a real Portuguese AD plant that currently processes 40000 t/y of OFMSW. The organic waste is coming from canteens, restaurants and malls located in the vicinity of the AD plant. This AD plant operates 302 d/y, 24 h/d. It includes (i) two wet anaerobic digesters operating continuously under thermophilic regime (50-55 °C) and producing 560 m^3 Nm^3/h of raw biogas (Personal Communication, 2016); (ii) a CHP unit producing electric energy that is sold to the Portuguese national grid and providing the heat for internal use; the heat excess is lost to the atmosphere as no industrial heat is needed in the vicinity. The electric energy needed for the operation of the plant is bought from the national grid. The AD plant produces an average of 560 t/y of compost that is sold as a soil organic amendment (Personal Communication, 2016).

The AcoD scenarios took into consideration the harvesting, grinding and transport of MCW from rural area sited 50 km far from the AD plant.

The harvesting of MCW required for the production of MCW(PA)3h activated carbon was carried out, according to the MCW local availability, in a rural area located approximately 86 km from the AD plant. The production of MCW(PA)3h activated carbon is performed in an industrial furnace that was intended to be built in the vicinity of MCW fields in order to reduce the transport costs and environmental impacts. The overall MCW availability was assessed on the basis of personal communication with the Portuguese national producers association of corn and sorghum (Anpromis, 2016).

The bioCH_4 upgrading unit is intended to be built in the existing AD plant area and includes: (i) an adsorption unit for H_2S removal, (ii) a compression and biogas drying unit, and (iii) a PSA unit (Hoyer et al., 2016).

The mass and energy flows for the alternative plant configurations analysed, and the identification and quantification of all the direct, indirect and avoided burdens are reported in Figures 6.2- 6.5 and Tables 6.1-6.4.

The background and foreground system boundaries, as defined by Frischknecht (1998), are reported in Figure 6.6. They include all the activities from bio-waste delivery at plant entry gates up to the management of all process products (e.g., compost, ACs, biomethane) and wastes produced. The analysis includes the capital goods, as they are estimated in Ecoinvent v.3.4 database and is performed following the cradle-to-gate approach.

The allocation of impacts was developed according to the system expansion methodology proposed by Clift et al. (2000). This methodology consists in the identification of the product obtained that can replace less sustainable products already present in the market. In the present study, these products were (i) the part of electric energy not yet produced from renewable sources, (ii) replacement of NG by biomethane, and (iii) replacement of chemical fertilizers by compost. This approach is known as the "avoided-burden method".

The quality of data is high since all the data used to calculate the impacts related to AD and AcoD derived from confidential information and measurements related to the mentioned AD plant, or from the laboratory assays performed by the authors in the previous published works (Surra et al., 2019, 2018a, 2018b). MCW availability and its distribution is based on real data provided by the Portuguese national producers association of corn and sorghum (Anpromis, 2016). The remaining data, mainly related to the indirect and avoided burdens, came from the Ecoinvent v.3.4 database, technical reports and studies recently published in scientific literature, which are all cited along this manuscript.

The avoided impacts, related to the use of biogas for electric energy production and NG substitution by bioCH_4 as fuel for automotive, have been evaluated on the basis of Ecoinvent v.3.4 database, referring to electric energy production mix, in Portugal, in the year of 2014, and to the NG production, transport and marketing from high pressure network (1-5 bar) at service station, respectively.

The compost production is intended to avoid the production of the equivalent amount of chemical fertilizers, being the organic compost able to guarantee

similar or even higher crop yields, reducing nutrient-leaching risks, while improving the chemical, physical and microbiological properties of soil (Han et al., 2016; Hernández et al., 2016; Oliveira et al., 2018).

No avoided burdens were considered for the MCW(PA)3h production process. The amount of MCW and hard coal needed for MCW(PA)3h and CAC production, respectively was calculated on the basis of the adsorption capacities measured by the authors under laboratory conditions (Surra et al., 2019).

The present LCA study is developed by using the ReCiPe2016 impact method, that allows to transform the long list of life cycle inventory results, into a limited number of environmental impact scores, known as the impact categories (Huijbregts et al., 2017). In this work, the impact categories were calculated at the "Endpoint" level and directly related to the damage to human health, ecosystem quality, and resource availability areas of protection. The perspective adopted is "Hierarquist", regarding the time and expectations that proper management or future technology development can avoid future damages.

The software package used for this study is the GreenDelta openLCA Version 1.8.0 (Mac OS x86_64), which allows the comparative analysis of the different scenarios through the application of the "System Project" tool.

6.3 Life Cycle Inventory

The study comprised the collection of all data, whether measured, calculated or estimated, necessary to quantify the inputs and outputs of each unit process included within the system boundaries. The specific values of the main parameters used are reported in Table 6.1. Tables 6.1 to 6.5 integrate the values reported in the different plant configurations analysed in this study (Figures 6.1 to 6.5).

Table 6.1: Integrated data of the flow sheets used to estimate the environmental burdens of OFMSW and MCW collection and transport for AD and AcoD processes.

Parameter	Unit	Amount		Reference
		OFMSW	MCW	
Total amount of OFMSW	t/y	40000 [1]	675 [2]	[1] (Personal Communication, 2016)
OFMSW (by diesel lorries)		24172 [3]	-	
OFMSW (by NG lorries)		15828 [3]	-	
Diesel for OFMSW transport		219 [3]	3.65 [2]	[2] Calculated from AcoD laboratory results
NG for OFMSW transport		349 [3]	-	
Diesel for MCW harvesting		-	11.8 [2]	[3] (Private Communication, 2016)
Emissions to air				
CO_2	kg/y	15.9E+05	3.96E+04	Calculated from the Emission Factors (EF) proposed by Ntziachristis et al. (2018)
CO		1.66E+03	2.81E+01	
CH_4		6.12E+02	1.41E+00	
N_2O		1.11E+01	4.87E-01	
NO_X		7.51E+03	4.34E+02	
NH_3		2.84E+00	1.13E-01	
SO_2		2.74E+00	1.36E-02	
NMVOC		4.20E+02	1.90E+02	
VOC		12.78E+02	3.96E+04	

Tables 6.2 and 6.3 summarize the specific values of the main parameters used together with those of flowsheets reported in Figure 6.1 and 6.2 to estimate the environmental burdens of AD and AcoD plant configurations.

The base-case scenario hOFMSW represents the current situation of the Portuguese AD plant used as the case-study in this work. Figure 6.1 and Tables 6.1 and 6.2 report an essential, but exhaustive description of the unit processes. The OFMSW are collected in the territories of three municipalities located nearby the AD pant and are transported by lorries fleet fuelled with diesel and NG (which are both fossil fuels). The impacts related to the specific air emissions due to OFMSW transport have been quantified on the basis of fuel consumption and distances travelled (Private Communication, 2016). The OFMSW amount fed to the plant is assumed to be the same for the AD and AcoD scenarios.

Table 6.2: Integrated data of the flow sheets used to estimate the environmental and avoided burdens of the AD and AcoD processes.

Parameter	Unit	AD and AcoD			Reference
		hOFMSW [1,2]	hOFMSW +Pre3 [2]	hOFMSW +MCW [2]	
Biogas production	m^3/h	560	906	940	[1] (Personal Communication, 2016), [2] Calculated on the basis of AcoD laboratory results (Surra et al., 2018b)
Biogas production	m^3/y	4.06E+06	6.57E+06	6.82E+06	
LHV	kWh/m^3	6.22	5.92	5.66	
EE production		7.57E+06	1.17E+07	1.16E+07	
Heat production	kWh/y	1.14E+07	1,75E+07	1.74E+07	
Emission to air from piping, tanks and valves during AD and AcoD					
		hOFMSW	hOFMSW +Pre3	hOFMSW +MCW	
CH_4 (biogenic)		4.03E-04	4.42E-04	2.50E-04	Calculated from EF proposed by Liebetrau et al. (2013)
N_20	kg/m^3	4.67E-07	4.44E-07	4.25E-07	
NH_3		1.62E-03	1.07E-03	6.17E-4	
Emission to air (Bobcat for MCW loading)					
CO_2 (fossil)		-	4.92E-04	4.74E-04	
CO		-	1.19E-06	1.14E-06	
N_2O		-	8.00E-09	7.70E-09	Calculated from the EF proposed by Bobcat-Dorsan (2018)
NOx	kg/m^3	-	5.23E-06	5.04E-06	
NH_3		-	2.04E-09	1.96E-09	
NMVOC		-	3.01E-07	2.90E-07	

Table. 6.2. *Continued*. Integrated Data of the flow sheets used to estimate the environmental and avoided burdens of the AD and AcoD processes.

Parameter	Unit	AD and AcoD			Reference
		hOFMSW	hOFMSW +Pre3	hOFMSW +MCW	
Emission to air from CHP (15% O_2)					
CH_4 (biogenic)	kg/m^3	1.41E-05	8.94E-06	8.56E-06	Calculated on the basis of EF proposed by Vicente (2015) and Kristensen et al. (2004)
CO_2 (biogenic)		5.80E-01	6.47E-01	7.10E-01	
CO		1.14E-04	1.09E-04	1.04E-04	
NOx		6.05E-04	5.75E-04	5.50E-04	
N_2O		1.41E-05	8.94E-06	8.56E-06	
NMVOC		1.68E-05	1,60E-05	1.53E-05	
PM_{10}		4.64E-05	4.41E-05	4.22E-05	
Emission to air from Biofilter					
		hOFMSW [1]	hOFMSW +Pre3 [1,2]	hOFMSW +MCW [1,2]	
NH_3	kg/m^3	7.01E-09	7.01E-09	7.01E-09	
Emissions to water from WWTP discharge					
		hOFMSW [1]	hOFMSW +Pre3 [1,2]	hOFMSW +MCW [1,2]	[1] (Personal Communication, 2016), [2] Estimated from AcoD laboratory results (Surra et al., 2018b)
BOD_5 (20 ° C)	kg/m^3	8.05E-03	5.74E+00	5.12E-03	
COD		7.52E-03	5.74E-03	4.78E-03	
TSS		8.05E-03	5.36E-03	5.12E-03	
Total Chlorides (Cl)		4.03E-03	5.74E-03	2.56E-03	
Nitrites (NO_2)		4.37E-03	2.87E-03	2.78E-03	
Nitrates (NO_3)		7.45E-04	3.12E-03	4.74E-04	
Nitrogen total (N)		3.28E-03	5.31E-04	2.09E-03	
P_{total} (P)		2.89E-04	2.34E-03	1.84E-04	
Fats (Ether soluble)		8.05E-04	2.06E-04	5.12E-04	
Avoided burdens					
Electricity, mix (PT)	kWh/y	7.57E+06	1.17E+07	1.16E+07	
Chemical fertilizers, as N	t/y	560	502	496	

MCW was considered as a co-substrate for both AcoD scenarios. MCW feeding rate was calculated on the basis of laboratory results obtained by the authors (Surra et al., 2018b), assuming an increase of the current OLR inside the digesters of 15% (Surra et al., 2018a). The bulk densities of MCW were of 190 kg/m^3 and 240 kg/m^3 for bulk and ground ($\phi < 1$ mm) MCW, respectively, as measured by authors.

It was assumed that MCW harvesting was carried out coupling the harvester with a cob harvester of 3.6 m^3 loading capacity, that can collect MCW separately from corn. The MCW harvesting operations are supported by a trailer tractor equipped with a dumper (30 m^3 capacity), travelling alongside the harvester to empty the cob harvester and transporting MCW to the limit of the corn fields. The dumpers containing the cobs were then collected by dedicated road trucks and transported to the grinding area. This area was in a central position in respect to the corn fields, in a place where electric energy is available. MCW grinding is required to reduce the transportation costs and to enhance its anaerobic biodegradability (Surra et al., 2018a). The impacts associated to the grinding of MCW were calculated assuming the electric energy consumption reported by Gu and Bergman (2016) for woody materials. The ground MCW was then transported to the AD plant. The crop area needed for harvesting the required amount of MCW was of 520 ha, being calculated in the basis of a MCW yield of 1.3 t_{MCW}/ha (Anpromis, 2016). The impacts related to the specific air emissions due to MCW harvesting and transportation were quantified based on the calculated fuel consumptions and distances travelled by collection machinery and trucks.

Fuel consumption and distance travelled by the corn harvester and environmental impacts due to the corn crop cultivation and harvesting were not taken into consideration as they can be allocated entirely to the corn production process. Independently of MCW harvesting and processing, corn crop would always be cultivated.

Table 6.3. Integrated data of the flow sheets used to estimate the environmental burdens associated to the production of MCW(PA)3h and CAC activated carbons.

Parameter	Unit	AC		Reference
		MCW(PA)3h	CAC	
MCW for AC production	t/y	2318	-	Estimated from AcoD laboratory results (Surra et al., 2019)
Hard Coal for CAC production		-	32882	
AC amount		487	14796	
H_2S amount to be removed	kg/y	7187	7187	
AC adsorption capacity	kg/kg	1.55E-02	5.10E-04	
Diesel for MCW harvesting	kg/y	29.3E+04	-	
Diesel for MCW(PA)3h transportation		3.7E+03	-	
Emissions to air for MCW collection and MCW(PA)3h transport				
CO_2	kg/y	1.04E+05	-	Calculated from the EF proposed by Ntziachristis et al. (2018)
CO		2.48E+02		
CH_4		2.15E-01	-	
N_2O		4.60E+00	-	
NO_X		1.25E+03	-	
NH_3		2.84E-01	-	
SO_2		1.48E-01	-	
NMVOC		1.14E+02	-	
VOC		6.11E+00		
Emission to air during MCW carbonization				
CO_2 (biogenic)	kg/y	1.64E+06	-	Calculated on the basis of the Ecoinvent database v3.4 and on the results of Mullen et al. (2010)
CO (biogenic)		1.16E+05	-	
CH_4		2.45E+04	-	
Ethane		4.26E+03	-	
Ethene		1.42E+03		
$PM_{2.5}$		2.74E+02		
PM_{10}		3.35E+01		
$PM_{2.5-10}$		3.04E+01		
Emission to water during MCW carbonization				
Water		1.18E+07	-	
Water, GLO		1.86E+07	-	

*T*able. 6.3. Continued. Integrated data of the flow sheets used to estimate the environmental burdens associated to the production of MCW(PA)3h and CAC activated carbons.

Parameter	Unit	AC		Reference
		MCW(PA)3h [1]	CAC [2]	
Emission to air during the activation process				
CO_2	kg/y	8.81E+05	7.83E+07	[1] Calculated on the basis of the results obtained by Gu et al. (2019) [2] Calculated according to the EF reported on Ecoinvent V3.4 database
H_2O		4.38E+04		
N_2		8.91E+05		
O_2		7.74E+05		
H_2		2.43E+03		
CO		4.38E+03	8.55E+04	
CH_4		4.87E+02	8.55E+03	
SO_2		4.87E+02	4.28E+05	
HCl		6.09E-01	3.46E+04	
NOx		4.41E+01	1.71E+05	
NMVOC			1.47E+03	
C_2H_4O/Acetaldehyde		5.55E+00		
C_6H_6/Benzene		4.17E+01	4.28E+02	
CH_2O/Formaldehyde		1.33E-02	6.84E+01	
CH_4O/Methanol		2.00E+00		
$C_{10}H_8$/Naphthalene		3.52E+00		
C_6H_6O/Phenol		9.93E+12		
C_3H_6O/Propanal		3.52E-02		
Aluminum			9.15E+03	
PM		2.24E+04	4.28E+04	
Polonium-210	kBq/y		7.27E+04	
Radium-228			5.56E+04	
Lead-210			3.98E+04	
Uranium-238			8.55E+03	
Potassium-40			1.15E+04	
Radium-226			1.03E+04	
Silicon			1.35E+04	
Emissions to water during the activation process				
Water, RER	kg/y	1.02E+06	2.49E+01	

For all the scenarios, the OFMSW received at the AD plant is mechanically sorted in order to recover recyclable materials (glass and metals, mainly) and to turn the substrate more biodegradable. 4400 t/y of glass, plastics and stones,

representing an average of 11% w/w of the waste inlet (Vaz et al., 2010). These materials are removed and recycled, except the stones that are landfilled.

In the scenario hOFMSW (Figure 6.1), the pre-treated OFMSW is fed to two wet thermophilic anaerobic reactors of 3400 m^3 nominal capacity and Hydraulic Retention Time (HRT) of 21 d. Periodic injections of compressed biogas guarantee the adequate mixing inside the bioreactors.

The anaerobic bioreactors produce liquid digestate and biogas (Figure 6.1). The raw digestate is dewatered through centrifugation. The liquid fraction is partially recirculated to the pre-treatment section (Recirculated Sludge 1) (Figure 6.1 a)) and partially treated in the internal Waste Water Treatment Plant (WWTP), consisting of a denitrifying-nitrifying biological system followed by a membrane filtering system (ultrafiltration membranes) able to retain the suspended solids. The sludge obtained from ultrafiltration membranes is recirculated to the pre-treatment section (Recirculated Sludge 2) (Figure 6.1a). The wastewater excess is than discharged into the municipal sewer: the treated wastewater mass flow rate is approximately 35990 t/y with the average pollutant concentrations reported in Table 6.2. All these values are below the limits imposed by the discharge license of the WWTP, as defined by the Portuguese legislation and the Environmental Portuguese Agency.

The dried solid digestate produced during the centrifugation process is sent to the composting tunnels. The compost is finally maturated in outdoor piles, where compost suitable for agronomic use is obtained.

The produced raw biogas in hOFMSW scenario is composed mainly by 66.1% v/v CH_4, 32.4% v/v CO_2, 970 ppmv H_2S , with a degradation rate of 60% Volatile Solids. These data are in agreement with scientific literature (Ardolino et al., 2018).

A combined heat and power (CHP) system burns the raw biogas, with an electric energy conversion efficiency of 30% and thermal energy conversion efficiency of 45%. The remaining 25% conversion rate represents the energy losses. The CHP system produces 7.57E+06 kWh/y and 1.14E+07 kWh/y of electric and thermal energy, respectively. Internal consumption of the AD plant corresponds to approximately 50% of the electric energy produced, which is used for the operations of pre-treatment, anaerobic digestion, wastewater treatment, and compost drying (3.90E+06 kWh/y).

Table 6.4: Main characteristics of the raw biogas sent to the upgrading unit and of the bioCH_4 produced. Characteristics of the PSA upgrading unit and the environmental and avoided burdens.

Parameters	Unit	Raw Biogas	bioCH_4 *	References
Flow rate	m^3/y	6.81E+06	-	Personal Communication, (2016) and estimated on AcoD laboratory results
	m^3/h	940	-	
	kg/y	7.45E+06	-	
Pressure	mbarg	21	-	
Temperature	° C	38-50	-	
Gas Composition				
CH_4	% v/v	60.3	96.0	Calculated on the basis of the AcoD laboratory results
CO		7.0E-04		
CO_2		39.6	2.41	
H_2S **		8.2E-02	-	
H_2O		1.4E+00	-	
NH_3		3.2E-03	-	
H_2		9.0E-3	9.0E-3	
LHV	kWh/kg	5.66	9.67	
PSA Upgrading Unit				
Feed	bar	-	8	(Grande, 2011)
Purge			5	
bioCH_4 purity	%	-	96	(Ecoinvent, 2018) and Q. Sun et al. (2015)
CH_4 Loss		-	4	
Emission to air during the upgrading process				
CH_4	kg/y	-	1.06E+05	Calculated on the basis of the Ecoinvent (2018), Grande (2011) and Q. Sun et al. (2015)
CO_2		-	4.50E+06	
CO		-	5.40E+01	
H_2S		-	2.34E+02	
NH_3		-	1.50E+02	
Emission to water during the upgrading process				
Water	kg/y	-	954	
Avoided burdens				
Natural gas, PT	kg/y	-	2.85E+06	

* It was assumed that half of the H_2S present in the biogas stream was adsorbed on the AC during the upgrading process, NH_3 exits entirely in the off gas stream (Hoyer et al., 2016), and water vapor is condensed and discharged as a condensate during the biogas the drying step before upgrading.

** The amount of the H_2S in the feed was calculated on the basis of the breakthrough value used for H_2S removal capacity assessment (ASTMD 6646) (50 ppmv).

Figure 6.1a)

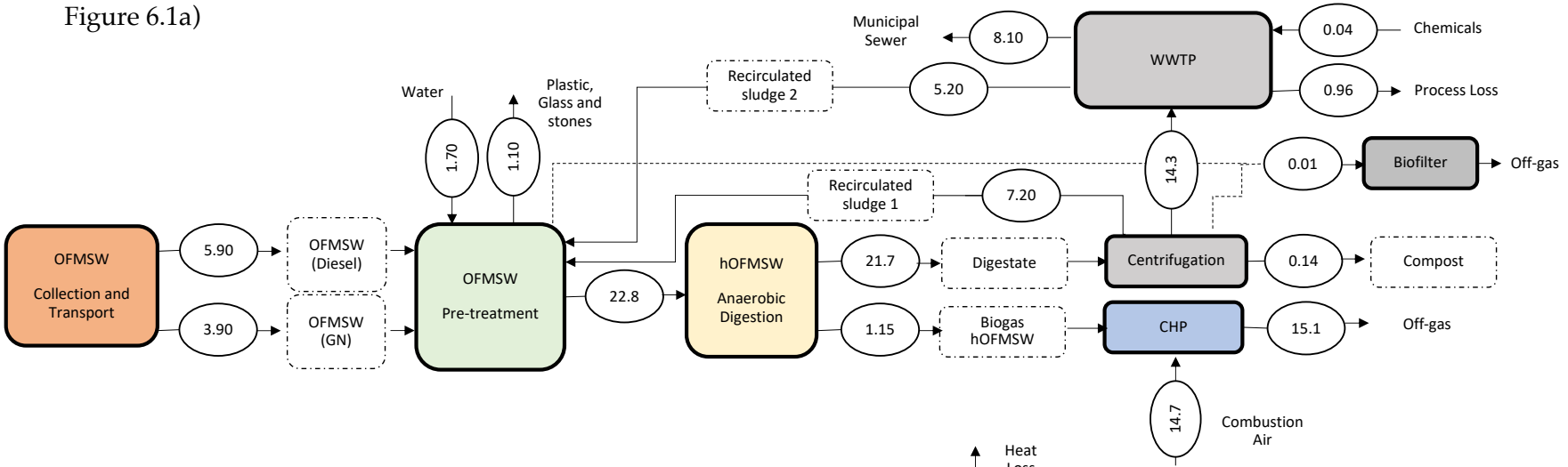

Figure 6.1b)

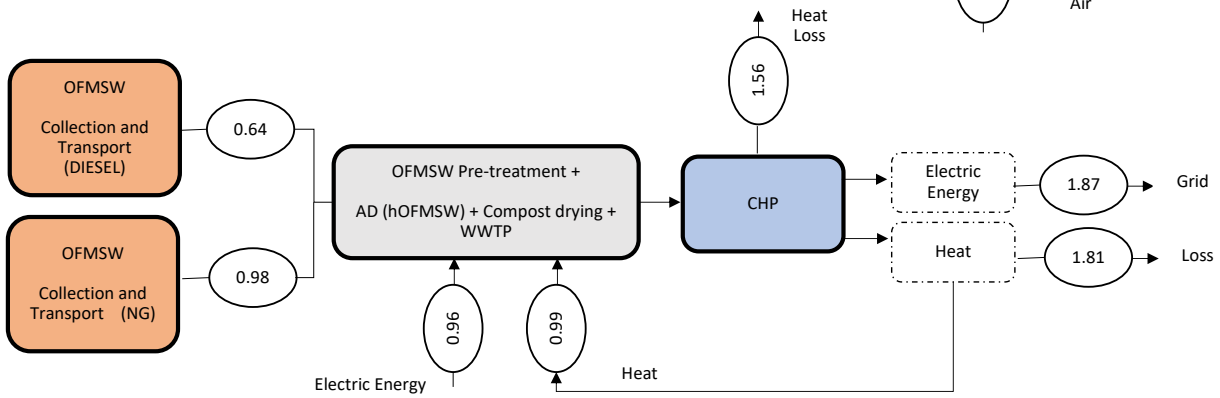

Figure 6.1: Flow sheets of mass (a) and energy (b) balances of the hOFMSW scenario (base case configuration). Data are expressed in kg/y for mass flow sheets (a) and in kWh/y for energy flow sheet (b) (functional unit: 1 m^3 biogas (STP)).

Figure 6.2a)

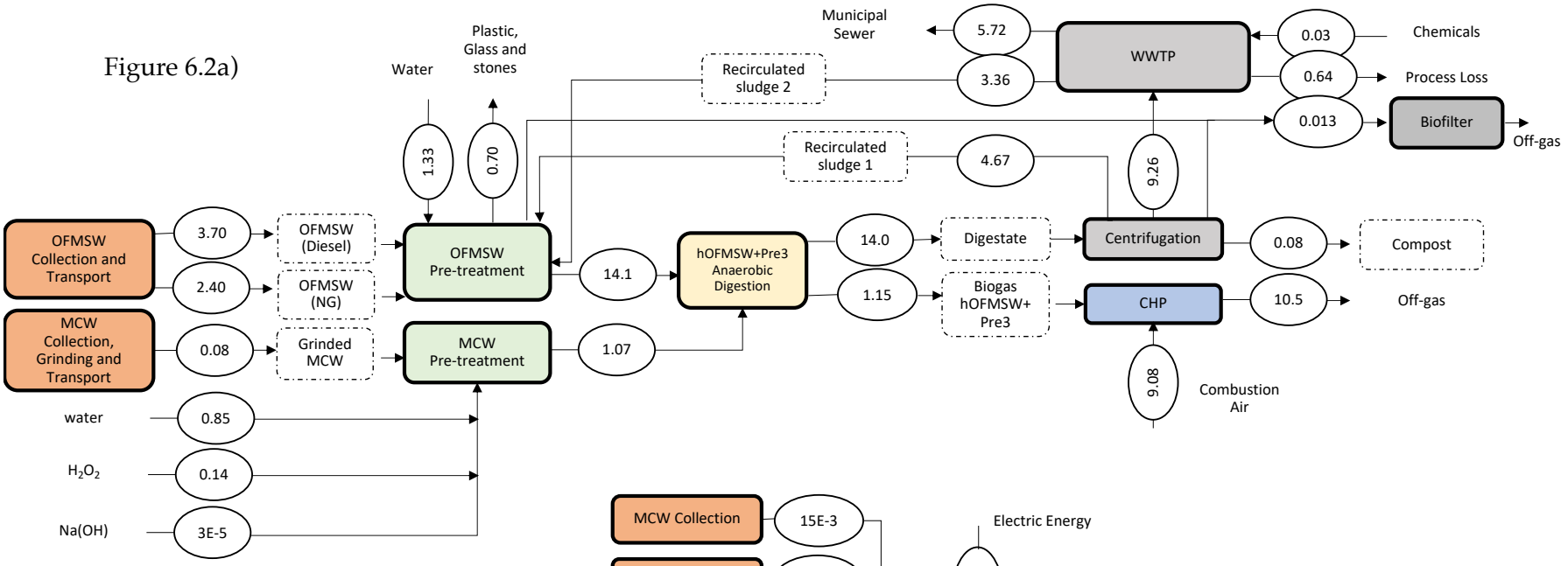

Figure 6.2b)

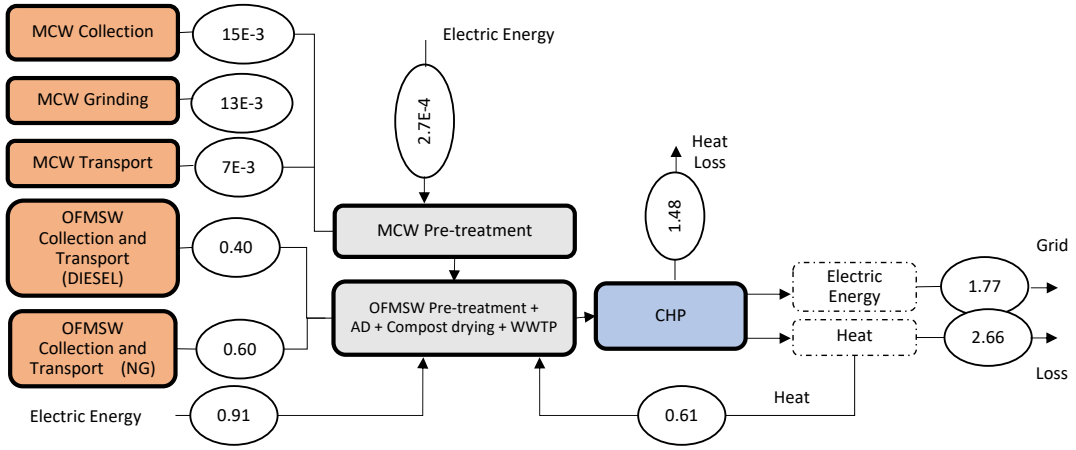

Figure 6.2: Flow sheets of mass (a) and energy (b) balances of the hOFMSW+Pre3 scenario. Data are expressed in kg/y for mass flow sheet (a) and in kWh/y for energy flow sheet (b) (functional unit: 1 m^3 biogas (STP)).

Figure 6.3a)

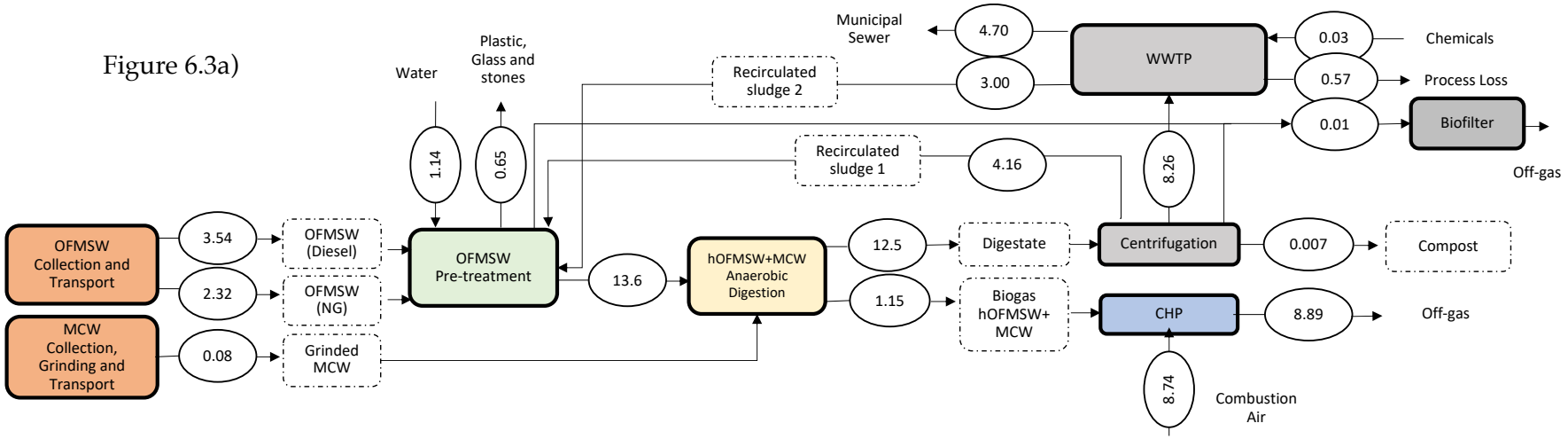

Figure 6.3b)

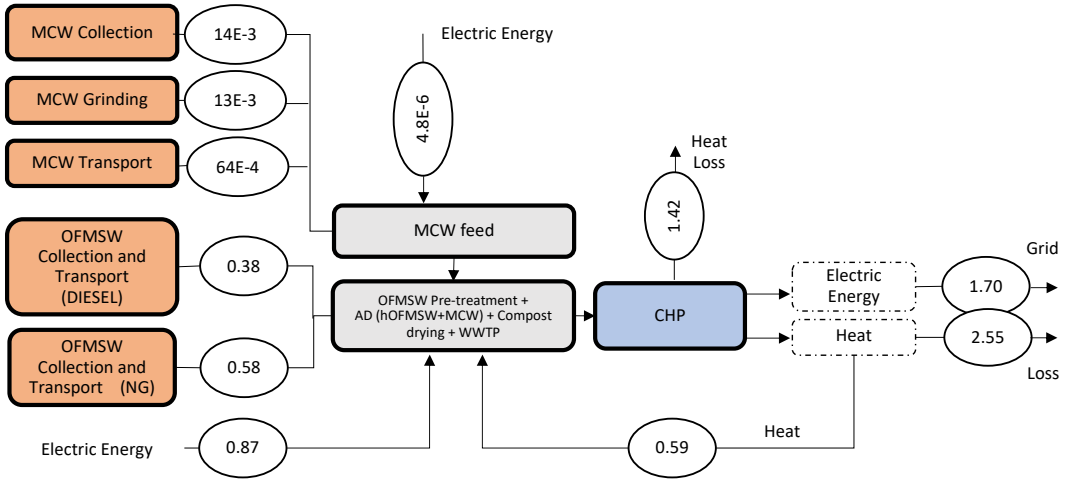

Figure 6.3: Flow sheets of mass (a) and energy (b) balances of the hOFMSW+MCW scenario. Data are expressed in kg/y for mass flow sheet (a) and in kWh/y for energy flow sheet (b) (functional unit: 1 m^3 biogas (STP)).

Figure 6.4a)

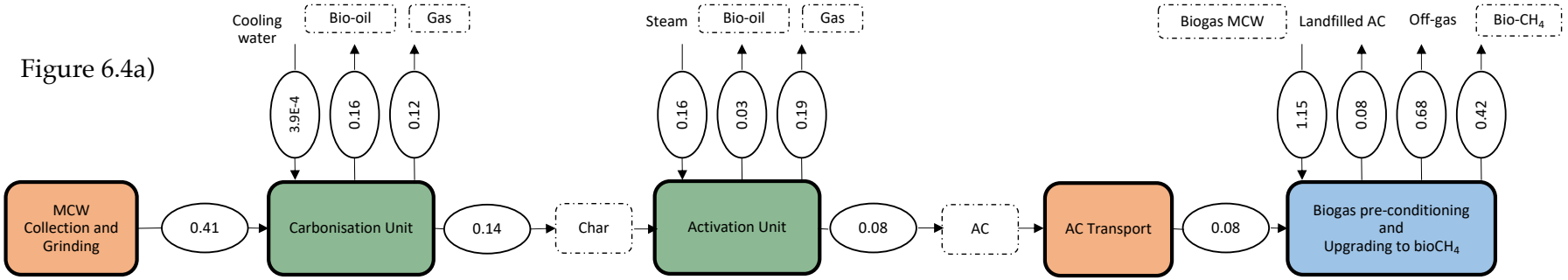

Figure 6.4b)

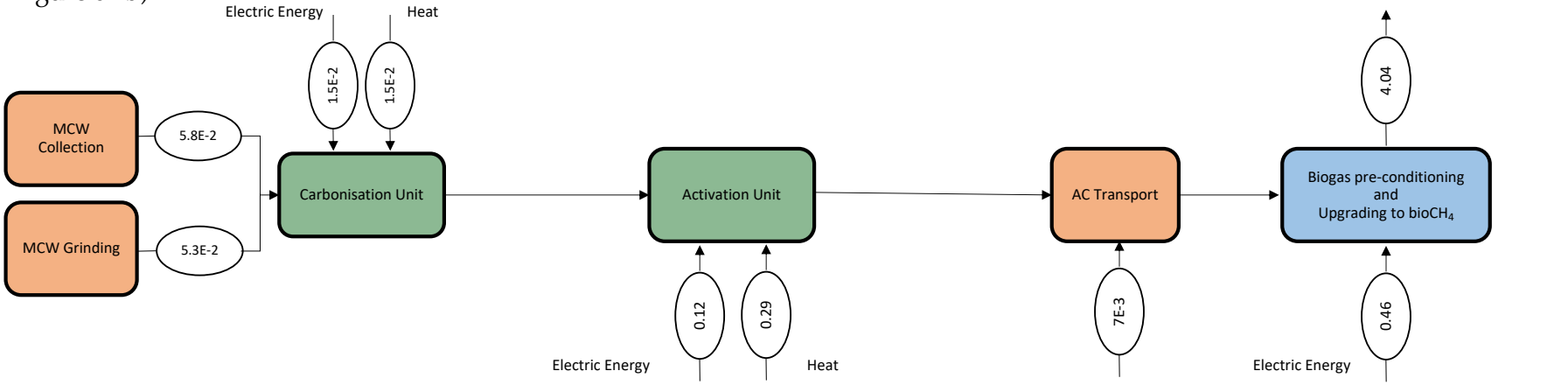

Figure 6.4: Flow sheets of mass (a) and energy (b) balances of the MCW(PA)3h scenario, including H_2S removal, and biogas upgrading to $bioCH_4$. The plant configuration adopted for the biogas production is of hOFMSW+MCW scenario. Data are expressed in kg/y for mass flow sheet (a) and in kWh/y for energy flow sheet (b) (functional unit: 1 m^3 biogas (STP)).

Figure 6.5a)

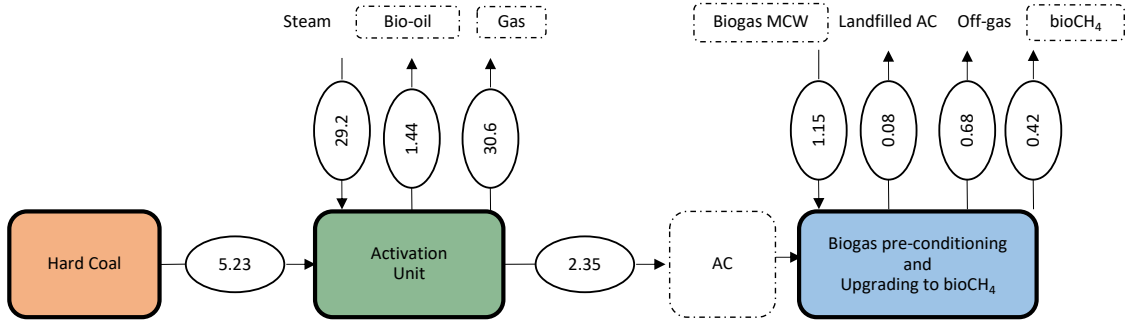

Figure 6.5b)

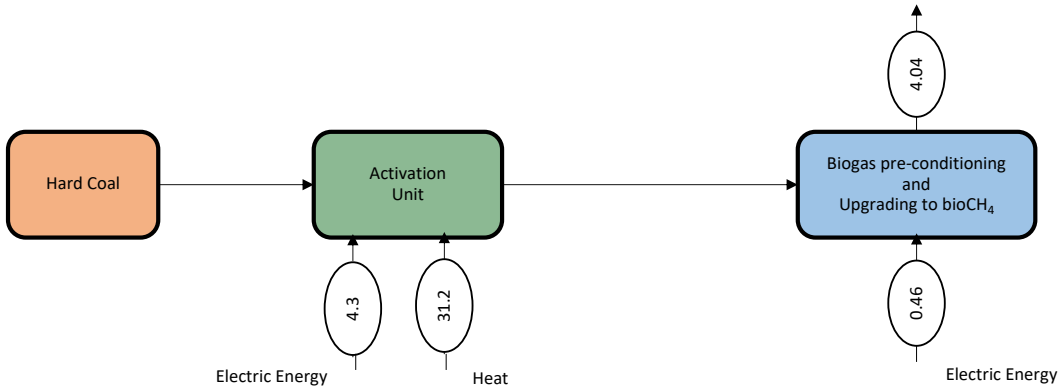

Figure 6.5: Flow sheets of mass (a) and energy (b) balances of CAC production, H_2S removal and biogas upgrading to $bioCH_4$. The plant configuration adopted for biogas production is the one for hOFMSW+MCW scenario. Data are expressed in kg/y for mass flow sheet (a) and in kWh/y for energy flow sheet (b) (functional unit: 1 m^3 biogas (STP)).

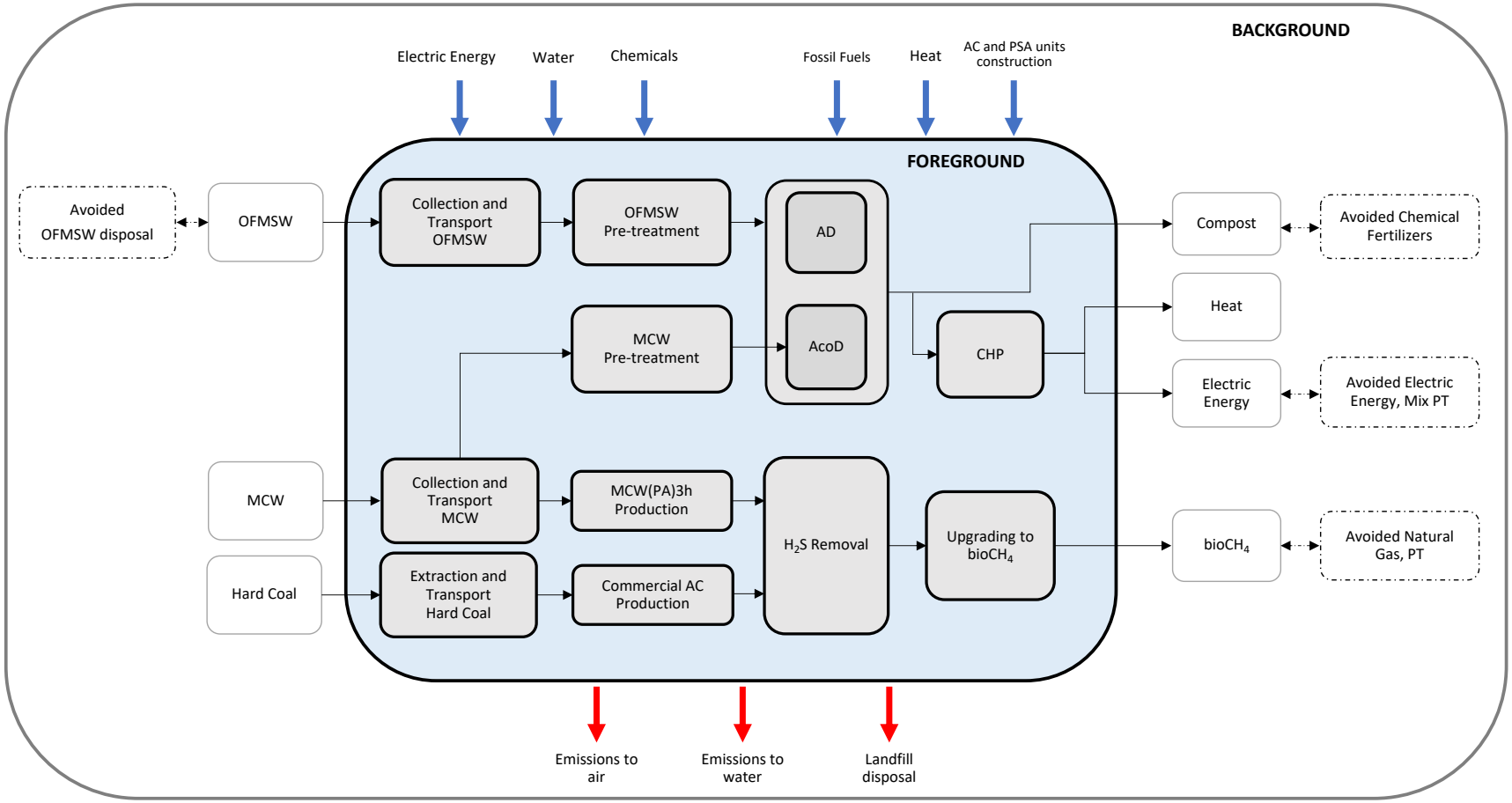

Figure 6.6: System boundaries with the indication of the foreground and background systems. Dashed lines refer to the avoided burdens

The recovered heat is completely used for the internal necessities of the AD plant, although, according to the calculation performed on the basis of the expected thermal energy requirements of the AD plant (Baccioli et al., 2019; van Haaren et al., 2010), most of the heat produced is currently lost (Figure 6.1).

Air emissions from CHP system in hOFMSW base case scenario have been quantified based on the measured flow rate and average pollutant concentrations of the flue gas at the engine stack (Table 6.2) (Personal Communication, 2016). The biofilter, consisting of a coconut shell packed column, receives the gas streams coming from the areas of OFMSW pre-treatment and digestate centrifugation and removes the volatile organic compounds present in that gas streams. The biofilter emissions consists mainly of NH_3 (Personal Communication, 2016) (Table 6.2).

The plant configuration of hOFMSW+Pre3 and hOFMSW+MCW scenarios are similar to that of hOFMSW scenario, only considering that 675 t/y of MCW is used as co-substrate with hOFMSW for AcoD.

In the case of hOFMSW+Pre3 scenario, the MCW is loaded to the pre-treatment reactor with a screw conveyor (standard pitch, single flight) with 1840 kg/h capacity, mechanically loaded with a bobcat fuelled by diesel. The estimated working time of the bobcat and of the screw conveyor is 150 h/y. Ground MCW is chemically pre-treated at ambient temperature with 926 t/y of H_2O_2, in alkaline water solution (5557 t/y H_2O and 0.023 t/y NaOH) prepared on site in a dedicated reactor equipped with an helicoidal mixer. The MCW pre-treatment is carried out in a dedicated pre-treatment reactor equipped with a Rushton turbine to guarantee adequate mixing. The pre-treated MCW is then mixed in line with the pre-hydrolysed OFMSW (hOFMSW) through a static mixer and pumped into anaerobic digesters. The estimated working time of the dynamic mixers is 50 h/y. The electric energy required for MCW pre-treatment operations under hOFMSW+Pre3 scenario is 2534 kWh/y, including over the equipment mentioned above the presence of three additional pumps for pre-treated fluid transfer.

In the case of AcoD with MCW, the ground MCW is mixed in line with hOFMSW through a static mixer fed by a screw conveyor of 1840 kg/h. The calculated energy demand of this system is 16.2 kWh/y.

The amount estimation of the different products and wastes obtained along the AcoD processes was performed on the basis of the laboratory results obtained in a previous study (Surra et al., 2018b) and on the following assumptions: (i) a

20% v/v reduction of biogas production may be expected as upscaling factor, (ii) digestate production was calculated by subtracting from the mass of substrate fed into the digesters the mass transformed into biogas, (iii) gaseous emissions from CHP during AcoD were estimated on the basis of the Estimation Factors (EF) reported by Kristensen et al. (2004) and Vicente (2015); (iv) the compost production was estimated assuming that the ratio of Total Solids (TS) in the digestate/compost produced (TS/Compost ratio) is constant during AD and AcoD; (iv) the wastewater sent to the municipal sewer and the amount of sludge recirculated to the pre-treatment section were calculated on the basis of the data reported by Neto (2011) on the AD plant.

Modelling of feedstocks, products, energy demand and emissions for the production of MCW(PA)3h AC for H_2S removal has been developed on the basis of the laboratory results obtained in a previous work (Surra et al., 2019), bibliographic references (Gu et al., 2019; Mullen et al., 2010) and Ecoinvent database (2018).

The MCW harvesting and grinding flow diagram considered for AC production and the calculation of emissions to air of these processes are similar to those described for AcoD (Table 6.3).

The production plant of MCW(PA)3h AC includes a carbonization unit followed by a physical activation unit. Steam was considered as activating agent (Figure 6.4a), assuming that the use of steam is able to produce an AC with similar adsorption capacity of MCW(PA)3h AC. The option for substituting CO_2 by steam is based on the evidence that the calculated amount of CO_2 required for activation (41.2 kg CO_2/kg AC) exceeds in approximately 700% w/w the total amount of CO_2 produced during biogas upgrading (5.10 kg CO_2/kg AC used). Moreover, the re-use of CO_2 produced during the upgrading process in AC activation would require the construction of the AC industrial furnace in the AD plant area instead in the vicinity of corn fields, increasing the transport costs. The option of using industrial CO_2 was not taken into consideration, due to its high costs.

Mass and energy balances of the carbonization and activation plants for the production of MCW(PA)3h AC are reported in Figures 6.4a) and b).

The required amount of MCW(PA)3h AC was calculated taking into consideration the production of 7790 kg/y of H_2S and an adsorption capacity of MCW(PA)3h of 1.55E-02 kg_{H2S}/kg AC.

MCW is heated up in the carbonization unit to approximately 500 ºC in the absence of air. It is considered that the production of 1 kg charcoal, including drying process requires 2.5 MJ heat, 0.075 kWh electricity and 50 L cooling water (Ecoinvent, 2018). The process produces charcoal, bio-oil and gas in the percentages (w/w) of 35%, 35% and 30%, respectively (Fałtynowicz et al., 2015; Shariff et al., 2016; Surra et al., 2019).

The configuration of the carbonization unit and the calculation of environmental burdens are based on the "charcoal production | charcoal | APOS, U" process reported on the Ecoinvent v.3.4 database for woody biomass. This approximation is justified by the great similarity of the chemical and physical characteristics of MCW with woody biomass (Gu et al., 2019; Mullen et al., 2010; Surra et al., 2019). Moreover, the comparison of the emissions to air and water calculated according to the Ecoinvent database v.3.4 is reasonably similar to those reported by Mullen et al. (2010) on the pyrolysis of MCW.

The activation step is assumed to be carried out at an activation temperature of 800 ºC with steam (activating agent) coming from a boiler. It was assumed that the activation process requires 1.6 kWh electric energy, 13.3 MJ heat to vaporize 2.1 L water for each 1 kg of produced AC (Ecoinvent, 2018; Gu et al., 2019).

For the calculation of the environmental burdens, it was assumed that the activation process presents yields for AC, gases and bio-oils of 20% w_{AC}/w_{MCW}, 37% w_{gases}/ w_{MCW} and 43% $w_{bio\text{-}oils}/w_{MCW}$, respectively.

Table 6.3 reports the activation process outputs. No heat recovery from the process was considered as avoided burden.

The environmental burden related with the production of commercial activated carbon CAC was assessed on the basis of the "activated carbon production, granular from hard coal | activated carbon, granular | APOS, U" process reported on the Ecoinvent v.3.4, assuming the adsorption capacity of 5.1E-04 kg_{H2S}/kg AC (Surra et al., 2019). The main energy demands are 1.6 kWh electricity and 0.33 m^3 of natural gas to heat 12 kg of water. Table 6.3 reports the main data and environmental burdens calculated. Figure 6.5 reports the mass and energy balances.

The biogas upgrading plant considered in this work is a PSA unit fed with 8 bar biogas. The biogas composition considered was the one that provided the most sustainable AcoD configuration (60.6% v/v CH_4; 39.3% v/v CO_2; 820 ppmv H_2S). The bioCH_4 leaves the plant at 5 bar with a CH_4 purity of 97% v/v (Ecoinvent, 2018) and a CH_4 slip of 3% v/v (Q. Sun et al., 2015). The upgrading process requires 0.46 kWh for each 1 m^3 of raw biogas, including biogas drying and compression, and H_2S removal.

The environmental burdens associated with the production and operation of the adsorbent materials required for PSA unit are neglected in the Ecoinvent (2018) database. This database does not detail neither the adsorbents used to achieve the declared environmental performances, nor their characteristics. In any case, being the PSA process cyclic and the adsorbent/s completely regenerable, their contribution to the overall environmental burdens was assumed to be negligible.

Table 6.4 summarizes all the data related with the operation of PSA upgrading unit and its direct and avoided burdens.

6.4 Life cycle impact assessment

Table 6.5 reports the comparison of the environmental burdens associated to AD and AcoD scenarios.

Most of the environmental impact categories are very low, highlighting that the AD and AcoD processes have associated low environmental impacts. This result suggests that the avoided burdens related to the production of renewable electric energy from biogas and, to a lesser extent, the avoided production of chemical fertilizers, are able in many cases to reduce the direct and indirect environmental burdens associated to the AD and AcoD processes.

The configuration of AcoD of hOFMSW+MCW scenario showed an overall better environmental performance than both AD scenario with standalone hOFMSW and AcoD of OFMSW+Pre3 scenario, presenting the lowest impacts in most of the impact categories and an increment lower than 10% in the majority of the remaining ones, when compared with AD of hOFMSW (Table 6.5). It must be noticed that the reduction of the environmental burdens related to hOFMSW+MCW scenario is very similar to that showed by AD of standalone hOFMSW. This is due to the increase of biogas and methane production in hOFMSW+MCW scenario that was able to compensate the added environmental

impacts caused by the collection, grinding and transport of MCW to the AD plant.

The AcoD of OFMSW+Pre3 scenario can be considered the less environmentally sustainable configuration, mainly due to the contribution to the indirect impacts of the hydrogen peroxide production that was responsible by percentages of 39%, 130% and 37% to the total value of FRS, MRS and fPMF impact categories, respectively.

The impact categories that showed the highest contribution to the environmental burdens of AD and AcoD processes are FRS, MRS, WC(hh), fPMF, and GW(hh) (Table 6.5).

Figure 6.7 reports the process contributions to the above-mentioned impact categories. The FRS impact category is mainly affected by the indirect impact, due to the production processes of fossil fuels that are used in the transport of wastes and production of the non-renewable part of electricity supplied to the AD and AcoD units.

The biogas production process contributes both to the impacts associated to WC(hh) impact categories, due to the supply of freshwater to the AD and AcoD processes in order to compensate the wastewater generated after digestate dewatering (

Figure 6.7 c). Finally, the avoided electric energy production can reduce on average by 55% and 63% the value of the overall impacts associated with fPMF and GW(hh) impact categories, respectively.

Table 6.6 reports the comparison of the environmental burdens associated to the production of MCW(PA)3h activated carbon and CAC. The production of MCW(PA)3h activated carbon is more favourable than CAC. The reason lays in the higher adsorption capacity provided by MCW(PA)3h than CAC (Figure 4.8), and thus in the lower amount of MCW(PA)3h activated carbon required to remove the same amount of H_2S present in the biogas stream. It must be noticed that the adsorption capacity of CAC was tested under real conditions of use and under the same experimental conditions as for MCW(PA)3h activated carbon. Real biogas samples have been used without adding supplemental oxygen or water vapor as required by standard conditions, in order to avoid biogas contamination before the upgrading process. The CAC manufacturer declared an adsorption capacity of 0.32 kg_{H2S}/kg AC, which is 1000 % higher (Cabot, 2016) than the capacity effectively measured under real conditions of use.

Table 6.5: Total impacts calculated for the different AD and AcoD configurations according to ReCiPe Endpoint (H) method. All values are referred to the functional unit of 1 m^3 biogas (STP). The yellow cells indicate the environmental impacts of the hOFMSW AD base scenario, the red and green ones, the impacts higher and lower, respectively than the corresponding impacts obtained in the AD base case scenario. The orange cells indicate the values when the % of increment is lower than 10%, when compared with AD with hOFMSW.

Acronyms	Impact category	AD and AcoD			Unit
		hOFMSW	hOFMSW +Pre3	hOFMSW +MCW	
FRS	Fossil resource scarcity	5.77E-02	5.02E-02	3.12E-02	USD2013
MRS	Mineral resource scarcity	-2.17E-05	1.00E-04	-2.49E-05	USD2013
WC(hh)	Water consumption, Human health	3.74E-06	2.97E-06	4.12E-06	DALY
fPMF	Fine particulate matter formation	6.19E-07	3.09E-07	1.18E-07	DALY
GW(hh)	Global warming, Human health	1.56E-07	1.72E-07	4.87E-09	DALY
WC(te)	Water consumption, Terrestrial ecosystem	4.56E-08	1.81E-08	2.51E-08	species.yr
OF(te)	Ozone formation, Terrestrial ecosystems	4.26E-10	5.63E-10	4.10E-08	species.yr
OF(hh)	Ozone formation, Human health	2.97E-09	3.94E-09	3.04E-09	DALY
TA	Terrestrial acidification	1.11E-09	5.86E-10	2.88E-10	species.yr
GW(te)	Global warming, Terrestrial ecosystems	4.72E-10	5.19E-10	1.45E-11	species.yr
IR	Ionizing radiation	2.29E-11	2.10E-10	8.27E-12	DALY
sOD	Stratospheric ozone depletion	2.10E-11	3.57E-11	4.23E-12	DALY
WC(ae)	Water consumption, Aquatic ecosystems	1.02E-12	8.08E-13	1.12E-12	species.yr
GW(fe)	Global warming, Freshwater ecosystems	1.29E-14	1.42E-14	4.01E-16	species.yr
ME	Marine eutrophication	-8.80E-15	3.46E-15	-8.63E-15	species.yr
MEco	Marine ecotoxicity	-5.16E-13	6.90E-13	-5.20E-13	species.yr
FEco	Freshwater ecotoxicity	-2.56E-12	3.34E-12	-2.55E-12	species.yr
TEco	Terrestrial ecotoxicity	-2.66E-12	3.19E-12	-2.60E-12	species.yr
FE	Freshwater eutrophication	-6.03E-11	-1.36E-11	-5.65E-11	species.yr
LU	Land use	-1.15E-10	-7.92E-11	-1.05E-10	species.yr
HT(c)	Human carcinogenic toxicity	-2.12E-08	5.77E-08	-4.06E-08	DALY
HT(nc)	Human non-carcinogenic toxicity	-2.07E-08	2.59E-08	-2.02E-08	DALY

Table 6.6: Total impacts calculated for the production of MCW(PA)3h and CAC activated carbons according to ReCiPe Endpoint (H). All values are referred to the functional unit 1 m3 of used biogas (STP).

Acronyms	Impact category	MCW(PA)3h	CAC	Unit
FRS	Fossil resource scarcity	0.0141	1.12E+05	USD2013
MRS	Mineral resource scarcity	3.30E-05	7.26E+03	USD2013
GW(hh)	Global warming, Human health	2.64E-07	1.75E+00	DALY
fPMF	Fine particulate matter formation	1.52E-07	2.69E+00	DALY
HT(c)	Human carcinogenic toxicity	1.17E-08	1.00E+00	DALY
HT(nc)	Human non-carcinogenic toxicity	7.24E-09	1.11E+00	DALY
GW(te)	Global warming, Terrestrial ecosystems	7.96E-10	5.29E-03	species.yr
OF(hh)	Ozone formation, Human health	4.47E-10	6.97E-03	DALY
TA	Terrestrial acidification	1.31E-10	2.01E-03	species.yr
IR	Ionizing radiation	8.94E-11	6.50E-04	DALY
OF(te)	Ozone formation, Terrestrial ecosystems	7.16E-11	1.01E-03	species.yr
LU	Land use	2.60E-11	1.20E-03	species.yr
sOD	Stratospheric Ozone depletion	2.30E-11	3.40E-04	DALY
FE	Freshwater eutrophication	1.58E-11	7.40E-04	species.yr
TEco	Terrestrial ecotoxicity	1.04E-12	1.90E-04	species.yr
FEco	Freshwater ecotoxicity	9.28E-13	1.00E-04	species.yr
MEco	Marine ecotoxicity	1.96E-13	2.17E-05	species.yr
GW(fe)	Global warming, Freshwater ecosystems	2.18E-14	1.44E-07	species.yr
ME	Marine eutrophication	3.09E-15	1.05E-07	species.yr
WC(ae)	Water consumption, Aquatic ecosystems	-1.74E-12	8.72E-09	species.yr
WC(te)	Water consumption, Terrestrial ecosystem	-3.89E-08	1.90E-04	species.yr
WC(hh)	Water consumption, Human health	-6.40E-06	3.21E-02	DALY

Figure 6.7a)

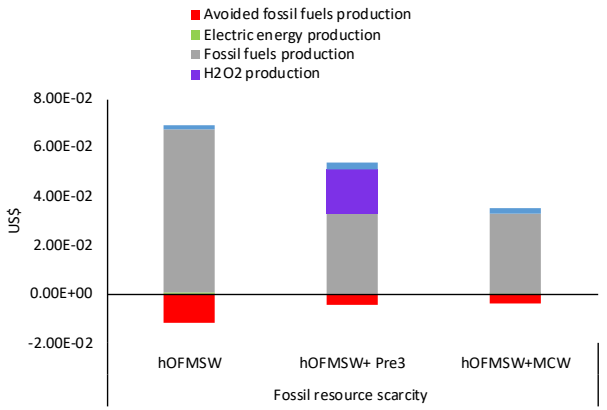

Figure 6.7b)

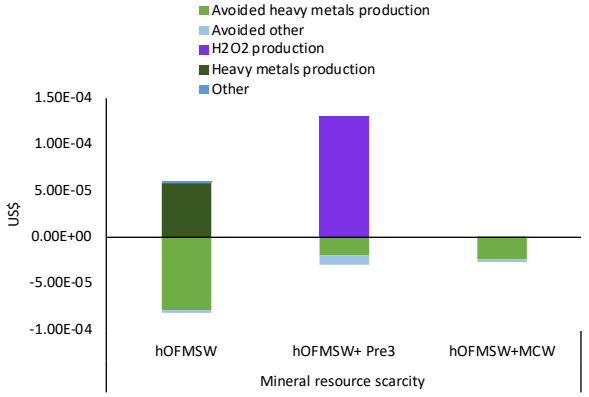

Figure 6.7c)

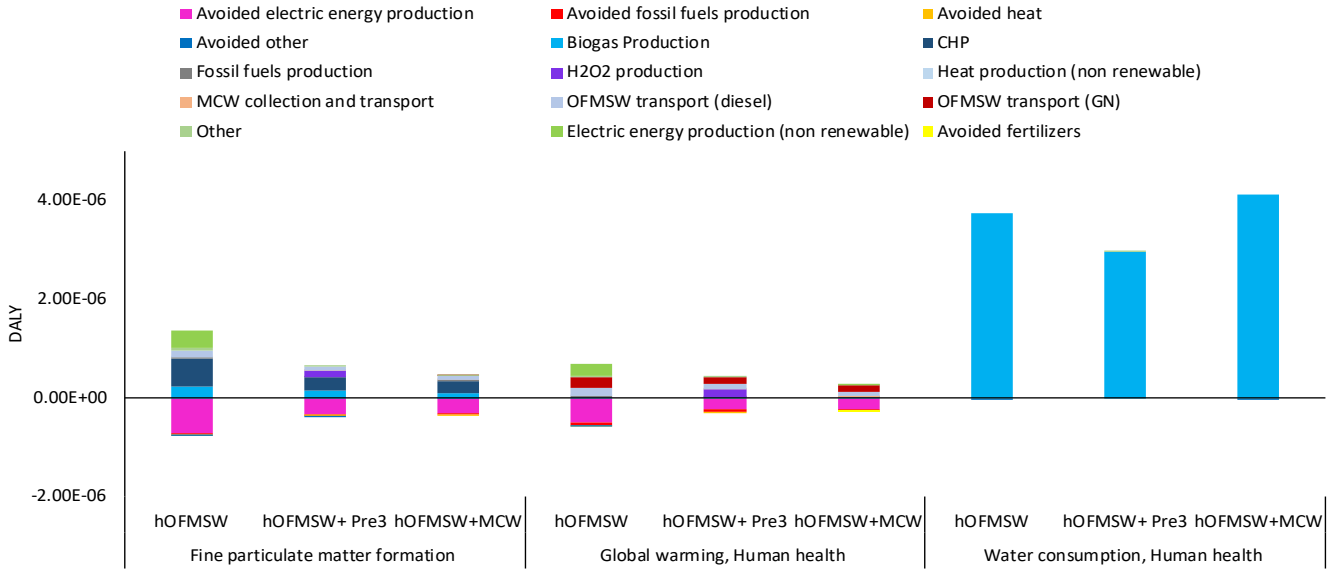

Figure 6.7: Contribution of the selected impact categories for the environmental burdens of AD and AcoD scenarios.

The impact categories that most affected the AC production were FRS, MRS, GW(hh), fPMF and HT(nc) (Table 6.6). The production of MCW(PA)3h AC showed the main impacts on FRS and in a lesser extent on GW(hh) and fPMF, being the indirect impacts of heat and electric energy production and the direct impact of the carbonization process, the main contributors for the environmental burdens (Figures 6.8a and b). Similarly, the production of CAC provided the main impacts on FRS, MRS and in a lesser extent on fPMF, being the indirect impacts of fossil fuel production and AC plant construction the main contributors for the environmental burdens (Figures 6.8c and d).

The biogas "upgrading to bioCH_4" scenario (Table 6.7) reports the comparison of LCA results of the most environmentally sustainable AcoD scenario (hOFMSW+MCW) with the three different upgrading scenarios of biogas stream to bioCH_4. The scenarios "Upgrading to bioCH_4 (Optimization 1 and 2)" will be discussed later in the sensitivity analysis reported in the following section, but, basically, they deal with the use of AC with optimised adsorption capacity and with the partial substitution of the fossil NG used to fuel fleet used for the OFMSW transportation.

The biogas "upgrading to bioCH_4" scenario (Table 6.7) showed less favourable environmental performances than the AcoD hOFMSW+MCW for the the majority of the categories of impact, with special emphasis to FRS, MRS, HT(nc), fPMF and GW(hh). In the "upgrading to bioCH_4" scenario, a reduction of the associated environmental burdens was observed for the impact categories related with the water consumption in the three areas of protection (WC(te), WC(ae) and WC(hh)).

Figure 6.8a)

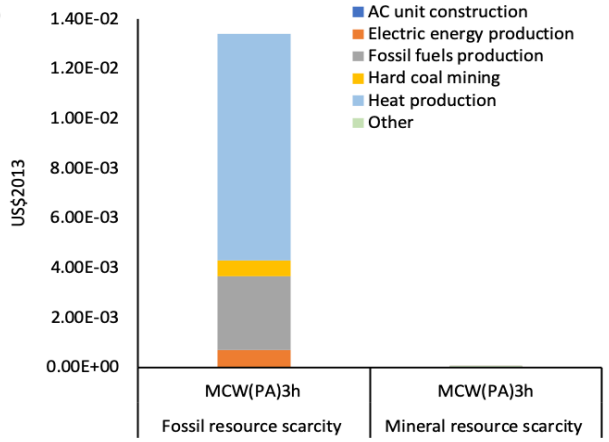

Figure 6.8b)

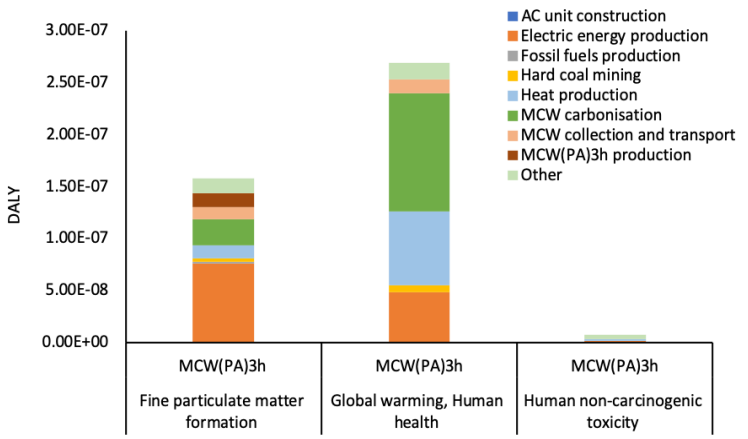

Figure 6.8c)

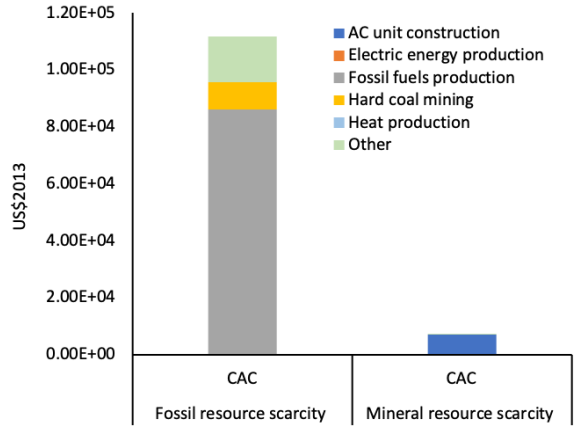

Figure 6.8d)

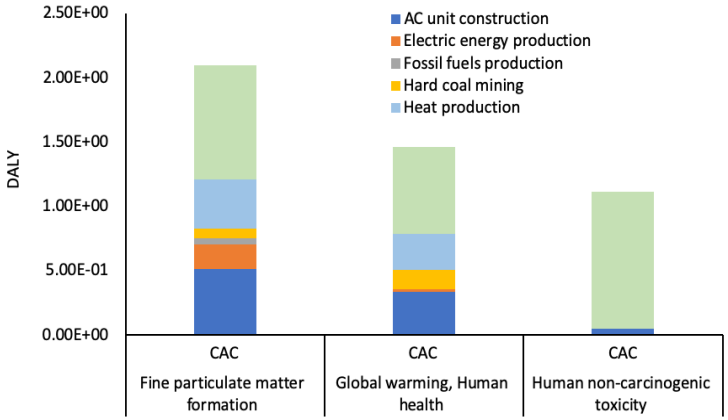

Figure 6.8: Contribution of the selected impact categories for the environmental burdens of MCW(PA)3h and CAC production process.

Table 6.7: Total impacts calculated for the different upgrading scenarios of biogas to bioCH_4, according to ReCiPe Endpoint (H) method. All values are referred to the functional unit of 1 m^3 biogas STP. The yellow cells indicate the environmental impacts of the hOFMSW+MCW AcoD scenario, the red and green ones indicate the impacts higher and lower, respectively than the corresponding impacts obtained in the hOFMSW+MCW AcoD scenario.

Acro-nyms	Impact category	AcoD (hOFMSW +MCW)	Upgrading to bio-CH_4	Upgrading (Optimization 1)	Upgrading (Optimization 2)	Unit
FRS	Fossil resource scarcity	3.12E-02	1.40E+00	5.54E-02	3.37E-02	USD2013
MRS	Mineral resource scarcity	-2.49E-05	1.94E-01	9.31E-05	8.42E-05	USD2013
fPMF	Fine particulate matter formation	1.18E-07	5.17E-05	8.34E-07	8.01E-07	DALY
HT(nc)	Human non-carcinogenic toxicity	-2.02E-08	4.69E-05	4.06E-08	3.87E-08	DALY
GW(hh)	Global warming, Human health	4.87E-09	2.61E-05	1.23E-06	1.07E-06	DALY
HT(c)	Human carcinogenic toxicity	-2.02E-08	1.52E-05	4.72E-08	4.48E-08	DALY
GW(te)	Global warming, Terrestrial ecosystems	1.45E-11	7.87E-08	3.71E-09	3.23E-09	species.yr
OF(hh)	Ozone formation, Human health	3.04E-09	6.56E-08	2.26E-09	2.18E-09	DALY
TA	Terrestrial acidification	2.88E-10	3.92E-08	1.04E-09	1.01E-09	species.yr
FE	Freshwater eutrophication	-5.65E-11	2.58E-08	1.04E-10	1.00E-10	species.yr
LU	Land use	-1.05E-10	2.18E-08	1.77E-10	1.75E-10	species.yr
IR	Ionizing radiation	8.27E-12	2.07E-08	5.08E-11	4.03E-11	DALY
OF(te)	Ozone formation, Terrestrial ecosystems	4.10E-10	9.49E-09	3.24E-10	3.11E-10	species.yr
sOD	Stratospheric ozone depletion	4.23E-12	7.56E-09	7.01E-11	5.69E-11	DALY
TEco	Terrestrial ecotoxicity	-2.60E-12	7.47E-09	5.35E-12	5.21E-12	species.yr
MEco	Freshwater ecotoxicity	-2.55E-12	4.18E-09	5.07E-12	4.82E-12	species.yr
ME	Marine ecotoxicity	-5.20E-13	8.94E-10	1.07E-12	1.01E-12	species.yr
ME	Marine eutrophication	-8.63E-15	3.59E-12	1.77E-14	1.68E-14	species.yr
GW(fe)	Global warming, Freshwater ecosystems	4.01E-16	2.15E-12	1.01E-13	8.83E-14	species.yr
WC(ae)	Water consumption, Aquatic ecosystems	1.12E-12	-4,63E-13	1.04E-12	1.04E-12	species.yr
WC(te)	Water consumption, Terrestrial ecosystem	2.51E-08	-1.04E-08	2.33E-08	2.33E-08	species.yr
WC(hh)	Water consumption, Human health	4.12E-06	-1.70E-06	3.83E-06	3.83E-06	DALY

This means that the avoided impacts related to bioCH_4 production and NG substitution are not always able to overcome the direct and indirect environmental impacts generated by the upgrading process. Thus, the impacts generated by biogas upgrading are, in most cases, higher than the environmental benefits gained due to the avoided production of NG. This result is in line with literature (Ardolino et al., 2018; Florio et al., 2019).

The impact categories that most contributed to the overall environmental burdens of biogas "upgrading to bioCH_4" scenario were FRS, MRS, HT(nc), fPMF and GW(hh). FRS impact category was affected by a percentage of 65% due the increased production of fossil fuels, petroleum and NG, required for both the AC and energy production, when compared to AcoD hOFMSW+MCW scenario in which biogas was converted into electric energy. MRS impact category was affected by the impacts associated to the construction of AC and PSA plants by a percentage of 90%, when compared to the same AcoD scenario. The other three impact categories are affected mainly by the indirect impacts provided by AC and PSA units construction and by energy production processes.

6.5 Sensitivity analysis

The biorefinery analysed in this work was submitted to a sensitivity analysis in order to assess how the variation of some parameters affects the LCA results.

The two parameters taken into consideration were the following ones: (i) adsorption capacity of the activated carbons used for H_2S removal, and (ii) amount of NG that fuels the fleet used for the collection of OFMSW. The former affects the amount of AC required for biogas pre-conditioning and thus the impacts associated with their production (this scenario was named as "upgrading to bioCH_4, Optimization 1"). The latter affects the amount of fossil NG used the in OFMSW collection fleet that is replaced by bioCH_4 produced in the biorefinery (this scenario was named as "upgrading to bio-CH_4, Optimisation 2"). In the "upgrading to bioCH_4, Optimization 2" scenario, the effects of NG substitution by bioCH_4 were added to those obtained by the optimized AC adsorption capacity provided by the "upgrading to bio-CH_4, Optimization 1" scenario.

Table 6.7 reports the results obtained with the two optimized conditions.

The use of an activated carbon with an optimized adsorption capacity (similar to those declared by the manufacturer of the commercial CAC) reduced drastically the environmental burdens associated to the "upgrading to bioCH_4" scenario in almost all the category of impacts (Table 6.7). Considering the substitution of NG by bioCH_4 in the OFMSW collection fleet ("upgrading to bioCH_4, Optimization 2" scenario), this reduction increases on average by an additional percentage of 8%, when compared with "upgrading to bioCH_4, Optimization 1" scenario.

If an AC with optimized adsorption capacity towards H_2S is used to upgrade biogas, the associated impacts of OF(hh), OF(te), WC(te), WC(ae) and WC(hh) categories were lower than the corresponding impacts of the AcoD of hOFMSW+MCW scenario in which the biogas is converted to electric energy. Furthermore, two of the main categories of impact, FRS and fPMF, decreased to the same order of magnitude of the corresponding values obtained with AcoD hOFMSW+MCW scenario.

The further substitution of NG for fuelling the OFMSW collection fleet with the produced bioCH_4 allowed a more sustainable configuration for all the impact categories when compared with "Upgrading to bioCH_4, Optimisation 1" scenario.

6.6 Conclusions

This study aims to assess the environmental benefits generated from different uses of biogas, namely to compare the bioCH_4 production and use in transportation with direct cogeneration of electricity and heat. A case-study of a real AD plant at industrial scale was studied. Currently, this AD plant is processing 40000 t/y of OFMSW. Among the three biogas production scenarios considered (hOFMSW, OFMSW+Pre3 and hOFMSW+MCW), the AcoD of hOFMSW+MCW was the most environmentally favourable, providing the lowest impacts in almost all the environmental categories analysed. The increase of biogas and methane yields in AcoD of hOFMSW+MCW scenario was able to compensate the added environmental impacts caused by the collection, grinding and transportation of MCW. AcoD of OFMSW+Pre3 can be considered the less sustainable scenario.

The MCW(PA)3h activated carbon, aiming to replace the commercial AC for the removal of H_2S from biogas stream, demonstrated to be more sustainable than the commercial activated carbon (CAC), tested under real conditions of use.

The reason lays in the higher adsorption capacity provided by MCW(PA)3h AC than by CAC, thus lowering the amount of activated carbon required to remove the same amount of H_2S present in the biogas stream.

The "upgrading to bioCH_4" scenario of biogas stream obtained with AcoD of hOFMSW+MCW provided higher environmental burdens than the classic co-generation scenario, mainly due to the contribution of the increased fossil fuel production and of the construction of AC and PSA plants. This means that the avoided impacts related to bioCH_4 production are not always able to overcome the direct and indirect environmental impacts produce by the upgrading process, indicating that the impacts generated are in most cases higher than the environmental benefits gained due to the avoided production of NG.

The results of the sensitivity analysis showed that for the "upgrading to bioCH_4, Optimization 2" scenario, the biogas upgrading to bioCH_4 is dramatically more sustainable than that "upgrading to bioCH_4" scenario and provided lower environmental impacts in OF(hh), OF(te), WC(te), WC(ae) and WC(hh) categories than of direct electric energy and heat production when bioCH_4 is used to replace NG in the collection and transportation fleet of OFMSW, at optimized H_2S adsorption capacity.

7

Conclusions and Future Challenges

7.1 General Conclusions

The biorefinery concept proposed in this work was based on the idea of valorising MCW as co-substrate for AcoD with OFMSW and as precursor to produce ACs suitable for H_2S removal and CO_2 separation from biogas. The main purpose was to produce bioCH_4. This biorefinery concept was developed according to the **Tasks 1-6** reported in Figure 1.1. The main conclusions and final remarks are as follows:

- **Task 1**: a strong interdisciplinary bibliographical review, concerning (i) the MCW pre-treatments prior to AcoD, (ii) the operational conditions for AcoD of MCW with OFMSW, (iii) the production of AC using MCW and liquid digestate as precursors for biogas conditioning, (iv) and the available biogas upgrading technologies, represented the starting point of the entire work:
  - (i) Regarding the possible pre-treatment that can be applied to MCW, most of the authors agree that an initial size reduction is an important step before any submission of MCW to AD (Chongkhong and Tongurai, 2014 ; Y. Zheng et al., 2014). Thermal and thermo-chemical pre-treatments can be very effective, although according to the temperature and the catalyst chosen, the formation of inhibitors may occur. Microwave Irradiation, as a non-conventional heating source, heats MCW uniformly, quickly and can help to avoid large temperature gradients, limiting the formation of inhibitors (Li et al., 2016). If a strict chemical pre-treatment is applied, the choice of the catalyst is crucial for the economic viability of the process. Among the catalysts that may be used for

MCW pre-treatment, NaOH is the most tested due to its high efficiency and low cost. Recently, High Boling Solvents such as glycerol were recognized by some authors to have a high solubilization potential and capacity to remain liquid at high temperatures (Diaz et al., 2015; Moretti De Souza et al., 2014). Finally, H_2O_2 can be considered as one of the most suitable catalysts for improving the methane yield on lignocellulosic biomass, due to its effectiveness without producing any significant inhibition to the AD process, and due to its relatively low cost (Banerjee et al., 2012; Song et al., 2014). On the base of these evidences, microwave irradiation catalysed by NaOH, glycerol and H_2O_2, and room temperature chemical pre-treatment catalysed by H_2O_2 have been tested for MCW pre-treatment before AcoD with OFMSW;

- (ii) Regarding the AcoD of MCW with OFMSW, several studies are available in the literature on AcoD of maize waste (Table 2.3). Owamah and Izinyon (2015) demonstrated that maize waste can enhance biogas and methane yields when used as co-substrate with food waste. Ramos-Suárez et al (2017) observed that oxidative pre-treatments on maize straw can enhance biogas and methane yields. On the other hand, Hutňan (2016) showed that the presence of standalone maize wastes submitted to size reduction without any other pre-treatment, provides biogas yields comparable to those obtained with pre-treated maize wastes, suggesting that the use of a pre-treatment prior to AcoD is not a guarantee of biogas and methane yields enhancement. Thus, AcoD of MCW pre-treated under conditions selected at point (i), as well as non-pre-treated MCW only submitted to size reduction, were tested and compared with the AD of standalone OFMSW;
- (iii) Regarding the different techniques that can be used for H_2S removal from biogas stream, adsorption onto ACs, namely lignocellulosic-derived ACs, is considered a safe, sustainable, reliable, highly efficient and in most cases an environmentally sound technique (Kwaśny and Balcerzak, 2016; Mohamad Nor et al., 2013). MCW is a lignocellulosic biowaste that can be considered a good precursor for ACs with relatively high surface area, due to its high carbon content and low percentage of ashes (Bagheri and Abedi, 2009; Flores et al., 2017; Tsai et al., 2001). The mechanisms underlying H_2S adsorption onto ACs are highly dependent on the porosity, on the surface chemistry and on the conditions applied

(relative humidity, O_2 concentration, presence of contaminants, and temperature) (Bandosz, 1999; Chen et al., 2010). It is usually considered that ACs surface chemistry is more important than the textural properties in H_2S adsorption (Adib et al., 2000a, 1999a; Bandosz, 1999). Moreover, the presence of water and oxygen is critical, since the H_2S removal mechanisms onto carbonaceous materials are ruled mainly by dissociative adsorption, favoured by the presence of water, and by oxidation mechanisms. Under dry conditions and without added oxygen, H_2S can also be oxidized in activated carbon by oxygen functional groups present on the carbon surface (Adib et al., 2000a; Bouzaza et al., 2004; Feng et al., 2005; Le Leuch et al., 2003). The enhancement of H_2S removal onto ACs can also be obtained through functionalization of the AC surface by introducing nitrogen-containing groups. This has a catalytic role in H_2S dissociation and oxidation, mainly due to the increase of basic sites on the carbon surface (Adib et al., 2000b; Bagreev et al., 2004; Bashkova et al., 2002; Seredych and Bandosz, 2008). In this context, a first set of ACs was physically activated with CO_2, to maximize ACs textural properties, and a second set of ACs was prepared by impregnating MCW with anaerobic LD, being this a sub-product of the anaerobic digestion. LD is a nitrogen rich material, that can catalyse the H_2S removal. The use of anaerobic LD is in line with the concept of the biorefinery concept proposed and can offer the opportunity to valorise the liquid digestate in a high added value product;

- (iv) Regarding CO_2 removal from biogas, among the several technologies available, PSA is an adsorption-based process that is attracting increasing interest for its low energy requirements and limited initial capital investment in comparison with other separation technologies (D.M. Ruthven et al., 1994 and Bauer et al., 2013). Moreover, PSA can process high throughputs and produce high-purity CH_4 (Esteves and Mota, 2007). In a PSA unit for biogas upgrading, the efficiency of adsorption of CO_2 depends, among other factors, specifically on the textural properties of the adsorbent material employed, on its working capacity, CO_2 selectivity and on its capability to be regenerated. Pellerano et al., 2009 observed that ACs can provide higher adsorption capacities than some zeolites at pressures higher than 2.5 bar and Siriwardane et al.

(2001) demonstrated that ACs can provide better performances than carbon molecular sieve , when CO_2 partial pressure is higher than 1.7 bar. Thus, ACs can be considered suitable candidates for biogas upgrading, since the typical CO_2 partial pressure used during the upgrading process commonly ranges from 1.8 bar to 4 bar (Grande, 2011). The use of agricultural residues as precursors to produce carbon adsorbent materials can be considered one of the main challenges in the manufacture of ACs, since these precursors are cheap, available in large amounts, environmentally friendly and have high potential as precursors of the adsorbent media for biogas upgrading and CO_2 separation (Vilella Costa et al., 2017, Álvarez-Gutiérrez et al., 2014 and 2016, Durán et al., 2018, Ogungbenro et al., 2018). Under this framework, among the produced ACs using MCW, the physically MCW (MCW(PA)2h and MCW(PA)3h ACs produced showed the best properties as potential adsorbents for CO_2 separation from a biogas stream;

- **Task 2**: the results obtained after MCW pre-treatment showed that, among the different conditions applied, the chemical pre-treatment catalysed by H_2O_2, at pH 9.8, with 4h of reaction time and at room temperature (Pre3), is a promising and low energy demanding pre-treatment applicable to MCW to allow its AcoD with hOFMSW. Higher reaction times (up to 3 d) produced inhibitors that affected the efficiency of the AcoD process. The co-digestion of OFMSW with pre-treated MCW under Pre3 increased the biogas yield by 65% and CH_4 yield by 48%, when compared to the results obtained using OFMSW alone. The co-digestion of hOFMSW with non-pre-treated MCW increased biogas and CH_4 yields by 84% and 57%, respectively. Despite the higher yields, the LHV of the biogas obtained in the AcoD of hOFMSW with non-pre-treated MCW were on average 4% lower, respectively, than the LHV obtained with the AcoD of hOFMSW+Pre3. Moreover, Pre3 favoured the stability of the AcoD process, providing reduced acetic acid and N-NH_4 accumulation when compared to non-treated MCW. These results allow concluding that a pre-treatment is recommended before submitting MCW to AD and that co-digestion of hOFMSW with pre-treated MCW allows a significant enhancement of biogas and methane yields.
- **Tasks 3 and 4**: the physically ACs performed better in H_2S removal assays than ACs impregnated with the anaerobic LD, with uptake capacities up to

15 folds higher than ACs impregnated with LD. Textural properties, such as surface area and microporosity, seemed to be more important than the mineral content for H_2S removal from real biogas samples. Effectively, both surface area and micropore volume were much higher in physically activated carbons than in the impregnated ones. Among the physically activated carbons produced, MCW(PA)3h showed the highest volume of micropores, with sizes between 0.7–1.8 nm. This may have played an important role in H_2S removal. Also, the higher oxygen content observed in this AC may have been involved in the catalytic oxidation reaction of H_2S, indicating that its better performance on H_2S removal is also probably due to the better surface chemistry properties. Finally, MCW(PA)3h showed a higher H_2S adsorption capacity (15.5 mg/g) than the commercial activated carbon (0.51 mg/g), which means that this new biomass-derived activated carbon suits better at non-optimized conditions of H_2S removal, namely in what concerns to moisture and oxygen deficiencies;

- **Task 5:** among the produced AC, the physically MCW(PA)3h AC can be considered the most suitable candidate for CO_2 separation due to its higher specific surface area, higher microporous volume, more favourable pore size distribution and higher working capacity, when compared to the others ACs produced and studied. The study of the adsorption equilibrium measurements of CO_2 and CH_4 on MCW(PA)3h activated carbon showed that the Sips isotherm model can be confidently employed to accurately correlate the adsorption equilibria of the two main constituents of biogas, CO_2 and CH_4. The MCW(PA)3h carbon adsorbent demonstrated to be sufficiently selective to CO_2 for making it a good candidate for biogas purification. Moreover, the experimental adsorption equilibrium data were successfully correlated using the APT in the form of a characteristic curve. The existence of little scatter in the characteristic curve data demonstrates that the isotherms of CO_2 and CH_4 were successfully correlated as a single temperature independent curve. This corroborates the applicability of the APT to the carbon under study. The regressed value of W_s is in good agreement with the total pore volume determined from the N_2 adsorption at 77 K. In the range of the partial pressures typical for biogas upgrading units, MCW(PA)3h showed higher CO_2 uptakes than the ones reported for coal-

based commercial ACs and similar uptakes to the ones reported for the bio-based ACs. Finally, the axial dispersed plug-flow and LDF approximation for lumped solid-diffusion mass transfer model used for the prediction of the dynamic behaviour of the adsorbate-adsorbent system, provided a good agreement with the laboratory experiments, demonstrating its applicability to the system. All these results give the basis for future design and modelling works of a PSA cycle based on the use of MCW derived renewable adsorbents;

- **Task 6:** referring to the biorefinery concept proposed in Figure 1.1 and on the laboratorial results obtained during Tasks 2, 3 and 4, an environmental LCA of a case study biorefinery was developed. The case study analysed was based on the hypothesis of implementing, at an existing Portuguese AD plant currently processing 40000 t/y OFMSW in the Lisbon area, (i) an AcoD using MCW as co-substrate; (ii) an H_2S removal unit from biogas stream based on the use of MCW(PA)3h as adsorbent, and (iii) a biogas upgrading unit to produce bio-CH_4 based on PSA technology. The study aimed to assess the environmental benefits generated from different uses of biogas with the purpose of comparing the bioCH_4 production to the direct cogeneration of electricity and heat, on the base of a real case scenario of an AD Portuguese plant. Among the three biogas production configurations considered (hOFMSW, OFMSW+Pre3 and hOFMSW+ MCW), the results obtained demonstrated that the AcoD of hOFMSW+ untreated MCW was the most environmentally favorable option, providing the lowest impacts in almost all the categories studied. The increase of biogas and methane yields occurred during AcoD of hOFMSW+ untreated MCW was able to compensate the added environmental impacts caused by the collection, grinding and transport of the MCW co-substrate. AcoD of OFMSW+Pre3 can be considered the less environmentally sustainable configuration among the tested ones, mainly due to the impacts associated with the production of the catalyst used for the pre-treatment of MCW. This suggests that the pre-treatment of MCW prior to AcoD favoured the biogas quality and the AcoD process stability but caused higher environmental impacts than the configuration based on the use of non-pre-treated MCW. Thus, the AcoD configuration that produced the biogas stream characterized by the highest HHV is not the most sustainable for the environment. This is an important conclusion that highlights that the use of a LCA methodological tool allowed to quantitatively analyse the life cycle of biogas, within the

context of the environmental impact providing a useful support for strategic future investment decisions. Regarding the MCW(PA)3h activated carbons, produced with the intent of substituting the commercial AC for the removal of H_2S from biogas stream, they demonstrated to be more sustainable than the CAC commercial sample, tested under real conditions and without the addition of oxygen or water vapour. The reason lays in the higher adsorption capacity provided by MCW(PA)3h than by CAC, and thus, in the lower amount of ACs required to remove the same amount of H_2S present in the biogas stream. Furthermore, the upgrading of the biogas obtained with AcoD of hOFMSW+MCW to bioCH_4 provided higher environmental loads than the classic cogeneration configuration. This is mainly due to the contribution of the increased fossil fuels production and of the AC and PSA unit's construction. This means that the avoided impacts related to the bioCH_4 production are not always able to overcome the direct and indirect environmental impacts produced by the upgrading process. This indicates that the impacts generated are, in most of the cases, higher than the benefits gained due to the avoided production of natural gas. Finally, the sensitivity analysis showed that the "upgrading to bio-CH_4, Optimization 2" configuration, in which the effects of the fossil-NG substitution by bioCH_4 were cumulated to those provided by an optimized AC adsorption capacity, is dramatically more sustainable than the "upgrading to bioCH_4" scenario and provided lower environmental impacts in OF(hh), OF(te), WC(te), WC(ae) and WC(hh) categories than direct electric energy and heat production.

7.2 Future Challenges

The idea of developing a biorefinery concept for bioCH_4 production from AcoD of MCW and OFMSW at an existing AD plant, currently processing standalone OFMSW, offers numerous hints for future research.

Some suggestions are as follows:

1. Assays of long term AcoD using OFMSW and not-pre-treated MCW as co-substrate, in order to finely tune the AcoD operational parameters, are proposed with the aim of maximizing the CH_4 production and increase the process stability. Different OLR and HRT, as well as MCW concentrations in the OFMSW, might be tested. The use of a pilot scale/demonstrating

scale AcoD unit located at the AD industrial unit might be extremely beneficial;

2. H_2S removal assays applying optimized conditions of water and/or oxygen are proposed, in order to maximize the H_2S removal capacity of the produced ACs and to reduce the amount of ACs required for biogas pre-conditioning;
3. Fixed bed experiments in presence of CO_2 concentrated mixture are required to obtain all the missing parameters useful for process energy balance assessment, PSA cycle modelling and validation;
4. Techno-Economic assessment of the proposed biorefinery, taking into consideration the energy local tariffs scenario and the existing infrastructures are suggested;
5. Updated environmental and economic LCA, including the new results obtained in the above points 1, 2, 3 and 4 are suggested.

A

Thermogravimetric Analysis

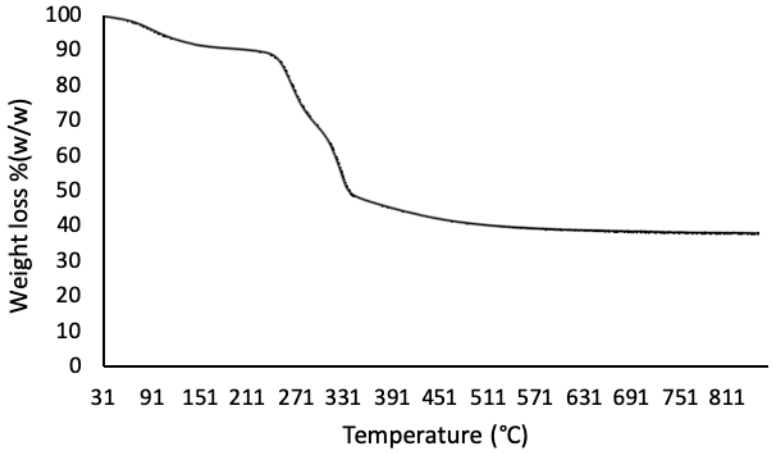

Figure A 1: TGA analysis of MCW

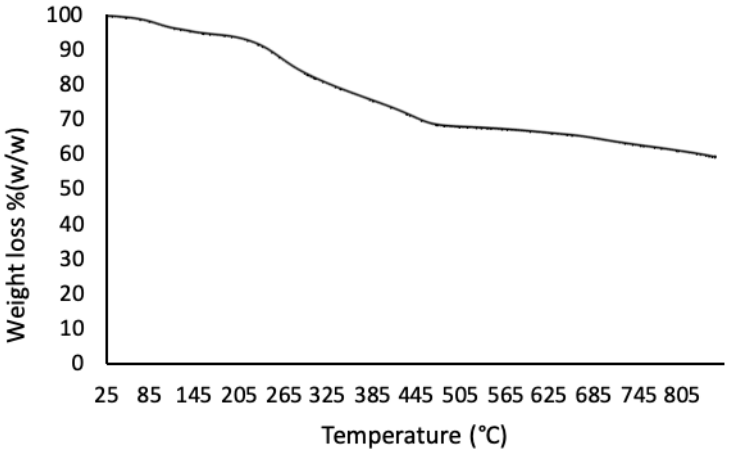

Figure A 2: TGA analysis of dried LD

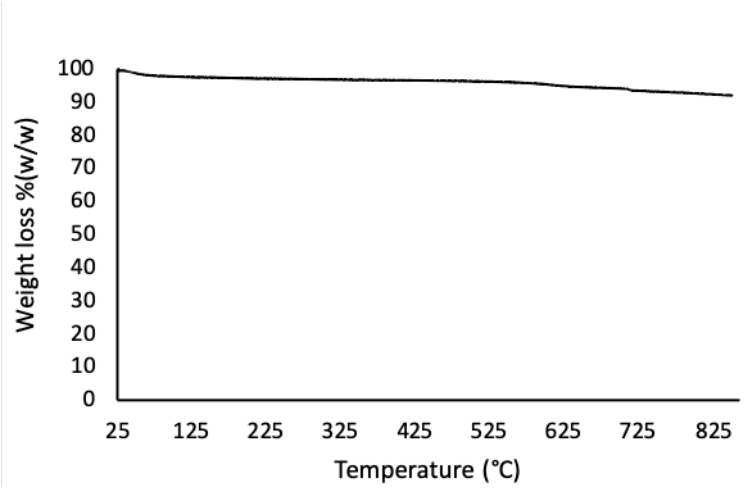

Figure A 3: TGA analysis of CAC

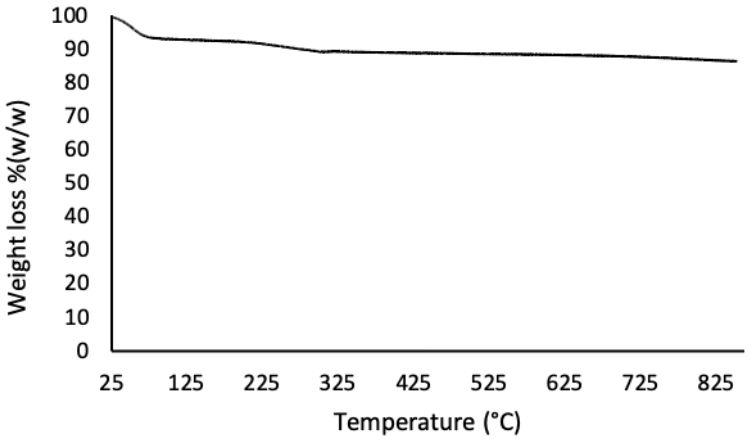

Figure A 4: TGA analysis of MCW(PA)2h

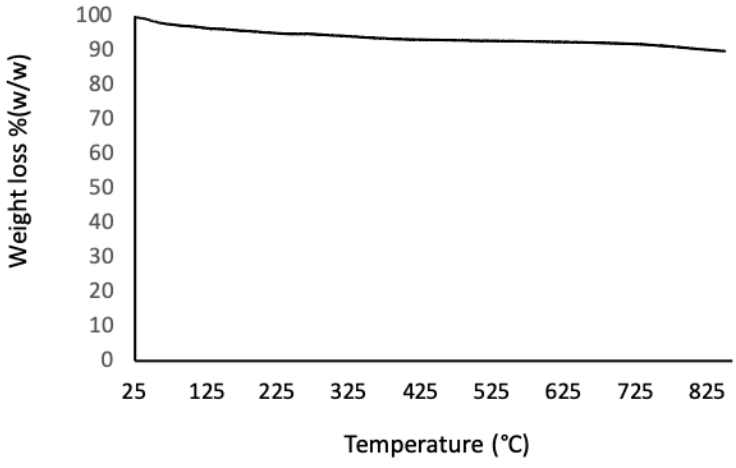

Figure A 5: TGA analysis of MCW(PA)3h

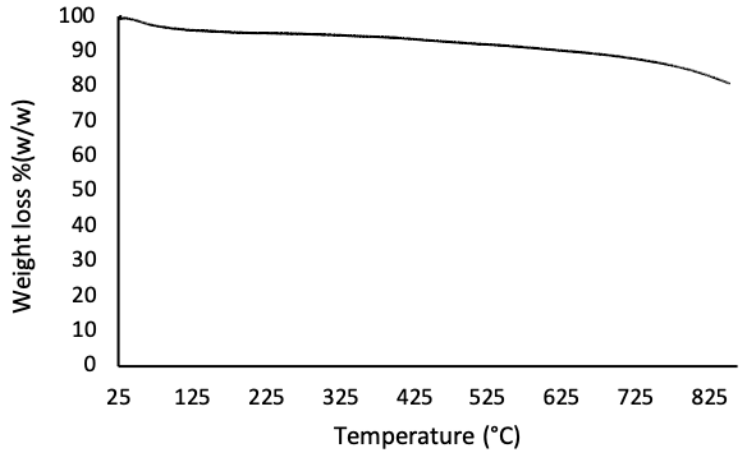

Figure A 6: TGA analysis of MCW(LD)

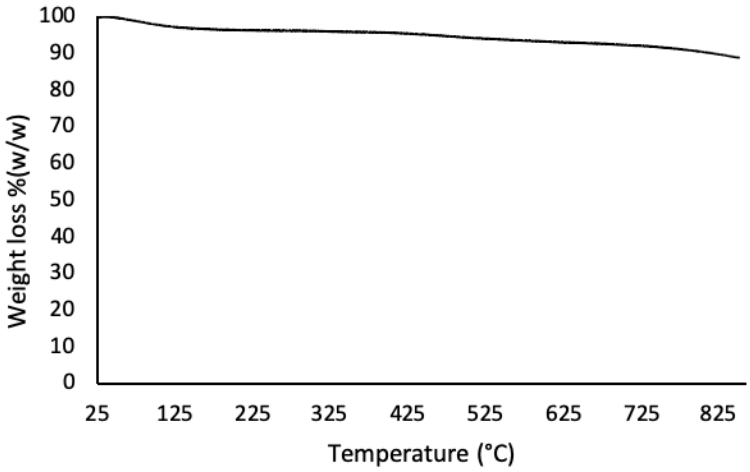

Figure A 7: TGA analysis of CAR-MCW(LD)

B

XRPD Analysis

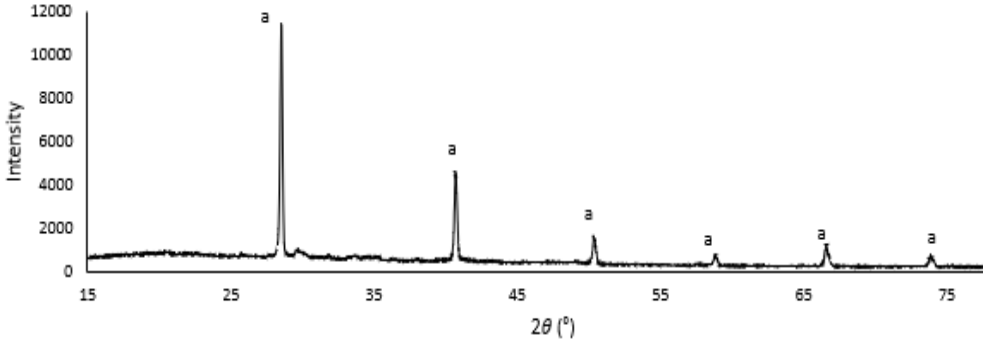

Figure B 1: XRPD pattern of dried LD. (a: sylvite, KCl).

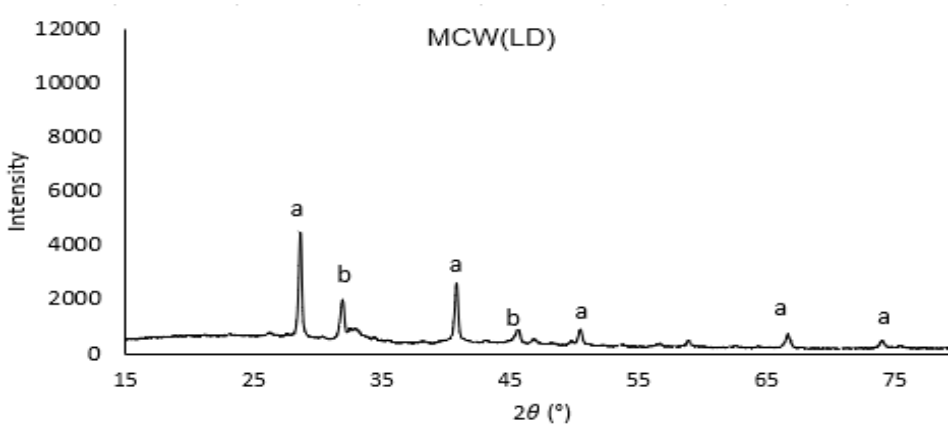

Figure B 2: XRPD pattern of MCW(LD) (a: sylvite, KCl; b: halite, NaCl)

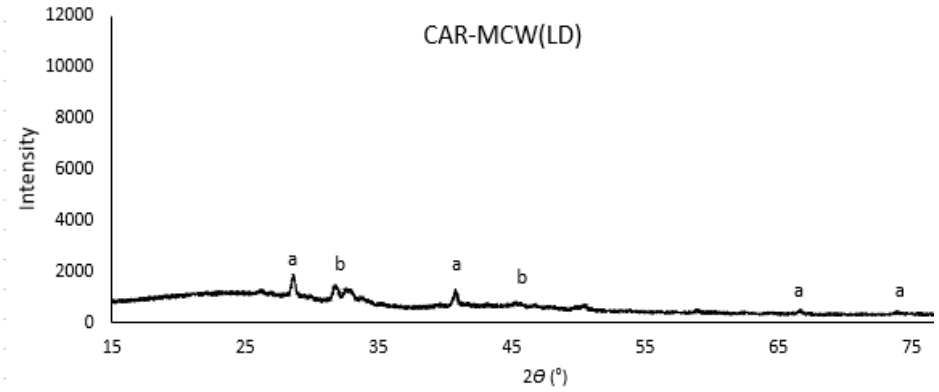

Figure B 3: CAR-MCW(LD) (a: sylvite, KCl; b: halite, NaCl).

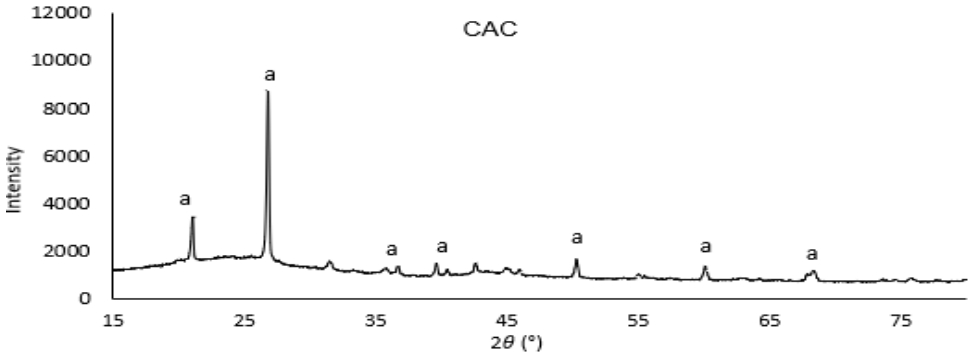

Figure B 4: XRPD pattern of CAC (a – Quartz, SiO2).

C

Adsorption-desorption isotherms N_2, 77 K

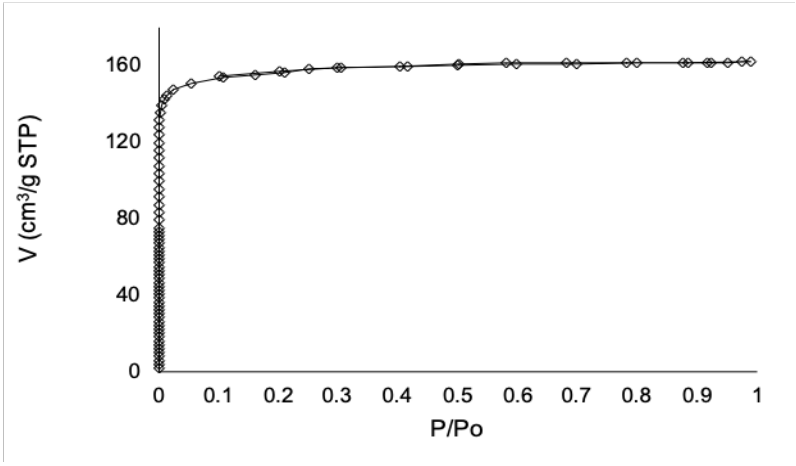

Figure C 1: N_2 adsorption-desorption isotherms of MCW(PA)2h.

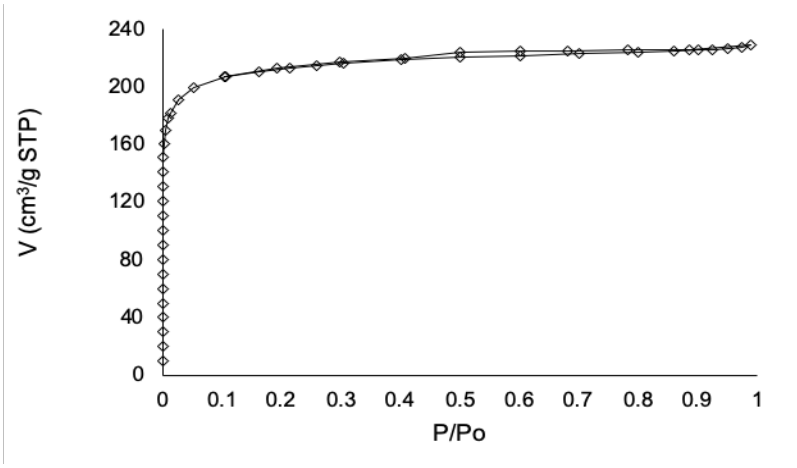

Figure C 2: N_2 adsorption-desorption isotherms of MCW(PA)3h.

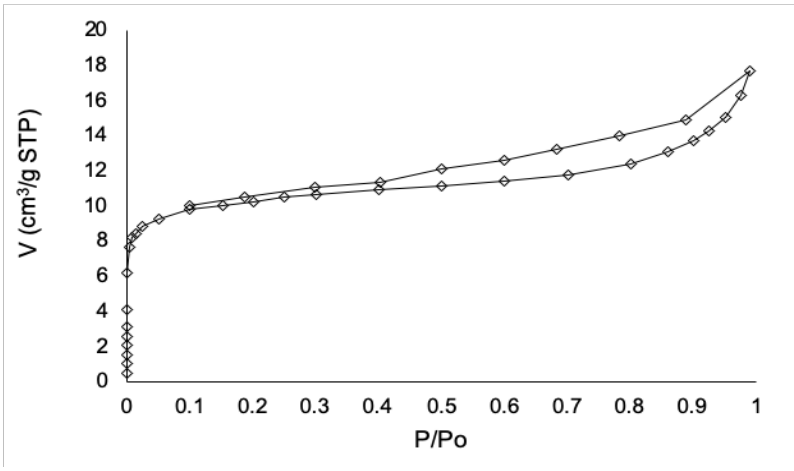

Figure C 3: N_2 adsorption-desorption isotherms of MCW(LD).

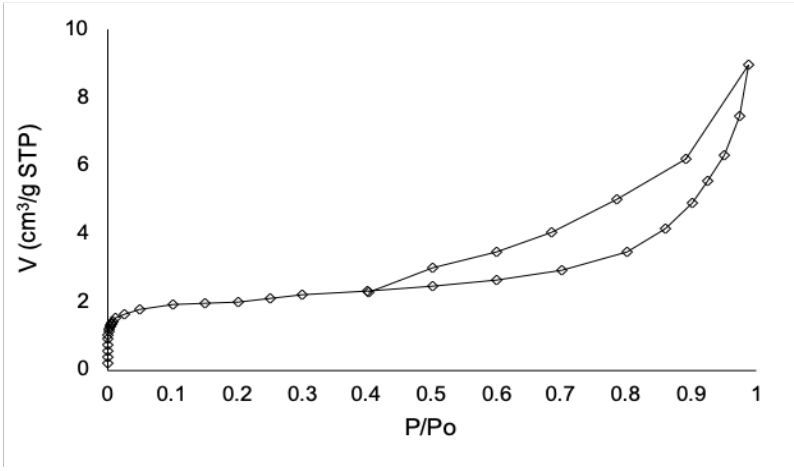

Figure C 4: N_2 adsorption-desorption isotherms of CAR-MCW(LD).

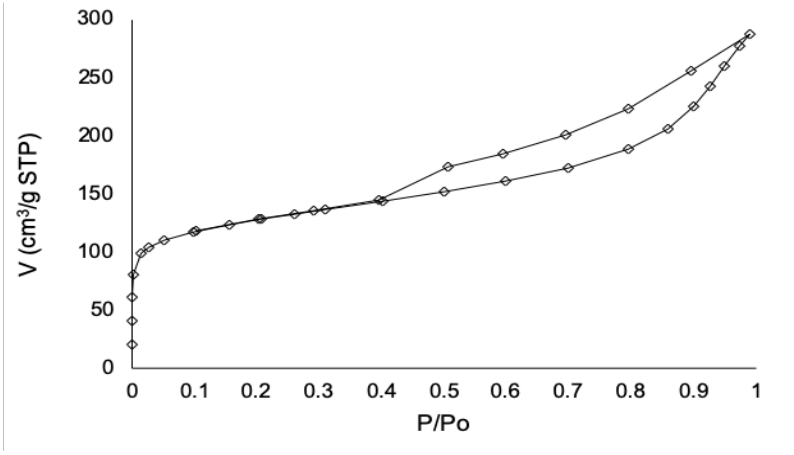

Figure C 5: N_2 adsorption-desorption isotherms of CAC.

D

Methodology for AC density and porosity assessment

Bulk Density (ρ_b)

The bulk density, ρ_b (g/cm^3) is the weight of clean material per unit bulk volume as packed in a column.

Carbon Matrix Density(ρ_s)

The carbon matrix density, ρ_s (g/cm^3) was measured through helium adsorption isotherm analysis with an adsorption/desorption equilibrium run in a Magnetic Suspension Balance (ISOSORP 2000 from Rubotherm (GmbH)) whose scheme and operating principles are reported elsewhere (Esteves, 2005)

The equilibrium measurements were performed at 333.15 K. Helium acts as an inert and does not adsorb into the carbon. Hence, the plot of gas density versus sample weight gives the carbon density. Table D 1 presents the experimental data results

Table D 1: Experimental data obtained from helium adsorption equilibrium measurements (333.15 K).

He density kg/m^3	Mass g
0.0000	6.3970
0.0731	6.5396
0.2074	6.53956
0.6756	6.5391
1.3526	6.5385
2.1824	6.5378
2.8786	6.5371
4.2901	6.5358
1.7516	6.5382
0.3147	6.5397
0.0500	6.5399
0.0000	6.5397

Table D 2:MCW(PA)3h density result assessed experimentally through helium adsorption equilibrium data (R2= 0.9998).

Parameter	Unit	Value
Mass	g	0.2111
Volume	cm^3	0.1194
ρ_b	g/cm^3	1.7685

The carbon weight M and the volume V average values, through which the carbon density ρ_s is calculated, are given in Table D 2. M of the AC and V of the AC are obtained from the intercept and slope of the fitting, respectively, after subtracting weight and volume of the calibrated measuring system.

Dry Particle Density (ρ_p)

The Dry Particle Density, ρ_p is determinated through the Mercury Porosimetry performed through intrusion/extrusion method giving the value of 0.4 g/cm³.

Void Fraction of Packing (ε_b)

The dry particle density, ρ_p, is related to the (external) void fraction of packing ε_b, by Eq. D1:

$$\rho_p = \frac{\rho_b}{(1 - \varepsilon_b)} \qquad (Eq.D1)$$

Intraparticle Porosity (ε_p)

For a given density of the carbon matrix, ρ_s, the internal or intraparticle porosity, ε_p is defined as Eq. D2

$$\varepsilon_p = \rho_p \left(\frac{1}{\rho_p} - \frac{1}{\rho_s}\right) \qquad (Eq.D2)$$

Total Voidage (ε)

The Total Voidage, ε, in a packed bed (outside and inside the particles is given by Eq. D3.

$$\varepsilon = \varepsilon_b + \left(1 - \frac{\varepsilon_b}{\varepsilon_p}\right) \qquad (Eq.D3)$$

References

Abatzoglou, N., Boivin, S., 2009. A review of biogas purification processes. Biofuels, Bioprod. Biorefining 3, 42–71. https://doi.org/10.1002/bbb.117

Achinas, S., Achinas, V., Euverink, G.J.W., 2017. A Technological Overview of Biogas Production from Biowaste. Engineering 3, 299–307. https://doi.org/10.1016/J.ENG.2017.03.002

Adib, F., Bagreev, A., Bandosz, T.J., 2000a. Analysis of the relationship between H2S removal capacity and surface properties of unimpregnated activated carbons. Environ. Sci. Technol. 34, 686–692. https://doi.org/10.1021/es990341g

Adib, F., Bagreev, A., Bandosz, T.J., 2000b. Adsorption/oxidation of hydrogen sulfide on nitrogen-containing activated carbons. Langmuir 16, 1980–1986. https://doi.org/10.1021/la990926o

Adib, F., Bagreev, A., Bandosz, T.J., 1999a. Effect of pH and surface chemistry on the mechanism of H2S removal by activated carbons. J. Colloid Interface Sci. 216, 360–369. https://doi.org/10.1006/jcis.1999.6335

Adib, F., Bagreev, A., Bandosz, T.J., 1999b. Effect of Surface Characteristics of Wood-Based Activated Carbons on Adsorption of Hydrogen Sulfide. J. Colloid Interface Sci. 214, 407–415. https://doi.org/10.1006/jcis.1999.6200

Agarwal, R.K., Schwarz, J.A., 1988. Analysis of high-pressure adsorption of gases on activated carbon by potential theory. Carbon N. Y. 26, 873.

Aguilar-Reynosa, A., Romaní-, A., Rodrí-guez-Jasso, R.M., Aguilar, C.N., Garrote, G., Ruiz, H.A., 2017. Comparison of microwave and conduction-convection heating autohydrolysis pretreatment for bioethanol production. Bioresour. Technol. 243,

273–283. https://doi.org/10.1016/j.biortech.2017.06.096

Akassou, M., Kaanane, A., Crolla, A., Kinsley, C., 2010. Statistical modelling of the impact of some polyphenols on the efficiency of anaerobic digestion and the co-digestion of the wine distillery wastewater with dairy cattle manure and cheese whey. Water Sci Technol. 62, 475–83.

Allman, M., Lawrence, D.F., 1972. Geological Laboratory Techniques. ARC0 Publishing Co., Inc., New York.

Almeida, J., Modig, T., Petersson, A., Hahn-Hagerdal, B., Lidén, G., Gorwa-Grauslund, M., 2007. Increased tolerance and conversion of inhibitors in lignocellulosic hydrolysates by Saccharomyces cerevisiae. J. Chem. Technol. Biotechnol. 82, 340–349. https://doi.org/10.1002/jctb.1676

Alqaralleh, R.M., 2012. Effect of Alkaline pretreatment on anaerobic digestion of organic fraction of municipal solid waste . Master thesis of Applied Sciences in Environmental Engineering. Ottawa-Carleton Institute for Environmental Engineering.

Altintig, E., Arabaci, G., Altundag, H., 2016. Preparation and characterization of the antibacterial effi ciency of silver loaded activated carbon from corncobs. Surf. Coat. Technol. 304, 63–67. https://doi.org/10.1016/j.surfcoat.2016.06.077

Álvarez-Gutiérrez, N., García, S., Gil, M. V., Rubiera, F., Pevida, C., 2014. Towards bio-upgrading of biogas: Biomass waste-based adsorbents. Energy Procedia 63, 6527–6533. https://doi.org/10.1016/j.egypro.2014.11.688

Álvarez-Gutiérrez, N., Gil, M. V, Rubiera, F., Pevida, C., 2017. Kinetics of CO2 adsorption on cherry stone-based carbons in CO2/CH4 separations. Chem. Eng. J. 307, 249–257. https://doi.org/10.1016/j.cej.2016.08.077

Álvarez-Gutiérrez, N., Gil, M. V, Rubiera, F., Pevida, C., 2016. Adsorption performance indicators for the CO 2 / CH 4 separation : Application to biomass-based activated carbons. Fuel Process. Technol. 142, 361–369. https://doi.org/10.1016/j.fuproc.2015.10.038

Alvira, P., Ballesteros, M., Negro, M.J., 2010. Pretreatment technologies for an efficient bioethanol production process based on enzymatic hydrolysis : A review. Bioresour. Technol. 101, 4851–4861. https://doi.org/10.1016/j.biortech.2009.11.093

Amon, T., Amon, B., Kryvoruchko, V., Bodiroza, V., Pötsch, E., Zollitsch, W., 2006. Optimising methane yield from anaerobic digestion of manure: Effects of dairy systems and of glycerine supplementation, in: International Congress Series. pp. 217–220. https://doi.org/10.1016/j.ics.2006.03.007

Angelidaki, I., Ellegaard, L., Ahring, B.K., 1993. A mathematical model for dynamic simulation of anaerobic digestion of complex substrates: Focusing on ammonia inhibition. Biotechnol Bioeng 42, 259–166. https://doi.org/10.1002/bit.26042020

Angelidaki, I., Treu, L., Tsapekos, P., Luo, G., Campanaro, S., Wenzel, H., Kougias, P.G., 2018. Biogas upgrading and utilization: Current status and perspectives. Biotechnol. Adv. 36, 452–466. https://doi.org/10.1016/j.biotechadv.2018.01.011

Anpromis, 2016. Production of corncob in Portugal in 2016. Personal Communication. Lisbon, PT.

Ansari, A., Bagreev, A., Bandosz, T.J., 2005. Effect of adsorbent composition on H2S removal on sewage sludge-based materials enriched with carbonaceous phase. Carbon N. Y. 43, 1039–1048. https://doi.org/10.1016/j.carbon.2004.11.042

Anukam, A.I., Boniswa, P.G., Omobola, O.O., Mamphweli, Sampson, N., 2017. Studies on Characterization of Corn Cob for Application in a Gasification Process for Energy Production. J. Chem. Volume 201. https://doi.org/doi.org/10.1155/2017/6478389

APHA, AWWA, WEF, 2005. Standard Methods for the examination of water and wastewater.

Ardolino, F., Parrillo, F., Arena, U., 2018. Biowaste-to-biomethane or biowaste-to-energy? An LCA study on anaerobic digestion of organic waste. J. Clean. Prod. 174, 462–476. https://doi.org/10.1016/j.jclepro.2017.10.320

Arefi Pour, a., Sharifnia, S., NeishaboriSalehi, R., Ghodrati, M., 2015. Performance evaluation of clinoptilolite and 13X zeolites in CO2 separation from CO2/CH4 mixture. J. Nat. Gas Sci. Eng. 26, 1246–1253. https://doi.org/10.1016/j.jngse.2015.08.033

Ask, M., Bettiga, M., Mapelli, V., Olsson, L., 2013. The influence of HMF and furfural on redox-balance and energy-state of xylose-utilizing Saccharomyces cerevisiae. Biotechnol Biofuels 6, 1–13.

Aslanzadeh, S., Berg, A., Taherzadeh, M.J., Sárvári Horváth, I., 2014. Biogas production from N-Methylmorpholine-N-oxide (NMMO) pretreated forest residues. Appl. Biochem. Biotechnol. 172, 2998–3008. https://doi.org/10.1007/s12010-014-0747-z

Augelletti, R., Conti, M., Annesini, M.C., 2017. Pressure swing adsorption for biogas upgrading . A new process configuration for the separation of biomethane and carbon dioxide. J. Clean. Prod. 140, 1390–1398. https://doi.org/10.1016/j.jclepro.2016.10.013

Awe, O.W., Zhao, Y., Nzihou, A., Minh, D.P., Lyczko, N., 2017. A Review of Biogas

Utilisation, Purification and Upgrading Technologies. Waste and Biomass Valorization 8, 267–283. https://doi.org/10.1007/s12649-016-9826-4

Ayeni, A.O., Daramola, M.O., 2017. Lignocellulosic biomass waste beneficiation: Evaluation of oxidative and non-oxidative pretreatment methodologies of South African corn cob. J. Environ. Chem. Eng. 5, 1771–1779. https://doi.org/https://doi.org/10.1016/j.jece.2017.03.019

Ayiania, M., Carbajal-Gamarra, F.M., Garcia-Perez, T., Frear, C., Suliman, W., Garcia-Perez, M., 2019. Production and characterization of H2S and PO43− carbonaceous adsorbents from anaerobic digested fibers. Biomass and Bioenergy 120, 339–349. https://doi.org/10.1016/j.biombioe.2018.11.028

Baccioli, A., Ferrari, L., Guiller, R., Yousfi, O., Vizza, F., Desideri, U., 2019. Feasibility Analysis of Bio-Methane Production in a Biogas Plant: A Case Study. Energies 12, 473. https://doi.org/10.3390/en12030473

Bagheri, N., Abedi, J., 2009. Preparation of high surface area activated carbon from corn by chemical activation using potassium hydroxide. Chem. Eng. Res. Des. 87, 1059–1064. https://doi.org/10.1016/j.cherd.2009.02.001

Bagreev, A., Adib, F., Bandosz, T.J., 1999. Initial heats of H2S adsorption on activated carbons: Effect of surface features. J. Colloid Interface Sci. 219, 327–332. https://doi.org/10.1006/jcis.1999.6485

Bagreev, A., Bandosz, T., 2002. A role of sodium hydroxide in the process of hydrogen sulfide adsorption/oxidation on caustic-impregnated activated carbons. Ind. Eng. Chem. Res. 41, 672–679. https://doi.org/10.1021/ie010599r

Bagreev, A., Bandosz, T.J., 2005. On the Mechanism of Hydrogen Sulfide Removal from Moist Air on Catalytic Carbonaceous Adsorbents. Ind. Eng. Chem. Res. 44, 530–538. https://doi.org/10.1021/ie049277o

Bagreev, A., Menendez, J.A., Dukhno, I., Tarasenko, Y., Bandosz, T.J., 2004. Bituminous coal-based activated carbons modified with nitrogen as adsorbents of hydrogen sulfide. Carbon N. Y. 42, 469–476. https://doi.org/10.1016/j.carbon.2003.10.042

Bailón Allegue, L., Hinge, J., 2014. Biogas upgrading Evaluation of methods for H2S removal, Danish Technological Institute.

Bailón Allegue, L., Hinge, J., 2012. Biogas and bio-syngas upgrading, Danish Technological Institute.

Bak, C., Lim, C.-J., Lee, J.-G., Kim, Y.-D., Kim, W.-S., 2019. Removal of sulfur compounds and siloxanes by physical and chemical sorption. Sep. Purif. Technol. 209, 542–549. https://doi.org/10.1016/j.seppur.2018.07.080

Bamdad, H., Hawboldt, K., MacQuarrie, S., 2018. A review on common adsorbents for acid gases removal: Focus on biochar. Renew. Sustain. Energy Rev. 81, 1705–1720. https://doi.org/10.1016/j.rser.2017.05.261

Bandosz, T.J., 2002. On the Adsorption/Oxidation of Hydrogen Sulfide on Activated Carbons at Ambient Temperatures. J. Colloid Interface Sci. 246, 1–20. https://doi.org/10.1006/jcis.2001.7952

Bandosz, T.J., 1999. Effect of pore structure and surface chemistry of virgin activated carbons on removal of hydrogen sulfide. Carbon N. Y. 37, 483–491. https://doi.org/10.1016/S0008-6223(98)00217-6

Banerjee, G., Car, S., Liu, T., Williams, D.L., Meza, S.L., Walton, J.D., Hodge, D.B., 2012. Scale-up and integration of alkaline hydrogen peroxide pretreatment, enzymatic hydrolysis, and ethanolic fermentation. Biotechnol. Bioeng. 109, 922–931. https://doi.org/10.1002/bit.24385

Banerjee, G., Car, S., Scott-craig, J.S., Hodge, D.B., Walton, J.D., 2011. Alkaline peroxide pretreatment of corn stover : effects of biomass , peroxide , and enzyme loading and composition on yields of glucose and xylose. Biotechnol Biofuels 4, 1–15.

Bashkova, S., Bagreev, A., Bandosz, T.J., 2002. Effect of surface characteristics on adsorption of methyl mercaptan on activated carbons. Ind. Eng. Chem. Res. 41, 4346–4352. https://doi.org/10.1021/ie020137t

Basu, S., Khan, A., Cano-Odena, A., Liu, C., Vankelecom, I., 2010. Membrane-based technologies for biogas separations. Chem. Soc. Rev. 39, 750–768. https://doi.org/10.1039/b817050a

Batstone, D.J., Keller, J., Angelidaki, I., Kalyuzhnyi, S. V., Pavlostathis, S.G., Rozzi, A., Sanders, W.T.M., Siegrist, H., Vavilin, V.A., 2002. The IWA Anaerobic Digestion Model No 1 (ADM1). Water Sci Technol. 45, 65–73. https://doi.org/http://dx.doi.org/10.1016/0043-1354(86)90189-2

Bauer, F., Hulteberg, C., Persson, T., Tamm, D., 2013. Biogas upgrading – Review of commercial technologies, SGC Rapport 2013:270.

Behera, S., Arora, R., Nandhagopal, N., Kumar, S., 2014. Importance of chemical pretreatment for bioconversion of lignocellulosic biomass. Renew. Sustain. Energy Rev. 36, 91–106. https://doi.org/10.1016/j.rser.2014.04.047

Belay, N., Voskuilen, G., 1997. Anaerobic Transformation of Furfural by Methanococcus deltae ⌬ LH. Appl. Environ. Microbiol. 63, 2092–2094.

Bernstad, A., Malmquist, L., Truedsson, C., Jansen, J.C., 2013. Need for improvements in physical pretreatment of source-separated household food waste. Waste Manag. 33,

746–754. https://doi.org/10.1016/j.wasman.2012.06.012

Beszédes, S., Kertész, S., László, Z., Szabó, G., Hodúr, C., 2009. Biogas production of ozone and/or microwave-pretreated canned maize production sludge. https://doi.org/10.1080/01919510902841218

Bhutto, A.W., Qureshi, K., Harijan, K., Abro, R., Abbas, T., Bazmi, A.A., Karim, S., Yu, G., 2017. Insight into progress in pre-treatment of lignocellulosic biomass. Energy 122, 724–745. https://doi.org/10.1016/J.ENERGY.2017.01.005

Biogas upgrading – Review of commercial technologies, n.d.

Biswas, R., Uellendahl, H., K.Ahring, B., 2015. Wet explosion: a universal and efficient pretreatment process for lignocellulosic biorefineries. Bioenergy Reseurce 8, 1101–1116. https://doi.org/I0.1007/s12155-015-9590-5

Bobcat-Dorsan, 2018. Bobcat S450 Skid-Steer Loader. Emission data [WWW Document]. Commer. Web site. URL http://www.bobcat.com/loaders/skid-steer-loaders/models/s450/features#lightbox-PerformanceEffectiveWeightBalance (accessed 11.5.18).

Bondesson, P., Galbe, M., Zacchi, G., 2013. Ethanol and biogas production after steam pretreatment of corn stover with or without the addition of sulphuric acid. Biotechnol. Biofuels 6, 11. https://doi.org/10.1186/1754-6834-6-11

Boonsombuti, A., Luengnaruemitchai, A., 2013. Enhancement of enzymatic hydrolysis of corncob by microwave-assisted alkali pretreatment and its effect in morphology. Cellulose 20, 1957–1966. https://doi.org/10.1007/s10570-013-9958-7

Bouzaza, A., Laplanche, A., Marsteau, S., 2004. Adsorption-oxidation of hydrogen sulfide on activated carbon fibers: effect of the composition and the relative humidity of the gas phase. Chemosphere 54, 481–488. https://doi.org/10.1016/j.chemosphere.2003.08.018

Budzianowski, W., Budzianowska, D., 2015. Economic analysis of biomethane and bioelectricity generation from biogas using different support schemes and plant configurations. Energy 88, 658–666. https://doi.org/10.1016/j.energy.2015.05.104

Builes, S., Sandler, S.I., Xiong, R., 2013. Isosteric Heats of Gas and Liquid Adsorption. Langmuir 29, 10416–10422. https://doi.org/10.1021/la401035p

Cabot, 2016. Darco ® Bg 1 Activated Carbon - a High Performance and Cost Effective Solution for H2S Removal [WWW Document]. Tech. Brocure. URL www.cabotcorp.com/~/.../infosheet-darco-bg-1-biogas-purification-united-states.pdf (accessed 6.24.19).

Calabrò, P., Greco, R., Evangelou, A., Komilis, D., 2015. Anaerobic digestion of tomato processing waste: Effect of alkaline pretreatment. J. Environ. Manage. 163, 49–52. https://doi.org/10.1016/j.jenvman.2015.07.061

Camacho, B.C.R., Ribeiro, R.P.P.L., Esteves, I.A.A.C., Mota, J.P.B., 2015. Adsorption equilibrium of carbon dioxide and nitrogen on the MIL-53(Al) metal organic framework. Sep. Purif. Technol. 141, 150–159. https://doi.org/10.1016/j.seppur.2014.11.040

Campos, F.M., Figueiredo, A.R., Hogg, T.A., Couto, J., 2009. Effect of phenolic acids on glucose and organic acid metabolism by lactic acid bacteria from wine. Food Microbiol. 26, 409–414. https://doi.org/10.1016/j.fm.2009.01.006

Campuzano, R., González-Martínez, S., 2016. Characteristics of the organic fraction of municipal solid waste and methane production: A review. Waste Manag. 54, 3–12. https://doi.org/10.1016/j.wasman.2016.05.016

Carrere, H., Antonopoulou, G., Affes, R., Passos, F., Battimelli, A., 2016. Review of feedstock pretreatment strategies for improved anaerobic digestion : from lab-scale research to full-scale application. Bioresour. Technol. 199, 386–397. https://doi.org/10.1016/j.biortech.2015.09.007

Casas, N., Schell, J., Blom, R., Mazzotti, M., 2013. MOF and UiO-67/MCM-41 adsorbents for pre-combustion CO2 capture by PSA: Breakthrough experiments and process design. Sep. Purif. Technol. 112, 34–48. https://doi.org/10.1016/j.seppur.2013.03.042

Castrillon, M.C., Moura, K.O., Alves, C.A., Bastos-Neto, M., Azevedo, D.C.S., Hofmann, J., Möllmer, J., Einicke, W.-D., Gläser, R., 2016. CO2 and H2S Removal from CH4-Rich Streams by Adsorption on Activated Carbons Modified with K2CO3, NaOH, or Fe2O3. Energy & Fuels 30, 9596–9604. https://doi.org/10.1021/acs.energyfuels.6b01667

Cesaro, A., Belgiorno, V., 2013. Sonolysis and ozonation as pretreatment for anaerobic digestion of solid organic waste. Ultrason. Sonochem. 20, 931–936. https://doi.org/10.1016/j.ultsonch.2012.10.017

Cesaro, A., Naddeo, V., Amodio, V., Belgiorno, V., 2012. Enhanced biogas production from anaerobic codigestion of solid waste by sonolysis. Ultrason. Sonochem. 19, 596–600. https://doi.org/10.1016/j.ultsonch.2011.09.002

Chandra, R., Takeuchi, H., Hasegawa, T., Kumar, R., 2012. Improving biodegradability and biogas production of wheat straw substrates using sodium hydroxide and hydrothermal pretreatments. Energy 43, 273–282. https://doi.org/10.1016/j.energy.2012.04.029

Chang, K.J., Talu, O., 1996. Behavior and performance of adsorptive natural gas storage cylinders during discharge. Appl. Therm. Eng. 16, 359–374. https://doi.org/https://doi.org/10.1016/1359-4311(95)00017-8

Chen, Q., Wang, Z., Long, D., Liu, X., Zhan, L., Liang, X., Qiao, W., Ling, L., 2010. Role of Pore Structure of Activated Carbon Fibers in the Catalytic Oxidation of H2S. Ind. Eng. Chem. Res. 49, 3152–3159. https://doi.org/10.1021/ie901223j

Chen, Y., Stevens, M.A., Zhu, Y., Holmes, J., Xu, H., 2013. Understanding of alkaline pretreatment parameters for corn stover enzymatic saccharification. Biotechnol. Biofuels 6, 2–11. https://doi.org/10.1186/1754-6834-6-8

Choi, D.-Y., Lee, J.-W., Jang, S.-C., Ahn, B.-S., Choi, D.-K., 2008. Adsorption dynamics of hydrogen sulfide in impregnated activated carbon bed. Adsorption 14, 533–538. https://doi.org/10.1007/s10450-008-9118-9

Chongkhong, S., Tongurai, C., 2014. Microwave-Assisted Organic Acid Hydrolysis of Corncob in Bioethanol Production. Adv. Mater. Res. 1033–1034. https://doi.org/10.4028/www.scientific.net/AMR.1033-1034.151

Choo, H.S., Lau, L.C., Mohamed, A.R., Lee, K.T., 2013. Hydrogen sulfide adsorption by alkaline impregnated coconut shell activated carbon. J. Eng. Sci. Technol. 8, 741–753.

Chornet, E., Overend, R., 1991. Phenomenological kinetics and reaction engineering aspects of steam/aqueous treatments. Amsterdam: Gordon and Breach Science Publishers; 1, in: Focher, B., Marzetti, A., Crescenzi, V. (Eds.), Steam Explosion Techniques—Fundamentals and Industrial Applications. Gordon and Breach Science Publishers, Amsterdam, pp. 21–58.

Chue, K.T., Kim, J.N., Yoo, J., Cho, S.H., Yang, T., 1995. Comparison of Activated Carbon and Zeolite 13X for CO_2 Recovery from Flue Gas by Pressure Swing Adsorption. Ind. Eng. Chem. Res. 34, 591–598. https://doi.org/10.1021/ie00041a020

Clift, R., Doig, A., Finnveden, G., 2000. The Application of Life Cycle Assessment to Integrated Solid Waste Management: Part 1—Methodology. Process Saf. Environ. Prot. 78, 279–287. https://doi.org/https://doi.org/10.1205/095758200530790

Cortez, D.V., Roberto, I.C., 2010. Individual and interaction effects of vanillin and syringaldehyde on the xylitol formation by Candida guilliermondii. Bioresour. Technol. 101, 1858–1865. https://doi.org/10.1016/j.biortech.2009.09.072

Costa, E., Calleja, G., Domingo, F., 1985. Adsorption of gaseous hydrocarbons on activated carbon: Characteristic kinetic curve. AIChE J. 31, 982.

CryoPur, 2017. Transforming Biogas into Bio-LNG and Liquid CO2, in: Biogas2020,

Skandinaviens Biogas Conference. Skive, 8-9 November, pp. 1–23.

da Costa Lopes, A.M., João, K.G., Rubik, D.F., Bogel-Łukasik, E., Duarte, L.C., Andreaus, J., Bogel-Łukasik, R., 2013. Pre-treatment of lignocellulosic biomass using ionic liquids: Wheat straw fractionation. Bioresour. Technol. 142, 198–208. https://doi.org/10.1016/J.BIORTECH.2013.05.032

Dalai, A.K., Cundall, M.T., De, M., 2008. Direct oxidation of hydrogen sulphide to sulphur using impregnated activated carbon catalysts. Can. J. Chem. Eng. 86, 768–777. https://doi.org/10.1002/cjce.20034

de Falco, G., Montagnaro, F., Balsamo, M., Erto, A., Alessandro Deorsola, F., Lisi, L., Cimino, S., 2017. Synergic effect of Zn and Cu oxides dispersed on activated carbon during reactive adsorption of H2S at room temperature. Microporous Mesoporous Mater. 257, 135–146. https://doi.org/10.1016/j.micromeso.2017.08.025

Demirer, G.N., Othma, M., 2008. Two-Phase Thermophilic Acidification and Mesophilic Methanogenesis Anaerobic Digestion of Waste-Activated Sludge. Environ. Eng. Sci. 25, 1291–1300. https://doi.org/10.1089/ees.2007.0242

Deublein, D., Steinhauser, A., 2010. Biogas from Waste and Renewable Resources: An Introduction, Second. ed. Wiley-VCVH, Federal Republic of Germany. https://doi.org/10.1002/9783527632794

Diaz, A.B., Moretti De Souza, M.M., Bezerra-bussoli, C., da Costa Carreira Nunes, C., da Silva, R., Blandino, A., Gomes, E., 2015. Evaluation of microwave-assisted pretreatment of lignocellulosic biomass immersed in alkaline glycerol for fermentable sugars production. Bioresour. Technol. 185, 316–323. https://doi.org/10.1016/j.biortech.2015.02.112

Do, D., 1998. Adsorption Analysis: Equilibria and Kinetics. Series in Chem. Eng.Vol 2: Imperial College Press.

Drosg, B., 2013. Process monitoring in biogas plants. IEA Bioenergy Technical Report.

Dubinin, M., 1975. Progress in Surface and Membrane Science, vol. 9. Academic Press, New York.

Dubinin, M.M., 1960. The potential theory of adsorption of gases and vapors for adsorbents with energetically nonuniform surfaces. Chem. Rev. 60.

Dubinin, M.M., Astakhov, V.A., 1970. Description of Adsorption Equilibria of Vapors on Zeolites over Wide Ranges of Temperature and Pressure. Adv. Chem. Ser.102, 69.

Dunne, J.A., Mariwala, R., Rao, M., Sircar, S., Gorte, R.J., Myers, A.L., 1996. Calorimetric heats of adsorption and adsorption isotherms. 1. O2,N2,Ar, CO2,CH4,C2H6,and

SF6 on silicalite. Langmuir 12, 5888–5895.

Durán, I., Álvarez-Gutiérrez, N., Rubiera, F., Pevida, C., 2018. Biogas purification by means of adsorption on pine sawdust-based activated carbon: Impact of water vapor. Chem. Eng. J. 353, 197–207. https://doi.org/10.1016/j.cej.2018.07.100

EBA, 2015. Biomethane & Biogas Report 2015, European Biogas Association.

Ecoinvent, 2018. Ecoinvent V.3.4 Database.

El-Hadj, T.B., Astals, S., Galí, A., Mace, S., Mata-Álvarez, J., 2009. Ammonia influence in anaerobic digestion of OFMSW. Water Sci Technol 59, 1153.

Esposito, G., Frunzo, L., Panico, A., Pirozzi, F., 2011. Modelling the effect of the OLR and OFMSW particle size on the performances of an anaerobic co-digestion reactor. Process Biochem. 46, 557–565. https://doi.org/10.1016/j.procbio.2010.10.010

Esteves, I., 2005. Gas Separation Processed by Integrated Adsorption And Permeation Technologies. PhD Thesis. Universidade Nova de Lisboa.

Esteves, I., M. R. P. L. Sousa, G., Silva, R., Ribeiro, R., F. J. Eusébio, M., P. B. Mota, J., 2016. A Sensitive Method Approach for Chromatographic Analysis of Gas Streams in Separation Processes Based on Columns Packed with an Adsorbent Material, Advances in Materials Science and Engineering. https://doi.org/10.1155/2016/3216267

Esteves, I., S.S. Lopes, M., M.C. Nunes, P., P.B. Mota, J., 2008. Adsorption of natural gas and biogas components on activated carbon, Separation and Purification Technology. https://doi.org/10.1016/j.seppur.2008.01.027

Esteves, I.A.A.C., Mota, J.P.B., 2007. Gas Separation by a Novel Hybrid Membrane/Pressure Swing Adsorption Process. Ind. Eng. Chem. Res. 46, 5723–5733. https://doi.org/10.1021/ie070139j

Esteves, I.A.A.C., Sousa, G.M.R.P.L., Silva, R.J.S., Ribeiro, R.P.P.L., Eusébio, M.F.J., Mota, J.P.B., 2016. A Sensitive Method Approach for Chromatographic Analysis of Gas Streams in Separation Processes Based on Columns Packed with an Adsorbent Material. Adv. Mater. Sci. Eng. Article ID, 9.

European Commission, 2019. EU Climate Action [WWW Document]. Policies, Inf. Serv. URL https://ec.europa.eu/clima/citizens/eu_en (accessed 7.16.19).

Eurostat, 2019. Municipal Solid Waste [WWW Document]. URL https://ec.europa.eu/eurostat/statistics-explained/index.php/Municipal_waste_statistics#Municipal_waste_generation (accessed 3.11.19).

Fałtynowicz, H., Kaczmarczyk, J., Kułazyński, M., 2015. Preparation and characterization of activated carbons from biomass material - Giant knotweed (Reynoutria sachalinensis). Open Chem. 13, 1150–1156. https://doi.org/10.1515/chem-2015-0128

Feng, W., Kwon, S., Borguet, E., Vidic, R., 2005. Adsorption of Hydrogen Sulfide onto Activated Carbon Fibers: Effect of Pore Structure and Surface Chemistry. Environ. Sci. Technol. 39, 9744–9749. https://doi.org/10.1021/es0507158

Férey, G., 2016. Yes, We Can! Eur. J. Inorg. Chem. 2016, 4275–4277. https://doi.org/10.1002/ejic.201600734

Flores, R.A.C., García, F.P., Sánchez, E.M.O., Miró, A.M.B., Sandoval, O.A.A., 2017. Physico-Chemical Characterization of Agricultural Residues as Precursors for Activated Carbon Preparation. https://doi.org/10.20944/preprints201712.0086.v1

Florio, C., Fiorentino, G., Corcelli, F., Ulgiati, S., Dumontet, S., Güsewell, J., Eltrop, L., 2019. A life cycle assessment of biomethane production from waste feedstock through different upgrading technologies. Energies 12, 1–12. https://doi.org/10.3390/en12040718

Forero, G.L.A., Velásquez, J.J.A., 2011. Wagner liquid – vapour pressure equation constants from a simple methodology. J. Chem. Thermodyn. 43, 1235–1251. https://doi.org/10.1016/j.jct.2011.03.011

Franchetti, M., 2013. Economic and environmental analysis of four different con fi gurations of anaerobic digestion for food waste to energy conversion using LCA for : A food service provider case study. J. Environ. Manage. 123, 42–48. https://doi.org/10.1016/j.jenvman.2013.03.003

Franke-Whittle, I.H., Walter, A., Ebner, C., Insam, H., 2014. Investigation into the effect of high concentrations of volatile fatty acids in anaerobic digestion on methanogenic communities. Waste Manag. 34, 2080–2089. https://doi.org/10.1016/j.wasman.2014.07.020

Frischknecht, R., 1998. Life cycle inventory analysis for decision-making: Scope-dependent inventory system models and context-specific joint product allocation, International Journal of Life Cycle Assessment. https://doi.org/10.1007/BF02978487

Fu, S.-F., Wang, F., Shi, X.-S., Guo, R.-B., 2016. Impacts of microaeration on the anaerobic digestion of corn straw and the microbial community structure. Chem. Eng. J. 287, 523–528. https://doi.org/10.1016/J.CEJ.2015.11.070

Fu, S, He, S., Shi, X., Katukuri, N., Dai, M., Guo, R., 2015. The chemical properties and microbial community characterization of the thermophilic microaerobic

pretreatment process. Bioresour. Technol. 198, 497–502. https://doi.org/10.1016/J.BIORTECH.2015.09.029

Fu, Shan-fei, Wang, F.F., Yuan, X., Yang, Z., Luo, S.-J., Wang, C.-S., Guo, R.-B., 2015. The thermophilic (55 ° C) microaerobic pretreatment of corn straw for anaerobic digestion. Bioresour. Technol. 175, 203–208. https://doi.org/10.1016/j.biortech.2014.10.072

Gao, J., Chen, L., Yan, Z., Wang, L., 2013. Effect of ionic liquid pretreatment on the composition, structure and biogas production of water hyacinth (Eichhornia crassipes). Bioresour. Technol. 132, 361–364. https://doi.org/10.1016/j.biortech.2012.10.136

Gil, M.V., Martínez, M., García, S., Rubiera, F., Pis, J.J., Pevida, C., 2013. Response surface methodology as an efficient tool for optimizing carbon adsorbents for CO2 capture. Fuel Process. Technol. 106, 55–61. https://doi.org/10.1016/J.FUPROC.2012.06.018

Goedkoop, M., Huijbregts, M., 2013. ReCiPe 2008 Characterisation 4–20.

Goering, H., Van Soest, P., 1970. Forage fiber analyses (aparatus, reagent procedures and some applications). Handbook n. 379. Washington, D.C.

Gonçalves, D. V, Paiva, M.A.G., Oliveira, J.C.A., Bastos-Neto, M., Lucena, S.M.P., 2018. Prediction of the monocomponent adsorption of H2S and mixtures with CO2 and CH4 on activated carbons. Colloids Surfaces A Physicochem. Eng. Asp. 559, 342–350. https://doi.org/10.1016/j.colsurfa.2018.09.082

González, A.S., Plaza, M.G., Rubiera, F., Pevida, C., 2013. Sustainable biomass-based carbon adsorbents for post-combustion CO2 capture. Chem. Eng. J. 230, 456–465. https://doi.org/10.1016/j.cej.2013.06.118

Gould, J., 1984. Alkaline peroxide delignification of agricultural residues to enhance enzymatic saccharification. Biotechnol Bioeng 26, 46–52.

Gould, J.M., 1985. Studies on the mechanism of alkaline peroxide delignification of agricultural residues. Biotechnol. Bioeng. 27, 225–231.

Grande, C., 2011. Biogas Upgrading by Pressure Swing Adsorption, in: Bernardes, D.M.A.S. (Ed.), Biofuel's Engineering Process Technology. pp. 65–84. https://doi.org/10.5772/18428

Gu, H., Bergman, R., 2016. Life-cycle Assessment of a Distributed-scale Thermochemical Bioenergy Conversion System. Wood Fiber Sci. 48, 129–141.

Gu, H., Bergman, R., Anderson, N., Alanya-Rosenbaum, S., 2019. Life-Cycle Assessment of Activated Carbon From Woody Biomass. Wood Fiber Sci. 50, 229–243.

https://doi.org/10.22382/wfs-2018-024

Gu, H., Zhang, J., Bao, J., 2014. Inhibitor analysis and adaptive evolution of Saccharomyces cerevisiae for simultaneous saccharification and ethanol fermentation from industrial waste corncob residues. Bioresour. Technol. 157, 6–13. https://doi.org/10.1016/j.biortech.2014.01.060

Guiochon, G., Felinger, A., Katti, A.M., Shirazi, D.G., 2006. Fundamentals of preparative and nonlinear chromatography., 2nd ed. Elsevier, Amsterdam.

Guo, J., Luo, Y., Lua, A.C., Chi, R., Chen, Y., Bao, X., Xiang, S., 2007. Adsorption of hydrogen sulphide (H2S) by activated carbons derived from oil-palm shell. Carbon N. Y. 45, 330–336. https://doi.org/https://doi.org/10.1016/j.carbon.2006.09.016

Guo, Q., Majeed, S., Xu, R., Zhang, K., Kakade, A., Khan, A., Hafeez, F.Y., Mao, C., Liu, P., Li, X., 2019. Heavy metals interact with the microbial community and affect biogas production in anaerobic digestion: A review. J. Environ. Manage. 240, 266–272. https://doi.org/10.1016/j.jenvman.2019.03.104

Guo, X., Zhang, L., Shu, S., Hao, J., 2014. Effects of hydrothermal pretreatment on the content and structure of lignin extracted from corncob. Appl. Mech. Mater. 154–158.

Gutiérrez Ortiz, F.J., Aguilera, P.G., Ollero, P., 2014. Biogas desulfurization by adsorption on thermally treated sewage-sludge. Sep. Purif. Technol. 123, 200–213. https://doi.org/10.1016/j.seppur.2013.12.025

Han, S.H., An, J.Y., Hwang, J., Kim, S. Bin, Park, B.B., 2016. The effects of organic manure and chemical fertilizer on the growth and nutrient concentrations of yellow poplar (Liriodendron tulipifera Lin.) in a nursery system. Forest Sci. Technol. 12, 137–143. https://doi.org/10.1080/21580103.2015.1135827

Hanaki, K., Hirunmasuwan, S., Matsuo, T., 1994. Protection of methanogenic bacteria from low pH and toxic materials by immobilization using polyvinyl alcohol. Water Res. 28, 877–885. https://doi.org/10.1016/0043-1354(94)90094-9

Heinze, T., Schwikal, K., Barthel, S., 2005. Ionic Liquids as Reaction Medium In Cellulose Functionalization. Macromol. Biosci. 5, 520–525. https://doi.org/10.1002/mabi.200500039

Hendriks, A., Zeeman, G., 2009. Pretreatments to enhance the digestibility of lignocellulosic biomass. Bioresour. Technol. 100, 10–18. https://doi.org/10.1016/j.biortech.2008.05.027

Hernandez, J.E., Edyvean, R.G.J., 2008. Inhibition of biogas production and biodegradability by substituted phenolic compounds in anaerobic sludge. J.

Hazard. Mater. 160, 20–28.

Hernández, T., Chocano, C., Moreno, J.L., Garcia, C., 2016. Use of compost as an alternative to conventional inorganic fertilizers in intensive lettuce (Lactuca sativa L.) crops—Effects on soil and plant. Soil Tillage Res. 160, 14–22. https://doi.org/10.1016/j.still.2016.02.005

Herrmann, C., Idler, C., Heiermann, M., 2015. Improving aerobic stability and biogas production of maize silage using silage additives. Bioresour. Technol. 197, 393–403. https://doi.org/10.1016/j.biortech.2015.08.114

Herrmann, C., Prochnow, A., Heiermann, M., Idler, C., 2012. Particle size reduction during harvesting of crop feedstock for biogas production II: effects on energy balance, greenhouse gas emissions and profitability. BioEnergy Res. 5, 937–948. https://doi.org/10.1007/s12155-012-9207-1

Hervy, M., Minh, D.P., Gerente, C., Weiss-Hortala, E., Nzihou, A., Villot, A., Le Coq, L., 2018. H2S removal from syngas using wastes pyrolysis chars. Chem. Eng. J. 334, 2179–2189. https://doi.org/10.1016/j.cej.2017.11.162

Hobson, P.N., Shaw, B.G., 1976. Inhibition of methane production by Methanobacterium formicicum. Water Res. 10, 849–852. https://doi.org/10.1016/0043-1354(76)90018-X

Holland, C.E., Al-Muhtaseb, S.A., Ritter, J.A., 2001a. Adsorption of C1−C7 Normal Alkanes on BAX Activated Carbon. Ind.Eng.Chem.Res. 40, 338.

Holland, C.E., Al-Muhtaseb, S.A., Ritter, J.A., 2001b. Adsorption of C1−C7 Normal Alkanes on BAX Activated Carbon. 1. Potential Theory Correlation and Adsorbent Characterization. Ind. Eng. Chem. Res. 40, 338–346. https://doi.org/10.1021/ie0004794

Hou, X.X., Deng, Q.F., Ren, T.Z., Yuan, Z.Y., 2013. Adsorption of Cu(2+) and methyl orange from aqueous solutions by activated carbons of corncob-derived char wastes. Environ. Sci. Pollut. Res. Int. 20, 8521–8534.

Hoyer, K., Hulteberg, C., Svensson, M., Jenberg, J., NØrregÅrd, Ø., 2016. Biogas upgrading: a technical review. Report 2016:275 . Energiforsk.

Huijbregts, M.A.J., Steinmann, Z.J.N., Elshout, P.M.F., Stam, G., Verones, F., Vieira, M., Zijp, M., Hollander, A., van Zelm, R., 2017. ReCiPe2016: a harmonised life cycle impact assessment method at midpoint and endpoint level. Int. J. Life Cycle Assess. 22.

Hutňan, M., 2016. Maize silage as substrate for biogas production, in: da Silva, T., Santos, E.M. (Eds.), Advances in Silage Production and Utilization. InTech, pp. 65–84.

Idrees, M., Adnan, A., Qureshi, F.A., 2014. Comparison of Acid and Alkali Catalytic Efficiency During Enzymatic Saccharification of Corncob and Lactic Acid Production. Pakistan J. Agric. Sci. 51, 1049–1058.

IGC (International Grain Council), 2018. Grain Market Report - September 2018 [WWW Document]. Grain Mark. Rep.

Inoue, A., Matsumoto, A., 2017. Rapid adsorption removal of hydrogen sulfide by surface-modified activated carbon, in: AIP Conference Proceedings. pp. 020003-1-020003–6. https://doi.org/10.1063/1.4993322

IPCC, 2006. Guidelines for National Greenhouse Gas Inventories [WWW Document]. URL IGES, Japan. %3Cipcc- nggip.iges.or.jp%3E (accessed 12.11.17).

Izumi, K., Okishio, Y., Nagao, N., Niwa, C., Yamamoto, S., Toda, T., 2010. Effects of particle size on anaerobic digestion of food waste. Int. Biodeterior. Biodegradation 64, 601–608. https://doi.org/https://doi.org/10.1016/j.ibiod.2010.06.013

Jain, S.S., Jain, S.S., Wolf, I.T., Lee, J., Tong, Y.W., 2015. A comprehensive review on operating parameters and different pretreatment methodologies for anaerobic digestion of municipal solid waste. Renew. Sustain. Energy Rev. 52, 142–154. https://doi.org/10.1016/j.rser.2015.07.091

Jeschke, M.R., Heggenstaller, A., 2012. Sustainable corn stover harvest for biofuel production. Crop Insights by Pioneer Agron. Sci. 22, 1–6.

Kabir, M.M., Forgács, G., Sárvári- Horváth, I., 2015. Biogas from lignocellulosic materials, in: Karimi, K. (Ed.), Lignocellulose Based Bio-Products. Springler International Pubblisher, Switzerland, pp. 207–251.

Kacem, M., Pellerano, M., Delebarre, A., 2015. Pressure swing adsorption for CO2/N2 and CO2/CH4 separation: Comparison between activated carbons and zeolites performances. Fuel Process. Technol. 138, 271–283. https://doi.org/10.1016/j.fuproc.2015.04.032

Kante, K., Nieto-Delgado, C., Rangel-Mendez, J.R., Bandosz, T.J., 2012. Spent coffee-based activated carbon: Specific surface features and their importance for H2S separation process. J. Hazard. Mater. 201–202, 141–147. https://doi.org/10.1016/j.jhazmat.2011.11.053

Karagöz, P., Vaitkeviciute-Rocha, I., Özkan M; Angelidaki, I., 2012. Alkaline peroxide pretreatment of rapeseed straw for enhancing bioethanol production by Same Vessel Saccharification and Co-Fermentation. Bioresour. Technol. 104, 349--357. https://doi.org/10.1016/j.biortech.2011.10.075

Karavias, F., Myers, A.L., 1991. Isosteric Heats of Multicomponent Adsorption:

Thermodynamics and Computer Simulations. Lagmuir 7, 3118–3126. https://doi.org/10.1021/la00060a035

Kaźmierczak-Raźna, J., Nowicki, P., Pietrzak, R., 2013. Sorption properties of activated carbons obtained from corn cobs by chemical and physical activation. Adsorption 19, 273–281. https://doi.org/10.1007/s10450-012-9450-y

Keramati, M., Ghoreyshi, A.A., 2014. Improving CO2 adsorption onto activated carbon through functionalization by chitosan and triethylenetetramine. Phys. E Low-dimensional Syst. Nanostructures 57, 161–168. https://doi.org/10.1016/j.physe.2013.10.024

Khanal, S.K., 2008. Bioenergy generation from residues of biofuel industries, in: Khanal, S.K. (Ed.), Anaerobic Biotechnology for Bioenergy Production: Principles and Applications. Wiley-Blackwell, Iowa, p. 179. https://doi.org/10.1002/9780813804545

Kim, D., 2018. Physico-chemical conversion of lignocellulose: Inhibitor effects and detoxification strategies: A mini review. Molecules 23. https://doi.org/10.3390/molecules23020309

Kim, H.W., Nam, J.Y., Shin, H.S., 2011. A comparison study on the high-rate co-digestion of sewage sludge and food waste using a temperature-phased anaerobic sequencing batch reactor system. Bioresour. Technol. 102, 7272–7279.

Kim, Y.J., Nam, Y.S., Kang, Y.T., 2015. Study on a numerical model and PSA (pressure swing adsorption) process experiment for CH4/CO2 separation from biogas. Energy 91, 732–741. https://doi.org/10.1016/j.energy.2015.08.086

Klein, J., Henning, K.-D., 1984. Catalytic oxidation of hydrogen sulphide on activated carbons. Fuel 63, 1064–1067. https://doi.org/10.1016/0016-2361(84)90189-3

Köchermann, J., Schneider, J., Matthischke, S., Rönsch, S., 2015. Sorptive H2S removal by impregnated activated carbons for the production of SNG. Fuel Process. Technol. 138, 37–41. https://doi.org/10.1016/j.fuproc.2015.05.004

Kondusamy, D., Kalamdhad, A.S., 2014. Pre-treatment and anaerobic digestion of food waste for high rate methane production – A review. J. Environ. Chem. Eng. 2, 1821–1830. https://doi.org/10.1016/j.jece.2014.07.024

Kowalski, S., Lukasiewicz, M., Duda-Chodak, A., Zięć, G., 2013. 5-Hydroxymethyl-2-Furfural (HMF) – Heat-induced formation , occurrence in food and biotransformation – a review. Pol. J. Food Nutr. Sci., 63, 207–225. https://doi.org/10.2478/v10222-012-0082-4

Kratky, L., Jirout, T., 2011. Biomass size reduction machines for enhancing biogas

production. Chem. Eng. Technol. 34, 391–399. https://doi.org/10.1002/ceat.201000357

Kreuger, E., Nges, I.A., Björnsson, L., 2011. Ensiling of crops for biogas production: effects on methane yield and total solids determination. Biotechnol. Biofuels 4, 44. https://doi.org/10.1186/1754-6834-4-44

Kristensen, P.G., Jensen, J.K., Nielsen, M., Illerup, J.B., 2004. Emission factors for gas fired CHP units< 25 MW. IGRC, Novemb.

KTBL, 2009. Brochure on biogas from energy crops. D-64289. Darmstadt.

Kumar, A.K., Sharma, S., 2017. Recent updates on different methods of pretreatment of lignocellulosic feedstocks: a review. Bioresour. Bioprocess. 4, 7. https://doi.org/10.1186/s40643-017-0137-9

Kvist, T., Aryal, N., 2019. Methane loss from commercially operating biogas upgrading plants. Waste Manag. 87, 295–300. https://doi.org/10.1016/j.wasman.2019.02.023

Kwaśny, J., Balcerzak, W., 2016. Sorbents Used for Biogas Desulfurization in the Adsorption Process. Polish J. Environ. Stud. 25, 37–43. https://doi.org/10.15244/pjoes/60259

Lapa, N., Surra, E., Esteves, I.A.A.., Ribeiro, R., Mota, J.P.B., 2017. Production of biogas and bioH2 – biochemical methods, in: Riazi, M.R., Chiaramonti, D. (Eds.), Biofuels Production and Processing Technology. CRC Press Taylor & Francis, pp. 65–84.

Le Leuch, L.M., Subrenat, A., Le Cloirec, P., 2003. Hydrogen Sulfide Adsorption and Oxidation onto Activated Carbon Cloths: Applications to Odorous Gaseous Emission Treatments. Langmuir 19, 10869–10877.

Lebuhn, M., Liu, F., Heuwinkel, H., Gronauer, A., 2008. Biogas production from mono-digestion of maize silage-long-term process stability and requirements. Water Sci. Technol. 58, 1645–1651. https://doi.org/10.2166/wst.2008.495

Lee, J., Kim, J., Jang, H., Lee, M., Park, J., 2015. Sequential dilute acid and alkali pretreatment of corn stover : Sugar recovery efficiency and structural characterization. Bioresour. Technol. 182, 296–301. https://doi.org/10.1016/j.biortech.2015.01.116

Lestinsky, P., Večeř, M., Navrátil, P., Stehlík, P., 2014. Removing CO2 from biogas - The optimisation of a pressure swing adsorption (PSA) unit using breakthrough curves, Chemical Engineering Transactions. https://doi.org/10.3303/CET1439045

Li, D., Liu, S., Mi, L., Li, Z., Yuan, Y., Yan, Z., Liu, X., 2015. Effects of feedstock ratio and organic loading rate on the anaerobic mesophilic co-digestion of rice straw and cow

manure. Bioresour. Technol. 189, 319–326. https://doi.org/10.1016/J.BIORTECH.2015.04.033

Li, H., Deng, A., Ren, J., Liu, C., Lu, Q., Zhong, L., Peng, F., Sun, R., 2014. Catalytic hydrothermal pretreatment of corncob into xylose and furfural via solid acid catalyst. Bioresour. Technol. 158, 313–320. https://doi.org/10.1016/j.biortech.2014.02.059

Li, H., Qu, Y., Yang, Y., Chang, S., Xu, J., 2016. Microwave irradiation – A green and efficient way to pretreat biomass. Bioresour. Technol. 199, 34–41. https://doi.org/10.1016/j.biortech.2015.08.099

Li, J., Zhang, R., Abdul, M., Siddhu, H., He, Y., Wang, W., Li, Y., Chen, C., Liu, G., 2015. Enhancing methane production of corn stover through a novel way : Sequent pretreatment of potassium hydroxide and steam explosion. Bioresour. Technol. 181, 345–350. https://doi.org/10.1016/j.biortech.2015.01.050

Li, M., Cheng, Y.-L., Fu, N., Li, D., Adhikari, B., Chen, X.D., 2014. Isolation and Characterization of Corncob Cellulose Fibers using Microwave-Assisted Chemical Treatments. Int. J. Food Eng. 0, 427–436. https://doi.org/10.1515/ijfe-2014-0052

Li, Q., Jiang, X., He, Y., Li, L., Xian, M., Yang, J., 2010. Evaluation of the biocompatibile ionic liquid 1-methyl-3-methylimidazolium dimethylphosphite pretreatment of corn cob for improved saccharification. Appl Microbiol Biotechnol 87, 117–126. https://doi.org/10.1007/s00253-010-2484-8

Li, Y.Y., Xu, F., Li, Y.Y., Lu, J., Li, S., Shah, A., Zhang, X., Zhang, H., Gong, X., Li, G., 2018. Reactor performance and energy analysis of solid state anaerobic co-digestion of dairy manure with corn stover and tomato residues. Waste Manag. 73, 130–139. https://doi.org/10.1016/j.wasman.2017.11.041

Li, Y., Li, Yu, Zhang, D., Li, G., Lu, J., Li, S., 2015. Solid state anaerobic co-digestion of tomato residues with dairy manure and corn stover for biogas production. Bioresour. Technol. 217, 50–55. https://doi.org/10.1016/j.biortech.2016.01.111

Liebetrau, J., Reinelt, T., Clemens, J., Hafermann, C., Friehe, J., Weiland, P., 2013. Analysis of greenhouse gas emissions from 10 biogas plants within the agricultural sector. Water Sci. Technol. 67, 1370–1379. https://doi.org/10.2166/wst.2013.005

Lindorfer, H., Waltenberger, R., Köllner, K., Braun, R., Kirchmayr, R., 2008. New data on temperature optimum and temperature changes in energy crop digesters. Bioresour. Technol. 99, 7011–7019. https://doi.org/https://doi.org/10.1016/j.biortech.2008.01.034

Liu, X., Bayard, R., Benbelkacem, H., Buffiere, P., Gourdon, R., 2015. Evaluation of the correlations between biodegradability of lignocellulosic feedstocks in anaerobic

digestion process and their biochemical characteristics. Biomass and Bioenergy 81, 534–543. https://doi.org/10.1016/j.biombioe.2015.06.021

Liu, X., Hiligsmann, S., Gourdon, R., Bayard, R., 2017. Anaerobic digestion of lignocellulosic biomasses pretreated with Ceriporiopsis subvermispora. J. Environ. Manage. 193, 154–162. https://doi.org/10.1016/j.jenvman.2017.01.075

Lo, H.M., Chiang, C.F., Tsao, H.C., Pai, T.Y., Liu, M.H., Kurniawan, T.A., Chao, K.P., Liou, C.T., Lin, K.C., Chang, C.Y., Wang, S.C., Banks, C.J., Lin, C.Y., Liu, W.F., Chen, P.H., Chen, C.K., Chiu, H.Y., Wu, H.Y., Chao, T.W., Chen, Y.R., Liou, D.W., Lo, F.C., 2012. Effects of spiked metals on the MSW anaerobic digestion. Waste Manag. Res. 30, 32–48. https://doi.org/10.1177/0734242X10383079

Lo, H.M., Kurniawan, T.A., Sillanpää, M.E.T., Pai, T.Y., Chiang, C.F., Chao, K.P., Liu, M.H., Chuang, S.H., Banks, C.J., Wang, S.C., Lin, K.C., Lin, C.Y., Liu, W.F., Cheng, P.H., Chen, C.K., Chiu, H.Y., Wu, H.Y., 2010. Modeling biogas production from organic fraction of MSW co-digested with MSWI ashes in anaerobic bioreactors. Bioresour. Technol. 101, 6329–6335. https://doi.org/10.1016/j.biortech.2010.03.048

Lopez Torres, M., Ma del C. Espinosa, L., 2008. Effect of alkaline pretreatment on anaerobic digestion of solid wastes. Waste Manag. 28, 2229–2234. https://doi.org/10.1016/j.wasman.2007.10.006

Lopez, V.M., De la Cruz, F., Barlaz, M., 2016. Chemical composition and methane potential of commercial food wastes. Waste Manag. 56, 477–490. https://doi.org/10.1016/j.wasman.2016.07.024

Luo, J., Cai, M., Gu, T., 2013. Pretreatment of lignocellulosic biomass using green ionic liquids, in: Gu, T. (Ed.), Green Biomass Pretreatment for Biofuels Production., SpringerBriefs in Molecular Science. SpringerBriefs in Molecular Science., Springer, Dordrecht, pp. 127–153. https://doi.org/10.1007/978-94-007-6052-3_6

Makawi, S.Z.A., Taha, M.I., Zakaria, B.., Siddig, B., Mahmod, H., Elhussein, A.R.M. Kariem, E.A.G., 2009. Identification and quantification of 5-hydroxymethyl furfural HMF in some sugar-containing food products by HPLC. Pakistan J. Nutr. 8, 1391–1396.

Mancini, G., Papirio, S., Lens, P.N.L., Esposito, G., 2016. Solvent pretreatments of lignocellulosic materials to enhance biogas production: a review. Energy and Fuels 30, 1892–1903. https://doi.org/10.1021/acs.energyfuels.5b02711

Mao, C., Feng, Y., Wang, X., Ren, G., 2015. Review on research achievements of biogas from anaerobic digestion. Renew. Sustain. Energy Rev. 45, 540–555. https://doi.org/10.1016/j.rser.2015.02.032

Masoud Kayhanian, 1994. Performance of a high-solids anaerobic digestion process

under various ammonia concentrations. J. Chem. Technol. Biotechnol. 59, 349–352. https://doi.org/10.1002/jctb.280590406

Mauky, E., Weinrich, S., Jacobi, H., Nägele, H., Liebetrau, J., Nelles, M., 2017. Demand-driven biogas production by flexible feeding in full-scale – Process stability and flexibility potentials. Anaerobe 46, 86–95. https://doi.org/10.1016/j.anaerobe.2017.03.010

Maurya, D.P., Singla, A., Negi, S., 2015. An overview of key pretreatment processes for biological conversion of lignocellulosic biomass to bioethanol. 3 Biotech 5, 597–609. https://doi.org/10.1007/s13205-015-0279-4

McCarty, P., 1964. Anaerobic waste treatment fundamentals – part one: chemistry and microbiology; part two: environmental requirements and control, part three: toxic materials and their control, part four: process design. Public Work 95, 91–112.

McCarty, P., McKinney, R., 1961. Salt toxicity in anaerobic digestion. J Water Pollut Control Fed. 33, 99–415.

McDonald, P., Henderson, N., Heron, S., 1991. The biochemistry of silage, 2nd ed. Chalcombe Publications, Great Britain.

McMillan, J.D., 1994. Pretreatment of lignocellulosic biomass, in: Himmel, M.E., Baker, J.O., Overend, R.P. (Ed.), Enzymatic Conversion of Biomass for Fuels Production. American Chemical Society, Washington, DC, pp. 292–324. https://doi.org/10.1021/bk-1994-0566.ch015

Meeyoo, V., Trimm, D.L., Cant, N.W., 1997. Adsorption-Reaction Processes for the Removal of Hydrogen Sulphide from Gas Streams. J. Chem. Technol. Biotechnol. 68, 411–416. https://doi.org/10.1002/(SICI)1097-4660(199704)68:4<411::AID-JCTB644>3.0.CO;2-9

Melbinger, N.R., Donnellon, J., Zablatzky, H.R., 1971. Toxic effects of ammonia nitrogen in high-rate digestion [with Discussion]. J. (Water Pollut. Control Fed. 43, 1658–1670.

Menardo, S., Airoldi, G., Balsari, P., 2012. The effect of particle size and thermal pre-treatment on the methane yield of four agricultural by-products. Bioresour. Technol. 104, 708–714. https://doi.org/10.1016/j.biortech.2011.10.061

Menezes, R.L.C.B., Moura, K.O., de Lucena, S.M.P., Azevedo, D.C.S., Bastos-Neto, M., 2018. Insights on the Mechanisms of H 2 S Retention at Low Concentration on Impregnated Carbons. Ind. Eng. Chem. Res. 57, 2248–2257. https://doi.org/10.1021/acs.iecr.7b03402

Menon, V., Rao, M., 2012. Trends in bioconversion of lignocellulose: Biofuels, platform

chemicals & biorefinery concept. Prog. Energy Combust. Sci. 38, 522–550. https://doi.org/10.1016/j.pecs.2012.02.002

Minh, P., Ketheesan, B., Yan, Z., Stuckey, D., 2016. Trace metal speciation and bioavailability in anaerobic digestion : A review. Biotechnol. Adv. 34, 122–136. https://doi.org/10.1016/j.biotechadv.2015.12.006

Modenbach, A.A., Nokes, S.E., 2013. Enzymatic hydrolysis of biomass at high-solids loadings e A review. Biomass and Bioenergy 56, 526–544. https://doi.org/10.1016/j.biombioe.2013.05.031

Mohamad Nor, N., Lau, L.C., Lee, K.T., Mohamed, A.R., 2013. Synthesis of activated carbon from lignocellulosic biomass and its applications in air pollution control—a review. J. Environ. Chem. Eng. 1, 658–666. https://doi.org/10.1016/j.jece.2013.09.017

Moretti De Souza, M.M., Alonso Bocchini-Martins, D., da Costa Carreira Nunes, C., Arévalo Villena, M., Micali Perrone, O., Da Silva, R., Boscolo, M., Gomes, E., 2014. Pretreatment of sugarcane bagasse with microwaves irradiation and its effects on the structure and on enzymatic hydrolysis. Appl. Energy 122, 189–195. https://doi.org/10.1016/j.apenergy.2014.02.020

Mota, J.P.B., Rodrigo, A.J.S., 2000. Calculations of Multicomponent Adsorption-Column Dynamics Combining the Potential and Ideal Adsorbed Solution Theories. Ind. Eng. Chem. Res. 39, 2459–2467. https://doi.org/10.1021/ie9908478

Mousa, L., Forster, C., 1999. The use of glucose as a growth factor to counteract inhibition in anaerobic digestion. Trans IChemE 77, 192–198.

Mullen, C.A., Boateng, A.A., Goldberg, N.M., Lima, I.M., Laird, D.A., Hicks, K.B., 2010. Bio-oil and bio-char production from corn cobs and stover by fast pyrolysis. Biomass and Bioenergy 34, 67–74. https://doi.org/10.1016/j.biombioe.2009.09.012

Muñoz, R., Meier, L., Diaz, I., Jeison, D., 2015. A review on the state-of-the-art of physical/chemical and biological technologies for biogas upgrading. Rev. Environ. Sci. Biotechnol. Technol. 14, 727–759. https://doi.org/10.1007/s11157-015-9379-1

Murphy, J., Braun, R., Weilnd, P., Wellinger, A., 2011. Biogas from Crop Digestion, IEA Bioenergy Report. Task 37.

Mussatto, S.I., Roberto, I.C., 2004. Alternatives for detoxification of diluted-acid lignocellulosic hydrolyzates for use in fermentative processes : a review. Bioresour Technol 93, 1–10. https://doi.org/10.1016/j.biortech.2003.10.005

Nam, H., Wang, S., Jeong, H.-R., 2018. TMA and H2S gas removals using metal loaded on rice husk activated carbon for indoor air purification. Fuel 213, 186–194.

https://doi.org/10.1016/J.FUEL.2017.10.089

Nasr, F.A., Shafy, H.I.A., 1992. Biodegradation of sewage sludge: toxic effects of heavy metals. Environ. Manag. Heal. 3, 18–25. https://doi.org/https://doi.org/10.1108/09566169210018187

National Research Cuncil, 1982. United States-Canadian Tables of Feed Composition. Nutritional Data for United States and Canadian Feed.third revision. National Academy Press, Washington, D.C.

National Research Institute Poland - Oil and Gas, 2014. The Agricultural Biogas Plants in Poland.Technical Report.

Nazari, L., Yuan, Z., Santoro, D., Sarathy, S., Ho, D., Batstone, D., Xu, C. (Charles), Ray, M.B., 2017. Low-temperature thermal pre-treatment of municipal wastewater sludge: Process optimization and effects on solubilization and anaerobic degradation. Water Res. 113, 111–123. https://doi.org/https://doi.org/10.1016/j.watres.2016.11.055

Negri, M., Bacenetti, J., Manfredini, A., Lovarelli, D., Fiala, M., Maggiore, T.M., Bocchi, S., 2014. Evaluation of methane production from maize silage by harvest of different plant portions. biomass and bioenergy 67, 339–346. https://doi.org/10.1016/j.biombioe.2014.05.016

Neto Franco, I.F., 2011. Estudo dos processos de nitrificação e desnitrificação numa Estação de Tratamento de Águas Residuais. Universidade Nova de Lisboa, Faculdade da Ciência e Tecnologia.

Ning, J., Zhou, M., Pan, X., Li, C., Lv, N., Wang, T., Cai, G., Wang, R., Li, J., Zhu, G., 2019. Simultaneous biogas and biogas slurry production from co-digestion of pig manure and corn straw: Performance optimization and microbial community shift. Bioresour. Technol. 282, 37–47. https://doi.org/10.1016/j.biortech.2019.02.122

Nogueira, M., 2017. Novos eco-adssorventes para o pré condicionamento do biogás.Tese de mestrado em Energias Renováveis. Universidade Nova de Lisboa.Faculdade de Ciência e Tecnologia.

Nowicki, P., Kaźmierczak-Raźna, J., Skibiszewska, P., Wiśniewska, M., Nosal-Wiercińska, A., Pietrzak, R., 2016. Production of activated carbons from biodegradable waste materials as an alternative way of their utilisation. Adsorption 22, 489–502. https://doi.org/10.1007/s10450-015-9719-z

Nowicki, P., Skibiszewska, P., Pietrzak, R., 2014. Hydrogen sulphide removal on carbonaceous adsorbents prepared from coffee industry waste materials. Chem. Eng. J. 248, 208–215. https://doi.org/10.1016/j.cej.2014.03.052

Ntziachristis, L., Samaras, Z., Kouridis, C., Samaras, C., Hassel, D., Mellios, G., Mccrae, I., Hickman, J., Zierock, H., Keller, M., Rexeis, M., Andre, M., Winther, M., Pastramas, N., Boulter, P., Katsis, P., Joumard, R., Rijkeboer, R., Geivanidis, S., 2018. EMEP/EEA air pollutant emission inventory guidebook 2016_Update Jul.2018.

Odhner, P.B., Horváth, I.S., Kabir, M.M., Schabbauer, A., 2012. Biogas from lignocellulosic biomass. Amsterdam.

Ogungbenro, A.E., Vega, L.F., Abu-Zahra, M.R.M., Quang, D. V., Al-Ali, K.A., 2018. Physical synthesis and characterization of activated carbon from date seeds for CO2 capture. J. Environ. Chem. Eng. 6, 4245–4252. https://doi.org/10.1016/j.jece.2018.06.030

Oliveira, J.J. de, Dalmazo, G.O., Morselli, T.B.G.A., Oliveira, V.F. da S. de, Corrêa, L.B., Nora, L., Corrêa, É.K., 2018. Composted slaughterhouse sludge as a substitute for chemical fertilizers in the cultures of lettuce (Lactuca sativa L.) and radish (Raphanus sativus L.). Food Sci. Technol. https://doi.org/http://dx.doi.org/10.1590/1678-457x.00717

Oliveira, J., 1982. Operações e processos fundamentais em engenharia sanitária: fundamentos de depuração biológica., UNL(ed.). ed. Lisboa.

Owamah, H.I., Izinyon, O.C., 2015. The effect of organic loading rates (OLRs) on the performances of food wastes and maize husks anaerobic co-digestion in continuous mode. Sustain. Energy Technol. Assessments 11, 71–76. https://doi.org/10.1016/j.seta.2015.06.002

Ozawa, S., Kusumi, S., Ogino, Y., 1976. Physical adsorption of gases at high pressure. IV. An improvement of the D–A adsorption equation. J. Colloids Interface Sci. 56, 83–91.

Pakarinen, O., Lehtomäki, A., Rissanen, S., Rintala, J., 2008. Storing energy crops for methane production: Effects of solids content and biological additive. Bioresour. Technol. 99, 7074–7082. https://doi.org/10.1016/J.BIORTECH.2008.01.007

Pakseresht, S., Kazemeini, M., Akbarnejad, M., 2002. Equilibrium isotherms for CO, CO2, CH4 and C2H4 on the 5A molecular sieve by a simple volumetric apparatus, Separation and Purification Technology. https://doi.org/10.1016/S1383-5866(02)00012-6

Palmqvist, E., Hahn-Hägerdal, B., 2000. Fermentation of lignocellulosic hydrolysates. II: inhibitors and mechanisms of inhibition. Bioresour. Technol. 74, 25–32.

Pang, F., Xue, S., Yu, S., Zhang, C., Li, B., Kang, Y., 2012. Effects of microwave power and microwave irradiation time on pretreatment efficiency and characteristics of corn stover using combination of steam explosion and microwave irradiation (SE –

MI) pretreatment. Bioresour. Technol. 118, 111–119. https://doi.org/10.1016/j.biortech.2012.05.041

Paolini, V., Petracchini, F., Carnevale, M., Gallucci, F., Perilli, M., Esposito, G., Segreto, M., Occulti, L.G., Scaglione, D., Ianniello, A., Frattoni, M., 2018. Characterisation and cleaning of biogas from sewage sludge for biomethane production. J. Environ. Manage. 217, 288–296. https://doi.org/10.1016/j.jenvman.2018.03.113

Papa, G., Rodriguez, S., George, A., Schievano, A., Orzi, V., Sale, K.L., Singh, S., Adani, F., 2015. Comparison of different pretreatments for the production of bioethanol and biomethane from corn stover and switchgrass. Bioresour. Technol. 183, 101–110. https://doi.org/10.1016/j.biortech.2015.01.121

Parajó, J.C., Dominguez, H., Domínguez, J.M., 1998. Biotechnological production of xylitol. Part 1: Interest of xylitol and fundamentals of its biosynthesis. Bioresour. Technol. 65, 191–201. https://doi.org/10.1016/S0960-8524(98)00038-8

Park, H., Um, Y., Jun, S., Yup, S., Min, H., 2015. Transcriptomic analysis of Corynebacterium glutamicum in the response to the toxicity of furfural present in lignocellulosic hydrolysates. Process Biochem. 50, 347–356. https://doi.org/10.1016/j.procbio.2014.11.014

Patel, B., Guo, M., Izadpanah, A., Shah, N., Hellgardt, K., 2016. A review on hydrothermal pre-treatment technologies and environmental profiles of algal biomass processing. Bioresour. Technol. 199, 288–299. https://doi.org/10.1016/j.biortech.2015.09.064

Paul, S., Dutta, A., 2018. Challenges and opportunities of lignocellulosic biomass for anaerobic digestion. Resour. Conserv. Recycl. 130, 164–174. https://doi.org/10.1016/j.resconrec.2017.12.005

Pekařová, S., Dvořáčková, M., Stloukal, P., Ingr, M., Šerá, J., Koutny, M., 2017. Quantitation of the inhibition effect of model compounds representing plant biomass degradation products on methane production. BioResources 12, 2421–2432.

Pellerano, M., Pré, P., Kacem, M., Delebarre, A., 2009. CO2 capture by adsorption on activated carbons using pressure modulation. Energy Procedia 1, 647–653. https://doi.org/10.1016/j.egypro.2009.01.085

Peng, K., Li, X., Luo, C., Shen, Z., 2006. Vegetation composition and heavy metal uptake by wild plants at three contaminated sites in Xiangxi area, China. J. Environ. Sci. Heal. Part A 41, 65–76. https://doi.org/10.1080/10934520500298838

Peredo-Mancilla, D., Ghouma, I., Hort, C., Ghimbeu, C.M., Jeguirim, M., Bessieres, D., 2018. CO2 and CH4 Adsorption Behavior of Biomass-Based Activated Carbons.

Energies 11, 1–13. https://doi.org/10.3390/en11113136

Pérez-Rodríguez, N., Garcí-a-Bernet, D., Domínguez, J.M., 2016. Effects of enzymatic hydrolysis and ultrasounds pretreatments on corn cob and vine trimming shoots for biogas production. Bioresour. Technol. 221, 130–138. https://doi.org/10.1016/j.biortech.2016.09.013

Personal Communication, 2016. Plant Operational Data.

Petersson, A., Wellinger, A., 2009. Biogas upgrading technologies – developments and innovations. IEA Bioenergy. Task 37. Report.

Pevida, C., Plaza, M.G., Arias, B., Fermoso, J., Rubiera, F., Pis, J.J., 2008. Surface modification of activated carbons for CO2 capture. Appl. Surf. Sci. 254, 7165–7172. https://doi.org/10.1016/j.apsusc.2008.05.239

Plaza, M.G., García, S., Rubiera, F., Pis, J.J., Pevida, C., 2010. Post-combustion CO 2 capture with a commercial activated carbon: comparison of different regeneration strategies. Chem. Eng. Process. Process Intensif. 163, 41–47. https://doi.org/10.1016/j.cej.2010.07.030

Plöchl, M., Zacharias, H., Herrmann, C., Heiermann, M., Prochnow, A., 2009. Influence of silage additives on methane yield and economic performance of selected feedstock. Agric. Eng. Int. CIGR J XI 1123, 1–16.

Policicchio, A., Maccallini, E., Kalantzopoulos, G.N., Cataldi, U., Abate, S., Desiderio, G., Agostino, R.G., 2013. Volumetric apparatus for hydrogen adsorption and diffusion measurements: Sources of systematic error and impact of their experimental resolutions. Rev. Sci. Instrum. 84, 103907. https://doi.org/10.1063/1.4824485

Private Communication, 2016. OFMSW transport data of some portuguese Municipalities.

Prorot, A., Laurent, J., Dagot, C., Leprat, P., 2011. Sludge disintegration during heat treatment at low temperature: A better understanding of involved mechanisms with a multiparametric approach. Biochem. Eng. J. 54, 178–184. https://doi.org/https://doi.org/10.1016/j.bej.2011.02.016

Rabemanolontsoa, H., Saka, S., 2015. Various pretreatments of lignocellulosics. Bioreseaurce Technol. 199, 83–91. https://doi.org/10.1016/j.biortech.2015.08.029

Rajagopal, R., Massé, D.I., Singh, G., 2013. A critical review on inhibition of anaerobic digestion process by excess ammonia. Bioresour. Technol. 143, 632–641. https://doi.org/10.1016/J.BIORTECH.2013.06.030

Ramos-Suárez, J.L., Gómez, D., Regueiro, L., Baeza, A., Hansen, F., 2017. Alkaline and

oxidative pretreatments for the anaerobic digestion of cow manure and maize straw: Factors influencing the process and preliminary economic viability of an industrial application. Bioresour. Technol. 241, 10–20. https://doi.org/10.1016/j.biortech.2017.05.054

Rashidi, A.N., Yusup, S., Borhan, A., 2016. Isotherm and thermodynamic analysis of carbon dioxide on activated carbon. Procedia Eng. 148, 630–637. https://doi.org/10.1016/j.proeng.2016.06.527

Raveendran, K., Ganesh, A., Khilar, K.C., 1995. Influence of mineral matter on biomass pyrolysis characteristics. Fuel 74, 1812–1822. https://doi.org/10.1016/0016-2361(95)80013-8

Redding, A.P., Wang, Z., Keshwani, D.R., Cheng, J.J., 2011. High temperature dilute acid pretreatment of coastal Bermuda grass for enzymatic hydrolysis. Bioresour. Technol. 102, 1415–1424. https://doi.org/10.1016/j.biortech.2010.09.053

Reid, R.C., Sherwood, T.K., Street, R.E., 2009. The Properties of Gases and Liquids , Physics Today. https://doi.org/10.1063/1.3060771

Ribeiro, R.P.P.L., Esteves, I.A.A.C., Mota, J.P.B., 2017. Two-column relay simulated moving-bed process for gas-phase separations. Sep. Purif. Technol. 182, 19–28. https://doi.org/10.1016/j.seppur.2017.03.037

Ribeiro, R.P.P.L., Silva, R.J.S., Esteves, I.A.A.C., Mota, J.P.B., 2015. Development, Construction, and Operation of a Multisample Volumetric Apparatus for the Study of Gas Adsorption Equilibrium. J. Chem. Educ. 92, 757–761. https://doi.org/10.1021/ed500633h

Riboldi, L., Bolland, O., 2017. Overview on Pressure Swing Adsorption (PSA) as CO2 capture technology: state-of-the-Art, limits and potentials. Energy Procedia 114, 2390–2400. https://doi.org/https://doi.org/10.1016/j.egypro.2017.03.1385

Riboldi, L., Bolland, O., 2015. Evaluating Pressure Swing Adsorption as a CO2 separation technique in coal-fired power plants. Int. J. Greenh. Gas Control 39, 1–16. https://doi.org/10.1016/j.ijggc.2015.02.001

Rouches, E., HerpoÃ«l-Gimbert, I., Steyer, J.P., Carrere, H., 2016. Improvement of anaerobic degradation by white-rot fungi pretreatment of lignocellulosic biomass: A review. Renew. Sustain. Energy Rev. 59, 179–198. https://doi.org/10.1016/j.rser.2015.12.317

Rouquerol, F., Rouquerol, J., Sing, K., 1999. Adsorption by Powders and Porous Solids—Principles, Methodology and Applications. Accademic Press.

Ruthven, D., Farooq, S., Knabel, K., 1994. Pressure Swing Adsorption. VCH Publisher,

Inc., USA.

Ruthven, D.M., 1984. Flow through packed beds, in: Principles of Adsorption & Adsorption Processes. Wiley-Interscience Publication, New York, pp. 206–219.

Ruthven, D.M., Farooq, S., Knabel, K.S., 1994. Pressure Swing Adsorption. VCH Publisher, Inc., USA.

Ryckebosch, E., Drouillon, M., Vervaeren, H., 2011. Techniques for transformation of biogas to biomethane. Biomass and Bioenergy 35, 1633–1645. https://doi.org/10.1016/j.biombioe.2011.02.033

S. Lyubchik, A. Lyubchik, O. Lygina, S. Lyubchik, and I.F., 2011. Comparison of the Thermodynamic Parameters Estimation for the Adsorption Process of the Metals from Liquid Phase on Activated Carbons, in: Moreno-Pirajan, J.C. (Ed.), Hermodynamics – Interaction Studies – Solids, Liquids and Gases. InTech, pp. 95–122.

S.D. Mehta, R.P.D., 1985. An improved potential theory method for predicting gas-mixture adsorption equilibria. Ind. Eng. Chem. Fundam 24, 325.

Saha, B., Cotta, M., 2007. Enzymatic saccharification and fermentation of alkaline peroxide pretreated rice hulls to ethanol. Enzyme Microb. Technol. 41, 528–532. https://doi.org/10.1016/j.enzmictec.2007.04.006

Schattauer, A., Abdoun, E., Weiland, P., Plo, M., 2011. Abundance of trace elements in demonstration biogas plants. Biosyst. Eng. 108, 57–65. https://doi.org/10.1016/j.biosystemseng.2010.10.010

Schell, J., Casas, N., Marx, D., Blom, R., Mazzotti, M., 2013. Comparison of commercial and new adsorbent materials for pre-combustion CO2 capture by pressure swing adsorption. Energy Procedia 37, 167–174. https://doi.org/10.1016/j.egypro.2013.05.098

Schimpf, U., Hanreich, A., Mähnert, P., Unmack, T., Junne, S., Renpenning, J., Lopez-Ulibarri, R., 2013. Improving the efficiency of large-scale biogas processes: pectinolytic enzymes accelerate the lignocellulose degradation. J. Sustain. Energy Environ. 4, 53–60.

Scholz, M., Melin, T., Wessling, M., 2013. Transforming biogas into biomethane using membrane technology. Renew. Sustain. Energy Rev. 17, 199–212. https://doi.org/10.1016/j.rser.2012.08.009

Schroyen, M., Vervaeren, H., Hulle, S.W.H. Van, Raes, K., 2014. Impact of enzymatic pretreatment on corn stover degradation and biogas production. Bioresour. Technol. 173, 59–66. https://doi.org/10.1016/j.biortech.2014.09.030

Selig, M., Vinzant, T., Himmel, M., Decker, S., 2009. The effect of lignin removal by alkaline peroxide pretreatment on the susceptibility of corn stover to purified cellulolytic and xylanolytic enzymes. Appl Biochem Biotechnol. 155, 397–406.

Selling, R., Håkansson, T., Björnsson, L., 2008. Two-stage anaerobic digestion enables heavy metal removal. Water Sci. Technol. 57, 553–558. https://doi.org/http://dx.doi.org/10.2166/wst.2008.054

Seredych, M., Bandosz, T.J., 2008. Role of microporosity and nitrogen functionality on the surface of activated carbon in the process of desulfurization of digester gas. J. Phys. Chem. C 112, 4704–4711. https://doi.org/10.1021/jp710271w

Seredych, M., Bandosz, T.J., 2006. Desulfurization of digester gas on catalytic carbonaceous adsorbents: complexity of interactions between the surface and components of the gaseous mixture. Ind. Eng. Chem. Res. 45, 3658–3665. https://doi.org/10.1021/ie051388f

Shahriari, H., Warith, M., Hamoda, M., Kennedy, K., 2013. Evaluation of single vs. staged mesophilic anaerobic digestion of kitchen waste with and without microwave pretreatment. J. Environ. Manage. 125, 74–84. https://doi.org/10.1016/j.jenvman.2013.03.042

Shang, G., Li, Q., Liu, L., Chen, P., Huang, X., 2016. Adsorption of hydrogen sulfide by biochars derived from pyrolysis of different agricultural/forestry wastes. J. Air Waste Manage. Assoc. 66, 8–16. https://doi.org/10.1080/10962247.2015.1094429

Shang, G., Shen, G., Liu, L., Chen, Q., Xu, Z., 2013. Kinetics and mechanisms of hydrogen sulfide adsorption by biochars. Bioresour. Technol. 133, 495–499. https://doi.org/10.1016/j.biortech.2013.01.114

Shariff, A., Noor, N.., Lau, A., Ali, M.A.M., 2016. A comparative study on biochar from slow pyrolysis of Corn Cob and Cassava wastes. Int. J. Biotechnol. Bioeng. 10, 767–771.

Sharma, S.K., Mishra, I.M., Sharma, M.P., Saini, J.S., 1988. Effect of particle size on biogas generation from biomass residues. Biomass 17, 251–263. https://doi.org/https://doi.org/10.1016/0144-4565(88)90107-2

Shen, D., Bilow, M., Siperstein, F.R., Engelhard, M., Myers, A.L., 2000. Comparison of Experimental Techniques for Measuring Isosteric Heat of Adsorption. Adsoprtion 6, 275.

Shen, F., Liu, J., Zhang, Z., Dong, Y., Gu, C., 2018. Density functional study of hydrogen sulfide adsorption mechanism on activated carbon. Fuel Process. Technol. 171, 258–264. https://doi.org/https://doi.org/10.1016/j.fuproc.2017.11.026

Shih-Perng, T., 1999. Production of biogas and bioH2 – biochemical methods, in: Radecki, P.P., Crittenden, J.C., Shonnard, D.R., Bulloch, J.L. (Eds.), Emerging Separation and Separative Reaction Technologies for Process Waste Reduction: Adsorption and Membrane Systems. Center for Waste Reduction Technologies, American Institute of Chemical Engineers, p. 319.

Siegrist, H., Vogt, D., Garcia-Heras, J.L., Gujer, W., 2002. Mathematical model for meso- and thermophilic anaerobic sewage sludge digestion. Environ. Sci. Technol. 36, 1113–1123. https://doi.org/10.1021/es010139p

Sigot, L., Fontseré Obis, M., Benbelkacem, H., Germain, P., Ducom, G., 2016. Comparing the performance of a 13X zeolite and an impregnated activated carbon for H 2 S removal from biogas to fuel an SOFC: Influence of water. Int. J. Hydrogen Energy 41, 18533–18541. https://doi.org/10.1016/j.ijhydene.2016.08.100

Sing, K., 1985. Reporting physisorption data for gas/solid systems with special reference to the determination of surface area and porosity (Recommendations 1984). Pure Appl. Chem. 57, 603–619. https://doi.org/10.1351/pac198557040603

Sircar, S., Cao, D.V., 2002. Heat of Adsorption. Chem. Eng. Technol.ology 25, 945.

Sircar, S., Cao, D. V., 2001. Heat of adsorption of pure sulfur hexafluoride on micro-mesoporous adsorbents. Adsoprtion 7.

Siriwardane, R. V, Shen, M., Fisher, E.P., Poston, J.A., 2001. Adsorption of CO2 on molecular sieves and activated carbon. Energy & Fuels 15, 279–284.

Sitthikhankaew, R., Chadwick, D., Assabumrungrat, S., Laosiripojana, N., 2014. Effects of humidity, O2, and CO2 on H2S adsorption onto upgraded and KOH impregnated activated carbons. Fuel Process. Technol. 124, 249–257. https://doi.org/10.1016/j.fuproc.2014.03.010

Song, M., Jin, B., Xiao, R., Yang, L., Wu, Y., Zhong, Z., Huang, Y., 2013. The comparison of two activation techniques to prepare activated carbon from corn cob. Biomass and Bioenergy 48, 250–256. https://doi.org/10.1016/j.biombioe.2012.11.007

Song, Y.-C., Kwon, S.-J., Woo, J.-H., 2004. Mesophilic and thermophilic temperature co-phase anaerobic digestion compared with single-stage mesophilic- and thermophilic digestion of sewage sludge. Water Res. 38, 1653–1662. https://doi.org/https://doi.org/10.1016/j.watres.2003.12.019

Song, Z., Yang, G., Liu, X., Yan, Z., Yuan, Y., Liao, Y., 2014. Comparison of seven chemical pretreatments of corn straw for improving methane yield by anaerobic digestion. PLoS One 9, 1–8. https://doi.org/10.1371/journal.pone.0093801

Špalková, V., Hutňan, M., Lazor, M., Kolesárová, N., 2009. Selectec problems of

anaerobic treatment of maize silage, in: Markoš, J. (Ed.), Proceedings of the 36th International Conference of Slovak Society of Chemical Engineering. pp. 157-[1-17].

Spencer, F., Danner, P., 1972. Improved Equation for Prediction of Saturated Liquid Density. J. Chem. Eng. Data 17, 236–241. https://doi.org/10.1021/je60053a012

Su, Y., Du, R., Guo, H., Cao, M., Wu, Q., 2015. Fractional pretreatment of lignocellulose by alkaline hydrogen peroxide : Characterization of its major components. Food Bioprod. Process. 94, 322–330. https://doi.org/10.1016/j.fbp.2014.04.001

Sun, Q., Li, H., Yan, J., Liu, L., Yu, Z., Yu, X., 2015. Selection of appropriate biogas upgrading technology-a review of biogas cleaning, upgrading and utilisation. Renew. Sustain. Energy Rev. 51, 521–532. https://doi.org/10.1016/j.rser.2015.06.029

Sun, S.S., Sun, S.S., Cao, X., Sun, R., 2015. The role of pretreatment in improving the enzymatic hydrolysis of lignocellulosic materials. Bioresour. Technol. 199, 49–58. https://doi.org/10.1016/j.biortech.2015.08.061

Sun, Y., Yang, G., Zhang, L., Sun, Z., 2017. Preparation of high performance H 2 S removal biochar by direct fluidized bed carbonization using potato peel waste. Process Saf. Environ. Prot. 107, 281–288. https://doi.org/10.1016/j.psep.2017.02.018

Sun, Y., Zhang, J.P., Wen, C., Zhang, L., 2016. An enhanced approach for biochar preparation using fluidized bed and its application for H2S removal. Chem. Eng. Process. Process Intensif. 104, 1–12. https://doi.org/10.1016/j.cep.2016.02.006

Surra, E., Bernardo, M., Lapa, N., Esteves, I., Fonseca, I., Mota, J.P., 2018a. Maize cob waste pre-treatments to enhance biogas production through co-anaerobic digestion with OFMSW. Waste Manag. 72, 193–205. https://doi.org/https://doi.org/10.1016/j.wasman.2017.11.004

Surra, E., Bernardo, M., Lapa, N., Esteves, I., Fonseca, I., Mota, J.P., 2018b. Enhanced Biogas Production through Anaerobic co-Digestion of OFMSW with Maize Cob Waste Pre-Treated with Hydrogen Peroxide. Chem. Eng. Trans. 65, 121–126.

Surra, E., Costa Nogueira, M., Bernardo, M., Lapa, N., Esteves, I., Fonseca, I., 2019. New adsorbents from maize cob wastes and anaerobic digestate for H2S removal from biogas. Waste Manag. 94, 136–145. https://doi.org/https://doi.org/10.1016/j.wasman.2019.05.048

Taherzadeh, M.J., Karimi, K., 2008. Pretreatment of lignocellulosic wastes to improve ethanol and biogas production: a review, International Journal of Molecular Sciences. https://doi.org/10.3390/ijms9091621

Tajima, H., Yamasaki, A., Kiyono, F., 2004. Energy consumption estimation for greenhouse gas separation processes by clathrate hydrate formation. Energies 29, 1713–1729. https://doi.org/10.1016/j.energy.2004.03.003

Taricska, J., Long, D., Chen, J., Hung, Y., Zou, S., 2009. Anaerobic digestion Biological Treatment Processes. Springer.

Teixeira Franco, R., Buffière, P., Bayard, R., 2016. Ensiling for biogas production: Critical parameters. A review. Biomass and Bioenergy 94, 94–104. https://doi.org/10.1016/J.BIOMBIOE.2016.08.014

Thaerzadeh, M., Nicklasson, C., Lidén, G., 2000. On-line control of fed-batch fermentation of dilute-acid hydrolyzates. Biotechnol Bioeng 69, 330–338.

Thommes, M., Kaneko, K., Neimark, A. V., Olivier, J.P., Rodriguez-Reinoso, F., Rouquerol, J., Sing, K.S., 2015. Physisorption of gases, with special reference to the evaluation of surface area and pore size distribution (IUPAC Technical Report). Pure Appl. Chem. 87, 1051–1069. https://doi.org/10.1515/pac-2014-1117

Tien, C., 1994. Adsorption Calculations and Modeling, first ed. ed. Butterworth-Heinemann, Boston.

Tiwari, D., Bhunia, H., Bajpai, P.K., 2018. Development of chemically activated N-enriched carbon adsorbents from urea-formaldehyde resin for CO2 adsorption: Kinetics, isotherm, and thermodynamics. J. Environ. Manage. 218, 579–592. https://doi.org/10.1016/j.jenvman.2018.04.088

Tong, M., Yao, C., 2009. Effects of microwave-assisted pretreatment on the enzymatic hydrolysis of corn stover. J. Nanjing For. Univ. (Natural Sci. Ed. 33, 91–95.

Torre, P., Aliakbarian, B., Rivas, B., Domínguez, J.M., Converti, A., 2008. Release of ferulic acid from corn cobs by alkaline hydrolysis. Biochem. Eng. J. 40, 500–506. https://doi.org/10.1016/j.bej.2008.02.005

Tsai, W.T., Chang, C.Y., Wang, S.Y., Chang, C.F., Chien, S.F., Sun, H.F., 2001. Cleaner production of carbon adsorbents by utilizing agricultural waste corn cob. Resour. Conserv. Recycl. 32, 43–53. https://doi.org/10.1016/S0921-3449(00)00093-8

TUV, 2012. Biogas To Biomethane Technology Review, Vienna University of Technology. Vienna.

URL1, 2018. N-methylmorpholine N-oxide [WWW Document]. Alibaba.com. URL https://www.alibaba.com/showroom/n-methylmorpholine-oxide.html (accessed 5.15.19).

URL2, 2016. IEA Bioenergy Task 37. Report Summaries 2016 [WWW Document]. IEA-

biogas.net. URL https://www.scribd.com/document/340646451/IEA-Bioerg-T37CRS-2015-Final (accessed 7.19.16).

van Haaren, R., Themelis, N.J., Barlaz, M., 2010. LCA comparison of windrow composting of yard wastes with use as alternative daily cover (ADC). Waste Manag. 30, 2649–2656. https://doi.org/https://doi.org/10.1016/j.wasman.2010.06.007

Vaswani, S., Kumar, R., Kumar, V., Roy, D., 2016. Nutritional and mineral composition of different varieties of normal and high quality protein maize fodder at post- cob stage. Int. J. Sci. Environ. Technol. 5, 2719–2727.

Vaz, F., Torres, A., Ribeiro, C.I., Neiva Correia, M.I., Vidal, N.D., 2010. Case study for collection schemes serving the Valorsul AD plant.VALORGAS Project, SEVENTH FRAMEWORK PROGRAMME THEME ENERGY.2009.3.2.2 Biowaste as feedstock for 2nd generation.

Velásquez-Piñas, J.A., Venturini, O.J., Silva Lora, E.E., Denisse, O., Roalcaba, C., 2018. Technical assessment of mono-digestion and co-digestion systems for the production of biogas from anaerobic digestion in Brazil. Renew. Energy 117, 447–458. https://doi.org/10.1016/j.renene.2017.10.085

Vicente, P., 2015. Formulário Único SIRAPA.Manual de Apoio ao Preenchimento do Formulário PRTR Emissões de Combustão Determinação de emissões ar por fatores de emissão.

Vidal, J., 1997. Predicting Thermodynamic Properties Of Pure Substances. General Principles. Corrisponding States. Group Contributions., in: Thermodynamics. Applications in Chemical Enigineering and Petroleoum Industry. Editions TECHNIP, Paris, p. 71.

Vilella, P.C., Lira, J.A., Azevedo, D.C.S.S., Bastos-Neto, M., Stefanutti, R., 2017. Preparation of biomass-based activated carbons and their evaluation for biogas upgrading purposes. Ind. Crop. Prod. 109, 134–140. https://doi.org/10.1016/j.indcrop.2017.08.017

Voss, C., 2005. Applications of pressure swing adsorption technology. Adsorption 11, 527–529. https://doi.org/10.1007/s10450-005-5979-3

Wallace, R., Seredych, M., Zhang, P., Bandosz, T.J., 2014. Municipal waste conversion to hydrogen sulfide adsorbents: Investigation of the synergistic effects of sewage sludge/fish waste mixture. Chem. Eng. J. 237, 88–94. https://doi.org/10.1016/j.cej.2013.10.005

Wang, L., Wu, D., Tang, P., Fan, X., Yuan, Q., 2012. Xylitol production from corncob hydrolysate using polyurethane foam with immobilized Candida tropicalis.

Carbohydr. Polym. 90, 1106–1113. https://doi.org/10.1016/j.carbpol.2012.06.050

Wang, X., Yang, G., Feng, Y., Ren, G., Han, X., 2012. Optimizing feeding composition and carbon – nitrogen ratios for improved methane yield during anaerobic co-digestion of dairy , chicken manure and wheat straw. Bioresour. Technol. 120, 78–83. https://doi.org/10.1016/j.biortech.2012.06.058

Wang, Y., Zhang, Y., Wang, J., Meng, L., 2009. Effects of volatile fatty acid concentrations on methane yield and methanogenic bacteria. Biomass and Bioenergy 33, 848–853. https://doi.org/10.1016/j.biombioe.2009.01.007

Wang, Y.X., Liu, B.S., Zheng, C., 2010. Preparation and adsorption properties of corncob-derived activated carbon with high surface area. J.Chem.Eng. 55, 4669–4676.

Ward, A.J., Hobbs, P.J., Holliman, P.J., Jones, D.L., 2008. Optimisation of the anaerobic digestion of agricultural resources. Bioresour. Technol. 99, 7928–7940. https://doi.org/10.1016/j.biortech.2008.02.044

Wellinger, A., 2017. BioSurf Project. D3.7. Report on the practical experiences with the applicaton of European Biomethane Standards.

Wilkinson, J.M., Davies, D.R., 2012. The aerobic stability of silage: key findings and recent developments. Grass Forage Sci. 68, 1–19. https://doi.org/10.1111/j.1365-2494.2012.00891.x

Wood, G., 2001. Affinity Coefficients of the Polanyi/Dubinin Adsoprtion Isotherm Equations. A review with Compilation and Correlations. Carbon N. Y. 39, 343–356.

Wood, G.O., 1992. Activated carbon adsorption capacities for vapors. Carbon N. Y. 30, 593.

Wu, S., Ni, P., Li, J., Sun, H., Wang, Y., Luo, H., Dach, J., Dong, R., 2016. Integrated approach to sustain biogas production in anaerobic digestion of chicken manure under recycled utilization of liquid digestate: Dynamics of ammonium accumulation and mitigation control. Bioresour. Technol. 205, 75–81. https://doi.org/10.1016/J.BIORTECH.2016.01.021

Xiao, Y., Wang, S., Wu, D., Yuan, Q., 2008. Catalytic oxidation of hydrogen sulfide over unmodified and impregnated activated carbon. Sep. Purif. Technol. 59, 326–332. https://doi.org/10.1016/j.seppur.2007.07.042

Xu, F., Wang, Z.-W., Li, Y., 2014. Predicting the methane yield of lignocellulosic biomass in mesophilic solid-state anaerobic digestion based on feedstock characteristics and process parameters. Bioresour. Technol. 173, 168–176. https://doi.org/https://doi.org/10.1016/j.biortech.2014.09.090

Xu, S., Selvam, A., Wong, J., 2014. Optimization of micro-aeration intensity in acidogenic reactor of a two-phase anaerobic digester treating food waste. Waste Manag. 34, 363–369. https://doi.org/10.1016/J.WASMAN.2013.10.038

Xu, X., Cao, X., Zhao, L., Sun, T., 2014. Comparison of sewage sludge- and pig manure-derived biochars for hydrogen sulfide removal. Chemosphere 111, 296–303. https://doi.org/10.1016/j.chemosphere.2014.04.014

Yan, R., Liang, D.T., Tsen, L., Tay, J.H., 2002. Kinetics and Mechanisms of H 2 S Adsorption by Alkaline Activated Carbon. Environ. Sci. Technol. 36, 4460–4466. https://doi.org/10.1021/es0205840

Yang, B., Wyman, C.E., 2008. Pretreatment: the key to unlocking low-cost cellulosic ethanol. Biofuels, Bioprod. Biorefining 2, 26–40.

Yang, H., Gong, M., Chen, Y., 2011. Preparation of activated carbons and their adsorption properties for greenhouse gases: CH4 and CO2. J. Nat. Gas Chem. 20, 460–464. https://doi.org/10.1016/S1003-9953(10)60232-0

Yang, R.T., 1987. Gas Separation by adsorption processes. Butterworths, Boston, USA.

Yenigün, O., Demirel, B., 2013. Ammonia inhibition in anaerobic digestion: A review. Process Biochem. 48, 901–911. https://doi.org/10.1016/j.procbio.2013.04.012

Yu, F., Steele, P.H., Ruan, R., 2010. Microwave Pyrolysis of Corn Cob and Characteristics of the Pyrolytic Chars. Energy Sources, Part A Recover. Util. Environ. Eff. 32, 475–484. https://doi.org/10.1080/15567030802612440

Yuan, W., Bandosz, T.J., 2007. Removal of hydrogen sulfide from biogas on sludge-derived adsorbents. Fuel 86, 2736–2746. https://doi.org/10.1016/j.fuel.2007.03.012

Yusuf, N.Y., Masdar, M.S., Isahak, W.N.R.W., Nordin, D., Husaini, T., Majlan, E.H., Rejab, S.A.M., Chew, C.L., 2017. Ionic liquid-impregnated activated carbon for biohydrogen purification in an adsorption unit. IOP Conf. Ser. Mater. Sci. Eng. 206, 12071.

Zhang, Q., Hu, J., Lee, D.-J., 2017. Pretreatment of biomass using ionic liquids: Research updates. Renew. Energy 111, 77–84. https://doi.org/10.1016/J.RENENE.2017.03.093

Zhang, T., Mao, C., Zhai, N., Wang, X., Yang, G., 2015. Influence of initial pH on thermophilic anaerobic co-digestion of swine manure and maize stalk. Waste Manag. 35, 119–126. https://doi.org/10.1016/j.wasman.2014.09.004

Zhang, X., Tang, Y., Qu, S., Da, J., Hao, Z., 2015. H 2 S-Selective Catalytic Oxidation: Catalysts and Processes. ACS Catal. 5, 1053–1067.

https://doi.org/10.1021/cs501476p

Zhang, X., Yuan, Q., Cheng, G., 2017. Deconstruction of corncob by steam explosion pretreatment: Correlations between sugar conversion and recalcitrant structures. Carbohydr. Polym. 156, 351–356.

Zhang, Y., Ghaly, A.E., Li, B., 2012. Physical Properties of Corn Residues. Am. J. Biochem. Biotechnol. 8, 44–53. https://doi.org/10.3844/ajbb.2012.44.53

Zhao, Q., Kugel, G., 1996. Thermophilic/mesophilic digestion of sewage sludge and organic wastes. J. Environ. Sci. Heal. . Part A Environ. Sci. Eng. Toxicol. 31, 2211–2231. https://doi.org/10.1080/10934529609376487

Zheng, J, Choo, K., Bradt, C., Lehoux, R., Rehmann, L., 2014. Enzymatic hydrolysis of steam exploded corncob residues after pretreatment in a twin-screw extruder. Biotechnol. Reports 3, 99–107. https://doi.org/10.1016/j.btre.2014.06.008

Zheng, Jun, Choo, K., Bradt, C., Lehoux, R., Rehmann, L., 2014. Enzymatic hydrolysis of steam exploded corncob residues after pretreatment in a twin-screw extruder. Biotechnol. Reports 3, 99–107. https://doi.org/10.1016/j.btre.2014.06.008

Zheng, M., Li, X., Li, L., Yang, X., He, Y., 2009. Enhancing anaerobic biogasification of corn stover through wet state NaOH pretreatment. Bioresour. Technol. 100, 5140–5145. https://doi.org/10.1016/j.biortech.2009.05.045

Zheng, Y., Zhao, J., Xu, F., Li, Y., 2014. Pretreatment of lignocellulosic biomass for enhanced biogas production. Prog. Energy Combust. Sci. 42, 35–53. https://doi.org/10.1016/j.pecs.2014.01.001

Zhu, J., Wan, C., Li, Y., 2010. Enhanced solid-state anaerobic digestion of corn stover by alkaline pretreatment. Bioresour. Technol. 101, 7523–7528. https://doi.org/10.1016/j.biortech.2010.04.060

Zhu, S., Wu, Y., Yu, Z., Liao, J., Zhang, Y., 2005. Pretreatment by microwave/alkali of rice straw and its enzymic hydrolysis. Process Biochem. 40, 3082–3086. https://doi.org/10.1016/J.PROCBIO.2005.03.016

Zulkurnai, N.Z., Ali, U.F.M., Ibrahim, N., Manan, N.S.A., 2017. Carbon Dioxide (CO2) Adsorption by Activated Carbon Functionalized with Deep Eutectic Solvent (DES). IOP Conf. Ser. Mater. Sci. Eng. 206, 12001.